

**SYNTHESIS AND CHARACTERIZATION OF FUNCTIONALIZED
ORDERED MESOPOROUS SILICA MCM-41 WITH
MACROCYCLIC COMPOUNDS FOR THE ADSORPTION OF
ORGANOTIN COMPOUNDS**

ALAHMADI SANA MOHAMMAD T

**THESIS SUBMITTED IN FULFILMENT OF
THE REQUIREMENTS FOR THE DEGREE
OF DOCTOR OF PHILOSOPHY**

**DEPARTMENT OF CHEMISTRY
FACULTY OF SCIENCE
UNIVERSITY OF MALAYA
KUALA LUMPUR**

2014

UNIVERSITI MALAYA

ORIGINAL LITERARY WORK DECLARATION

Name of Candidate: **ALAHMADI SANA MOHAMMAD T** (I.C/Passport No: **H440357**)

Registration/Matric No: **SHC70084**

Name of Degree: **Doctor of Philosophy**

Title of Thesis: **Synthesis and Characterization of Functionalized Ordered Mesoporous Silica MCM-41 with Macrocyclic Compounds for the Adsorption of Organotin Compounds**

Field of Study: **Analytical Chemistry**

I do solemnly and sincerely declare that:

- I am the sole author/writer of this Work;
- This Work is original;
- Any use of any work in which copyright exists was done by way of fair dealing and for permitted purposes and any excerpt or extract from, or reference to or reproduction of any copyright work has been disclosed expressly and sufficiently and the title of the Work and its authorship have been acknowledged in this Work;
- I do not have any actual knowledge nor do I ought reasonably to know that the making of this work constitutes an infringement of any copyright work;
- I hereby assign all and every rights in the copyright to this Work to the University of Malaya ("UM"), who henceforth shall be owner of the copyright in this Work and that any reproduction or use in any form or by any means whatsoever is prohibited without the written consent of UM having been first had and obtained;
- I am fully aware that if in the course of making this Work I have infringed any copyright whether intentionally or otherwise, I may be subject to legal action or any other action as may be determined by UM.

Candidate's Signature

Date

Subscribed and solemnly declared before,

Witness's Signature

Date

Name:

Designation:

ABSTRACT

The work presented in this thesis consists of two parts, focusing on the synthesis and characterization of modified mesoporous MCM-41 with macrocyclic compounds and their application as an adsorbent for organotin compounds removal. The first part of work dealt with the modification of mesoporous silica MCM-41 with macrocyclic compound via a post-synthesis grafting method with calix[4]arene, calix[4]arene sulfonate, para-tert-butylcalix[4]arene and β -cyclodextrin by using toluene-2,4-diisocyanate as the coupling agent (MCM-TDI-C4, MCM-TDI-PC4, MCM-TDI-C4S and MCM-TDI- β -CD) in the first method, and also by using toluene-2,4-diisocyanate and organosilane (3-chloropropyl triethoxysilane-CIPTS) as coupling agents in the second method (MCM-PS-TDI-C4, MCM-PS-TDI-PC4, MCM-PS-TDI-C4S, and MCM-PS-TDI- β -CD). Different techniques such as infrared (FTIR), elemental analysis, thermal gravimetric analysis (TGA) and X-ray powder diffraction (XRD) were used to confirm the production of the desired products. The surface area, pore size and pore size distribution were determined using the surface area analysis (BET) method. The functionalized mesoporous materials with calix[4]arene derivatives and toluene diisocyanate as coupling agent (MCM-TDI-C4, MCM-TDI-PC4 and MCM-TDI-C4S) possessed high surface areas, large pore sizes and narrow pore size distributions compared to other synthetic materials. The screening study of the adsorption of organotin compounds (tributyltin TBT, triphenyltin TPT and dibutyltin DBT) onto prepared materials showed that functionalized mesoporous materials with calix[4]arene derivatives by using toluene-2,4-diisocyanate as coupling agent materials have a higher

adsorption capacity compared to the other prepared materials. A percentage removal for TBT, TPT and DBT from aqueous solution of 98, 95 and 97 %, respectively, by MCM-TDI-PC4 were produced in this study. Isotherms, kinetics and thermodynamics of the adsorption of TBT, TPT and DBT on the prepared mesoporous materials (MCM-TDI-C4, MCM-TDI-PC4 and MCM-TDI-C4S) were investigated. The effect of operating parameters, such as contact time, adsorbate initial concentration, initial pH and temperature were studied. The adsorption capacity was affected by these parameters. The contact time of adsorbent reached equilibrium within 2 h. The maximum adsorption capacity of TBT, TPT and DBT occurred at pH 6. It was found that the maximum adsorption capacities of TBT, TPT and DBT were 16.42, 19.31 and 18.82 mg/g, respectively, for the prepared material MCM-TDI-PC4. Equilibrium modelling of the adsorption isotherm showed that adsorption of those three organotin compounds was able to be described by the three-parameter model better than the two-parameter model. The empirical kinetic data of the adsorption of TBT, TPT and DBT by prepared materials were well described by the second order model. Values of ΔG° indicate that the adsorption of TBT, TPT and DBT onto all adsorbents were spontaneous processes.

ABSTRAK

Kajian yang terkandung dalam tesis ini terdiri daripada dua bahagian yang memberi tumpuan kepada sintesis dan pencirian mesoliang MCM-41 yang diubahsuai dengan bahan makrosiklik serta penggunaannya sebagai penjerap bagi penyingkiran kompaun organotimah. Bahagian pertama kajian ini berkaitan dengan pengubahsuaian silika mesoliang MCM-41 dengan bahan makrosiklik menggunakan kaedah cantuman pos-sintesis, di mana kaedah pertama menggunakan kaliks[4]arene, kaliks[4]arene sulfonat, para-tert-butil kaliks[4]arene and β -siklodekstrin dengan toluena menggunakan 2,4-diisosianat sebagai agen gandingan (MCM-TDI-C4, MCM-TDI-PC4, MCM-TDI-C4S dan MCM-TDI- β -CD), manakala toluena 2,4-di-iso-sianat dan organosilana (3-kloroprofiltrimetoksisilana-CIPTS) digunakan dalam kaedah kedua (MCM-PS-TDI-C4, MCM-PS-TDI-PC4, MCM-PS-TDI-C4S, dan MCM-PS-TDI- β -CD). Pelbagai kaedah seperti spektroskopi inframerah (FTIR), analisis unsur, analisis gravimetri terma (TGA) dan pembelauan serbuk sinar-X (XRD) telah digunakan untuk mengesahkan penghasilan produk yang dikehendaki. Keluasan permukaan, saiz liang dan taburan saiz liang telah ditentukan dengan menggunakan kaedah analisis keluasan permukaan (BET). Bahan mesoliang dengan derivatif kaliks[4]arene dan toluena diisosianat sebagai agen gandingan (MCM-TDI-C4, MCM-TDI-PC4 and MCM-TDI-C4S) mempunyai luas permukaan yang tinggi, saiz liang yang besar dan taburan saiz liang yang sempit berbanding dengan bahan-bahan sintetik yang lain. Kajian pemeriksaan mengenai penjerapan kompaun-kompaun organotin (tributyltimah TBT, trifeniltimah TPT dan dibutyltimah DBT) terhadap bahan-bahan yang disediakan menunjukkan bahawa bahan-bahan mesoliang berfungsi

derivatif-derivatif kaliks[4]arene dengan menggunakan toluena 2,4-di-iso-sianat sebagai agen gandingan mempunyai kapasiti penjerapan yang lebih tinggi berbanding dengan bahan-bahan lain yang disediakan. Peratusan penyingkiran bagi TBT, TPT dan DBT daripada larutan akueus dengan menggunakan MCM-TDI-PC4 yang dihasilkan dalam kajian ini adalah masing-masing 98, 95 dan 97%. Kajian mengenai isoterma, kinetik dan termodinamik bagi penjerapan TBT, TPT dan DBT bagi bahan-bahan mesoliang yang disediakan (MCM-TDI-C4, MCM-TDI-PC4 dan MCM-TDI-C4S) telah dilakukan. Kesan parameter-parameter operasi seperti masa sentuhan, kepekatan awal bahan terjerap, pH awal dan suhu telah dikaji. Kapasiti penjerapan telah didapati dipengaruhi oleh parameter-parameter ini. Masa sentuhan bagi penjerap untuk mencapai keseimbangan adalah dalam tempoh 2 jam. Kapasiti penjerapan maksima bagi TBT, TPT dan DBT berlaku pada pH 6. Kapasiti penjerapan maksima bagi TBT, TPT dan DBT dengan menggunakan MCM-TDI-PC4 yang telah dihasilkan adalah masing-masing 16.42, 19.31 dan 18.82 mg/g. Model keseimbangan bagi isoterma penjerapan menunjukkan bahawa penjerapan bagi ketiga-tiga sebatian organotimah telah berjaya diterangkan lebih baik oleh model dengan tiga parameter berbanding model dengan dua parameter. Data kinetik empirikal bagi penjerapan TBT, TPT dan DBT dengan menggunakan bahan-bahan yang disediakan telah diterangkan dengan baik oleh model tertib kedua. Nilai-nilai ΔG° menunjukkan bahawa penjerapan TBT, TPT dan DBT ke atas semua penjerap adalah merupakan proses spontan.

ACKNOWLEDGEMENTS

In the Name of Allah, Most Gracious, Most Merciful

First and foremost, greatest thanks to Allah (SWT) for giving me the health, ability, strength and blessing to make this work possible. My success in everything can only come from Allah. In Him I trust, and unto Him I turn.

I would like to thank all people who have helped me along the way. First of all, I wish to express my sincere appreciation and gratefulness to my thesis advisors, Dr. Sharifah Mohamad and Prof. Dato' Dr. Mohamad Jamil Maah as this thesis would not have been possible without their guidance, encouragement, understanding, patience and support throughout this research.

I must, of course, express my appreciation to academic and technical staff in the Department of Chemistry, Universiti Malaya for their assistances. Special thanks go to my labmates for both their generous assistance and their valuable friendship in my life. I would also like to express my thanks for all the assistance, support and services provided by the Institute of Postgraduate Studies (IPS), laboratories, computer facilities and the library of UM.

My deepest gratitude goes to my parents for their unflagging love and support in my life. I am indebted to my father, Mr. Mohammad and my mother, Ms. Aisha, for their praying and everlasting love to me.

Profound appreciations and grateful honor to my husband, Ahmad, who has been constantly taking good care of me and stands by me to help cope with whatever difficulties I have encountered these years and to my children Badr, Abdulrahman, Sara and Yousef for their everlasting love, encouragement, understanding and support throughout these years.

Last, but by no means the least, I would like to acknowledge the financial support of my sponsor Taibah University (TU), Madinah, Kingdom of Saudi Arabia.

TABLE OF CONTENTS

ABSTRACT	iii
ABSTRAK	v
ACKNOWLEDGEMENTS	vii
TABLE OF CONTENTS	ix
LIST OF FIGURE	xiii
LIST OF TABLE	xix
LIST OF SYMBOLS	xxii
LIST OF ABBREVIATIONS	xxv
CHAPTER 1: INTRODUCTION	1
1.1 Background of the research	1
1.2 Research objectives	8
1.3 Structure of the thesis	10
CHAPTER 2: LITERATURE REVIEW AND THEORY	12
2.1 Literature review	12
2.1.1 Organotin compounds and organotin compounds pollution	12
2.1.1.1 Organotin compounds in the aquatic environment	12
2.1.1.2 Toxicity of organotin compounds	14
2.1.2 Techniques available for organotin compounds removal	20
2.1.2.1 Biological methods	21
2.1.2.2 Chemical methods	23
2.1.2.3 Physical methods	25
2.1.3 Adsorption study	30
2.1.3.1 Background history	30
2.1.3.2 Types of adsorption	33
2.1.3.3 Adsorption isotherms	36
2.1.3.4 Adsorbent	38
2.1.4 Ordered mesoporous silica	39
2.1.4.1 History and synthesis of mesoporous silica type MCM-41	43
2.1.4.2 Surface modification of MCM-41	45
2.1.4.2.1 Grafting method	46
2.1.4.2.2 Co-condensation method	49
2.1.4.3 Applications of mesoporous silica	52
2.1.5 Macrocyclic compounds	55
2.1.5.1 Calix[4]arene	55
2.1.5.2 β -cyclodextrin	62
2.2 Theory	68
2.2.1 Two-parameter adsorption isotherms models	68
2.2.1.1 Langmuir isotherm	68

2.2.1.2	Freundlich isotherm	71
2.2.1.3	Temkin isotherm	72
2.2.1.4	Dubinin-Radushkevitch isotherm	72
2.2.2	Three-parameter adsorption isotherm models	74
2.2.2.1	Redlich-Peterson isotherm	74
2.2.2.2	Koble-Corrigan isotherm	75
2.2.3	Adsorption kinetics	76
2.2.3.1	Pseudo-first order model	76
2.2.3.2	Pseudo-second order model	77
2.2.3.3	Intraparticle diffusion model	78
2.2.4	Thermodynamic studies	79
 CHAPTER 3: SYNTHESIS AND CHARACTERIZATION OF FUNCTIONALIZED ORDERED MESOPOROUS SILICA MCM-41 WITH CALIX[4]ARENE DERIVATIVES		82
3.1	Introduction	82
3.2	Experimental	84
3.2.1	Materials	84
3.2.2	Instrumentation	86
3.2.3	Synthesis methods	87
3.2.3.1	Synthesis of p-sulfonatocalix[4]arene	87
3.2.3.2	Functionalization of MCM-41 mesoporous surfaces with calix[4]arene derivatives	87
3.2.3.3	Determination of isocyanate groups of the reaction system	92
3.3	Results and discussion	93
3.3.1	Characterization of functionalized MCM-41 with TDI as linker	93
3.3.2	Characterization of functionalized MCM-TDI with calix[4]arene derivatives	98
3.3.3	Characterization of functionalized MCM-41 with CIPTS and TDI as a linker	106
3.3.4	Characterization of functionalized MCM-PS-TDI with calix[4]arene derivatives	110
3.4	Summary	118
 CHAPTER 4: SYNTHESIS AND CHARACTERIZATION OF FUNCTIONALIZED ORDERED MESOPOROUS SILICA MCM-41 WITH β-CYCLODEXTRIN		120
4.1	Introduction	120
4.2	Experimental	122
4.2.1	Materials	122
4.2.2	Instrumentation	124
4.2.3	Synthesis methods	124
4.2.3.1	Preparation of 3-hydroxypropyl triethylsilyl functionalized MCM-41	124
4.2.3.2	Immobilizing β -cyclodextrins onto the functionalized MCM-41	125

4.2.3.3	Screening experiments	127
4.3	Results and discussion	128
4.3.1	Characterization of functionalized MCM-41 with β -cyclodextrin	129
4.3.2	Screening results	136
4.4	Summary	140
 CHAPTER 5: ISOTHERMS, KINETICS AND THERMODYNAMICS OF TRIBUTYLTIN (TBT) ADSORPTION ON MODIFIED MESOPOROUS SILICA WITH CALIX[4]ARENE DERIVATIVES		142
5.1	Introduction	142
5.2	Experimental	144
5.2.1	Materials	144
5.2.1.1	Adsorbents	144
5.2.1.2	Adsorbate	145
5.2.2	Adsorption studies	146
5.2.2.1	Equilibrium contact time	146
5.2.2.2	Effect of pH	146
5.2.2.3	Effect of initial TBT concentration	147
5.2.2.4	Effect of temperature on the adsorption of TBT	147
5.2.3	Analytical procedure	148
5.3	Results and discussion	148
5.3.1	Effect of contact time	148
5.3.2	Effect of pH	151
5.3.3	Effect of initial TBT concentration	153
5.3.4	Effect of solution temperature	155
5.3.5	Adsorption isotherm models	157
5.3.6	Adsorption Kinetic	171
5.3.7	Adsorption thermodynamic	178
5.4	Summary	181
 CHAPTER 6: ISOTHERMS, KINETICS AND THERMODYNAMICS OF TRIPHENYLTIN (TPT) ADSORPTION ON MODIFIED MESOPOROUS SILICA WITH CALIX[4]ARENE DERIVATIVES		185
6.1	Introduction	185
6.2	Experimental	187
6.2.1	Materials	187
6.2.1.1	Adsorbents	187
6.2.1.2	Adsorbate	187
6.2.2	Equilibrium isotherm and kinetics studies	188
6.2.3	Analytical procedure	189
6.3	Results and discussion	190
6.3.1	Effect of contact time	190
6.3.2	Effect of pH	192
6.3.3	Effect of initial TPT concentration	194

6.3.4	Effect of solution temperature	196
6.3.5	Adsorption isotherm models	198
6.3.6	Adsorption kinetic	210
6.3.7	Adsorption thermodynamic	216
6.4	Summary	218
CHAPTER 7: ISOTHERMS, KINETICS AND THERMODYNAMICS OF DIBUTYLTIN (DBT) ADSORPTION ON MODIFIED MESOPOROUS SILICA WITH CALIX[4]ARENE DERIVATIVES		221
7.1	Introduction	221
7.2	Experimental	223
7.2.1	Materials	223
7.2.2	Equilibrium isotherm and kinetics studies	223
7.2.3	Analytical procedure	225
7.3	Results and discussion	225
7.3.1	Effect of contact time	225
7.3.2	Effect of pH	227
7.3.3	Effect of initial DBT concentration	230
7.3.4	Effect of solution temperature	231
7.3.5	Adsorption isotherm models	233
7.3.6	Adsorption kinetic	243
7.3.7	Adsorption thermodynamic	249
7.4	Summary	251
CHAPTER 8: CONCLUSIONS AND RECOMMENDATIONS		253
8.1	Conclusions	253
8.2	Recommendations for future work	256
REFERENCE		257
	List of publications and international conferences attended	313

LIST OF FIGURE

Figure 1.1	From molecular to supramolecular chemistry	6
Figure 1.2	Schematic representation of a sensitive layer of receptor molecules in the vicinity of the liquid of the analyte	8
Figure 2.1	Most common adsorption isotherms for dilute aqueous solutions on carbon materials	37
Figure 2.2	Schematic illustrating pore size distribution of some porous materials	40
Figure 2.3	The IUPAC classification of adsorption isotherms showing both adsorption and desorption pathways.	41
Figure 2.4	The relationship between the pore shape and the adsorption-desorption isotherm	42
Figure 2.5	Proposed mechanism of MCM-41 formation	44
Figure 2.6	The X-ray diffraction patterns and proposed structures of MCM-41, MCM-48, and MCM-50	45
Figure 2.7	Different types of silanols on the surface	47
Figure 2.8	Difference in the coverage between hydrated and non-hydrated surfaces	49
Figure 2.9	Calix[4]arenes	57
Figure 2.10	Structural representation of β -cyclodextrin	62
Figure 2.11	Proposed schematic of the inclusion compound	64
Figure 3.1	Molecular structures of some materials	85
Figure 3.2	Schematic diagram for the functionalization of MCM-41 mesoporous silica material surface with of calix[4]arene derivatives using toluene-2,4-diisocyanate (TDI) as linker	89
Figure 3.3	Schematic diagram for the functionalization of MCM-41 mesoporous silica material surface with calix[4]arene	

	derivatives using 3-chloropropyl triethoxysilane (CIPTS) and toluene-2,4-diisocyanate (TDI) as linker	92
Figure 3.4	Fourier transform infrared spectroscopy (FTIR) spectra of MCM-41 (A) and MCM-TDI (B)	96
Figure 3.5	Thermogravimetric analysis (TGA) of MCM-41(...) and MCM-TDI (—)	97
Figure 3.6	FTIR spectra of MCM-TDI-C4 (A), MCM-TDI-C4S (B) and MCM-TDI-PC4 (C)	100
Figure 3.7	TGA analysis of MCM-TDI-C4, MCM-TDI-C4S and MCM-TDI-PC4	102
Figure 3.8	X-ray powder diffraction (XRD) analysis of MCM-TDI-C4, MCM-TDI-C4S and MCM-TDI-PC4	103
Figure 3.9	Nitrogen adsorption-desorption isotherms of MCM-TDI-C4, MCM-TDI-C4S, and MCM-TDI-PC4	104
Figure 3.10	Fourier transform infrared spectroscopy (FTIR) spectra of MCM-PS-TDI (A) and MCM-41 (B)	108
Figure 3.11	Thermogravimetric analysis (TGA) of MCM-PS-TDI	110
Figure 3.12	FTIR spectra of MCM-PS-TDI-C4 (A), MCM-PS-TDI-C4S (B) and MCM-PS-TDI-PC4 (C)	112
Figure 3.13	TGA analysis of MCM-PS-TDI-C4, MCM-PS-TDI-C4S and MCM-PS-TDI-PC4	114
Figure 3.14	XRD analysis of MCM-PS-TDI-C4, MCM-PS-TDI-C4S and MCM-PS-TDI-PC4	115
Figure 3.15	Nitrogen adsorption-desorption isotherms of MCM-PS-TDI-C4 (Δ), MCM-PS-TDI-C4S (\square) and MCM-PS-TDI-PC4 (\diamond)	117
Figure 4.1	Molecular structures of some materials	123
Figure 4.2	Preparation of modified mesoporous silica with β -cyclodextrin	126
Figure 4.3	FTIR spectra of MCM-41 (A), MCM-PS-TDI, (B) MCM-TDI (C), MCM-PS-TDI- β -CD (D) and MCM-TDI- β -CD (E)	131
Figure 4.4	TGA analysis of MCM-PS-TDI- β -CD and MCM-TDI- β -CD	132

Figure 4.5	XRD analysis of MCM-PS-TDI- β -CD and MCM-TDI- β -CD	134
Figure 4.6	Nitrogen adsorption-desorption isotherms of (\diamond) MCM-PS-TDI- β -CD, and (\square)MCM-TDI- β -CD	135
Figure 4.7	Removal percentage of TBT, TPT and DBT by modified mesoporous silica MCM-41 with calix[4]arenes derivatives and β -cyclodextrin adsorbents	137
Figure 4.8	BET pore size distribution patterns of the MCM-TDI-C4, MCM-TDI-PC4 and MCM-TDI-C4S.	139
Figure 5.1	Tributyltin molecular formula	145
Figure 5.2	Effect of contact time on removal of TBT onto MCM-TDI-C4 (a), MCM-TDI-PC4 (b) and MCM-TDI-C4S (c)	150
Figure 5.3	Effect of pH on removal of TBT	152
Figure 5.4	Effect of initial TBT concentration on the TBT removal efficiency and uptake capacity by MCM-TDI-C4 (a), MCM-TDI-PC4 (b) and MCM-TDI-C4S (c)	154
Figure 5.5	Adsorption isotherm for TBT on MCM-TDI-C4 (a), MCM-TDI-PC4 (b) and MCM-TDI-C4S (c) at different temperatures	156
Figure 5.6	Freundlich isotherm of TBT adsorbed onto MCM-TDI-C4 (a), MCM-TDI-PC4 (b) and MCM-TDI-C4S (c)	158
Figure 5.7	Langmuir isotherm Type II of TBT adsorbed onto MCM-TDI-C4 (a), MCM-TDI-PC4 (b) and MCM-TDI-C4S (c)	162
Figure 5.8	Values of R_L for adsorption of TBT onto MCM-TDI-C4, MCM-TDI-PC4 and MCM-TDI-C4S	164
Figure 5.9	Temkin isotherm of TBT adsorbed onto MCM-TDI-C4 (a), MCM-TDI-PC4 (b) and MCM-TDI-C4S (c)	165
Figure 5.10	Dubinin–Radushkevitch isotherm of TBT adsorbed onto MCM-TDI-C4 (a), MCM-TDI-PC4 (b) and MCM-TDI-C4S (c)	167
Figure 5.11	Redlich–Peterson isotherm of TBT adsorbed onto MCM-TDI-C4 (a), MCM-TDI-PC4 (b) and MCM-TDI-C4S (c)	169

Figure 5.12	Koble–Corrigan isotherm of TBT adsorbed onto MCM-TDI-C4 (a), MCM-TDI-PC4 (b) and MCM-TDI-C4S (c)	171
Figure 5.13	Pseudo-first order model plot for the adsorption of TBT onto MCM-TDI-C4 (a), MCM-TDI-PC4 (b) and MCM-TDI-C4S (c)	173
Figure 5.14	Pseudo-second order model plot for the adsorption of TBT onto MCM-TDI-C4 (a), MCM-TDI-PC4 (b) and MCM-TDI-C4S (c)	175
Figure 5.15	Intraparticle diffusion model plot for the adsorption of TBT onto MCM-TDI-C4 (a), MCM-TDI-PC4 (b) and MCM-TDI-C4S (c)	177
Figure 5.16	Plot of $\ln K_c$ versus $1/T$ for TBT adsorption	180
<i>Figure 6.1</i>	Molecular structure of triphenyltin chloride	187
Figure 6.2	Effect of contact time on removal of TPT by MCM-TDI-C4 (a), MCM-TDI-PC4 (b) and MCM-TDI-C4S (c)	191
Figure 6.3	Effect of pH on removal of TPT by MCM-TDI-C4, MCM-TDI-PC4 and MCM-TDI-C4S	193
Figure 6.4	Effect of initial TPT concentration on the TPT removal efficiency and uptake capacity by MCM-TDI-C4 (a), MCM-TDI-PC4 (b) and MCM-TDI-C4S (c)	195
Figure 6.5	Adsorption isotherms for TPT on MCM-TDI-C4 (a), MCM-TDI-PC4 (b) and MCM-TDI-C4S (c) at different temperature	197
Figure 6.6	Langmuir isotherm Type II of TPT adsorbed onto MCM-TDI-C4 (a), MCM-TDI-PC4 (b) and MCM-TDI-C4S (c)	199
Figure 6.7	Freundlich isotherm of TPT adsorbed onto MCM-TDI-C4 (a), MCM-TDI-PC4 (b) and MCM-TDI-C4S (c)	200
Figure 6.8	Values of R_L for adsorption of TPT onto MCM-TDI-C4, MCM-TDI-PC4 and MCM-TDI-C4S	203
Figure 6.9	Temkin isotherm of TPT adsorbed onto MCM-TDI-C4 (a), MCM-TDI-PC4 (b) and MCM-TDI-C4S (c)	204
Figure 6.10	Dubinin–Radushkevitch isotherm of TPT adsorbed onto MCM-TDI-C4 (a), MCM-TDI-PC4 (b) and MCM-TDI-C4S (c)	206

Figure 6.11	Redlich-Peterson isotherm of TPT adsorbed onto MCM-TDI-C4 (a), MCM-TDI-PC4 (b) and MCM-TDI-C4S (c)	207
Figure 6.12	Koble-Corrigan isotherm of TPT adsorbed onto MCM-TDI-C4 (a), MCM-TDI-PC4 (b) and MCM-TDI-C4S (c)	209
Figure 6.13	Pseudo-first order model plot for the adsorption of TPT onto MCM-TDI-C4 (a), MCM-TDI-PC4 (b) and MCM-TDI-C4S (c)	211
Figure 6.14	Pseudo-second order model plot for the adsorption of TPT onto MCM-TDI-C4 (a), MCM-TDI-PC4 (b) and MCM-TDI-C4S (c)	213
Figure 6.15	Intraparticle diffusion model plot for the adsorption of TPT onto MCM-TDI-C4 (a), MCM-TDI-PC4 (b) and MCM-TDI-C4S (c)	215
Figure 6.16	Plot of $\ln K_c$ versus $1/T$ for TPT adsorption	216
Figure 7.1	Dibutyltin molecular formula	223
Figure 7.2	Effect of contact time on removal of DBT onto MCM-TDI-C4 (a), MCM-TDI-PC4 (b) and MCM-TDI-C4S (c)	226
Figure 7.3	Effect of pH on removal of DBT onto MCM-TDI-C4, MCM-TDI-PC4 and MCM-TDI-C4S	227
Figure 7.4	Predicted adsorption edges of DBT, calculated by using the pH-dependent Dual Langmuir model	229
Figure 7.5	Effect of initial DBT concentration on the DBT removal efficiency and uptake capacity by MCM-TDI-C4 (a), MCM-TDI-PC4 (b) and MCM-TDI-C4S (c)	231
Figure 7.6	Adsorption isotherms for DBT on MCM-TDI-C4 (a), MCM-TDI-PC4 (b) and MCM-TDI-C4S (c) at different temperatures	233
Figure 7.7	Freundlich isotherm of DBT adsorbed onto MCM-TDI-C4 (a), MCM-TDI-PC4 (b) and MCM-TDI-C4S (c)	237
Figure 7.8	Values of R_L for adsorption of DBT onto MCM-TDI-C4, MCM-TDI-PC4 and MCM-TDI-C4S	238
Figure 7.9	Temkin isotherm of DBT adsorbed onto MCM-TDI-C4 (a), MCM-TDI-PC4 (b) and MCM-TDI-C4S (c)	240

Figure 7.10	Dubinin–Radushkevitch isotherm of DBT adsorbed onto MCM-TDI-C4 (a), MCM-TDI-PC4 (b) and MCM-TDI-C4S (c)	241
Figure 7.11	Koble–Corrigan isotherm of DBT adsorbed onto MCM-TDI-C4 (a), MCM-TDI-PC4 (b) and MCM-TDI-C4S (c)	242
Figure 7.12	Pseudo-first order model plot for the adsorption of DBT onto MCM-TDI-C4 (a), MCM-TDI-PC4 (b) and MCM-TDI-C4S (c)	244
Figure 7.13	Pseudo-second order model plot for the adsorption of DBT onto MCM-TDI-C4 (a), MCM-TDI-PC4 (b) and MCM-TDI-C4S (c)	246
Figure 7.14	Intraparticle diffusion model plot for the adsorption of DBT onto MCM-TDI-C4 (a), MCM-TDI-PC4 (b) and MCM-TDI-C4S (c)	248
Figure 7.15	Plot of $\ln K_c$ versus $1/T$ for DBT adsorption	250

LIST OF TABLE

Table 2.1	Sources and possible pathways for the introduction of organotins to the environment	13
Table 2.2	Brief history of adsorption development and application	31
Table 2.3	Characteristics associated with physical/chemical adsorption	35
Table 2.4	Surface modification of MCM-41 in the recent years (2000–2013) for the adsorption application	50
Table 2.5	Applications of modified calix[4]arene as adsorbent in the recent years (2000–2013)	59
Table 2.6	Physical properties of cyclodextrin	63
Table 2.7	Applications of modified β -cyclodextrin as adsorbent in the recent years (2000–2013)	65
Table 3.1	Results of elemental analysis for mesoporous silica-TDI, MCM-TDI-C4, MCM-TDI-C4S and MCM-TDI-PC4	101
Table 3.2	Thermogravimetric analysis results of MCM-TDI-C4, MCM-TDI-C4S and MCM-TDI-PC4	101
Table 3.3	Structural parameters of MCM-41, MCM-TDI-C4, MCM-TDI-C4S and MCM-TDI-PC4	105
Table 3.4	Results of elemental analysis for MCM-PS-TDI functionalized with calix[4]arene derivatives	113
Table 3.5	Results of thermogravimetric analysis for MCM-PS-TDI-C4, MCM-PS-TDI-C4S and MCM-PS-TDI-PC4	114
Table 3.6	Structural parameters of MCM-41, MCM-PS-TDI-C4, MCM-PS-TDI-C4S and MCM-PS-TDI-PC4	117
Table 4.1	ICP-MS conditions	124
Table 4.2	Thermogravimetric analysis results of MCM-PS-TDI- β -CD and MCM-TDI- β -CD	132
Table 4.3	Results of elemental analysis for MCM-PS, MCM-PS-TDI, MCM-PS-TDI- β -CD, MCM-TDI, MCM-TDI- β -CD	133

Table 4.4	Structural parameters of MCM-41, MCM-PS-TDI- β -CD and MCM-TDI- β -CD	135
Table 5.1	Isotherm constants and correlation coefficient of determination for various adsorption isotherms for the adsorption of TBT onto MCM-TDI-C4 (a), MCM-TDI-PC4 (b) and MCM-TDI-C4S (c)	159
Table 5.2	Calculated kinetic parameters for pseudo-first order and pseudo-second order kinetic models for the adsorption of TBT using MCM-TDI-C4 (a), MCM-TDI-PC4 (b) and MCM-TDI-C4S (c) as adsorbents	173
Table 5.3	Calculated kinetic parameters for intraparticle diffusion model for the adsorption of TBT using MCM-TDI-C4 (a), MCM-TDI-PC4 (b) and MCM-TDI-C4S (c) as adsorbents	177
Table 5.4	Thermodynamic parameters of TBT adsorption on MCM-TDI-C4, MCM-TDI-PC4 and MCM-TDI-C4S	180
Table 5.5	Comparison of adsorption capacities of various materials for TBT	183
Table 6.1	Isotherm constants and correlation coefficient of determination for various adsorption isotherms for the adsorption of TPT onto MCM-TDI-C4 (a), MCM-TDI-PC4 (b) and MCM-TDI-C4S (c)	201
Table 6.2	Calculated kinetic parameters for pseudo first-order and pseudo-second order kinetic models for the adsorption of TPT using MCM-TDI-C4 (a), MCM-TDI-PC4 (b) and MCM-TDI-C4S (c) as adsorbents	211
Table 6.3	Calculated kinetic parameters for intraparticle diffusion model for the adsorption of TPT using MCM-TDI-C4 (a), MCM-TDI-PC4 (b) and MCM-TDI-C4S (c) as adsorbents	214
Table 6.4	Thermodynamic parameters of TPT adsorption on MCM-TDI-C4, MCM-TDI-PC4 and MCM-TDI-C4S	217
Table 7.1	Isotherm constants and correlation coefficients of determination for various adsorption isotherms for the adsorption of DBT onto MCM-TDI-C4 (a), MCM-TDI-PC4 (b) and MCM-TDI-C4S (c)	234

Table 7.2	Calculated kinetic parameters for pseudo-first order and pseudo-second order kinetic models for the adsorption of DBT using MCM-TDI-C4 (a), MCM-TDI-PC4 (b) and MCM-TDI-C4S (c) as adsorbents	243
Table 7.3	Calculated kinetic parameters for intraparticle diffusion model for the adsorption of DBT using MCM-TDI-C4 (a), MCM-TDI-PC4 (b) and MCM-TDI-C4S (c) as adsorbents	247
Table 7.4	Thermodynamic parameters of DBT adsorption on MCM-TDI-C4, MCM-TDI-PC4 and MCM-TDI-C4S	250
Table 8.1	Summarized results for adsorption of TBT, TPT, and DBT onto MCM-TDI-C4, MCM-TDI-PC4 and MCM-TDI-C4S	255

LIST OF SYMBOLS

Symbol	Description	Unit
nSiO ₂	Silica nanoparticles	----
nFe ₃ O ₄ ,	Nano-magnetite	----
nZnO	Nano zinc oxide	----
SiO ₂	Silica oxide	----
Si-O-Si	Siloxane	----
Si-OH	Silanol	----
Ni (II)	Nickel (II)	----
Cd (II)	Cadmium (II)	----
Pb (II)	Lead (II)	----
CO ₂	Carbon dioxide	----
Ce (III)	Cerium (III)	----
Nd(III)	Neodymium (III)	----
Eu (III)	Europium (III)	----
Gd (III)	Gadolinium (III)	----
Lu(III)	Lutetium (III)	----
Cr (VI)	Chromium (VI)	----
Zn (II)	Zinc (II)	----
Cu (II)	Copper (II)	----
CHCl ₃	Chloroform	----
CS ₂	Carbon disulfide	----
HCHO	Formaldehyde	----
HSO ₃ Cl	Chlorosulfonic acid	----
CH ₂ Cl ₂	Dichloromethane	----
HCl	Hydrochloric acid	----
Cs ⁺	Cesium	----

K^+	Potassium	----
Hg (II)	Mercury (II)	----
As (III) and As (V)	Arsenic (III) and arsenic (V)	----
U(VI)	Uranium (VI)	----
Co (II)	Cobalt (II)	----
α -, β -, γ - and δ -	Alpha, beta, gamma and delta	----
TiO ₂	Titanium dioxide	----
q_{max}	Maximum surface coverage of adsorbent	mg/g
K_L	Adsorption energy constant of Langmuir isotherm	L/mg
C_e	Equilibrium liquid phase concentration	mg/L
R_L	Langmuir dimensionless separation factor	----
C_o	Initial liquid phase concentration	mg/L
q_e	Equilibrium solid phase adsorbate concentration	mg/g
K_F	Freundlich isotherm constant	L/g
n	Freundlich isotherm constant related to adsorption intensity	----
K_T	Equilibrium binding constant	L/mg
b_T	Temkin energy constant	J/mol
A_T	Constant relates to the heat of adsorption	
R	Gas constant = 8.314	J/(mol K)
T	Absolute temperature	K
q_d	Dubin-Radushkevitch constant refer to maximum adsorption capacity	(mg/g)
β	Constant related to free energy	mol ² /kJ ²
ϵ	Polanyi potential	----
E	Mean free energy	kJ/mol
A_R	Redlich-Peterson isotherm constant	L/g
B_R	Redlich-Peterson isotherm constant	L/mg
g	Exponent which lies between 0 and 1	----
A_K	Koble-Corrigan isotherm constant	----

B_K	Koble-Corrigan isotherm constant	----
p	Koble-Corrigan isotherm constant	----
q_t	Amount of adsorption at any time, t	mg/g
K_1	Rate constant of first-order adsorption	min ⁻¹
t	Time	min
K_2	Rate constant of second order adsorption	g/mg min
K_i	Intraparticle diffusion rate constant	mg/ g min ^{1/2}
C	Constant related to the thickness of the boundary layer	----
ΔH°	Change in standard enthalpy	kJ/mol
ΔG°	Change in standard free energy	kJ/mol
ΔS°	Change in standard entropy	J/mol K
K_c	Standard thermodynamic equilibrium constant	L/g
S_{BET}	Surface area calculated using a Brunauer-Emmett-Teller analysis	m ² /g
V_0	The titer of 0.1 mol/L HCl for blank	ml
V_s	The titer of 0.1 mol/L HCl for sample	ml
w	Weight of the sample	g
f	Factor of 0.1 mol/L HCl	----
V	Volume of solution	L
R^2	Correlation coefficient	----
$q_{e, cal}$	Calculated equilibrium adsorption capacity	mg/g
h	Initial adsorption rates	mg/ g min
pK_a	Dissociation constant	----

LIST OF ABBREVIATIONS

Tributyltin	TBT
Triphenyltin	TPT
Dibutyltin	DBT
Polyvinyl chloride	PVC
Part per billion	ppb
Silica and aluminosilica mesoporous molecular sieves	M41S
Mesoporous silica with hexagonal arrangement of uniform cylindrical mesopores	MCM-41
Toluene-2,4-diisocyanate	TDI
3-Chloropropyl triethoxysilane	CIPTS
Organotin compounds	OTCs
Monobutyltin	MBT
Adenosine triphosphate	ATP
An enzyme that catalyzes the hydrolysis of adenosine triphosphate to adenosine diphosphate, releasing energy that is used in the cell	ATPases
Deoxyribonucleic acid (a molecule that encodes the genetic instructions used in the development and functioning of all known living organisms)	DNA
Enzymes catalyze the oxidation of organic substances	Cytochrome P450
A type of white blood cell that assists other white blood cells in immunologic processes	CD4 ⁺ thymocytes
A type of white blood cell that virally destroys infected cells and tumor cells, and is also implicated in transplant rejection	CD8 ⁺ thymocytes
Triphenyltin hydroxide	TPTOH
Parts per trillion	ppt
Triorganotin compounds	TOTCs

The solution with pH at which the surface charge is zero	pH _{ZPC}
The International Union of Pure and Applied Chemistry	IUPAC
The ordered mesoporous silica materials	OMS
Mesoporous silica with cubic pore shapes	MCM-48
Mesoporous silica with lamellar structures	MCM-50
Tetraethylorthosilicate	TEOS
Tetramethylorthosilicate	TMOS
Nuclear magnetic resonance	NMR
The Dubinin-Radushkevitch isotherm	D-R
Fourier transform infrared spectroscopy	FT-IR
Thermogravimetric analyses	TGA
The X-ray powder diffraction	XRD
Brunauer, Emmett and Teller model	BET
Elemental analysis	CHN
Dichloromethane	DCM
Calix[4]arene	C4
para-tert-butylcalix[4]arene	PC4
Calix[4]arene sulfonate	C4S
Mesoporous silica modified with toluene-2,4-diisocyanate	MCM-TDI
Mesoporous silica functionalized with calix[4]arene using toluene-2,4-diisocyanate as linker	MCM-TDI-C4
Mesoporous silica functionalized with para-tert-butylcalix[4]arene using toluene-2,4-diisocyanate as linker	MCM-TDI-PC4
Mesoporous silica functionalized with calix[4]arene sulfonate using toluene-2,4-diisocyanate as linker	MCM-TDI-C4S
Volume/volume	v/v
Mesoporous silica modified with 3-chloropropyl triethoxysilane	CIPTS-MCM
Hydrolysed mesoporous silica modified with 3-chloropropyl triethoxysilane	OHPTS-MCM

Mesoporous silica modified with 3-chloropropyl triethoxysilane and toluene-2,4-diisocyanate	MCM-PS-TDI
Mesoporous silica functionalized with calix[4]arene using 3-chloropropyl triethoxysilane and toluene-2,4-diisocyanate as linker	MCM-PS-TDI-C4
Mesoporous silica functionalized with para-tert-butylcalix[4]arene using 3-chloropropyl triethoxysilane and toluene-2,4-diisocyanate as linker	MCM-PS-TDI-PC4
Mesoporous silica functionalized with calix[4]arene sulfonate using 3-chloropropyl triethoxysilane and toluene-2,4-diisocyanate as linker	MCM-PS-TDI-C4S
β -cyclodextrins	β -CDs
Inductively coupled plasma mass spectrometry	ICP-MS
Tin	Sn
Mesoporous silica functionalized with β -cyclodextrins using toluene-2,4-diisocyanate as linker	MCM-TDI- β -CD
Mesoporous silica functionalized with β -cyclodextrins using 3-chloropropyl triethoxysilane and toluene-2,4-diisocyanate as linker	MCM-PS-TDI- β -CD
Lethal dose, 50% (the dose required to kill half the members of a tested population after a specified test duration)	LD ₅₀
Revolutions per minute	rpm
Minute	min
Hour	h

CHAPTER 1

INTRODUCTION

1.1 Background of the research

In the past thirty years, there was a notable increase in the use of organotin compounds as evidenced by their widespread applications (Hoch, 2001). Organotin compounds are basically utilized in the form of fungicides, bactericides, pesticides, biocides, preservatives of wood and stabilizing agents in polymers and catalysts (Fent, 1996a; Forsyth & Jay, 1997). They are also utilized as an antifouling agent in paints in the form of tributyltin (TBT) and triphenyltin (TPT), where they are released into marine and freshwater environment in a continuous manner that contaminate the environment.

Several legislation efforts have been undertaken to minimize the release of such compounds but to date, there are still significant concentrations and metabolites of such compounds in the water (Reader & Pelletier, 1992) along with suspended matters (Fent & Mueller, 1991), sediments (Jantzen & Prange, 1995) and sewage sludge (Fent, 1996b).

Dibutyltin (DBT) is defined as an organotin compound found in polyvinyl chloride (PVC) plastics, agricultural pesticides and other consumer products such as a plastic stabilizer (e.g. carpet, textiles and wallpaper) (Fent, 1996a). Due to the popular use of consumer and agricultural products, DBT has been found on the surface water and drinking water at the

level of 2 ppb and 53 ng/L, basically from leaching of PVC piping (Jones-Lepp, Varner, & Heggem, 2004; Sadiki & Williams, 1999).

In the USA and other countries, PVC piping is extensively utilized for water transportation to and from residential places and according to research, DBT is leached from PVC pipes in a continuous indefinite manner (Forsyth & Jay, 1997; Quevauviller, Donard, & Bruchet, 1991). DBT is also known to be utilized as an anti-helminthic for poultry prior to 1992, resulting in agricultural runoff from soil contamination as a secondary DBT exposure source (Epstein, 1991; Jones-Lepp, et al., 2004). While DBT has lower toxicity compared to TBT, the former has higher toxicity when it comes to immune systems (Bouchard, Pelletier, & Fournier, 1999; St-Jean, Pelletier, & Courtenay, 2002). TBT degrades into DBT and monobutyltin (MBT), which are more polar and less toxic compounds to aquatic living organisms. Because of this degradation, DBT reaches the same or even higher concentrations compared to its parent compound (TBT) in coastal waters (H Frouin, Pelletier, Lebeuf, Saint-Louis, & Fournier, 2010) along with sediments (Berto et al., 2007). As these compounds (TBT, TPT and DBT) are the most toxic compounds among organotins owing to their widespread use. Efficient methods of their removal have been given priority and have led to the increasing research and technological interest over the last few years.

In the past thirty years, three methods have been used for the removal of organotin compounds involving physical (Ayanda, Fatoki, Adekola, & Ximba, 2013; Behra, Lecarme-Théobald, Bueno, & Ehrhardt, 2003; Fang, Borggaard, Christensen, Holm, &

Hansen, 2012; Fang, Borggaard, Marcussen, Holm, & Bruun Hansen, 2010), chemical (Gabbianelli, Falcioni, & Lupidi, 2002; R. Prasad & Schafran, 2006; Schafran, Prasad, Thorn, Ewing, & Soles, 2003; Stichnothe, Thöming, & Calmano, 2001; Yvon, Hécho, & Donard, 2011) and biological methods (Gadd, 2000; Jin et al., 2011; S. E. Lee, Chung, Won, Lee, & Lee, 2012; Luan, Jin, Chan, Wong, & Tam, 2006; N. Tam, Chong, & Wong, 2003; N. F. Y. Tam, Chong, & Wong, 2002).

From many methods that were brought forward to remove pollutants, adsorption is gaining a significant attention because of its effectiveness in removing various types of pollutants and producing high quality treated water (Sze, Lee, & McKay, 2008). It is also known for its simplicity of design, ease of operation, insensitivity to toxic pollutants (Tamez Uddin, Rukanuzzaman, Maksudur Rahman Khan, & Akhtarul Islam, 2009) and its resulting in the absence of harmful substances (Ahmad & Hameed, 2010). Moreover, the most attracting element of adsorption is the veritable array of adsorbents selection with an extensive functionalization potential, which makes adsorption suitable to be used in removing pollutants. Basic cases are created through the use of chelating resins, chemically-modified activated carbon, nanotubes, biomass or functionalized silica gel as materials for adsorption.

Back in 1992, Mobil scientists proposed the synthesis, characterization and mechanism that leads to the formation of a new family of silica and alumino-silica mesoporous molecular sieves known as M41S (Beck, Vartuli, et al., 1992). They stated that MCM-41, a member

of the said family indicates a hexagonal arrangement of uniform cylindrical mesopores that may be engineered in the range of 20Å to higher than 100Å.

Following the discovery of M41S, increasing interest has been shown for the material synthesis of well-defined mesoporous structure due to their potential catalysis applications (Armengol, Corma, Fernández, García, & Primo, 1997; Morey, Davidson, & Stucky, 1998; Pater, Jacobs, & Martens, 1999; Reynhardt, Yang, Sayari, & Alper, 2004; Sayari, 1996), in separation science (Hata, Saeki, Kimura, Sugahara, & Kuroda, 1999; Mattigod, Feng, Fryxell, Liu, & Gong, 1999; Newalkar, Choudary, Kumar, Komarneni, & Bhat, 2002; Shiraishi, Nishimura, Hirai, & Komasawa, 2002) and environmental protection, including the adsorption of heavy metals from aqueous solutions (Antochshuk & Jaroniec, 2002; A. Liu, Hidajat, Kawi, & Zhao, 2000; Mercier & Pinnavaia, 1998; Pinnavaia, 1999), adsorption of carbon dioxide (Harlick & Sayari, 2006; Zelenák et al., 2008) and adsorption of organic pollutants (Sayari, Hamoudi, & Yang, 2005; Serna-Guerrero & Sayari, 2007). The increasing interest in the materials stems from their flexibility of synthetic conditions, pore sizes, particle geometry and advanced materials applications.

For the purpose of applications for the environment, mesoporous materials often undergo appropriate surface modification to provide the specific surface chemistry and bonding sites. The occurrence of high density of functional groups while retaining its open structure would lead to high performance. Hence, to achieve a high load of functional groups, mesoporous silica has been receiving increasing attention. Several researchers have

revealed surface modification with various functional groups through the use of various routes and for various purposes (Sayari & Hamoudi, 2001).

In the previous decades, supramolecular chemistry has been developed in the scientific triangular field of chemistry, physics and biology. As a concept, supramolecular chemistry was proposed by Lehn et al. (1978). It refers to the area of chemistry defined as the ‘chemistry beyond the molecule’ on the basis of organized entities of higher complexity resulting from the association between two or more chemical species bound together by intermolecular forces (Lehn, 1988).

While molecular chemistry concentrates on molecules, supramolecular chemistry handles supramolecular species known as ‘molecular receptor’ and ‘substrate’ (Figure 1.1). A receptor’s binding of a substrate produces supramolecules and this process of binding presents molecular recognition (the particular inter-action between two molecules, which complement each other in terms of geometric and electronic features like two fitting pieces of a jigsaw puzzle). The substrates may be anything from cations, anions, neutral organic molecules or even gases, whereas receptor molecules should complement the substrates in terms of their size, shape and architecture in order to create non-covalent binding interactions (Lehn, 1995). In addition, macrocyclic compounds have various branches, bridges and linkages, which in majority of cases have intramolecular cavities for various substances and therefore have become common receptors. The most extensively examined macrocyclic compounds include crown ethers, cyclodextrins and calixarenes (Atwood & Lehn, 1996).

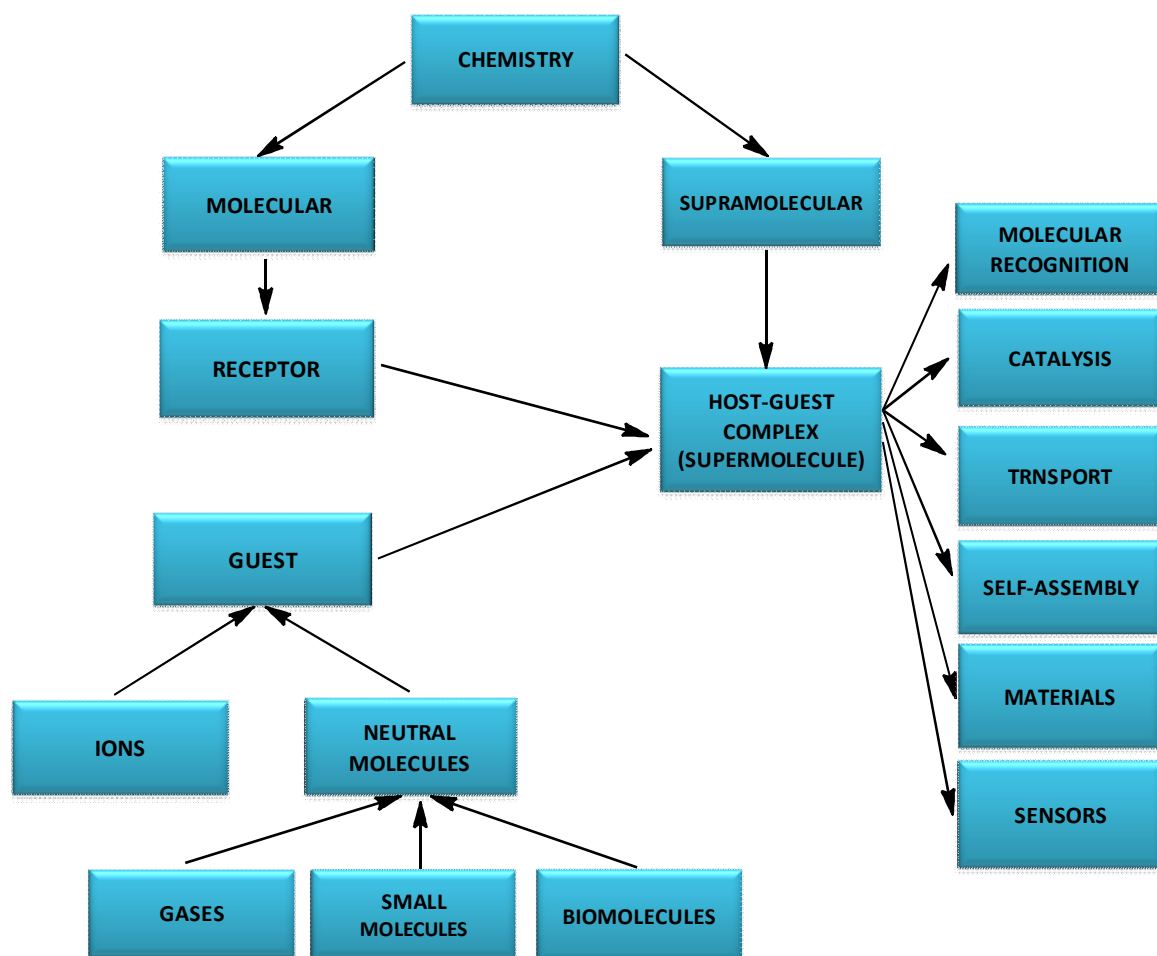


Figure 1.1 From molecular to supramolecular chemistry

Meanwhile, cyclodextrins, which consist of 6, 7 and 8 glucose units, are described as bucket-shaped oligosaccharides generated from starch. Owing to their molecular structure and shape, they have a distinct ability to be molecular containers by capturing guest molecules in their internal cavities. The produced inclusion complexes are one of the most common host-guest supramolecules categories in academic research and they provide various potential benefits to the pharmaceutical formulations (Uekama, Hirayama, & Irie, 1998).

Gutsche & Muthukrishnan (Gutsche & Muthukrishnan, 1978) were the pioneering researchers to introduce calixarenes and described them as cup-like shapes, having the ability of complexing guest molecules. Since their introduction, they have proliferated in the extensive field of molecular recognition. Previous work dedicated to functionalizing calixarenes on the upper as well as the lower rims that offer various cavities of different sizes and shapes. These calixarenes were commonly studied regarding their receptor capability for metal cations.

The combined physical properties of mesoporous materials, along with the molecular recognition ability of macrocyclic molecules, have encouraged researchers to explore new adsorbents that can be applied in various fields. For a more extensive field of applications, recognition structures have to be created in a way that they reversibly interact and are highly selective with any desired analyte. Accordingly, Figure 1.2 presents a monolayer architecture of a recognition structure that is capable of interacting with analytes in the liquid stage. Because of various interactions, several adsorption positions are possible. For instance, supramolecular inclusion of analyte or solvent (A), interaction with the linker that links recognition structure to the surface (B), or surface adsorption (C). Macrocyclic compounds like crown ethers, calixarenes and cyclodextrins are incorporated in particular substrates (polymeric resin, silica gel, supported liquid membrane, and others) and selective recognition of various analytes is achieved on the basis of interaction between host and guest (M. Chen, Ding, Wang, & Diao, 2013).

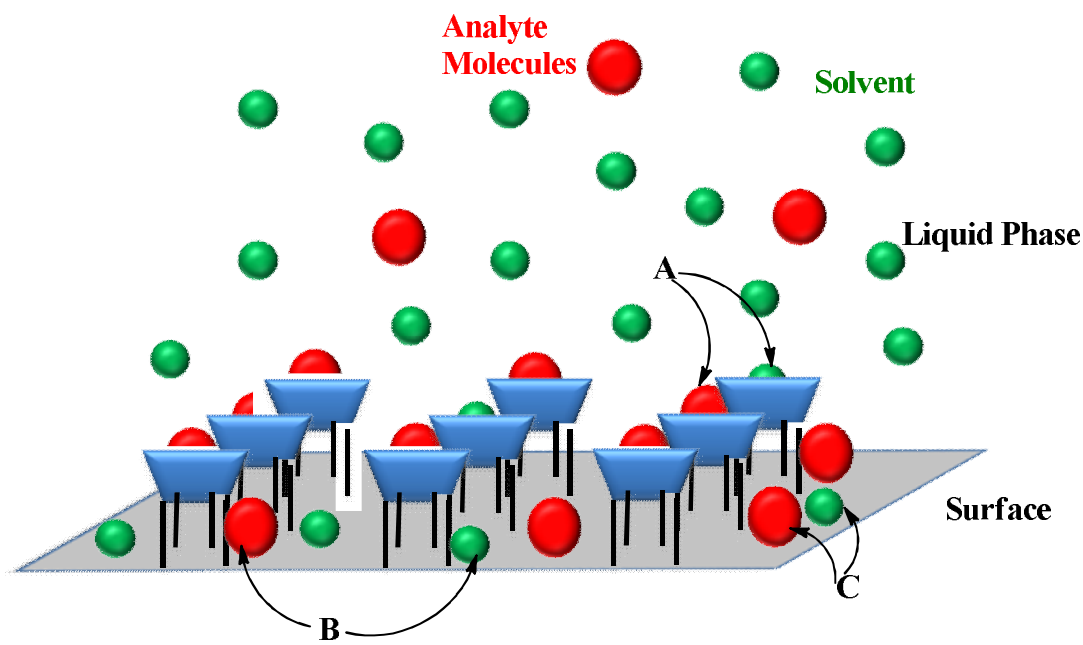


Figure 1.2 Schematic representation of a sensitive layer of receptor molecules in the vicinity of the liquid of the analyte

Summarily, further requirements for a clean environment will result in superior standards for air and water pollutants. The challenges entailed call for better sorbents that have not been made available commercial-wise. Therefore, in order to provide the solution, tailored sorbents have to be created based on fundamental principles prompting the interest for the present study to come up with an in-depth understanding of the topic and to create new advanced materials having chemical functionalities for the elimination of pollutants from the environment.

1.2 Research objectives

The purpose of this research is to modify ordered mesoporous silica with functionalized macrocyclic compound for removal of organotin compounds from aqueous solutions. This mesoporous silica has been synthesised by tailoring the surface chemistry of ordered

mesoporous silica with toluene-2,4-diisocyanate (TDI) and 3-chloropropyl triethoxysilane (CIPTS) as linkers, while calix[4]arene derivatives and β -cyclodextrin as organic hosts. Tributyltin, triphenyltin and dibutyltin were selected as the model target pollutants to evaluate the efficiency of new adsorbents. Emphasis was focused on studying the adsorption equilibrium, kinetics and thermodynamics in a single component system. The equilibrium data were fitted into two-parameter models and three-parameter models. The objectives of this research can be summarized as follows:

- (1) to functionalize ordered mesoporous silica MCM-41 with calix[4]arene, p-sulfonatocalix[4]arene and p-tert-butylcalix[4]arene;
- (2) to characterize functionalized MCM-41 with calix[4]arene derivatives;
- (3) to functionalize ordered mesoporous silica MCM-41 with β -cyclodextrin;
- (4) to characterize functionalized MCM-41 with β -cyclodextrin;
- (5) to screen the prepared materials as adsorbent for the removal of organotin compounds (tributyltin TBT, triphenyltin TPT and dibutyltin DBT);
- (6) to investigate and compare the adsorption capacity of prepared materials (MCM-TDI-C4, MCM-TDI-PC4 and MCM-TDI-C4S) for organotin compounds from aqueous solution, and different isotherm models (two- and three-parameter models) will be compared and evaluated;
- (7) to evaluate the kinetics and thermodynamics parameters of adsorption, i.e. free energy, enthalpy and entropy of adsorption.

1.3 Structure of the thesis

This thesis consists of eight chapters. In Chapter 1, the background information about this research is presented. Chapter 2 contains a literature review on the fundamentals and major findings related to the research project. The achievements from the dissertation work are mainly presented in Chapters 3 to 7, followed by conclusions in Chapter 8.

Chapter 3 and Chapter 4 deal with the synthesis and characterization of modified mesoporous silica MCM-41 with calix[4]arene derivatives and β -cyclodextrin, respectively. Study on the characterization of these new materials was carried out in details in order to observe the surface and structure evolution of the modified mesoporous silica MCM-41 materials. The adsorption of organotin compounds from aqueous solution was conducted to evaluate the performance of these new materials.

Based on the screening findings in Chapter 4, the adsorption equilibrium of tributyltin on the adsorbent synthesized was studied in Chapter 5. The effect of solution pH, adsorption temperatures and initial concentrations on the adsorption behavior was investigated to understand the adsorption mechanism. Two-parameter isotherm models, namely Freundlich, Langmuir, Temkin, and Dubinin-Radushkevitch and three-parameter isotherm models, namely Redlich–Peterson and Koble–Corrigan, were used to correlate the experimental data in order to gain a better understanding of the adsorption behavior and the surface heterogeneity of the adsorbent. The batch kinetic data were simulated using the pseudo-first order, pseudo-second order and intraparticle diffusion models. The study of the

thermodynamics for the adsorption of tributyltin on synthesized adsorbents can be used for evaluation of the free energy, enthalpy and entropy of adsorption.

Following the study of adsorption, kinetics and thermodynamics of tributyltin onto functionalized materials, study of adsorption, kinetics and thermodynamics of triphenyltin and dibutyltin were conducted in Chapter 6 and 7, respectively. Finally, the main conclusions of this research work, as well as the recommendations for future studies were presented in Chapter 8.

CHAPTER 2

LITERATURE REVIEW AND THEORY

2.1 Literature review

2.1.1 Organotin compounds and organotin compounds pollution

2.1.1.1 Organotin compounds in the aquatic environment

The pioneering synthesis of the organotin compound was conducted by Frankland (Frankland, 1852). Throughout 160 years following his initial study, a variety of organotin compounds have been synthesized through numerous procedures. Consequently, in the current times, tin has more organometallic derivatives uses compared to other metals (Maguire, 1991). Organotin is utilized in the form of $R_nS_nX_{(4-n)}$ (R = alkyl or aryl group, X = anionic group). This type of compound possess a wide variety of industrial applications, where they are used as thermal stabilizers in the PVC polymers productions and as catalysts in the polyurethane foams preparation besides their use in the vulcanization of silicone rubbers.

Moreover, they are also applied for wood preservations and as antifouling agents in marine paints, where their utilization entails slow but on-going release and accumulation of the compounds in water, sediments and aquatic organisms (Morabito, Chiavarini, & Cremisini, 1995; Strand & Jacobsen, 2005). Furthermore, their application extends to biocides, where organotin compounds (OTCs) are immediately spread in the environment and affects target

as well as non-target organisms. Due to their wide variety of uses, organotin compounds have a multitude of ways to be introduced into the environment. The sources and possible ways of OTCs seeping into the environment are provided in Table 2.1 (Becker van Slooten, Merlini, Stegmueller, Alencastro, & Tarradellas, 1994).

In hindsight, due to their toxic characteristic, the use of organotin compounds was regulated in some developed nations including England, France and the U.S. in the 1980s. However, tributyltin (TBT) is still being detected in marine environment of the same countries at a dangerous level and negatively impacts the environment. No controls of the utilization of OTCs in the developing countries have been reported. The International Maritime Organization adopted the international convention on the control of harmful antifouling systems in October 2001. The convention prohibits the use of OTCs as ingredients of antifouling systems for ships.

Table 2.1 Sources and possible pathways for the introduction of organotins to the environment

Compound	Application
Monobutyltin (MBT)	PVC stabilizer, catalyst and precursor for glass treatment
Dibutyltin (DBT)	PVC stabilizer, catalyst for polyurethane foams and silicones
Tributyltin (TBT, biocide, used mainly against fungi and molluscs)	Antifouling and water paints, wood and stone treatment, textile preservation, industrial water systems, paper and leather industry, breweries and anti-parasite
Triphenyltin (TPT, fungicide)	Agrochemical pesticide and antifouling paints

2.1.1.2 Toxicity of organotin compounds

The continuous addition of organic groups into the tin atom in any $R_nSn^{(4-n)}$ series leads to the increased biological activity to the maximum against almost all organisms when $n=3$ (i.e., for the triorganotin compounds) (Cremer, 1958; Maguire, 1991; P. Wong, Chau, Kramar, & Bengert, 1982). In this class of compounds, there is a variety of toxicity based on terms of the organic substituent's nature, with the C_4H_9 groups having the most toxicity. Moreover, tributyltin is considered to be the most toxic compound that has been introduced by human into the environment (Cooney & Wuertz, 1989). However, regardless of the various toxic impact of this compound, only little is known regarding the mechanisms that underlie the impact particularly at the molecular level.

Tributyltin compounds are considered to restrict energy production in cells by attacking and minimizing ATP levels (Chow, Kass, McCabe, & Orrenius, 1992; Marinovich, Viviani, & Galli, 1990) and in turn negatively impacts the macromolecular synthesis (Girard, Ferrua, & Pesando, 1997; Marinovich, et al., 1990). This constriction seems to be stemming from the action against the membrane-bound ATPases (A. Singh & Bragg, 1979; Tseng & Cooney, 1995) and the attack upon the mitochondria and chloroplasts (Matsuno-Yagi & Hatefi, 1993; Rugh & Miles, 1996).

According to Chicano et.al., (2001) and Tseng and Cooney (1995), organotin compounds also adversely impact the cellular membranes and inhibit ion pumps (Kodavanti, Cameron, Yallapragada, Vig, & Desaiyah, 1991), resulting in the modification of calcium homeostasis (Kass & Orrenius, 1999; Orrenius, McCabe, & Nicotera, 1992).

Organotin compounds are categorized into immunotoxins (Cooke et al., 2004; Whalen, Loganathan, & Kannan, 1999), neurotoxins (Oberdörster & McClellan-Green, 2002; Weis & Perlmutter, 1987) and hepatotoxins (Cooke, et al., 2004; Kawanishi et al., 1999). Moreover, tributyltin compounds may not be considered as inhibitors of enzymes, but they inhibit various enzymatic activity (Girard, et al., 1997; Y. M. Kim et al., 2002; Tseng & Cooney, 1995) through their interaction with thiol groups present in the proteins (Marinovich, et al., 1990; Stridh, Orrenius, & Hampton, 1999). Due to the tributyltin toxic actions occurrence at the concentrations that are one hundred times lower than those required for necrotic mode of action (Meador, 1997; Zaucke, Zöltzer, & Krug, 1998), they are considered to have high toxicity at low environmental concentrations, specifically to organisms having high uptake and low elimination rate constants.

Research concerning genotoxic and carcinogen activity of tributyltin compounds reveals inconsistent results (Hamasaki, Sato, Nagase, & Kito, 1993; Jensen, O. Andersen, & Ronne., 1991; Mirisola et al., 1997). Nevertheless, it seems literature is of the consensus that the compounds above can lead to the enhancement of the impact of DNA-damaging agents (Nirmala et al., 1999; Sasaki, Yamada, Sugiyama, & Kinae, 1993), even if they do not damage their own.

On the other hand, in *Vivo*, TBT is primarily metabolized into DBT inside the liver with the help of cytochrome P450 enzymes (Ohhira, Watanabe, & Matsui, 2003; Ueno et al., 2003). As DBT is utilized in the production of polyvinyl chloride (PVC) plastic tubes and bottles (J.-y. Liu & Jiang, 2002), this exposes humans to DBT through their direct uptake from

drinking water, which is leached from PVC water distribution pipes (Sadiki & Williams, 1999). Due to the assertions of the DBT's lower eco-toxicity to aquatic organisms compared to TBT (Gumy et al., 2008; Vighi & Calamari, 1985), DBT constantly enters into ecosystems but with little attention. However, some studies have shown that among butyltin compounds, DBT has the highest immunotoxicity to mammals (Héloïse Frouin et al., 2008; Gumy, et al., 2008), while other studies have shown that DBT is highly neurotoxic and immunotoxic (Jenkins, Ehman, & Barone Jr, 2004; Seinen et al., 1977; Whalen, et al., 1999).

DBT concentrations ranging from 11-401 nM were reported in human blood (Whalen, et al., 1999). To this end, DBT has to be viewed as potentially toxic. The toxicity of TBT and DBT stems causes thymus involution by inhibiting the proliferation of immature CD4⁻/CD8⁺ thymocytes and in high concentrations, they lead to induced thymocyte apoptosis (Gennari et al., 2000). The DBT's immunotoxic effects are quicker and more pronounced as compared to the effects of TBT, which indicates that some TBT effects stem from metabolite (DBT) (Snoeij, Penninks, & Seinen, 1988). Additionally, the DBT immunotoxic actions target(s) has still not been determined.

OTCs have also been largely viewed to disrupt endocrines by studies dedicated to aquatic organisms, among which imposex of marine gastropods is the most structured endocrinal impact of OTCs. Hence, imposex overseeing in neogastropod species has become the widespread technique to monitor OTCs effect in coastal marine environment on a global scale.

Imposex is considered as the development of vas deferens and penis in females (Gibbs, Bebianno, & Coelho, 1997), which may result in failure to reproduce and eventually minimizes the populations where imposex is present (Gibbs, Bryan, Pascoe, & Burt, 1987; Gibbs, Pascoe, & Burt, 1988). It was initially related with TBT in the earlier parts of 1980s and it has been revealed to be present in 195 gastropods species (Lima et al., 2011), including *Nucella lapillus*, *Nassarius reticulatus*, *Thais bronni* and *Thais clavigera* (Bryan, Gibbs, & Burt, 1988; Gibbs & Bryan, 1986; Horiguchi, Shiraishi, Shimizu, Yamazaki, & Morita, 1995).

Despite the occurrence of TPT in coastal areas, triphenyltin compounds causing imposex in gastropods was not known until the mid-1990 by Japanese scientists (Horiguchi, Shiraishi, Shimizu, & Morita, 1994). Currently, imposex occurrence in marine gastropods gathered from various countries' coastal areas has been related with TPT (Japan: (Horiguchi, et al., 1994); Spain: (Solé, Morcillo, & Porte, 1998); Korea:(Shim et al., 2000)). Study findings of laboratory experiments in which TPT was injected into *T. clavigera* showed TPT causing imposex (Horiguchi, Shiraishi, Shimizu, & Morita, 1997). Similarly, the same result was revealed for *Bolinus brandaris* (M. M. Santos, Armanda Reis-Henriques, Natividade Vieira, & Solé, 2006). Also, reports have been brought forward regarding TPT-induced effects on fish endocrine system through their reproduction. Fish reproduction is suppressed by spawning frequency and the number of eggs produced by female *Medaka*, *Oryzias latipes* is reduced (Z. Zhang, Hu, Zhen, Wu, & Huang, 2008), or the testicular development of male rockfish, *Sebastes marmoratus* is inhibited (Sun et al., 2011).

Besides gastropods and fish, TPT also induces malformation in amphibian embryos including the African clawed frog, *Xenopus tropicalis* (Yuan et al., 2011).

Humans are exposed to various chemicals in the environment and in their diet such as OTCs and hence, their potential toxicity to humans should be considered (Golub & Doherty, 2004). OTCs sources are multitude and commonly present in food containers made from PVC polymers (Kannan, Tanabe, & Tatsukawa, 1995), seafood sold in markets (Guérin, Sirot, Volatier, & Leblanc, 2007) and even from tap water distributed by PVC pipes (Sadiki, Williams, Carrier, & Thomas, 1996). This is specifically true for seafood and fishery products, which are the primary sources of OTCs for humans (Guérin, et al., 2007).

Additionally to oral uptake through contaminated foodstuffs, cutaneous absorption through the respiratory tract has a high potential of occurring and should be considered (Colosio et al., 1991). Two reports have been brought forward concerning the negative impact of TPT compounds to human (Colosio, et al., 1991; Manzo, Richelmi, & Sabbioni, 1981) through the accidentally exposure of farmers to TPT-based pesticides. The patients showed symptoms of TPT poisoning, such as dizziness and nausea. Moreover, TPT may also result in the central nervous system's impairment and liver damage.

Owing to the absence of quantitative toxicological data on humans, potential toxic effects on humans can be taken from other mammals tests such as rats, rabbits or pigs and thus the human intake of the chemicals are estimated. For instance, a diet containing 50 mg of TPTOH kg⁻¹ of diet did not negatively affect rats even following 276 day of the constant

dietary exposure (Kimbrough, 1976). On the other hand, on guinea pigs, the most sensitive species, growth inhibition was reported in as little as 1 mg concentration of TPT kg⁻¹ (Stoner, 1966). TPT compounds are also eliminated slowly from rats and guinea pigs (Stoner, 1966; Verschuuren, Kroes, Vink, & Van Esch, 1966).

In the context of mammals, aromatase may be a toxicological target of TPT just as it is in marine organisms. For instance, rats exposed to TPT reveal negative impact on brain and gonadal aromatase activity in a sex-dependent manner (Hobler et al., 2010). Immunotoxicity is viewed as the highly sensitive critical endpoint of mammal exposure to TPT (Boyer, 1989). On the basis of immunological reaction of experimental animals, an acceptable daily intake of TPT is set at 0.5 lg kg⁻¹ body weight d⁻¹ for humans (Lu, 1994). As TBT, DBT and TPT share common modes of immunotoxic impacts upon organisms, it is logical to derive an acceptable daily intake for the whole group compounds (Guérin, et al., 2007).

On the basis of the notion that the toxic effects of the compounds are additive, the European Food Safety Authority laid down the value of tolerable daily intake of the group of OTCs at 0.25 lg kg⁻¹ body weight d⁻¹ (EFSA, 2004).

Most surveys concerning OTCs in foodstuff revealed the daily uptake from food is lower than the acceptable daily intake or tolerable daily intake values and their risks are negligible to average consumers. These surveys are, however, not without limitations. For example, OTCs source may also be from other products like potatoes, fruits and vegetables and is not

confined to seafood (Rantakokko, Kuningas, Saastamoinen, & Vartiainen, 2006). Also, the surveys failed to estimate the dietary intakes of OTCs among children of less than average bodyweights. Moreover, the daily intake may be higher for those consuming large portions of the contaminated food.

OTCs have been reported to be present in human blood and liver. The first detection was in human blood in the late 1990s (Kannan, Senthilkumar, & Giesy, 1999) and the detection in human liver in the latter came from samples from Japanese and Polish population (Kannan & Falandysz, 1997; S. Takahashi et al., 1999). Average concentrations of butyltin compounds found in livers of Polish people (2.4–11 ng g⁻¹ wet weight) were not as high as those found in Japanese (59–96 ng g⁻¹ wet weight). TPT concentrations in human blood are higher for people consuming more seafood (Rantakokko et al., 2008). Hence, from the public health view point, it is logical to expend more effort to minimize OTCs presence in the environment. Advocates have also stressed for the OTCs and degradants monitoring in human blood and breast milk samples, particularly in a population that consumes great amounts of seafood like fishermen and people living near the coast.

2.1.2 Techniques available for organotin compounds removal

About thirty years ago, three types of organotin compounds removal methods have been proposed to remove organotin compounds from effluents; these methods are biological, chemical and physical methods. Each method has its own benefits and drawbacks.

2.1.2.1 Biological methods

Inorganic tin types have relatively low toxicity towards microorganisms, but more lipid-soluble organotin compounds are highly toxic. In a general sense, trisubstituted organotin compounds are highly toxic compared to its di- and monosubstituted forms. Nevertheless, several microorganisms show resistance against organotin compounds, a fact that is significant to the organotin compounds environmental cycle and to the biological approaches of treatment. The degradation of organotin can entail the step-by-step removal of organic moieties that results in less toxic derivatives, such as debutylation of tributyltin compounds to di- and monobutyltins. This type of degradation may occur in algae, fungi and bacteria and this offers a way for detoxification.

Additionally, microorganisms are able to accumulate tributyltin compounds, which are considered another process of removal from solution. The high lipid solubility organotin compounds guarantees cell penetration and relation with intracellular sites, although the cell wall components have an equal role to play. Among the components of the fungal wall, melanin pigments are able to achieve TBT binding and the extra melanin to grow cultures can eradicate the toxicity. In addition, melanised strains are more sensitive as compared to albino strains of the same species of organism (Gadd, 2000).

In a related study Luan et.al., (2006) examined the TBT removal and degradation through the alginate-immobilized *Chlorella vulgaris* beads, where they revealed that over 90% of TBT was expediently removed in a day. The spiked nutrient concentrations impact upon the removal capacity and degradation of TBT in the alginate immobilized *C. vulgaris* were

examined. The nutrients addition in the contaminated water encouraged the growth and physiological activity of *C. vulgaris* immobilized in alginate beads and enhanced its TBT degradation enhancement (Jin, et al., 2011).

Similarly, the TBT removal from artificial wastewater through dead and live cells of four microalgal species namely *Chlorella miniata*, *C. sorokiniana*, *Scenedesmus dimorphus* and *S. platydiscus* was examined. Dead cells were revealed to be better in eradicating TBT after three days of exposure. The degradation products, DBT and MBT, were noted primarily within the cells, and intracellular MBT concentrations were higher as compared to DBT. With regards to the removal of TBT, *Scenedesmus* cells were better in removal as compared to *Chlorella* due to the significant sizes of cell and biomass. However, the specific uptake and degradation of TBT through *Chlorella* proved to be greater as compared to *Scenedesmus*. The greatest specific TBT uptake values and the greatest degradation was revealed in *C. miniata*, a Hong Kong isolate (N. Tam, et al., 2003; N. F. Y. Tam, et al., 2002).

More recently, a study by Lee et.al., (2012) isolated a marine species of bacteria capable of degrading tributyltin contaminants. The findings showed that *Shewanella putrefaciens* bacteria degraded 88% of tributyltin in real wastewater in a duration of 36 h, indicating the efficient decomposition strength of *S. putrefaciens* of the targeted substances and the same species may be employed in a real wastewater.

2.1.2.2 Chemical methods

The treatment of organotins-containing effluent with the use of chemical methods entails a series of reactions with the attempt to break down the triorganotin molecules into simpler and less toxic substances such as monoorganotin compounds.

The electrochemical treatment of sediment is able to decompose both dibutyltin and tributyltin. Two distinct processes were described and compared, and the findings showed that a slurry electrolysis of the suspended sediment appeared to be more efficient as compared to the column leaching and electrolysis. Under oxidizing and under reduced process conditions, tributyltin was destroyed and the detoxification process appears to follow a step-by-step elimination of the butyl groups. Moreover, a partial debutylation of tri- and dibutyltin could be reached although monobutyltin was not impacted (Stichnothe, et al., 2001).

The eradication of triphenyltin chloride from water through the use of photoinduced degradation was looked into and it was revealed that the photoredox process took place in iron (III) aquacomplexes. In addition, aquacomplexes were utilized to cause the overall degradation of triphenyltin. The initial step was the formation of an adduct between hydroxyl radicals and the benzene ring. The primary process was a step-by-step dephenylation of the TPT. The formation of hydroxylated phenyltin derivatives also occurred but merely as minor photoproducts. The process was efficient for both artificial and solar light (Gabbianelli, et al., 2002).

The removal of TBT with the help of the current full-scale treatment plant to the degree complying with a 50 parts per trillion (ppt) discharge limit was carried out by Schafran et al., (2003). This was conducted through the use of ultraviolet irradiation or ozonation, where both processes were significantly enhanced by adding hydrogen peroxide to encourage the formation of hydroxyl radical.

In 2006, R. Prasad and his colleague examined the tributyltin removal through laboratory and full-scale treatment (R. Prasad & Schafran, 2006). Laboratory studies and operation of a full-scale treatment plant were utilized to investigate options of TBT removal treatment with the inclusion of physicochemical treatment processes of coagulation-clarification, filtration, and granular activated carbon adsorption. Laboratory tests with aluminum sulfate along with ferric sulfate revealed that at an average level, 90% of TBT in shipyard waters could be eliminated through coagulation-flocculation-clarification under optimum environment. A significantly lower removal was shown for the coagulation-flocculation-clarification part for the full-scale plant, while the complete full-scale treatment plant showed an average of 99.8% of TBT removal over a 3-year period.

Furthermore, in a more recent study, Yvon et.al., (2011) investigated tributyltin solubilization and degradation from spiked kaolin through various reagents. The best results were revealed under acidic conditions ($2 < \text{pH} < 5$) characterized by up to 87% TBT removal from the spiked kaolin. Acids having reducing properties were shown to be much more effective, such as ascorbic and formic acid, which reached 87% and 82% of TBT removal, respectively. In addition, final concentrations of monobutyltin and dibutyltin were

examined to pinpoint the species that predominate in the solid matrix following batch experiments. Speciation of OTCs revealed that TBT degradation happened simultaneously with solubilization in the existence of several reagents. The findings enable the selection of favorable/optimal operating conditions for the elimination of OTCs.

2.1.2.3 Physical methods

Some of the physical methods used to remove pollutants are membrane filtration, ion exchange and adsorption. The first method (membrane filtration) involves the physical separation of dissolved pollutant molecules from the effluent with the help of permeable membranes under pressure (Mui, 2009), and it includes various separation processes ranging from filtration, ultra-filtration to osmosis. The method's main drawback is the issues concerning concentrated residue disposal that is left over following the separation, the expensive cost and the probability of clogging that often occurs when concentrated pollutant layer builds up, which consequently minimizes the overall removal efficiency.

The second method (ion exchange) is used for the removal of cationic and anionic pollutant by having effluents passing through the ion exchange resin until the saturation of the available exchange sites (Robinson, McMullan, Marchant, & Nigam, 2001). The ion exchange resins comprise of organic/inorganic network structure along with functional groups. The majority of ion exchange resins utilized in the treatment of effluents are synthetic resins originating from the organic compounds polymerization into a porous three-dimensional structure. The major disadvantage of this method is the utilization of pricey organic solvents for regeneration of the ion-exchanger.

Pollutants adsorption on adsorbents is described as a phenomenon in which molecules of pollutant attach onto the adsorbent surface as influenced by different forces of adsorption. This method is popular due to its ability to remove various types of pollutants and generate a good quality of treated water (Sze, et al., 2008), for its simple design, operational ease, insensitivity to toxic pollutants and its resulting in no formation of toxic substances (Ahmad & Hameed, 2010; Tamez Uddin, et al., 2009). It is described as an economically feasible process that could be impacted by various factors including adsorbate structure, textural properties and adsorbents surface chemistry, and specific interactions between the adsorbate and the adsorbent surface (Dabrowski, 2001).

The most commonly utilized adsorbent for the pollutants removal from effluents is activated carbon due to its great degree of porosity and expended surface area (Chiu & Ng, 2012; Chowdhury, Zain, Khan, & Ashraf, 2011; Mamun et al., 2009; Marwani, Albishri, Soliman, & Jalal, 2012; Revathi, Ramalingam, Subramaniam, & Ganapathi, 2011; Treviño-Cordero et al., 2013). Nevertheless, its microporous characters greatly confine its applications as an adsorbent, especially for cases of bulky molecules or macromolecule adsorption (Zhuang, Wan, Feng, Shen, & Zhao, 2009). Furthermore, its widespread use is restricted due to high cost.

The triorganotin compounds (TOTCs) sorption from aqueous solution to mineral surfaces was studied in batch sorption experiments using homoionic clay minerals including kaolinites, montmorillonites, illites, aluminum, iron, and silicon (hydr) oxides (Weidenhaupt, Arnold, Müller, Haderlein, & Schwarzenbach, 1997). Triorganotin

compounds sorption was led by cation exchange of the TOT^+ species with clay minerals. TOTCs adsorption at homoionic clays was heightened with the decrease in selectivity coefficients of the exchangeable cations ($\text{Na}^+ > \text{K}^+ \approx \text{Rb}^+ \gg \text{Cs}^+, \text{Ba}^{2+}, \text{Ca}^{2+}, \text{Mg}^{2+}$). On the basis of surface area, the sorption of TOTCs to montmorillonite and illite was lower as compared to kaolinite, which is consistent with the densities of the surface charge of clays and the lack of intercalation of TOT^+ . Because the leading TOTCs interaction with every mineral was the sorption of TOT^+ cations to negatively charged surface sites, $\equiv\text{XO}^-$, the sorption was significantly pH dependent and sorption maximum appeared at the TOT^+ maximum overlap with $\equiv\text{XO}^-$ concentrations. Hence, high sorption of TOTCs to hydroxide or oxide minerals happens if a significant fraction of negatively charged surface sites exist at pH values where TOT^+ species predominate, i.e., minerals possessing low values of pH_{ZPC} .

Various parameters impact, including the TBT concentration and the sorbents nature were examined by a study for the sorption of tributyltin on a natural quartz sand through traditional batch experiments (Behra, et al., 2003; Bueno, Astruc, Astruc, & Behra, 1998). The main species of TBT at $\text{pH} < 6$ was the cation TOT^+ . In addition, owing to the existence of the cationic part as well as the butyl chains, it comes to reason that TBT should exhibit amphiphilic features. TBT sorption happens as homovalent 1:1 cation exchange between H^+ or Na^+ and TOT^+ for concentrations less than $40 \mu\text{M}$. TBT's increasing affinity with various materials was according to the following series; kaolinite << natural sand < treated sand < pure quartz.

TBT adsorption on soot and two charcoals having certain surface area range from 62–111 $\text{m}^2 \text{g}^{-1}$ have been examined while concentrating on the impacts of pH (Fang, et al., 2010). The charcoals were found to have an acidic function group but not those that were not soot. The adsorption of TBT reached its highest at pH 6-7 for charcoals and for soot at pH > 6. Additionally, soot has 1.5-15 times greater density of adsorption ($0.09\text{--}1.77 \mu\text{mol m}^{-2}$) as compared to charcoals but the latter exhibited up to 17 times higher sorption affinities compared to the former.

Zhang and his colleagues (2009) examined the adsorption behaviour of multiple-wall carbon nanotubes to tributyltin. They studied several factors such as pH and salinity, and concluded that multiple-wall carbon nanotubes showed strong adsorption to TBT.

Moreover, the efficiency of activated carbon-fly ash-nanometal oxide composite materials for the removal of tributyltin were studied and compared (Ayanda, et al., 2013). The findings revealed that activated carbon, nSiO_2 activated carbon-fly ash, activated carbon-fly ash- nFe_3O_4 , activated carbon-fly ash- nSiO_2 and activated carbon-fly ash- nZnO composite materials revealed a net negative charge on the surfaces. On the other hand, fly ash, nFe_3O_4 and nZnO revealed a net positive charge. The relative higher removal efficiency (>99%) of TBT was noted for the entire composite materials and compared to their precursors with the exception of activated carbon. The composite materials provide higher potentials for the TBT remediation in wastewaters.

The dibutyltin sorption behavior of four kinds of natural clay-rich sediments in comparison to the highly toxic tributyltin was examined (Burton, Phillips, & Hawker, 2004; Hoch, Alonso-Azcarate, & Lischick, 2003). The most significant DBT affinity was revealed to be the montmorillonite-rich sediment, which is known for having the highest specific surface area and cation exchange capacity of the four utilized sediments. At a salinity of 0‰ with pH 6, a maximum DBT adsorption was revealed. With a higher pH of 8, the butyltin compounds affinity of the sediment phase shifts towards the sequence TBT>DBT, which is consistent to the hydrophobicity order of the compounds. It is therefore suggested that the hydrophobic feature is the factor that drives the adsorption when butyltin compounds primarily arises as neutral hydroxides in the water phase (Hoch, et al., 2003).

The adsorption of mono- and dibutyltin (MBT and DBT) onto wheat charcoal was also examined (Fang, et al., 2012). The behavior of adsorption was showed to be dependent on pH owing to butyltin speciation and the pH-dependent charcoal surface charge. The adsorption of MBT to the charcoal showed a dip with the pH increase from 4-8. Meanwhile, for DBT, the greatest adsorption appeared at pH 6.

Many commercial adsorbents were examined for their ability to get rid of organotin compounds (TBT and DBT) from the artificial contaminated wastewater, as well as actual dockyard wastewater (Vreysen, Maes, & Wullaert, 2008). There are three kinds of adsorbents namely bentonite-based adsorbent, powdered activated carbon and granular activated carbons were utilized. The second type of adsorbent revealed a more significant organotin compounds adsorption ability as compared to the final type, which is due to its

larger surface area. The greater ability of activated carbon adsorbents to eliminate organotin compounds from wastewater shows that organotin compounds are primarily eliminated from water by hydrophobic adsorption on the activated carbon. In addition, the organically-modified bentonite adsorbent revealed the highest ability to remove organotin, which indicates the significance of the hydrophobic adsorption mechanism.

An imprinting approach based adsorbent with high retention capacity and pre-concentration factor has been examined for organotin compounds retention (TBT, DBT, MBT and TPT) (Puri, Muñoz-Olivas, & Cámara, 2004). These compounds may be retained in a quantitative manner on the adsorbent over a wide pH range and following elution, these compounds were determined by graphite furnace atomic absorption spectrometry. The process of screening has been employed to determine organotin compounds in natural sediments and samples of seawater, with the recovery between 82%-90% for TBT, DBT and TPT and 50%-55% for MBT in the samples of sediment. On the other hand, it was 97–103% recovery for the entire organotin compounds in samples of seawater. This process has been validated through the use of a standard sediment reference material.

2.1.3 Adsorption study

2.1.3.1 Background history

Adsorption is found to be more effective as compared to the various techniques proposed for the removal of pollutants because of the reasons stated above (Section 2.1.2.3). Adsorption is a process first proposed by Kayser in 1881 to explain his observations of the

gases condensation on free surfaces, a process that was independently discovered by Scheele in 1773 and Fontana in 1777 (Sykut, Saba, & Dabrowski, 1999; Tien, 1994). Currently, adsorption is described as the change in concentration of a given substance at the interface in comparison to the next phases (Sykut, et al., 1999). A summary of the history of the adsorption development and application is provided in Table 2.2 (Inglezakis & Pouloupoulos, 2006).

Table 2.2 Brief history of adsorption development and application

Year	Scientist (s) Name (s)	Significance
1773-1777	C.W. Scheele, F. Fontana	Experiments on the uptake of gases by charcoal and clays.
1776-1778	T. Lowitz	Decolorization of tartaric acid utilizing charcoal.
1793	D.D. Kehl	Application of carbons of animal origin for the removal of colors from sugar. The English sugar industry used charcoal as a decolorization agent in 1794.
1814	T. de Saussure	Systematic studies on adsorption. The author discovered the exothermic character of adsorption.
1881	H. Kayser	Introduced the term “adsorption”.
1888	Van Bemmelen, H. Freundlich	The Freundlich equation was first proposed by Van Bemmelen and popularized by Freundlich.
1901	R. Von Ostreyko	Set the basis for the commercial development of activated carbons.

1903	M.S. Tswett	Discovered selective adsorption. The author used the term and technology of “column solid-liquid adsorption chromatography”.
1904	J. Dewar	Found selective adsorption of oxygen from a mixture with nitrogen during the uptake of air by charcoal.
1915	W.A. Zelinsky	Applied the use of active carbon as an adsorption medium in a gas mask for the needs during World War I.
1918	I. Langmuir	Derived the concept of monolayer adsorption formed on energetically homogeneous solid surfaces. Was awarded the Nobel Prize in chemistry in 1932.

Table 2.2 (Continued)

1938	S. Brunauer, P.H. Emmet, E. Teller	The milestone in the development of adsorption science was the multilayer isotherm equation known as BET.
1941	A.J.P. Martin B.L.M. Synge	Introduced to laboratory practice about the solid-liquid partition chromatography, both in column and planar form.
1956	R.M. Barrer D.W. Breck	Invented the method of zeolite synthesis. The Linde Company started the production of synthetic zeolites on a commercial scale.

A species existing in the fluid phase is revealed to be adsorbed on the solid surface in cases where the species concentration in the fluid-solid boundary is greater as compared to the bulk fluid (Tien, 1994). The adsorbed species is known as adsorbate, where in one adsorption situation, there may be a single or more adsorbates. In addition, adsorbent is the solid substance upon whose surfaces adsorption takes place.

Adsorption is described as a surface phenomenon that occurs due to the interaction between adsorbate and adsorbent (Tien, 1994). Based on the interaction's strength, the adsorption processes can be categorized into two; physical and chemical adsorption (Lowell, Shields, Thomas, & Thommes, 2006; Sykut, et al., 1999). The extent of adsorption of an adsorbate on an adsorbent that takes place under a certain condition is attributable to the adsorbate-adsorbent system and depends on the way in which the adsorbate and adsorbent interact. The different adsorptive affinity of various chemical species with respect to a certain adsorbent lays down the basis of the removal or separation of the species from their mixtures through the application of this adsorbent.

2.1.3.2 Types of adsorption

There are two adsorption categories; physical adsorption (physisorption)/van der Waals adsorption, and chemical adsorption (chemisorption) where the occurrence of chemical bonds can be determined during the process. Physisorption can be applied to all adsorbate-adsorbent systems on the condition that the pressure and temperature situations are appropriate, while chemisorption may only take place if the system creates a chemical bond.

I. Physical adsorption

This type of adsorption is known as a dynamic process, where an equilibrium state is present with molecules and the adsorbate and adsorbent interaction. The compatible interaction between the adsorbent and adsorbate comes from the intermolecular

electrostatic force, London dispersion force or van der Waals force from induced dipole-dipole interactions. It may depend sometimes on the physical configuration of the adsorbent such as porosity.

Adsorbent molecules/atoms should have an expanded specific surface area in order to have the optimum capacity for adsorption. Therefore, most adsorbents utilized are known for their high porosity and adsorption takes place on the specific sites on the walls of internal particles. In addition, both size and distribution of micropores within the particles are considered as significant characteristics, which impact the adsorbent's adsorption capacity (McCabe, Smith, & Harriott, 1956; Sohn & Kim, 2005). Another property that affects the adsorption capacity is the surface polarity, as polar surfaces have the affinity with polar substances like water. Surfaces like zeolites, porous alumina, silica gel or silica-alumina are considered hydrophilic, while non-polar surfaces like carbonaceous adsorbents, polymer adsorbents and silicate are considered hydrophobic, and they are characterized as more likely to be adsorbents of non-aqueous solutions as opposed to aqueous solutions like water (McCabe, et al., 1956; Sohn & Kim, 2005).

Differences in surface area and polarity provide adsorbents with the ability to separate various compounds from the primary solution. In addition to the adsorption surface properties, mass, size, shape and polarity of different adsorbate molecules results in the irreversible adsorption of some molecules to the surface so that separation takes place (McCabe, et al., 1956).

The physical adsorption process is always exothermic with the physisorption increased with a decrease in temperature or increase in pressure. Meanwhile, adsorption occurs on a heterogeneous surface at the sites of the greatest potential of adsorption. In addition, according to Lamond & Marsh (1964), physical adsorption does not depend on the adsorbent surface chemistry.

II. Chemical Adsorption

This type of adsorption entails the creation of chemical bonds between the adsorbate and adsorbent through a chemical reaction. It is not as common compared to physical adsorption. The adsorbent regeneration for subsequent reuse is almost always challenging or impossible due to the developed chemical bonds (Cheremisinoff & Cheremisinoff, 1993).

The differences between the two adsorption types are enumerated in Table 2.3 (O'Malley, 1983). The level of adsorption on a surface is primarily a function of the temperature, pressure and nature of both adsorbent and adsorbate.

Table 2.3 Characteristics associated with physical/chemical adsorption

	Physical Adsorption	Chemical Adsorption
Heat of adsorption (kJmol ⁻¹)	2.1-20.9 (low heat of adsorption) c.f. heat of vaporization	20.9-418.4 (High heat of adsorption) c.f. bulk-phase chemical reactions
Kinetics of adsorption (at 273 K)	Fast	Slow
Temperature dependence of uptake (with Increasing T)	Decreases	Increases or decreases
Desorption	Adsorbate unchanged	May be different from original adsorptive
Specificity	Non-specific	Highly specific
Monolayer coverage	Mono- or multilayer, depending on conditions	Monolayer only

2.1.3.3 Adsorption isotherms

Adsorption isotherm is a basic concept in the field of adsorption science (Dabrowski, 2001). It is described as an equilibrium relation between the amount of adsorbed substance and its concentration or pressure in the bulk fluid phase at a controlled temperature (Dabrowski, 2001). These adsorption isotherms are commonly utilized to describe the adsorption capacity of a particular adsorbent for a particular molecule (Moreno-Castilla, 2004). The basic experimental information comprised of these isotherms are generally utilized to distinguish different types of adsorbents; in other words, the selection of one that fits most for a specific application (Moreno-Castilla, 2004).

The first experimental tool used to analyze specific adsorption phenomenon and to organize the most frequent types phenomenologically is the isotherms shape (Lyklema, 1995). On

the basis of the initial isotherm part, adsorption isotherms frequently noted in adsorption of solutes from aqueous solution have five categories; linear, S, L, H and F types (Lyklema, 1995). The shapes of these five common types of isotherms are depicted in Figure 2.1 (Moreno-Castilla, 2004).

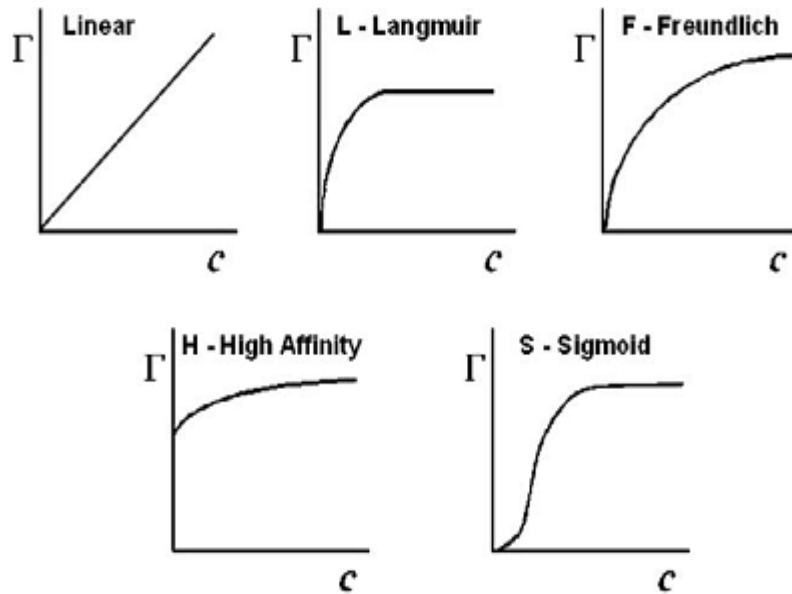


Figure 2.1 Most common adsorption isotherms for dilute aqueous solutions on carbon materials

The effectiveness of adsorption isotherm model in aqueous systems depends on various factors including the surface functional groups, temperature, solution pH and equilibrium contact time (Kumar, Kumar, Kumar, & Gupta, 2007). Two or more parameters are available to describe the experimental data of adsorption isotherm.

2.1.3.4 Adsorbent

In an adsorption process, the adsorbent is an important variable because the process success or failure depends on the way the solid performs in kinetics as well as equilibrium (Do Duong, 1998). A solid having a great capacity of adsorption but low kinetics and a solid having fast kinetics but low capacity of adsorption are both ineffective. Slow kinetics refers to the long duration of time that adsorbate molecules take to reach the interior of the particle and this result in long residence time in a column and consequently, low throughput. Similarly, due to the low capacity for adsorption, a high solid amount is required to achieve a specific throughput. Hence, an effective adsorbent is the one that shows a reasonable high surface area per unit mass (or volume), which offers good capacity of adsorption and has relatively huge pore network for the transference and diffusion of adsorbate molecule that gives good kinetics (Do Duong, 1998; Tien, 1994).

There are four types of adsorbents that dominate the commercial use of adsorption; they are activated carbon, silica gel, activated alumina and zeolites (Do Duong, 1998; R. T. Yang, 2003). Activated carbon is considered to be the most versatile adsorbent and it has been widely used for many purposes owing to its extensively high surface area and micropore volume (Do Duong, 1998; R. T. Yang, 2003). It is utilized for the removal of negative odor, color, taste and other organic materials, as well as inorganic impurities existing in the domestic and industrial wastewater, solvent recovery, air purification and pollution control, and finally various applications of gas-phase (Bansal, 2005).

Both silica gel and activated alumina are utilized primarily for desiccants, even though several modified forms are utilized for the specific process of purification (Do Duong, 1998; R. T. Yang, 2003). Meanwhile, zeolite, or specifically synthetic zeolite, is a significant type of solid utilized as widely as activated carbon. It is primarily utilized as adsorbents for their specific surface chemistries and crystalline pore structures (Do Duong, 1998; R. T. Yang, 2003).

The adsorption applications are confined as only some generic adsorbents are commercially available (R. T. Yang, 2003). A new development in adsorbent is required in order to enhance its performance and satisfy current challenges. In the last 20 years, there has been a marked development in the new nanoporous materials such as the ordered mesoporous silica (Beck, Vartuli, et al., 1992; Tanev & Pinnavaia, 1995, 1996; D. Zhao et al., 1998; D. Zhao, Huo, Feng, Chmelka, & Stucky, 1998). Nevertheless, the wide utilization of new materials as adsorbents is not extensively explored.

2.1.4 Ordered mesoporous silica

Porous material is a term utilized for all materials that are characterized as full of pores, channels, vessels, holes or cavities, which are deep and wide and allow the fluid or gases movement (Rouquerol, Rouquerol, & Sing, 1998).

This type of material has been synthesized in a successful way with pore diameters encompassing the whole nanometer size range. For the purpose of a specific working term, the International Union of Pure and Applied Chemistry (IUPAC) has categorized porous

supports into three main types according to pore diameter; microporous (<2 nm), mesoporous (2-50 nm), and macroporous (>50 nm) (McCusker, Liebau, & Engelhardt, 2001). A few examples of porous materials that fit into the aforementioned pore types are presented in Figure 2.2 (X. S. Zhao, Lu, & Millar, 1996).

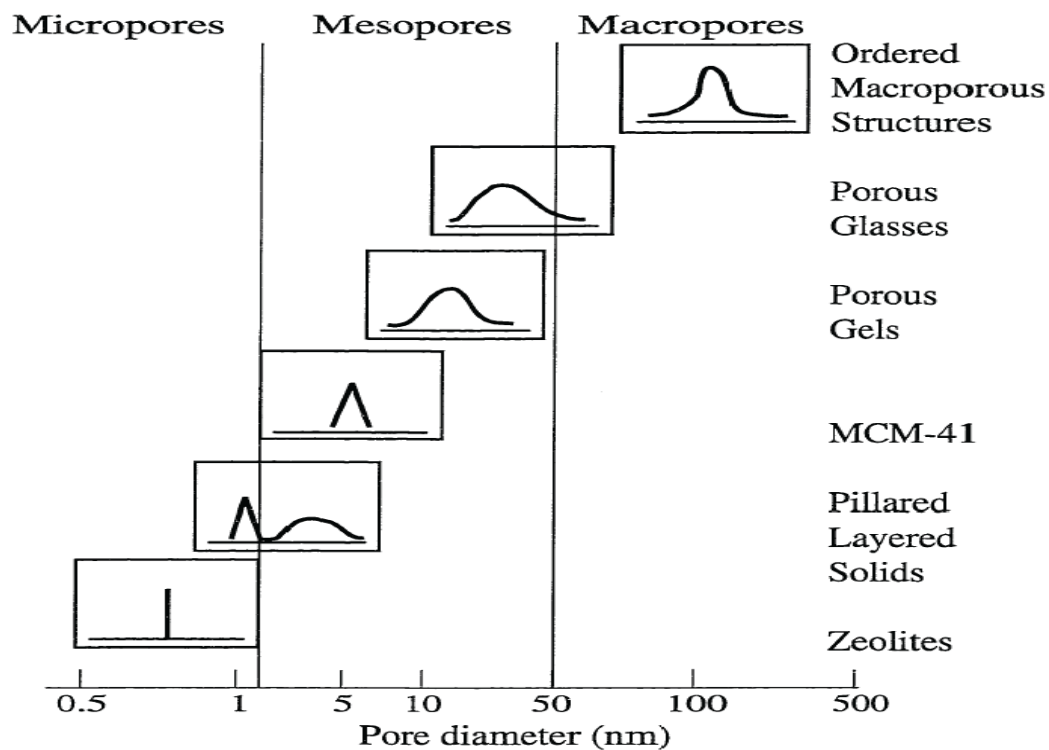


Figure 2.2 Schematic illustrating pore size distribution of some porous materials

Moreover, porous materials are categorized according to their properties of adsorption. The ‘adsorption’ terminology refers to the gas condensation on a free surface and not its entry into the bulk (absorption). This distinction is often not observed and the porous materials taking up gas is often described as adsorption or sorption, no matter what the physical mechanism involved. Gas adsorption by a porous material is described quantitatively by an adsorption isotherm, which is the amount of gas adsorbed by the material at a fixed

temperature as a function of pressure. Porous materials are often described according to pore sizes gauged through data of gas sorption, and IUPAC conventions have been brought forward to classify pore sizes and gas sorption isotherms that reflect the relationship between porosity and sorption (Rouquerol, et al., 1998).

The classification of IUPAC for adsorption isotherms is presented in Figure 2.3 (Rouquerol, et al., 1998). There are six types of isotherms that characterize adsorbents, namely microporous (type I), non-porous or macroporous (types II, III, and VI) or mesoporous (types IV and V) (Rouquerol, et al., 1998).

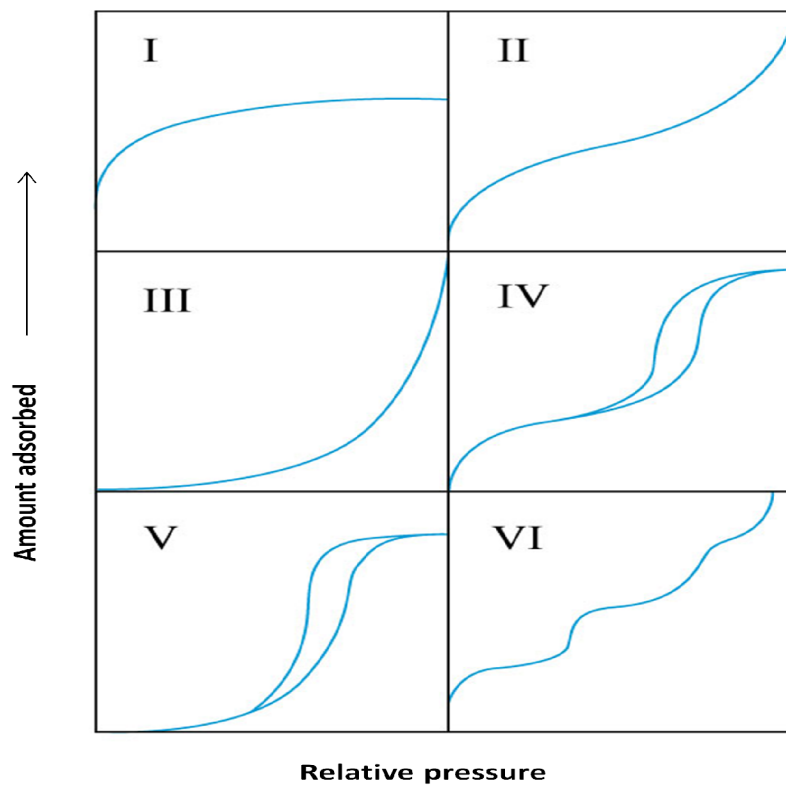


Figure 2.3 The IUPAC classification of adsorption isotherms showing both adsorption and desorption pathways. Note the hysteresis in types IV and V

The hysteresis of adsorption presented in Figure 2.4 (IV and V) are categorized and commonly acknowledged to have a correlation based on the shape of the hysteresis loop and texture (for instance pore size distribution, pore geometry, and connectivity) of a mesoporous material. The IUPAC provided the empirical classification of hysteresis loops according to the previous classification by De Boer (Broekhoff, 1979; Sing et al., 1985).

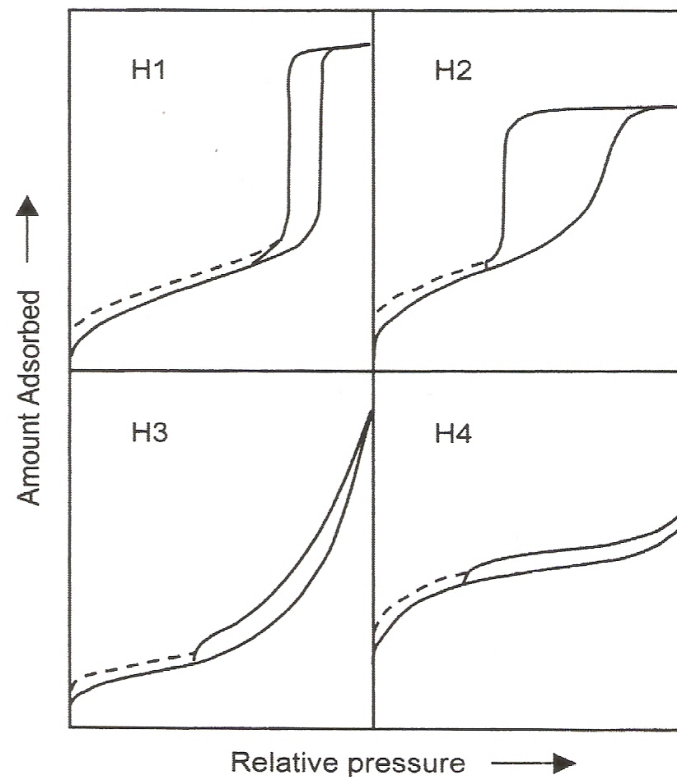


Figure 2.4 The relationship between the pore shape and the adsorption-desorption isotherm

The IUPAC classification is depicted in Figure 2.4. Type H1 is frequently related with porous materials comprising well-defined cylindrical-like pore channels or agglomerates of uniform spheres, while H2 describes materials that are frequently disordered with not well-defined pore size and shape indicating bottleneck constrictions. On the other hand, H3

hysteresis possess slit-shaped pores and isotherms showing no constricting adsorption at high P/P_0 , which is often prevalent in non-rigid aggregates of plate-like particles. The desorption curve of H3 hysteresis has a steep related with a forced hysteresis loop due to the tensile strength impact, which shows an occurrence of nitrogen at 77 K in the pressure ranging from 0.4-0.45. Type H4 hysteresis is often linked with slit pores that are narrow (Lowell, et al., 2006).

The dashed curves in the hysteresis loops presented in Figure 2.4 indicate low-pressure hysteresis which may be linked with the volume change of the adsorbent; for instance, the swelling of non-rigid pores or the irreversible uptake of molecules in pores having similar width with the adsorptive molecule (Lowell, et al., 2006).

2.1.4.1 History and synthesis of mesoporous silica type MCM-41

The ordered mesoporous silica materials or OMS were synthesized for the first time in the early years of 1990s by Mobil Corp. scientists (Beck, Vartuli, et al., 1992). Their main characteristics are high surface areas, narrow pore size distribution and uniform pore size that commonly ranges from 3-10 nm. Three mesophases were synthesized in a collective way called the M41S materials and are mesoporous according to the nomenclature of IUPAC owing to their pore diameters, which differ from $2 \text{ nm} < d < 50 \text{ nm}$ (McCusker, et al., 2001). The most commonly utilized OMS is the MCM-41 (a Mobil code for mesoporous catalytic material) having a regular hexagonal pore structure. The remaining two phases possess cubic pore shapes (MCM-48) or lamellar structures (MCM-50).

Under basic conditions, the synthetic protocol makes use of quaternary alkylammonium salts like cetyltrimethylammonium bromide in an aqueous solution. These conditions facilitate the formation of spherical micelles of ionic surfactants, which in turn form the supramolecular aggregates of micellar rods that serve as structure-directing agents or templates through the formation of a liquid crystalline phase (Sayari, 1996). In addition, the hydrolysis and condensation of silica precursors like tetraethylorthosilicate (TEOS) or tetramethylorthosilicate (TMOS) create a solid silicate mesostructure surrounding the template (Path 1 in Figure 2.5) owing to the electrostatic interactions between the silica species that are negatively charged and the head groups of the surfactant, or by the interactions of the hydrogen bonding. It is also brought forward that the process of liquid crystalline formation phase is promoted through the introduction of the silicate species (Path 2 in Figure 2.5) (Beck, Vartuli, et al., 1992).

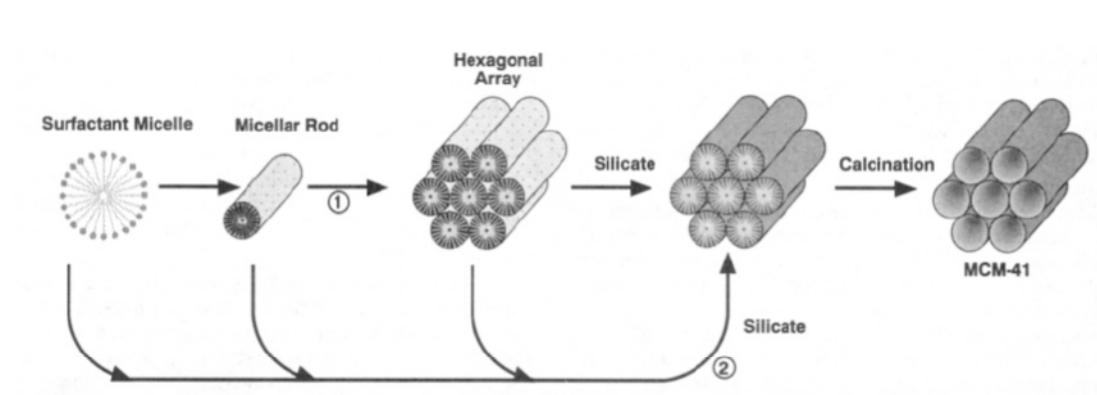


Figure 2.5 Proposed mechanism of MCM-41 formation

Following the formation of the silicate mesostructure, the template is taken off either by extraction using solvents such as ethanol or diethyl/ethanol ether mixtures, or by high temperature calcinations at 400-550°C. Changes in the experimental parameters in terms of

alkyl chain length, pH and surfactant concentration has led to mesoporous silicates having hexagonal pore structure, cubic pore shapes and lamellar structures (Figure 2.6 (Barton et al., 1999)), resulting in MCM-41, MCM-48 and MCM-50 respectively, which possessed different distributions of pore size, wall thickness of pore and surface areas (Stucky et al., 1994).

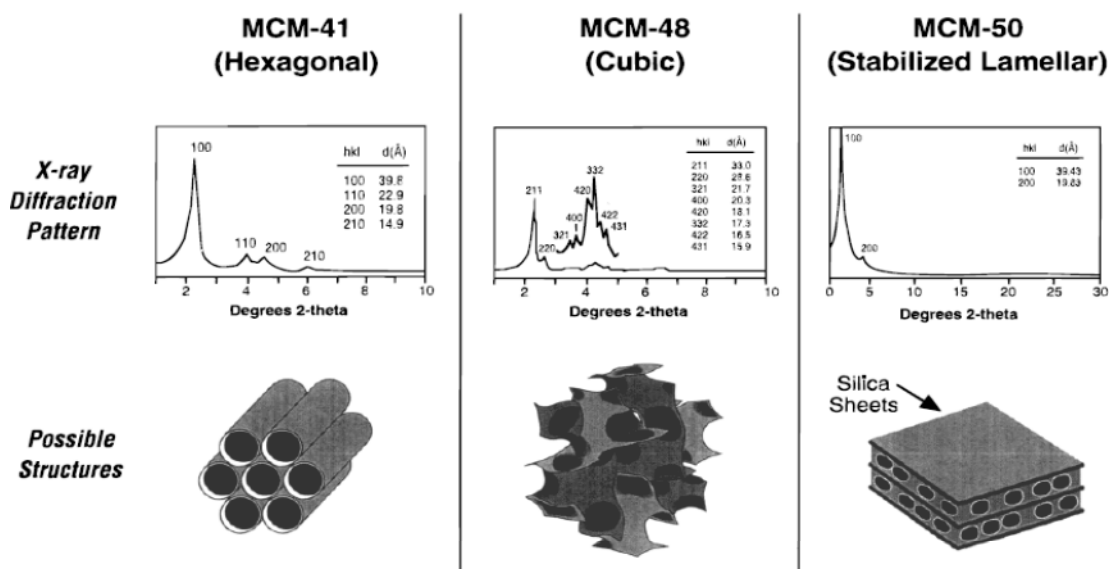


Figure 2.6 The X-ray diffraction patterns and proposed structures of MCM-41, MCM-48, and MCM-50

2.1.4.2 Surface modification of MCM-41

Several approaches have been applied in the modification of the surface of mesoporous silica materials. Functionalization of the surface with inorganic or organic groups tries to modify the surface properties accordingly for appropriate particular applications.

Inorganic modification, particularly direct doping of the silica surface with metal ions is also important but it is external to the present research scope and will not be dealt with.

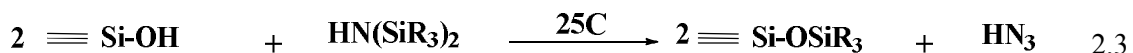
Through the introduction of organic groups in the MCM-41, accessible pores facilitate the manipulation of the chemical and physical properties of these materials while keeping the basic geometry and mechanical strength. Surface modification may be carried out chemically (covalent attachment) or physically by the adsorption of the functional group (Price, Clark, & Macquarrie, 2000).

The MCM-41 silica material framework has SiO_2 tetrahedra that is terminated in siloxane (Si-O-Si) or silanols (Si-OH) on the surface. These two groups are characterized as reactive to functionalization but their reaction to silanols is the core modification pathway (Price, et al., 2000). Covalent attachment of organic moieties on the surface is referred to as chemisorptions and can be carried out through two main methods, namely co-condensation and post-synthetic modification or grafting.

2.1.4.2.1 Grafting method

Grafting is referred to as a post-synthesis method and it is the most popular functionalization method used due to its synthetic simplicity and the flexibility of the introduction of surface groups. This is done following the removal of surfactant and the drying of mature MCM-41. The existence of silanols on the surface in high concentration is an important criterion in this method. Surface functionalization with organic groups through grafting is the most generally employed by silylation and carried out through any of the three procedures; (Eq. 2.1, 2.2 and 2.3) (Anwander, Palm, Stelzer, Groeger, & Engelhardt, 1998). In addition, esterification is another reaction that could be employed for

surface modification (Beck, Calabro, et al., 1992; Kimura, Saeki, Sugahara, & Kuroda, 1999).



As previously mentioned, high concentration of silanols is important for chemisorptions reaction. The surface silanols may be single (isolated or hydrogen bonded) or geminal (two hydroxyls on a single silicon) as depicted in Figure 2.7 (Jal, Patel, & Mishra, 2004).

Silylation is carried out on the entire surface groups of the silica, even on the free or geminal silanols. However, hydrogen-bonded silanol groups are not as accessible to the modification due to the formation of hydrophilic networks (X. Zhao & Lu, 1998).

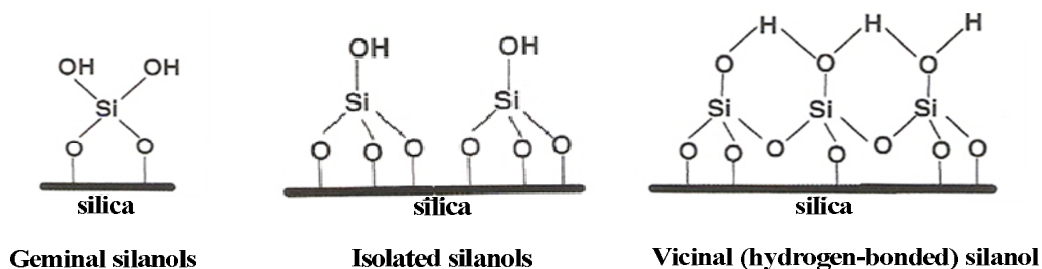


Figure 2.7 Different types of silanols on the surface

The calcinations process of the creation of ordered mesoporous silica leads to the loss of majority of the surface silanols due to high temperature exposure. According to the study by X. S. Zhao et.al., (1997), the calcination temperature during the MCM-41 materials synthesis impacts the silanols' surface density. In ideal situations, a greater concentration of silanol groups is desired because they play a role as active sites to anchor organic groups on the surface. However at lower degrees of calcinations temperature, a huge number of silanols were not available for the purpose of covalent grafting owing to the hydrogen bonding between them. On the other hand, exposure to higher temperature may result in the loss of many silanols because of the condensation reactions.

The surface may be rehydrated by boiling ordered mesoporous silica (e.g. MCM-41) in water and then by azeotropic distillation using benzene or toluene for the removal of excess water. In the direct method, on the basis of the surface area of MCM-41, a stoichiometric amount of water is added, where an approach created by Pacific Northwest National Laboratory scientists through the addition of just enough water for the formation of monolayer on the pore surface resulting in a more uniform coat of organosilane (Stein, Melde, & Schrodin, 2000) in a process known as 'self-assembled monolayer on mesoporous supports'. This is followed by the hydrolyzation of organosilanes to form trihydroxysilanes, which carries out self-assembly leading to dense silica coverage on the surface (X. Feng et al., 1997).

Excess water should not be added as it may lead to the formation of non-surface bound silanol clumps of the organosilane reagent, which may lead to pore blockage owing to the

polymerization of silane. The difference in coverage between hydrated and non-hydrated surfaces is depicted in Figure 2.8. (Fryxell, 2006).

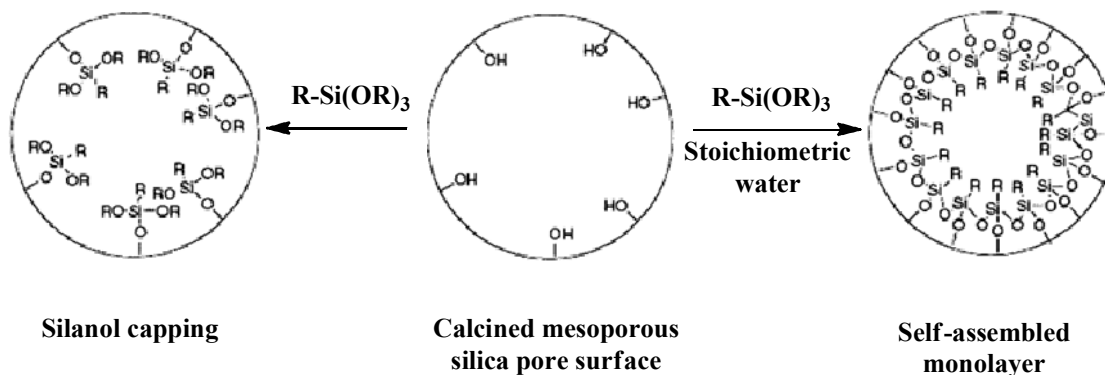


Figure 2.8 Difference in the coverage between hydrated and non-hydrated surfaces

2.1.4.2.2 Co-condensation method

The co-condensation method was pioneered by Mann et al. (Burkett, Sims, & Mann, 1996). It is a one-pot synthetic method analogous to MCM-41 synthesis, where incorporation of trialkoxyorganosilane species is carried out into TEOS (or TMOS) solution to undergo hydrolysis and condensation with structure directing agents or templates. This process results in mesostructures with organic functionalities that are attached covalently on the pore walls.

In comparison to the grafting method in which the functional groups distribution is frequently inhomogeneous, the co-condensation provides homogeneously distributed organic groups on all the surfaces of the inner pore. The organosilane may be buried into the silica matrix walls and becomes inaccessible. However, every functionalized

organosilane group is a defect of the silica matrix and therefore, negatively impacts the silica structure's stability. This confines the concentration of surface silane groups due to the fact that the greater the silane concentration, the more unstable will be the silica structure.

There are some evident disadvantages of this method. One of the main issues is the resulting templating agent removal. Calcination is considered to completely remove the structure directing agent but such high temperatures will damage the covalently attached organic functionality. This means the only recourse is the solvent extraction. The co-condensation is also superior to the post-synthesis grafting because of its easy control of the particle morphology of final mesoporous silicate (Ozin, 2000; H. Yang, Coombs, & Ozin, 1997).

The methodologies to characterize the modified MCM-41 are structural analyses like gas sorption studies, powder X-ray diffraction and transmission electron microscopy. In addition, compositional studies comprising of solid-state NMR, Fourier transform infrared, and X-ray photoelectron spectroscopic methods along with elemental and thermogravimetric analyses. The MCM-41's various surface modifications (organic modification) in the recent years for the adsorption application are presented in Table 2.4.

Table 2.4 Surface modification of MCM-41 in the recent years (2000–2013) for the adsorption application

Modified group	Adsorbate	Reference
Amino group (NH ₂ -)	Ni(II), Cd(II), Pb(II), Cr(VI), CO ₂ , remazol red dye, heparin, chlorophenols and plasmid DNA	(Anbia & Lashgari, 2009; Heidari, Younesi, & Mehraban, 2009; M. L. Kim, Stripeikis, & Tudino, 2009; Klinthong, Chao, & Tan, 2013; Marília, Delphine, Gleiciani, Philip, & Célia, 2011; D. O. Santos et al., 2013; Wan et al., 2012; H. Yang et al., 2012)
Ionic liquid	CO ₂	(G. H. Fu, Lv, & Ma, 2013)
2-mercaptobenzothiazole	Lead	(Pu, Ren, Tan, & Jiang, 2012)
Glycopyranose	Borate	(Fried, Schlossbauer, & Bein, 2012)
Iminodiacetamide	Ce(III), Nd(III), Eu(III), Gd(III), and Lu(III)	(Fryxell, Chouyyok, & Rutledge, 2011)
Polyacrylonitrile-derived carbon	Methyl–ethyl ketone	(R. Janus et al., 2011)
Lanthanum (III)-coordinated diamino modified MCM-41	Phosphate	(J. Zhang, Shen, Shan, Mei, & Wang, 2011)

Table 2.4 (Continued)

Trimethylchlorosilane and methyltrimethoxysilane	Phenol and hydroquinone	(J. Fu, He, Wang, Liu, & Hu, 2011)
--	-------------------------	------------------------------------

5-nitro-2-furaldehyde (fural)	Uranium(VI) and thorium(IV)	(Yousefi, Ahmadi, Shemirani, Jamali, & Salavati-Niasari, 2009)
5-mercapto-1-methyltetrazole	Zn(II)	(Pérez-Quintanilla, Sánchez, del Hierro, Fajardo, & Sierra, 2007)
3-phenyl-4-benzoyl-isoxazol-5-one	Cu(II)	(Miloudi et al., 2007)
Thiophene-2-carbaldehyde	Palladium(II)	(Jamali, Assadi, Shemirani, & Salavati-Niasari, 2007)
Salicylaldehyde	Uranium	(Jamali et al., 2006)
<i>N</i> -methylglucamine	Boron	(Kaftan et al., 2005)

2.1.4.3 Applications of mesoporous silica

Mesoporous silicates provide various favorable properties with possibilities for use in a range of applications. The main applications that will be explained are catalysis, chemo and biosensing, and chemical separations.

I. Catalysis

Mesoporous silica offers a one-of-a-kind platform for catalytic processes with various benefits compared to traditional homogenous catalysis. Pore size distributions and arrangements characterized as highly tunable (e.g. hexagonal, lamellar, cubic, spherical and others) enable size and shape selective catalysis. In addition, high surface areas and site isolation techniques enable the covalent attachment of huge amounts of non-interacting

catalytic sites. Also, homogenous materials like organometallic compounds are too pricey to synthesize and they require time and/or unique recovery approaches.

Catalytic reagents like acids/basic in acid or base catalyzed reactions may confine the selection of solvent systems and call for an extensive work-up procedure. However, silica mesostructure may be altered (i.e. hydrophilicity/-phobicity, size and shape) for stability unlike homogenous catalysts, in a varying range of reaction media, temperatures and pressures, and they may be conveniently separated from the reaction mixture through vacuum or gravity filtration and recycled for recurring use with little or no catalytic activity loss. Currently, there has been a variety of organic, inorganic and organometallic catalysts immobilized on highly ordered mesoporous silica. For instance, 3-aminopropyl functionalized mesoporous silicates have been revealed to be an efficient heterogeneous base catalyst for nitroaldol and Michael addition (D. J. Macquarrie, Maggi, Mazzacani, Sartori, & Sartorio, 2003; Sharma & Asefa, 2007).

II. Mesoporous chemosensors

Among the many major applications of mesoporous silica, one of them is their potential as platforms for chemosensing applications. The detection of metal ion through fluorescence and ultraviolet-visible spectroscopic measures has been extensively examined to create functionalized mesoporous silicates having high metal ion specificities (Gao et al., 2006).

Additionally, mesoporous silica has also been shown as an invaluable scaffold for volatile organic compound and applications of explosive chemosensing (Sasahara, Kido, Ishihara,

Sunayama, & Egashira, 2005). Moreover, various studies have made use of mesoporous silica as a scaffold in gas sensing applications in addition to fabricating sensors for metal ions and volatile organic compounds (Yuliarto, Honma, Katsumura, & Zhou, 2006).

III. Mesoporous biosensors

Intensive studies making use of mesoporous silica as a scaffold for many biological sensing methods are already existed. Huge surface areas and pore diameters enable the incorporation of biomolecules toward the fabrication of bioelectrochemical sensors (Chouyyok, Panpranot, Thanachayanant, & Prichanont, 2009; X. Xu, Lu, Zhou, Zhao, & Guo, 2009). Imaging biological processes are allowed through the surface functionalization with target specific compounds and the high biocompatibility of mesoporous silica. Currently, there are various studies concerning the immobilization of biological species.

IV. Chemical separations

Mesoporous silicates are widely examined for chemical separations and absorbents because of their large surface areas, easily tunable pore size distributions, mechanical and thermal stabilities and their resistance to decomposition in a wide pH range. Moreover, their ability to change the hydrophilicity/-phobicity through the addition of non-polar organic groups (alkyl, vinyl, or phenyl substituents), or the incorporation of reactive functional groups, for instance amines, thiols, or specialized chelating agents, enable the specific reactivity for size, shape and functionality. These properties are leveraged in the separation or the adsorption of heavy metals, organic compounds possessing high target material specificities

and efficiencies; for example, N- (2-aminoethyl) dithiocarbamate functionalized MCM-41 has been developed by Stathi et al., (2010). These materials are effective heavy metal adsorbents due to the existence of an effective dithiocarbamate group and the low pH value (3.2) of the point of zero charge.

As previously mentioned, functionalized mesoporous silicates are revealed to be as effective as chromatographic packings when used in organic compounds separation. Yasmin and Muller (2010) showed that several n-butyl and n-octyl functionalized MCM-41 spheres were examined for their separation of five organic components; uracil, toluene, ethylbenzene, quinizarin and amitriptyline.

In addition, the separation of chiral compound has also been performed successfully. Zhu et al., (2008) separated enantiomeric mixtures of R/S-1,10-bi-2-naphthol with the help of mesoporous organic-inorganic spheres possessing covalently bridged trans-(1R, 2R)-bis-(ureido)-cyclohexane synthesized by co-condensation of N,N'-bis [triethoxysilyl]propyl-trans-(1R,2R)-bis-(ureido)-cyclohexane and 1,2-bis (trimethoxysilyl) ethane.

2.1.5 Macrocyclic compounds

2.1.5.1 Calix[4]arene

The pioneering study dedicated to phenol-formaldehyde chemistry was attributed to Adolf Von Baeyer in 1872 (Takemura, 2002). However, the reaction products were not isolated and remained in its original form, and it was not characterized accurately due to the

limitations of available analytical methods. Following this pioneering study were the steps taken by Lederer (1894) and O. Manasse (1894) to introduce the method of hydroxymethyl phenol preparation under mild and well-controlled basic conditions in 1894. Baekeland (1908) then prepared phenol-formaldehyde resins in 1902 under its commercial name “Bakelite” under controlled basic condensation of phenol and formaldehyde, resulting in cross-linked polymers.

However, in 1944, the story took an unexpected turn when Alois Zinke and Eric Zeigler (1944) produced a crystalline compound as opposed to resin with controlled cross-linking using p-substituted phenols. In addition, Joseph Niederl and Heinz Vogel (1940) managed to synthesize a cyclic-tetrameric compound from acetaldehyde and resorcinol. Then, Cornforth and his colleagues repeated Zinke reactions and unearthed the potential of calixarenes as basket analogues of enzymes. X-ray crystallography concluded that Zinke reaction produced only cyclic tetramers (Cornforth, Hart, Nicholls, Rees, & Stock, 1955; Cornforth, Morgan, Potts, & Rees, 1973).

The term ‘calixarene’ was proposed by David Gutsche in 1975 and it stems from the Greek word, ‘calix’ which means ‘vase’ or ‘chalice’ and ‘arene’, indicating the existence of aryl rings, as shown in Figure 2.9. Calixarenes are defined as a class of cyclooligomers having distinct upper and lower rims and central annulus (Gutsche, 1991; Stewart & Gutsche, 1999).

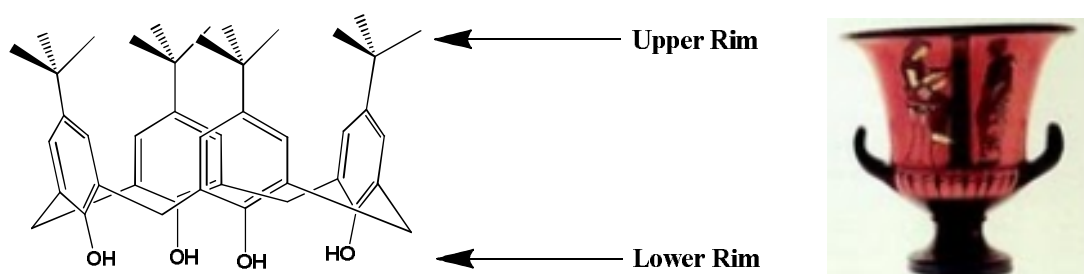
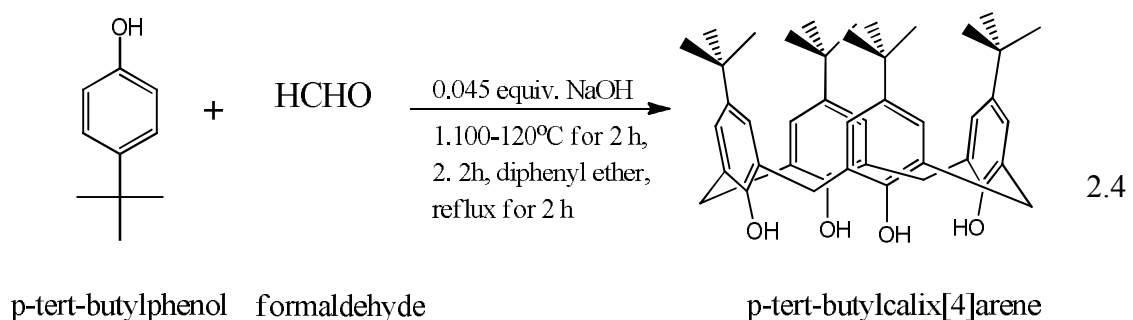


Figure 2.9 Calix[4]arenes

Calixarenes are categorized according to their number of aryl units as major, minor and large calixarenes (Gutsche, Rogers, Stewart, & See, 1990) (the major one has aryl units = 4, 6, 8; the minor one has aryl units = 5, 7, and the large one has aryl units = 9-20).

Currently, calixarenes are also known as the third generation supramolecules after cyclodextrins and crown ethers (Gutsche, 2008). The features of p-substituted calix[n]arenes are high melting points, potential for many functionalization at both the upper and lower rims and the methylene bridge (Gutsche, Iqbal, & Stewart, 1986), and frequently very low solubility in general organic solvents. Enough solubility of calixarenes in CHCl_3 , CS_2 and pyridine enables their use in NMR solvents for the characterization of calixarenes. David Gutsche was the pioneering researcher who first optimized the synthetic procedure of p-tert-butylcalix[4]arene (Eq. 2.4) by condensing p-tert-butyl phenol and 37% of formaldehyde (initially heated at the temperature of 100-120°C and afterwards refluxed in diphenyl ether) (Gutsche, Dhawan, No, & Muthukrishnan, 1981).



Calixarenes chemistry is a curious combination of academic and industrial research. The varying calixarenes applications are attributed to their cup-like shape, selective complexation with several metal ions and neutral molecules, stability, solubility and their large scale availability (Izatt, Christensen, & Hawkins, 1984).

Calixarenes have been commonly utilized for the purpose of separation. Separation of Cs^+ and K^+ from alkali metal ions mixture was carried out by incorporating a calix[4]arene-crown compound upon silica gel for the purpose of column chromatography (Arena et al., 1996).

Other calixarenes applications are the selective removal of actinium-125 (X. Chen, Ji, M. Wai, & R. Fisher, 1998) by p-tert-butylcalix[4, 6]arenes with OCH_3COOH -groups upon endo-rim, the extraction of Ra^{2+} by tert-butylthiacalix[4]arene-derived hosts (van Leeuwen et al., 2005), and the Hg(II) (over Cd(II), and Pb(II)) separation through the selection of strong complexation with (mercapto)thiacalix[4]arenes (Rao et al., 2000).

They have also been utilized in several chemical sensor devices including ion and molecule-selective electrodes for ions and molecules (Gale, Chen, Drew, Heath, & Beer, 1998; Gupta, Ludwig, & Agarwal, 2005), fluorescent sensors (H. Liu, Xu, Li, Yin, & Xu, 2001; Narita, Higuchi, Hamada, & Kumagai, 1998), and non-linear optical sensors (Regayeg et al., 2002). The applications of modified calix[4]arene as adsorbent in the recent years are presented in Table 2.5.

Table 2.5 Applications of modified calix[4]arene as adsorbent in the recent years (2000 –2013)

Modified calix[4]arene	Adsorbate	Reference
Thiacalixarenes-based silica nanoparticles	Oligonucleotides and proteins	(Yuskova, Ignacio-De Leon, Khabibullin, Stoikov, & Zharov, 2013)
p-sulfonated calix[4,6]arene derivatives immobilized onto magnetic nanoparticles	Aromatic amines	(Aksoy, Erdemir, Yildiz, & Yilmaz, 2012)
para-sulphonato-thiacalix[4]arene	Cadmium (Cd)	(Y. Li, Hu, Song, & Sun, 2012)
p-tert-butylcalix[4]-aza-crown immobilized sporopollenin	Cu(II), Pb(II) and Zn(II)	(Gubbuk, Gürfidan, Erdemir, & Yilmaz, 2012)
Calix[4]arene appended resins	As(III) and As(V)	(Qureshi et al., 2011)

Table 2.5 (Continued)

Calixarene-based magnetic nanoparticles	Cr(VI), As(V) and U(VI)	(Sayin & Yilmaz, 2011a, 2011b)
Polyvinylcalix[4]arene tetraacetic acid resin	Lead	(Adhikari, Kanemitsu, Kawakita, Jumina, & Ohto, 2011)

p-tert-butylcalix[4]arene 3-diethylaminopropyl diamide	Cr(VI)	(Alpaydin, Saf, Bozkurt, & Sirit, 2011)
Functioned calix [4] arene and calix [4] resorcarene derivative	Mercury	(Danil De Namor et al., 2011)
Diamine substituted 1,3-distal calix[4]arene-based magnetite nanoparticles	Uranyl ions	(Sayin, Yilmaz, & Tavasli, 2011)
p-tetraaminocalix[4]arene- and p-tetrathioureacalix[4]arene-based resins	Fluoride	(Solangi, Bhatti, Kamboh, Memon, & Bhanger, 2011)
Diamide derivatives of p-tert-butylcalix[4]arene immobilized onto [3-(2,3-epoxypropoxy)-propyl]-trimethoxysilane-modified Fe ₃ O ₄ magnetite nanoparticles	Arsenate and dichromate anions	(Sayin, Ozcan, & Yilmaz, 2011)
p-tert-butyl-calix[4]arene-based silica resin	Reactive black-5 and reactive red-45 azo dyes	(M. A. Kamboh, B. Solangi, S. T. H. Sherazi, & S. Memon, 2011a; M. A. Kamboh, I. B. Solangi, S. T. H. Sherazi, & S. Memon, 2011b)
Calix[4]arene-based silica	Endosulfan	(Memon, Memon, & Latif, 2011)
Starch grafted p-tert-butyl-calix[n]arene	Butyl Rhodamine B solution	(M. Chen, Shang, Fang, & Diao, 2011)

Table 2.5 (Continued)

Calix[4] arene containing PBT- poly(dimethylsiloxane) copolyester	Benzene	(G. Xu, Zhu, Gou, Zhu, & Shen, 2010)
Calix[4]arene amide ionophores	Chromate and phosphate anion	(Ertul, Bayrakci, & Yilmaz, 2010)

N-methylglucamine derivative of calix[4]arene immobilized onto poly[(phenyl glycidyl ether)-co-formaldehyde]	Oxonians (dichromate/arsenate)	(Sayin, Ozcan, Memon, & Yilmaz, 2010)
N-methylglucamine derivative of calix[4]arene immobilized onto magnetic nanoparticles	Chromate and arsenate	(Sayin, Ozcan, & Yilmaz, 2010)
Calix[4]arene modified Amberlite XAD-4 resin	Reactive Black-5, Reactive Red-45 and Congo Red	(Kamboh, Solangi, Sherazi, & Memon, 2009)
Tetraester calix[4]arene (TC4)-based resin	Pb (II)	(Solangi, Memon, & Bhanger, 2009)
Amino calix[4]arene derivative	Chromium anions	(Tabakci, Erdemir, & Yilmaz, 2007)
Cellulose-grafted with calix[4]arene polymers	Heavy metals (Co(II), Ni(II), Cu(II), Cd(II), Hg(II) and Pb(II)) and dichromate anions	(Tabakci, et al., 2007)
Calixarene-filled poly(dimethylsiloxane) composite membranes	Benzene	(Wu, Liu, Pan, Hu, & Jiang, 2006)
Calix[4]arene-based polysiloxane resin	Heavy metals and dichromate anion	(Tabakci, Ersoz, & Yilmaz, 2006)
Butylcalix[4]arene to cross-linked poly(dimethylsiloxane)	Benzene	(Ohshima, Miyata, & Uragami, 2005)

Table 2.5 (Continued)

Butylcalix[4]arene to cross-linked poly(dimethylsiloxane)	Volatile organic compounds	(Uragami, Ohshima, & Miyata, 2005)
p-tert-butyl-calix[4]arenes	Aluminum	(Gartner, Berends, & Witkamp, 1999; Gärtner, Berends, & Witkamp, 2002)

Anion-exchange resin with thiacalix[4]arenetetrasulfonate	Co(II), Ni(II), Cu(II), Zn(II), Cd(II), Hg(II), and Pb(II)	(Gärtner, et al., 2002)
Calixarene amide ionophores	Strontium ion	(Casnati et al., 2001)

2.1.5.2 β -cyclodextrin

Cyclodextrins have been in the limelight of research in the past five decades. The most commonly isolated compounds are α -, β -, γ - and δ - cyclodextrins (comprising respectively of 6, 7, 8, and 9 glucopyranose units). Cyclodextrins have led to the stimulation of innumerable investigations. They have unique chemical structure of three various hydroxyl groups in each 1, 4-linked glucopyranose structural unit and a spatial arrangement in a hollow truncated cone-shaped molecule, allowing the formation of inclusion complexes.

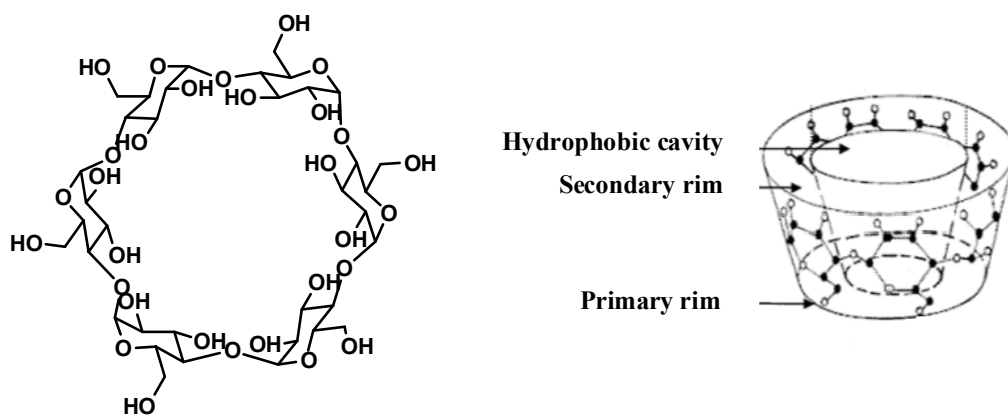


Figure 2.10 Structural representation of β -cyclodextrin

They have cylindrical shapes along with an axial cavity as presented in Figure 2.10. A part of the cavity is hydrophilic due to the existence of hydroxyl groups at the smaller cavity lip, as well as the larger cavity lip (Bender & Komiyama, 1978). The primary hydroxyl group

can freely rotate and interact with each other through hydrogen bonds that are not present among secondary hydroxyl groups. The latter is rigidly bonded. The internal part of the cavity is formed by C-H groups and glycosidic oxygen bridges and because of this, it is characterized as hydrophobic. The internal cavity also presents a Lewis base character stemming from the glycosidic oxygen. Some of the cyclodextrin properties are listed in Table 2.6 (Osa & Suzuki, 1996).

Table 2.6 Physical properties of cyclodextrin

	α - cyclodextrin	β -cyclodextrin	γ -cyclodextrin
Molecular weight	972	1134	1296
Inner cavity diameter (pm)	500	620	800
Outer diameter (pm)	1460	1540	1750
Volume cavity (10^6 pm ³)	174	262	427
Surface tension	71	71	71
Number of water molecule in cavity	6	11	17
Crystal water content	10.2	13-15	8-18

Currently, the preparation of cyclodextrins is carried out through the action of bacterial (Cyclodextrin glycosyl transferase) upon linear gelatinized starch. Because the enzymes do not present length specificity, the cyclodextrins comprise of 6-12 glucose units in each ring. There have been notable developments in the examination of novel enzymes for the cyclodextrin production (Seltzer, 1987).

The derivatives of cyclodextrin possess much greater scope and a more common range of applications (Croft & Bartsch, 1983). The relative functionalities in all α -, β -, and γ -cyclodextrins are the primary (position 6) hydroxyls and secondary (position 2 and 3) hydroxyls. The cyclodextrin derivatives are then allowed to react at either these three positions or selectively at one of them. Some derivatives that were prepared are acylated

cyclodextrins (Czarniecki & Breslow, 1978; Ogawa & Matsui, 1977), alkylated cyclodextrins (Casu, Reggiani, & Sanderson, 1979), amino and azido derivatives of cyclodextrins (Fujita, Yamamura, Egashira, & Imoto, 1992; Petter, Salek, Sikorski, Kumaravel, & Lin, 1990), halogen derivatives (Debouzy, Crouzier, & Gabelle, 2007), and derivatives with alcohols, aldehydes, and ketones (Furue, Harada, & Nozakura, 1975; Tabushi, Kuroda, Yokota, & Yuan, 1981). If cyclodextrins are related to polyethers, they produce soluble polymers (Akira, 1996, 1997).

The ability of the cyclodextrins to form inclusion complexes with various molecules is their most unique property (Figure 2.11). The guest compounds are situated in the cyclodextrins' cavity and this involves non-covalent bonding in the process known as complexation. Various molecular interactions are responsible for the cyclodextrin inclusion complexes formation in an aqueous solution such as hydrophobic interaction, hydrogen bonding and the relief of high energy water from the cyclodextrin cavity on substrate inclusion.

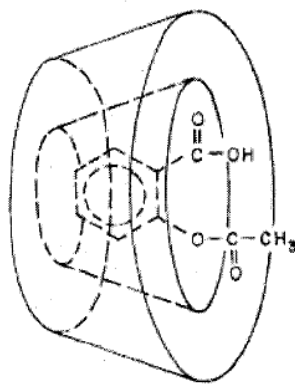


Figure 2.11 Proposed schematic of the inclusion compound

Some of the practical applications of cyclodextrin are cosmetics, personal care (N. Prasad, Strauss, & Reichart, 1999; Tatsuya, 1999; Trinh et al., 1999), food preservation (Hedges, 1998; Muñoz-Botella, Del Castillo, & Martín, 1995), catalysis (Badi et al., 2010; Cabou, Bricout, Hapiot, & Monflier, 2004; Tilloy, Bertoux, Mortreux, & Monflier, 1999), pharmaceuticals (Brewster & Loftsson, 2007; Hermens, Deurloo, Romeyn, Verhoef, & Merkus, 1990; Kristmundsdóttir, Loftsson, & Holbrook, 1996; Uekama et al., 1992), agriculture (Hedges, 1998; Szejtli, 1998) and chromatography (Cucinotta, Contino, Giuffrida, Maccarrone, & Messina, 2010; Rodríguez-Bonilla, López-Nicolás, Méndez-Cazorla, & García-Carmona, 2011; Schurig, 2010) The applications of modified β -cyclodextrin as adsorbent in the recent years are presented in Table 2.7.

Table 2.7 Applications of modified β -cyclodextrin as adsorbent in the recent years (2000–2013)

Modified β -cyclodextrin	Adsorbate	Reference
SiO ₂ - β -cyclodextrin	Azo dye-Congo red	(M. Chen, et al., 2013)
β -cyclodextrin-carboxymethylcellulose-based hydrogels	Bisphenol A	(Kono, Onishi, & Nakamura, 2013)
β -cyclodextrin modified graphene oxide	Co(II)	(Song, Hu, Zhao, Shao, & Li, 2013)
β -cyclodextrin grafting wood flour copolymer	Methylene blue	(Si, Wang, & Xu, 2013)
β -cyclodextrin-chitosan	Azo dyes, phenol, m-cresol, m-catechol, bisphenol and puerarin	(Q. Y. Chen et al., 2006; Karim, Adnan, & Husain, 2012; Q. Lin, Huo, Su, & Wang, 2013; Nishiki, Tojima, Nishi, & Sakairi, 2000)

Polysulfone- β -cyclodextrin	Endocrine	(Choi, Chung, Priestley, & Kwak, 2012)
Glycine- β -cyclodextrin	Atrazine	(Wang, Xu, Wang, & Huang, 2012)
Cross-linking β -cyclodextrin	Cholesterol	(Dias, Berbicz, Pedrochi, Baesso, & Matioli, 2010; Han, Kim, Ahn, & Kwak, 2005; S. H. Kim, Ahn, & Kwak, 2004; S. H. Kim, Kim, & Kwak, 2007; Kwak, Kim, Kim, Choi, & Kang, 2004; J. E. Lee, Seo, Chang, & Kwak, 2010; Y. K. Lee, Ganesan, & Kwak, 2012)
Magnetic β -cyclodextrin-chitosan nanoparticles	Methyl blue	(Fan et al., 2012)

Table 2.7 (Continued)

β -cyclodextrin modified zeolites	Nitrophenols	(X. Li, Zhao, Zhu, & Hao, 2011; X. Li, Zhu, & Hao, 2009)
β -cyclodextrin and phospholipase	Soy protein	(Arora & Damodaran, 2011)
β -cyclodextrin conjugated magnetic nanoparticles	Diazepam, copper ions and methylene blue	(Cai et al., 2011) (Badruddoza, Tay, Tan, Hidajat, & Uddin, 2011) (Badruddoza, Hazel, Hidajat, & Uddin, 2010)
β -cyclodextrin/attapulgit	2,4-didichlorophenol and 2,6-didichlorophenol	(J. Pan et al., 2011)
Glycine- β -cyclodextrin	Phenanthrene and lead	(Wang et al., 2010)

β -cyclodextrin polymer	Estrogen, Phenol, azo dyes, aromatic amines and bilirubin	(Oishi & Moriuchi, 2010; Yamasaki, Makihata, & Fukunaga, 2008; A. Yilmaz, Yilmaz, Yilmaz, & Bartsch, 2006; E. Yilmaz, Memon, & Yilmaz, 2010; Zheng, Huang, Kong, Li, & Zou, 2004)
β -cyclodextrin-ionic liquid polymer	P-nitrophenol, 2,4,6-trichlorophenol, 2,4-dichloropheno and Cr(VI)	(Mahlambi, Malefetse, Mamba, & Krause, 2010; Raoov, Mohamad, & Abas, 2013)
β -cyclodextrin grafted multi-walled carbon nanotubes	Polychlorinated biphenyls	(Shao, Sheng, Chen, Wang, & Nagatsu, 2010)

Table 2.7 (Continued)

Polyester β -cyclodextrin and polycarboxylic acids	Pb(II), Cd(II), Zn(II) and Ni(II)	(Ducoroy, Bacquet, Martel, & Morcellet, 2008)
β -cyclodextrin polyurethanes	Geosmin, 2-methylisorboneol, Pb(II) and Azo Dye Eriochrome Black T	(Dong et al., 2013; Mamba et al., 2007; Mirzajani, Pourreza, & Najjar, 2013)
β -cyclodextrin modified poly(hydroxyethylmethacrylate-ethyleneglycoldimethacrylate)	O-chloro phenol, p-nitro phenol, p-chloro phenol, o-nitro phenol, and phenol	(Abay, Denizli, Bişkin, & Salih, 2005)
Quaternary ammonium β -cyclodextrin	Palmitic acid	(Zhong, Ohvo-Rekilä, Ramstedt, Slotte, & Bittman, 2001)

2.2 Theory

2.2.1 Two-parameter adsorption isotherms models

In predictive modelling, an equilibrium isotherm has a critical role in analyzing and designing adsorption systems. The resulting adsorption isotherm is an important tool to theoretically evaluate and interpret thermodynamic parameters such as heats of adsorption.

For the purpose of creating a reliable predictive modelling of adsorption systems and a quantitative comparison of their behavior, an accurate mathematical description of equilibrium adsorption capacities is required. This applies for various adsorbent systems and for different conditions within a given single system. It is imperative to lay down the most suitable correlation for the description of equilibrium curves for optimum design of a system in order to remove the pollutants from the water. In the present study, a two-parameter models (Langmuir, Freundlich, Temkin and Dubinin-Radushkevitch) and three-parameter models (Redlich-Peterson and Koble-Corrigan) are utilized to correlate the organotins compound (TBT, TPT, DBT) adsorption onto modified mesoporous silica with calix[4]arene derivatives.

2.2.1.1 Langmuir isotherm

Langmuir (1916, as cited by Ho and Porter (2002)) proposed theoretical equilibrium isotherm that links the amount of gas sorbed to the gas pressure. The Langmuir isotherm is described as an equilibrium model developed on the basis of evaporation and condensation rates of gas molecules at solid surfaces (Weber Jr & DiGiano, 1996). It is also useful for the

characterization of the equilibrium adsorption of analytes from aqueous to solid systems according to the following assumptions:

- (1) Energy of adsorption is constant and independent of surface coverage.
- (2) Adsorption happens only on sites that are localized, with no interaction between adsorbate molecules.
- (3) Adsorption is limited by the presence of monolayer of solute on the surface.

A point of saturation is achieved at equilibrium where adsorption can no longer occur. The Langmuir isotherm appears to be the most commonly employed sorption isotherm. It may be represented as follows:

$$q_e = \frac{q_{\max} K_L C_e}{1 + K_L C_e} \quad 2.5$$

q_{\max} (mg/g) represents the concentration of solid phase that corresponds to a condition where the entire sites are filled or maximum adsorption capacity is attained, while K_L (L/mg) is the adsorption equilibrium constant and C_e is the equilibrium liquid phase concentration (mg/L).

The model parameters can be determined by using linearization methods using various approaches:

$$\frac{C_e}{q_e} = \frac{1}{q_{\max} K_L} + \frac{C_e}{q_{\max}} \quad \text{Langmuir I} \quad 2.6$$

$$\frac{1}{q_e} = \frac{1}{q_{\max} K_L C_e} + \frac{1}{q_{\max}} \quad \text{Langmuir II} \quad 2.7$$

$$q_e = q_{\max} - \left[\frac{1}{K_L} \right] \frac{q_e}{C_e} \quad \text{Langmuir III} \quad 2.8$$

$$\frac{q_e}{C_e} = K_L q_{\max} - K_L q_e \quad \text{Langmuir IV} \quad 2.9$$

All these approaches are equivalent although one specific form may offer a more dependable fit to specific data set compared to others according to the range and spread of the data to be described (Weber Jr & DiGiano, 1996).

The Langmuir model is suitable for homogeneous sorption and is consistent with Henry's law at low concentrations (Allen, McKay, & Porter, 2004). The essential characteristics of the Langmuir isotherm can be expressed in terms of a dimensionless separation factor (R_L) (Hall, Eagleton, Acrivos, & Vermeulen, 1966), which is defined by Eq. 2.10

$$R_L = \frac{1}{1 + K_L C_0} \quad 2.10$$

where K_L is the Langmuir constant and C_0 is the initial concentration (mg/L) of adsorbate. The value of R_L indicates the type of the isotherm to be either unfavorable ($R_L > 1$), linear ($R_L = 1$), favorable ($0 < R_L < 1$) or irreversible ($R_L = 0$).

2.2.1.2 Freundlich isotherm

Freundlich (1906, as cited by Ho and Porter (2002)) proposed the pioneering sorption isotherm equation. He, along with other authors recommended that data of sorption from solutions are accurately represented by a general exponential concentration that depends on the form's relationship:

$$q_e = K_F C_e^{1/n} \quad 2.11$$

where q_e (mg/g) is the amount of solute adsorbed per unit weight of adsorbent at equilibrium, C_e (mg/L) is the equilibrium liquid phase concentration, and K_F (L/g) and n are Freundlich empirical constants. K_F represents the specific capacity showing the capacity of sorption at a particular solution phase concentration. The value $1/n$, ranging between 0 and 1, is a measure of the adsorption intensity or surface heterogeneity, which becomes more heterogeneous as its value gets closer to zero. A value for $1/n$ below 1 indicates a normal Langmuir isotherm, while $1/n$ exceeding 1 is indicative of cooperative adsorption. Despite the wide use of this model, critics have highlighted its lack of basic thermodynamic as it fails to reduce to the linear model (Henry's law) at low levels of concentration (Weber Jr & DiGiano, 1996). The linearity of data by logarithmic transformation can solve the determinants of the coefficients of Eq. 2.12:

$$\log q_e = \log K_L + \frac{1}{n} \log C_e \quad 2.12$$

2.2.1.3 Temkin isotherm

The impact of adsorbent-adsorbate interactions upon the adsorption isotherms was examined by Temkin and Pyzhev (1940), and they stated that the heat of adsorption would decrease linearly with coverage. This type of isotherm has been utilized in the function of temperature:

$$q_e = \left(\frac{RT}{b_T}\right) \ln (K_T C_e) \quad 2.13$$

where K_T and b_T are Temkin isotherm constant and energy constant (J/mol), respectively. R (8.314 J/ mol K) is the gas constant and T (K) is the absolute temperature. The Eq. 2.13 is able to transform to a linear form:

$$q_e = \left(\frac{RT}{b_T}\right) \ln K_T + \left(\frac{RT}{b_T}\right) \ln C_e \quad 2.14$$

$$A_T = \frac{RT}{b_T} \quad 2.15$$

A plot of q_e versus $\ln C_e$ enables the determination of the constants K_T and A_T .

2.2.1.4 Dubinin-Radushkevitch isotherm

The Dubinin-Radushkevitch (D-R) equation has been utilized in an effective manner to provide a description of adsorption by microporous solids (Huber, Stoeckli, & Houriet, 1978). The D-R equation represents an adaptation of the prior Polanyi potential theory of

adsorption, which is also considered as the theory of volume filling of micropores. It postulates that adsorption is characterized by multi-layer involving van der Waals forces and is suitable for physical process of adsorption (Hutson & Yang, 1997). The expression of linear form of D-R isotherm model is represented as:

$$\ln q_e = \ln q_d - \beta \varepsilon^2 \quad 2.16$$

where q_d is the D-R constant which refers to maximum adsorption capacity (mg/g), β (mol^2/kJ^2) is the constant related to free energy and ε is the Polanyi potential which is defined as:

$$\varepsilon = R T \ln \left(1 + \frac{1}{C_e} \right) \quad 2.17$$

where R is the gas constant (8.31 J/mol K) and T (K) is the absolute temperature. The constant β gives the mean free energy E of adsorption per molecule of the adsorbate when it is transferred to the surface of the solid from infinity in the solution and can be computed by using the relationship:

$$E = \frac{1}{\sqrt{2\beta}} \quad 2.18$$

E values that are between 1-16 kJ/mol facilitate physical adsorption, while values over 16 kJ/mol facilitate chemisorptions (Apiratikul & Pavasant, 2008; Vijayaraghavan, Padmesh, Palanivelu, & Velan, 2006).

2.2.2 Three-parameter adsorption isotherm models

2.2.2.1 Redlich-Peterson isotherm

Redlich and Peterson (1959) brought forward an empirical equation including three parameters which may be useful in representing adsorption equilibria over a wide range of concentration and the equation can be employed in either homogeneous or heterogeneous systems due to its versatility. The Redlich-Peterson equation is represented by Eq. 2.19.

$$q_e = \frac{A_R C_e}{1 + B_R C_e^g} \quad 2.19$$

This equation can be converted to a linear form by taking logarithms:

$$\ln \left(A_R \frac{C_e}{q_e} - 1 \right) = g \ln C_e + \ln B_R \quad 2.20$$

where q_e is the concentration of solid phase sorbate in equilibrium (mg/g), C_e is the concentration of liquid phase sorbate in equilibrium (mg/L), A_R (L/g) and B_R (L/mg) are R-P isotherm constants, and g is the exponent which lies between 0 and 1.

The isotherm combines both Langmuir and Freundlich equations elements and the adsorption mechanism is described as a hybrid that does not follow an ideal monolayer adsorption. The isotherm is linearly dependent on the concentration in the numerator and has an exponential function in the denominator. The value ‘g’ is between 0 and 1 and characterizing the isotherm as; if g=1, the Langmuir is the preferable isotherm while if it is zero, then the Freundlich will be the isotherm preferred (Özer, Akkaya, & Turabik, 2005).

Despite the fact that the two-parameter equations may be determined graphically, Redlich-Peterson constants are not suitable due to the three unknown parameters. Normally, a minimization process is employed in solving the equations through the maximization of the correlation coefficient between the experimental data points and the predictions of the theoretical model with Solver add-in of the Microsoft Excel function (Y. Wong, Szeto, Cheung, & McKay, 2004).

2.2.2.2 Koble-Corrigan isotherm

Koble-Corrigan model is described as a three-parameter empirical model that represents the equilibrium adsorption data. This equilibrium relation is significantly non-linear in comparison to the Redlich-Peterson model. Similar to the isotherm above, it is a combination of the Langmuir and Freundlich isotherm models and is represented by Eq. 2.21 (Koble & Corrigan, 1952):

$$q_e = \frac{A_K C_e^P}{1 - B_K C_e^P} \quad 2.21$$

The linear form of this equation is

$$\frac{1}{q_e} = \left(\frac{1}{A_K C_e^p} \right) + \frac{B_K}{A_K} \quad 2.22$$

where A_K , B_K and p are the Koble-Corrigan parameters. The Koble-Corrigan model's three isotherm constants are also evaluated through the use of Solver add-in function of the Microsoft Excel.

2.2.3 Adsorption kinetics

The adsorption kinetics reveals the rate of adsorbate uptake by the adsorbent during the timeframe (Ho & McKay, 1999a). There are some specific models that are normally utilized to represent the adsorption kinetics, and the most common models among them are pseudo-first-order, pseudo-second order and intra-particle diffusion models. In the comparison of the adsorption kinetics of one compound on different adsorbents, it can be found which adsorbent has been adsorbed to a greater extent, or which adsorbent shows the faster rate of adsorbate adsorption.

2.2.3.1 Pseudo-first order model

The pseudo-first order model of Lagergren (Lagergren, 1898) is the pioneering equation that describes the rate of adsorption on the basis of the capacity of adsorption. The differential equation is commonly expressed as follows:

$$\frac{dq_t}{dt} = k_1 (q_e - q_t) \quad 2.23$$

where q_e and q_t (mg/g) are the adsorption capacities at equilibrium and at time t (min), respectively, and k_1 is the equilibrium rate constant of pseudo-first order adsorption (min^{-1}). Integrating Eq. 2.23 for the boundary conditions $t=0$ to t and $q_t=0$ to q_t gives:

$$\log \frac{q_e}{(q_e - q_t)} = \frac{k_1}{2.303} t \quad 2.24$$

which is the integrated rate law for a pseudo-first order reaction. Eq. 2.24 can be rearranged to obtain the linear form:

$$\log (q_e - q_t) = \log q_e - \frac{k_1 t}{2.303} \quad 2.25$$

The slope and intercept of plot of $\log (q_e - q_t)$ versus t are then used to determine the first-order rate constant, k_1 . In most cases, the first order equation of Lagergren is unfit with the whole range of contact time but is generally suitable over the initial stage of the processes of adsorption (Ho & McKay, 1999b).

2.2.3.2 Pseudo-second order model

This model also has its basis on the sorption capacity of the solid phase (Ho & McKay, 1999a). It is however distinct from the first model as it predicts the behavior throughout the

whole range of adsorption and it agrees with an adsorption mechanism as the rate controlling step:

$$\frac{dq_t}{dt} = k_2 (q_e - q_t)^2 \quad 2.26$$

where k_2 is the equilibrium rate constant of pseudo-second order adsorption (g/mg min).

Integrating Eq. 2.26 for the boundary condition $t=0$ to t and $q_t=0$ to q_t gives:

$$\frac{1}{(q_e - q_t)} = \frac{1}{q_e} + k_2 t \quad 2.27$$

which is the integrated rate law for a pseudo-second order reaction. Eq. 2.27 can be rearranged to obtain a linear form:

$$\frac{t}{q_t} = \frac{1}{k_2 q_e^2} + \frac{1}{q_e} t \quad 2.28$$

The slope and intercept of plot t/q_t versus t are then used to calculate the second order rate constant, k_2 .

2.2.3.3 Intraparticle diffusion model

The adsorption of adsorbate from an aqueous to a solid phase comprises of many steps and involves the transport of adsorbate from the aqueous phase to the solid particles surface (bulk diffusion), and then the diffusion of adsorbate through the boundary layer to the solid

particles surface (film diffusion), and followed by the transport of adsorbate from the solid particles surface towards the interior pores (pore diffusion or intraparticle diffusion). This is likely to be a slow process, hence it may be the rate-determining step. In cases in which the experiment is a batch system with rapid stirring, the possibility of that intraparticle diffusion to be the rate-determining step arises (McKay, 1983). According to Weber & Morris (1963), the rate for intraparticle diffusion is represented by the relationship between q_t and the square root of time, $t^{1/2}$, as presented in Eq. 2.29.

$$q = k_i t^{1/2} + C \quad 2.29$$

Where K_i ($\text{mg/g min}^{1/2}$) is the intraparticle diffusion rate constant and C is related to the thickness of the boundary layer. K_i and C values are calculated from the slope and intercept of q_t versus $t^{1/2}$ plots, respectively. With $C=0$, the adsorption rate is controlled by the intraparticle diffusion for the whole period of adsorption. However, the plot of q_t against $t^{1/2}$ often reveals more than a single linear portion and if the first portion slope is not equal to 0, then film diffusion or boundary layer controls the rate of adsorption at the initial stage.

2.2.4 Thermodynamic studies

The parameters of isotherm and kinetics are significant in the process of adsorption. It has to be noted that the parameters of thermodynamics like the change in standard enthalpy (ΔH°), change in standard free energy (ΔG°) and the change in standard entropy (ΔS°) have a key role in this process. Through these parameters, the adsorption type can be discerned

which is primarily either physisorption or chemisorption, and the process can be estimated as endothermic or exothermic.

Thermodynamic studies concerning adsorption process need to determine whether or not the process is spontaneous. The change of Gibbs free energy, ΔG° , indicates the spontaneity of chemical reaction and thus it is an important criterion for spontaneity. The energy and entropy factors must be kept into consideration for the determination of the Gibbs free energy of the process. Spontaneous reactions occur at a given temperature if ΔG° is a negative quantity.

The thermodynamic parameters can be determined from the thermodynamic equilibrium constant K_c . The standard Gibbs free energy ΔG° (kJ/ mol), standard enthalpy change ΔH° (kJ/ mol), and standard entropy change ΔS° (J/mol K) can be calculated using the following equations:

$$\ln K_c = \frac{\Delta S^\circ}{R} - \frac{\Delta H^\circ}{RT} \quad 2.30$$

$$\Delta G^\circ = \Delta H^\circ - T\Delta S^\circ \quad 2.31$$

where R (8.314 J/mol K) is the gas constant, T (K) is the absolute temperature and K_c (L/g) is the standard thermodynamic equilibrium constant defined by q_e/C_e .

The positive ΔH° value indicates that the adsorption is endothermic, while the negative value indicates that the adsorption is exothermic in nature. Furthermore, the ΔH° magnitude

gives information on the type of sorption, which can be either physical or chemical. Physisorption is distinguished from chemisorption by considering the absolute value of a physisorption process that is lower than 20.9 kJ/mol, while the adsorption heat of a chemisorption process ranging from 20.9 to 418.4 kJ/mol (Deng, Su, Su, Wang, & Zhu, 2007; Smith, 1981).

CHAPTER 3

SYNTHESIS AND CHARACTERIZATION OF FUNCTIONALIZED ORDERED MESOPOROUS SILICA MCM-41 WITH CALIX[4]ARENE DERIVATIVES

3.1 Introduction

Since the discovery of a new family of mesoporous molecular sieves M41S (Beck, Vartuli, et al., 1992; Kresge, Leonowicz, Roth, Vartuli, & Beck, 1992) with tailorable pore sizes ranging from 2.0 to 10 nm and with the surface areas often exceeding 1000 m²/g, these materials have attracted much attention in the field of catalysis, separation and adsorption. As mentioned before, mesoporous silica usually have very high surface and their surfaces are covered by silanol groups, which makes the functionalization of the pore surface of the mesoporous materials adjustable. Additionally, the surface functionalization of mesoporous silicates could change the chemical and physical properties of these materials dramatically.

Therefore, the surface functionalization of mesoporous silica has been intensively investigated (Stein, et al., 2000). Several kinds of surface modification have been conducted for providing new functions for the surfaces. Chemical surface modification of periodic mesoporous silica by covalent bonding of organic molecules has been achieved using two general strategies. The post-synthesis procedure was the first method to be used as it was already described in the early work by Mobil on M41S silica (Beck, Vartuli, et al., 1992). Subsequently, co-condensation procedures were introduced by Burkett et al.,(1996)

and Macquarrie (1996). Both methods were discussed in details in Chapter two Section 2.1.4.2.

The use of organosilanes in the surface functionalization of several materials such as MCM-41, MCM-48 and silica gels (Okutomo, Kuroda, & Ogawa, 1999; X. Zhao & Lu, 1998; X. S. Zhao, et al., 1996) is a well-known approach to control and change the surface characteristics of the underlying material. Among the great variety of different organosilanes that can be used for surface functionalization, monofunctional organosilanes ($R_3Si X$) with only one hydrolyzable group ($X = Cl, OR, NR_2,$ and OH) are far superior in terms of reproducibility as only one type of reaction is possible, which is the covalent attachment of the silane to the underlying substrate through M-O-Si bonds (Fadeev & McCarthy, 2000).

Isocyanates are considered to highly react with $-OH$ groups to produce urethane bonds (Chun et al., 2002; Xia & Song, 2006). The high reactivity of isocyanate groups towards nucleophilic reagents is mainly due to the pronounced positive character of the C atom in the cumulative double bond sequence consisting of nitrogen, carbon and oxygen, especially in aromatic systems. The electronegativity of the oxygen and nitrogen imparts a large electrophilic character to the carbon in the isocyanate group. Isocyanate can be aromatic, aliphatic or cycloaliphatic in structure. Aromatic isocyanates have high reactivity than aliphatic or cycloaliphatic diisocyanates. Based on the utilization of isocyanate, the binding strength to the surface of the support can be greater or at least equal to those obtained for the organosilane binders (Chun, et al., 2002).

Calixarenes are described as supramolecules that come after the second generation crown ethers and cyclodextrins, and are based on phenol macrocycles which are capable of creating stable and selective complexes with the following; cations, anions, or neutral molecules.

Here, we report a novel kind of mesoporous silica MCM-41 adsorbent with the macrocyclic compound calix[4]arene derivatives covalently attached on the substrate using: a linking agent consisting of an organosilane (3-chloropropyl trimethoxysilane-CIPTS) and a diisocyanate (TDI) for the adsorption of organotin compounds. Organic functionalizations of mesoporous silica were synthesized via a post-synthesis grafting method.

3.2 Experimental

3.2.1 Materials

The chemicals used in this part of the thesis are as follows: Mesoporous silica [Aldrich, surface area of 993 m²/g, average diameter of 2.9 nm] as silica source. Calix[4]arene [C₂₈H₂₄O₄, Acros] and p-tert-butylcalix[4]arene [C₄₄H₅₆O₄, Fluka] were the organic modifier, while 3-chloropropyl triethoxysilane (CIPTS) [C₉H₂₁ClO₃Si, Aldrich] and toluene-2,4-diisocyanate (TDI) [C₉H₆N₂O₂, Aldrich] were the organic linker. Triethylamine [C₆H₁₅N, SAFC] was used as catalyst. The structures of Di-n-butylamine [C₈H₁₉N, Acros] and hydrochloric acid [HCl, Fisher] were used for the determination of isocyanate groups. Dichloromethane (CH₂Cl₂, Sigma Aldrich), chlorosulfonic acid (HSO₃Cl, Merck) and methanol were utilized for the synthesis of p-sulfonatocalix[4]arene

as described in the literature (Makha & Raston, 2001). Toluene [Fisher, dried before use by using molecular sieves], ethanol [Fisher] and acetone [Fisher] were used as solvents. Water was purified using Milli-Q purification equipment. Some of these compounds are shown in Figure 3.1.

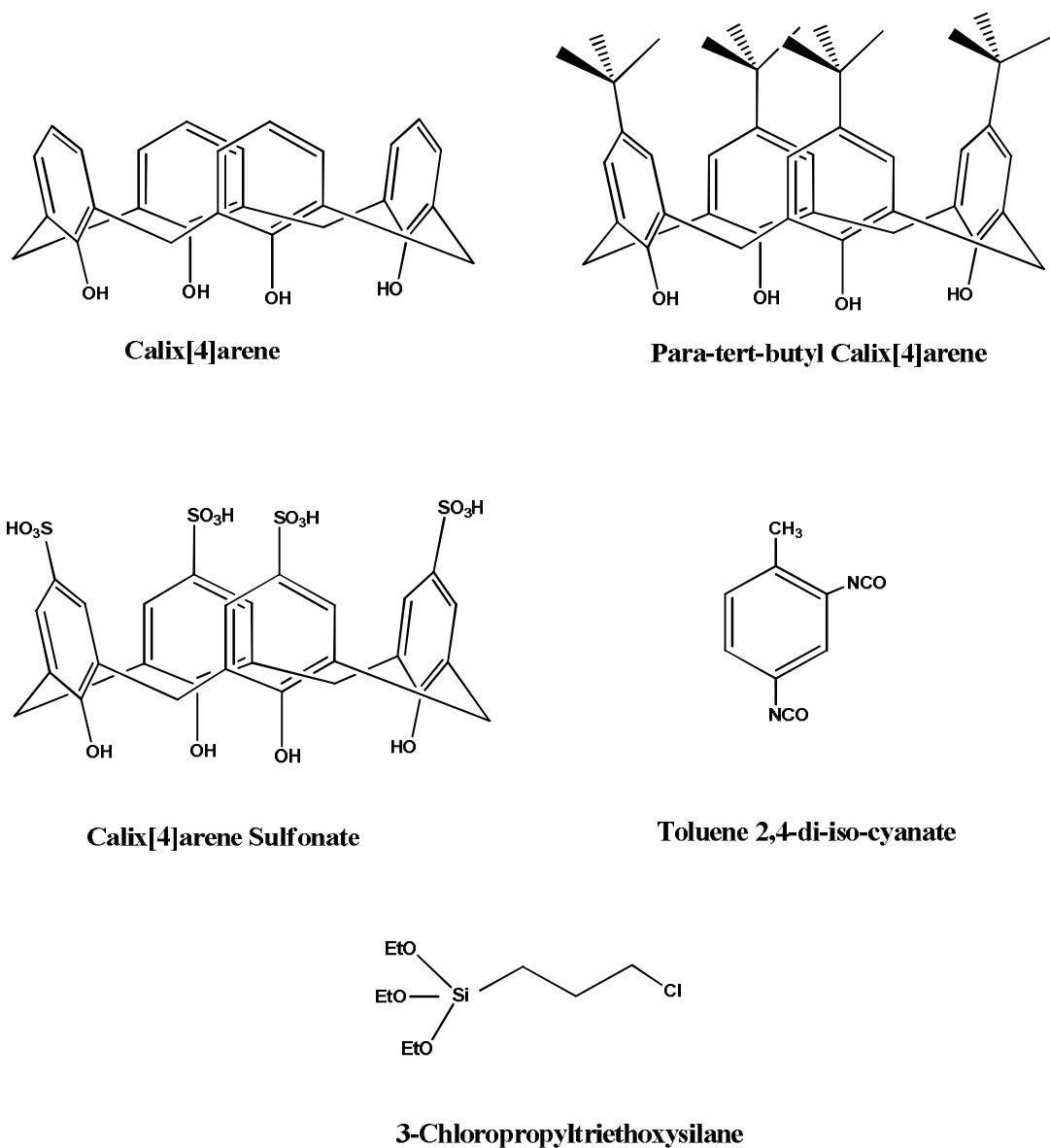


Figure 3.1 Molecular structures of some materials

3.2.2 Instrumentation

Fourier transform infrared spectra (FTIR) were recorded on a Perkin Elmer FTIR Spectrum RX1 ATR. The spectra were collected for all samples in the range from 400 to 4,000 cm^{-1} . The samples were ground to powders and diluted with potassium bromide in an approximate ratio of 1:6.

Thermogravimetric analyses (TGA) were performed on a Perkin Elmer TGA 4000 TG/DTA instrument using 2-3 mg samples and a flow of nitrogen of 100 ml/min. The temperature was ramped from 45 °C to 900 °C at a rate of 20 °C/min.

Chemical elemental analysis for C, H, N and S was carried out using a Perkin Elmer CHNS-2400 analyzer.

The X-ray powder diffraction (XRD) patterns were obtained on a Bruker AXS D-8 advance diffractometer using Cu K radiation ($\lambda = 0.154056 \text{ nm}$) at 40 kV and 30 mA within the 2θ range of 2 to 10. The samples were prepared as a thin, flat layer in a plastic holder.

Textural properties (surface areas, pore sizes, pore volumes and pore size distribution) were determined at 76.53°K using Brunauer-Emmett-Teller (BET) multilayer nitrogen adsorption method by a quantachrome autosorb automated gas sorption system. The Brunauer-Emmett-Teller surface area (S_{BET}) was calculated from the linearity of the BET equation. The surface area, volume and pore diameter were calculated from the pore size distribution curves using the density functional theory method.

3.2.3 Synthesis methods

3.2.3.1 Synthesis of p-sulfonatocalix[4]arene

The calixarene was sulfonated by chlorosulfonation method as described in the literature (Makha & Raston, 2001). To a solution of calix[4]arene (1.0 g, 2.4 mmol) dissolved in 30 ml of dry dichloromethane, 1.0 ml of chlorosulfonic acid was added dropwise at 0°C. The mixture was stirred at room temperature for 5 h to form a bright rose biphasic mixture. The reaction mixture was poured over ice, and the aqueous phase was evaporated to remove dichloromethane and boiled for 2 h. Water was evaporated to produce a light green solid, which was crystallized from acetone to obtain the acidic product. Water was added and the mixture was neutralized to pH=7. Water was then evaporated to produce a deliquescent green solid and upon addition of methanol, a fine gray precipitate formed which was then filtered to obtain p-sulfonatocalix[4]arene. The structure of this compound was characterized by FTIR analyses.

3.2.3.2 Functionalization of MCM-41 mesoporous surfaces with calix[4]arene derivatives

Calix[4]arene derivatives were chemically attached to the mesoporous MCM-41 material surfaces by means of the post-synthesis grafting method. Two synthetic procedures were applied, which are based on a combination of different synthetic methods used by previous researchers.

I. Surface functionalization of MCM-41 using toluene-2,4-diisocyanate (TDI) as a linker

The functionalization of isocyanate groups onto MCM-41 surface was carried out by refluxing of the activated mesoporous silica with excess of TDI (M. Yang, Gao, He, & Li, 2007). 5.0 g of mesoporous silica (150°C, overnight) and 200 ml TDI (1.41 mol, dried by molecular sieve for 24 h) were mixed in a 400 ml round-bottom flask using magnetic stirrer, and the functionalization was conducted in a dry nitrogen atmosphere at 80°C for 4 h. The chemical reaction is shown in Figure 3.2. The refluxed mixture was then cooled down to room temperature. In order to remove all the substances physically adsorbed on the surface of the particles, the sample of MCM-TDI was separated by centrifugation and sequentially rinsed with toluene three times (3 X 20 ml), and followed by acetone to wash away any excess TDI. Toluene and TDI were dried using molecular sieves (5A, beads, 4-8 mesh) prior to use. The white solid was then dried at 80°C for 24 h and the sample was marked as MCM-TDI.

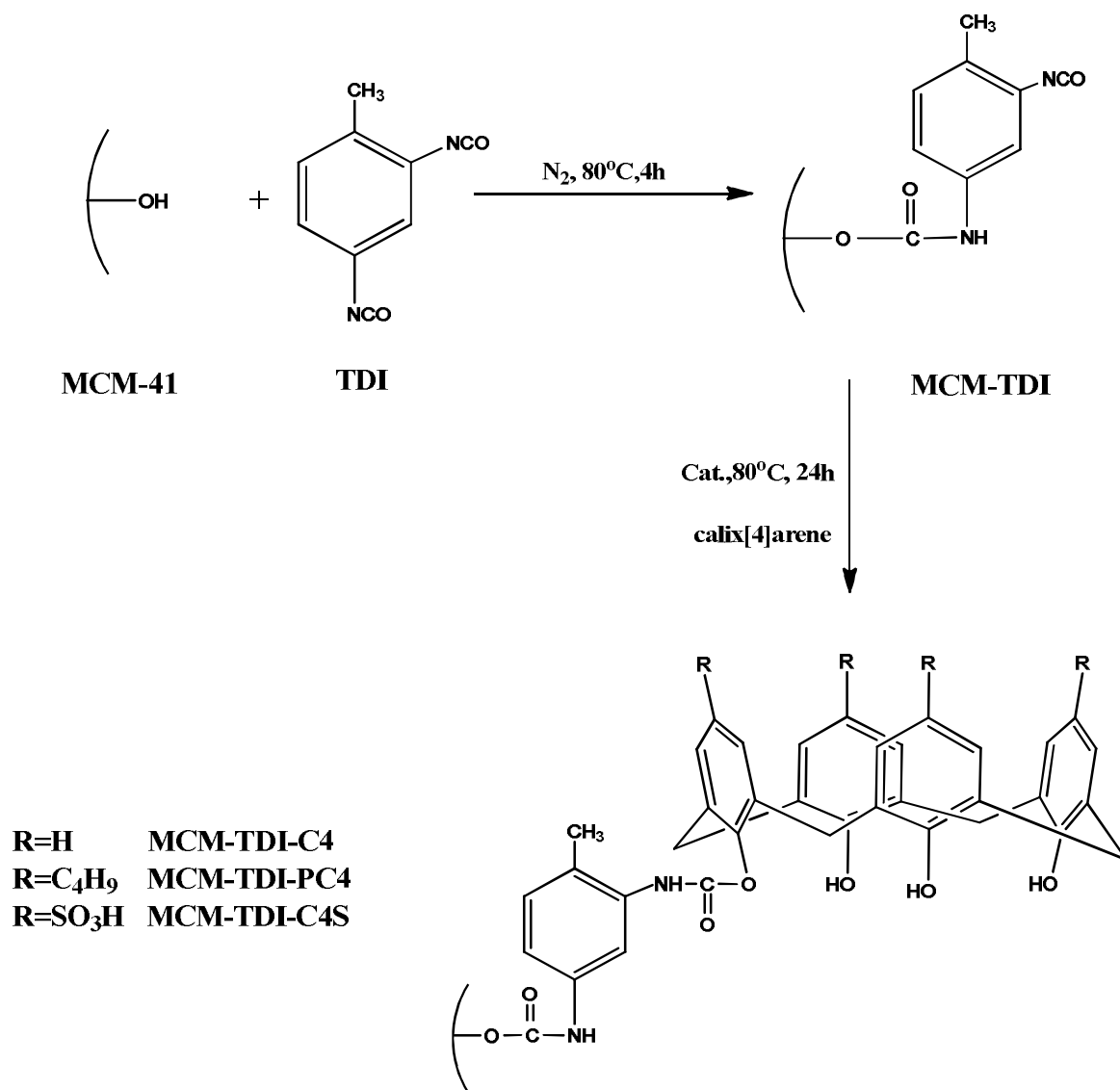


Figure 3.2 Schematic diagram for the functionalization of MCM-41 mesoporous silica material surface with of calix[4]arene derivatives using toluene-2,4-diisocyanate as linker

Functionalization of mesoporous silica with the calix[4]arene derivatives was carried out as follows (Figure 3.2): 1.0 g of the modified mesoporous silica MCM-TDI was stirred with 2.0 mmol of calix[4]arene (calculated from Section 3.2.3.3) derivatives in dry toluene and few drops of triethylamine was added into a 125 ml round-bottom flask for 24 h around

70°C under reflux. After cooling, the solid product was isolated by filtration and washed with toluene and acetone and dried for a day. The samples were marked as MCM-TDI-C4 for calix[4]arene, MCM-TDI-C4S for calix[4]arene sulfonate and MCM-TDI-PC4 for para-tert-butylcalix[4]arene.

II. Surface functionalization of MCM-41 using 3-chloropropyltriethoxysilane (CIPTS) and toluene-2,4-diisocyanate(TDI) as a linker

Surface functionalization of MCM-41 with CIPTS was carried out by a procedure described by Feng et. al., (1997), whereby the concentration of surface silanols was calculated based on the surface area and an estimate of 5×10^{18} surface silanols/m². This is achieved by multiplying the number above with the surface area to give the number of silanols per gram of the MCM-41, followed by dividing the number by Avogadro's number to get the total number of moles of surface silanols. The amount of the silane to be used was calculated accordingly. To optimize the functionalization process, hydration of the surface was carried out with approximately two monolayers (calculated based on the surface area by the procedure described above) of deionized water (DI).

In a general procedure, a self-assembled monolayer of the initial silane was produced by suspending 1.0 g of MCM-41 in 40 ml of toluene in a 100 ml round-bottom flask. The suspension was stirred vigorously for 5 min before adding 0.30 ml of DI water (calculated based on the surface area of 993 m²/g), and the stirring was resumed for 2 h. A slight excess of silane (10 % v/v), 2.18 ml of 3-chloropropyl triethoxysilane corresponding to 9.07 mmol, was added and the solution was refluxed for 6 h. The solids were then filtered and

washed copiously with toluene and ethanol to remove un-reacted silane and the dried overnight. For convenience, the following term CIPTS-MCM will be used. The chlorine groups present in the CIPTS-MCM were hydrolysed into hydroxyl groups (OHPTS-MCM) by heating the solid material with a solution of methanol: water (1:1) for 2 h and at 60°C (Xia & Song, 2006) (Figure 3.3). After cooling to room temperature, the reaction mixture was filtered with a fine filter funnel and dried at 110°C overnight.

The functionalization MCM-41 with CIPTS and TDI was prepared by refluxing the hydroxyl modified material, OHPTS-MCM with excess of TDI (dried by molecular sieve for 24 h) in a dry nitrogen atmosphere at 80°C for 4 h (M. Yang, et al., 2007) (Figure 3.3). After cooling down, the material was filtered, washed and dried overnight and marked as MCM-PS-TDI.

Mesoporous silica-supported calix[4]arene derivatives were prepared by refluxing 1.0 g of the functionalized mesoporous silica (MCM-PS-TDI) with 1.8 mmol of calix[4]arene (calculated from Section 3.2.3.3) derivatives and few drops of triethylamine in 100 ml of dry toluene in a 250 ml round-bottom flask and the reaction temperature was kept at 80°C for 24 h under continuous stirring, as shown in Figure 3.3. The mixture was then cooled to room temperature and then the resulting white mixture was filtered with a fine filter funnel. The solid was washed three times with toluene (3 X 20 ml) and then acetone. The white solid was then dried at 80°C for 24 h. The samples were marked as MCM-PS-TDI-C4 for calix[4]arene, MCM-PS-TDI-C4S for calix[4]arene sulfonate and MCM-PS-TDI-PC4 for para-tert-butylcalix[4]arene.

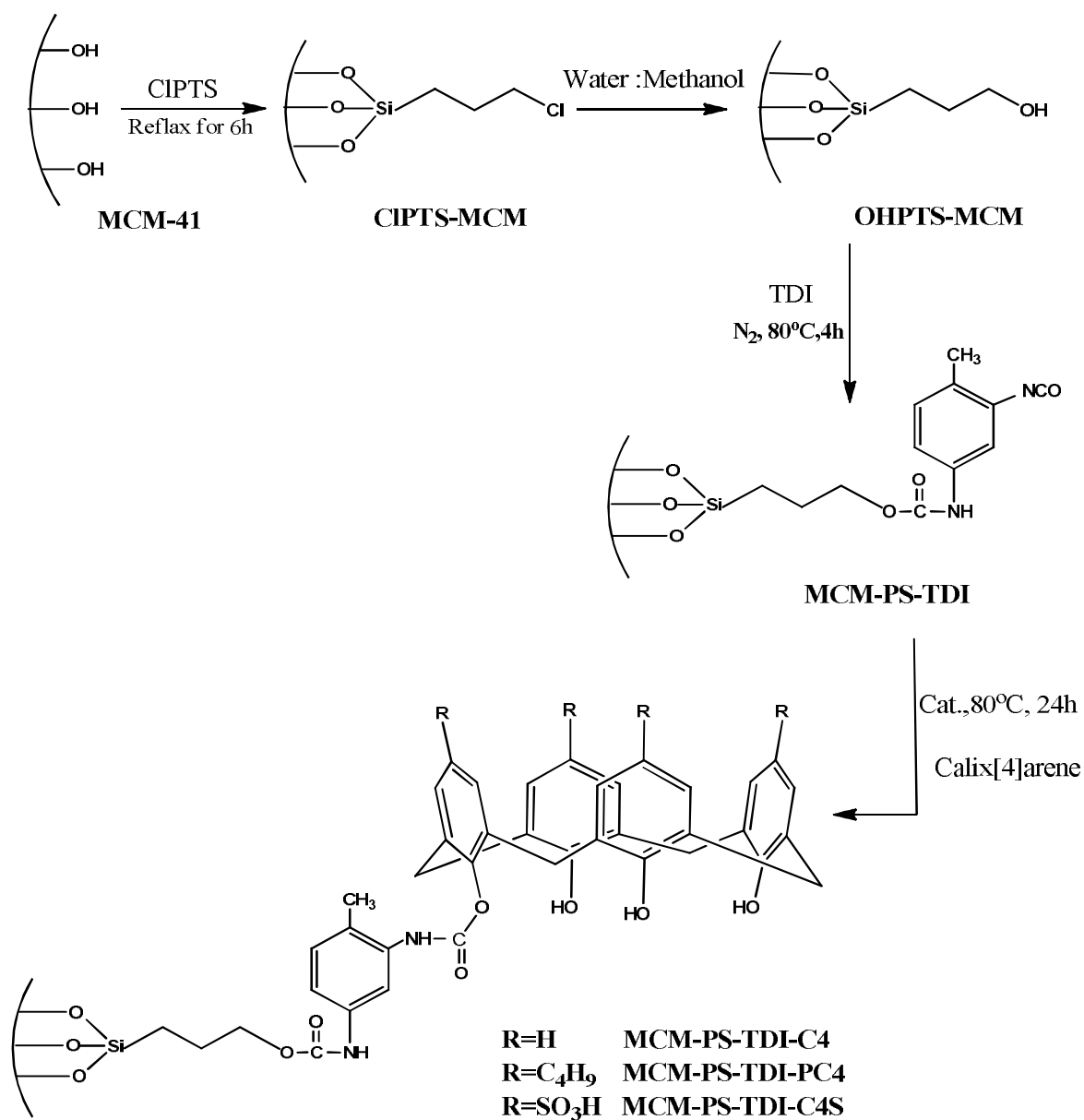


Figure 3.3 Schematic diagram for the functionalization of MCM-41 mesoporous silica material surface with calix[4]arene derivatives using 3-chloropropyl triethoxysilane (CIPTS) and toluene-2,4-diisocyanate (TDI) as linker

3.2.3.3 Determination of isocyanate groups of the reaction system

The content of isocyanate groups of the reaction system was determined by titration. 200 mg of MCM-TDI and MCM-PS-TDI samples and 20 ml of 0.1 mol/L di-n-butylamine in

toluene were charged into a flask and the mixture was stirred at room temperature for 1 h. The unreacted di-n-butylamine was backtitrated with 0.1 mol/L HCl using bromophenol blue as an indicator. The content of isocyanate groups was calculated using Equation 3.1:

$$\text{Isocyanate group (mmol/gm)} = 0.1 (V_0 - V_s) \frac{f}{w} \quad 3.1$$

where V_0 (ml) is the titer of 0.1 mol/L HCl for blank, V_s (ml) is the titer of 0.1 mol/L HCl for the sample, f is the factor of 0.1 mol/L HCl and w (g) is the weight of the sample.

3.3 Results and discussion

3.3.1 Characterization of functionalized MCM-41 with TDI as linker

In this part of this study, three mesoporous silica modified with calix[4]arene derivatives have been prepared via modification of activated mesoporous silica with toluene-2,4-diisocyanate (TDI) as linker and C4, C4S and PC4 as organic modifier. Toluene-2,4-diisocyanate was utilized to establish a bridge between the surface of mesoporous silica and calix[4]arene derivatives. TDI has highly unsaturated bonds and two isocyanate groups with different activities towards hydroxyl groups, located at a para-position and an ortho-position, respectively, and consequently, it is very active towards hydroxyls.

The isocyanate groups at para-positions would react with the hydroxyl groups on the surface of mesoporous silica preferentially, whereas those at the ortho-positions would be preserved due to the steric hindrance within the TDI molecule (R. Arnold, Nelson, &

Verbanc, 1957; Simons & Arnold, 1956). The mole amount of the isocyanate groups that reacted with mesoporous silica can be regarded as TDI that reacted with mesoporous silica. The amounts of TDI that reacted with mesoporous silica are largely dependent on the amount of hydroxyls on the mesoporous silica surface, therefore in the case of excess of TDI, the amounts of TDI that reacted with silica were invariable (Che et al., 2007). Excess TDI was used to serve two functions; as a solvent to disperse silica and as a reactant in order to drive the reactions to completion, and it was easily removed after reaction by centrifugation and prolonged washing with anhydrous toluene.

I. Fourier transform infrared spectroscopy (FTIR)

FTIR spectroscopic analysis provided the evidence that the mesoporous silica surface reaction proceeded as illustrated in Figure 3.4. Figure 3.4 shows the FTIR spectra of activated mesoporous silica and MCM-TDI. The FTIR spectrum of unmodified mesoporous silica is relatively simple and well assigned as shown in Figure 3.4 A (Boven, Oosterling, Challa, & Jan Schouten, 1990).

The spectra of MCM-41 and MCM-TDI were dominated by strong bands characteristic of the support matrix. These bands are due to the surface hydroxyl groups in the range of $3770\text{--}3300\text{ cm}^{-1}$, and to lattice vibrations in the range of $1300\text{--}750\text{ cm}^{-1}$. Two strong bands were present at about 1085 cm^{-1} and 801 cm^{-1} , which can be assigned to the asymmetrical Si-O-Si stretching and symmetrical Si-O-Si, respectively. The band present at about 970 cm^{-1} was attributable to Si-OH vibrations (Alba, Luan, & Klinowski, 1996; Kureshy et al., 2005; Shylesh & Singh, 2004). Any adsorbed water on the surface was seen in the region of

,3400 – 3500 cm^{-1} (Vansant, Van Der Voort, & Vrancken, 1995). The bending O-H mode of any adsorbed molecular water was found around 1625 cm^{-1} .

Addition of excess TDI to the mesoporous silica resulted in the incorporation of isocyanate functionalities on the surface of the mesoporous silica. This was evidenced by the appearance of a clearly discernible band at 2275 cm^{-1} corresponding to the asymmetric stretching of the appended terminal isocyanate groups, and the appearance of an aromatic C–C stretch at 1549 cm^{-1} in the FTIR spectrum Figure 3.4 B.

The signals corresponding to the C=O and C–N stretches of the formed carbamate linkages between the mesoporous silica and the isocyanate functionality in the compound mesoporous silica-TDI at 1647 cm^{-1} and 1197 cm^{-1} may be merged with the band of surface hydroxyl groups of mesoporous silica and Si–O–Si band, respectively. Other bands at 1522 cm^{-1} and 1560 cm^{-1} are referred to -CO-NH-. Also, a decrease in the peak intensity at about 970 cm^{-1} was observed, and when compared with the parent material, it is suggested that the silanol surface groups were functionalized (Oliveira et al., 2007).

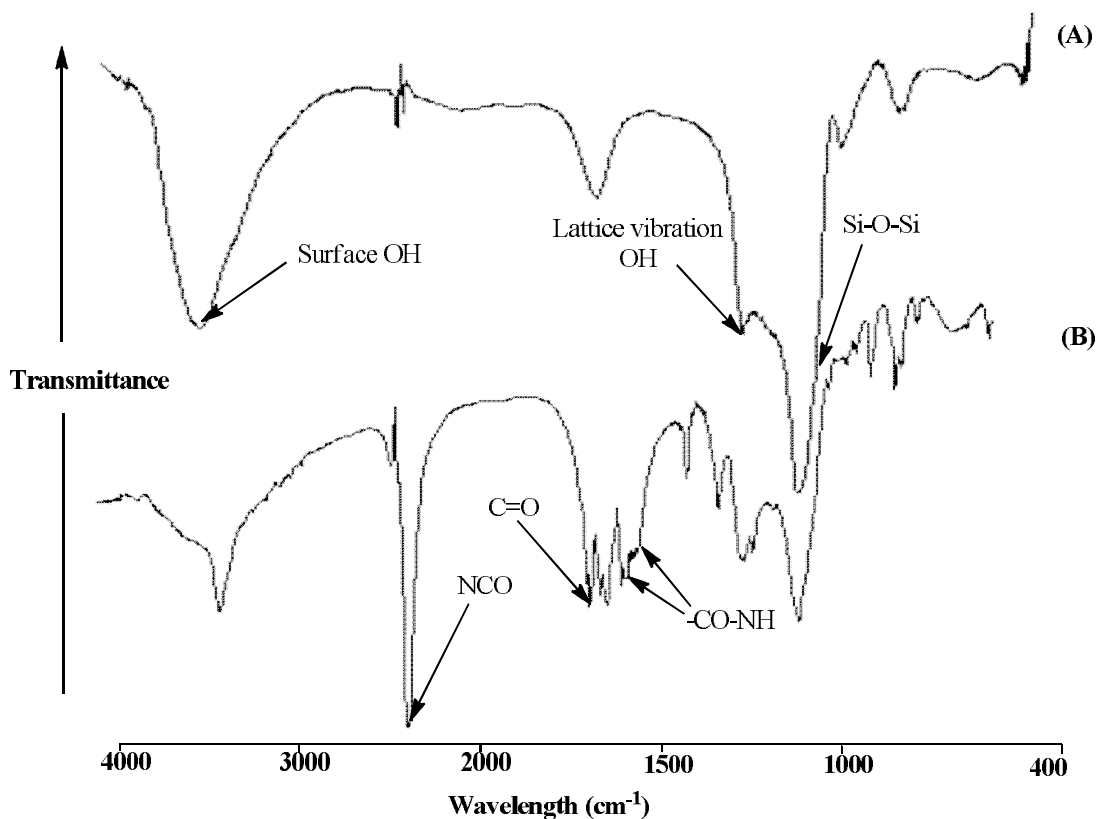


Figure 3.4 Fourier transform infrared spectroscopy (FTIR) spectra of MCM-41 (A) and MCM-TDI (B)

II. Elemental analysis

Elemental analysis provided further evidence of the successful modification of mesoporous silica. The carbon, hydrogen, nitrogen and sulfur contents of MCM-TDI were 18.64, 3.04, 5.93 and 0.0 respectively. It can be observed that the amount of carbon and nitrogen in mesoporous silica increased after the modification with TDI.

III. Thermogravimetric analysis (TGA)

Thermogravimetric analysis of mesoporous silica and MCM-TDI were determined (Figure 3.5). The unmodified MCM-41 exhibited a weight loss at about 50°C, corresponding to the loss of physically adsorbed water and suggesting the surface to be hydrophilic in nature (Iler, 1979; Jaroniec, Gilpin, & Jaroniec, 1997). With increase in the temperature, the weight loss remains constant, indicating no appreciable condensation of silanol groups on the surface (Iler, 1979; Jaroniec, et al., 1997).

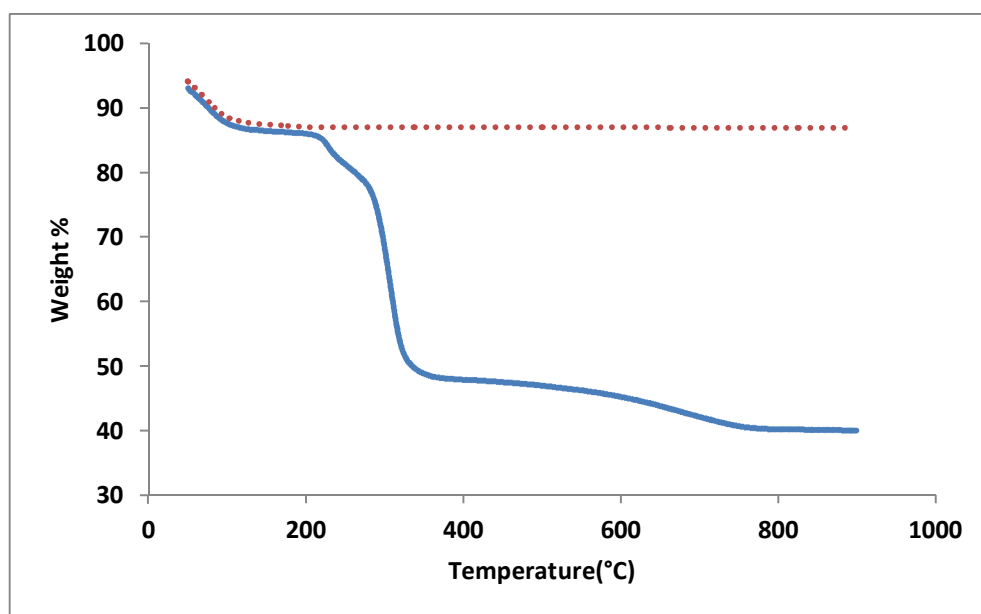


Figure 3.5 Thermogravimetric analysis (TGA) of MCM-41(...) and MCM-TDI (—)

There is a significant change in the weight loss curve with modification of MCM-41 (Figure 3.5). The decrease in weight from 50-100°C was due to the physically adsorbed water. A slight weight loss from 220-280°C was due to the decomposition of the organic moiety. The third sharp decrease in weight at 280°C was because of loss of the carbamate group. The last region of the weight loss curve, above 600°C, may be due to the dehydroxylation of the silicate network (Hashemi, Yarahmadi, Azizi, & Sabouri, 2008).

3.3.2 Characterization of functionalized MCM-TDI with calix[4]arene derivatives

I. Fourier transform infrared spectroscopy (FTIR)

Three mesoporous silica modified with calix[4]arene derivatives have been prepared via functionalization of modified mesoporous silica with toluene-2,4-diisocyanate (TDI) as linker and C4, C4S and PC4 as organic modifier. Toluene-2,4-diisocyanate was utilized to establish a bridge between the surface of mesoporous silica and calix[4]arene derivatives.

The remaining isocyanate groups at ortho-positions in modified mesoporous silica (MCM-TDI) reacted with hydroxyl groups at the lower rim of calix[4]arene derivatives to form modified mesoporous silica with toluene-2,4-diisocyanate (TDI) as linker and C4, C4S and PC4 as organic modifier. These functionalization reactions were again examined by FTIR spectroscopy to monitor the appearance and disappearance of some peaks. In detail, by comparison with the spectrum of MCM-TDI, MCM-TDI-C4 (Figure 3.6 A) present a strong band at 3423 cm^{-1} and its shoulder near 3198 cm^{-1} , which correspond to the -OH group of the mesoporous silica surface and the aromatic OH, respectively. There were two bands at 1420 and 1379 cm^{-1} , and both bands seem to belong to COH bending vibration. The medium-intensity peak and the weak intensity peaks at 1449 cm^{-1} , 2941 and 2862 cm^{-1} , respectively, corresponds to methylene bridges $-\text{CH}_2-$. The band at 1078 – 1229 cm^{-1} of mesoporous silica-TDI spectra, which was referred to Si–O–Si, was broadened with C_{ar} -O stretching at 1241 cm^{-1} . The bands at 807 and 755 cm^{-1} were related to aromatic torsion vibrations (Furer, Borisoglebskaya, Zverev, & Kovalenko, 2006). The band at 487 cm^{-1} may be assigned to the macrocycle torsion (Furer, et al., 2006).

The spectra of MCM-TDI-C4S (Figure 3.6 B) shows three main bands at 3449, 1446 and 1051 cm^{-1} assigned to the N-H and -OH groups of both hydroxides for the mesoporous silica and the C4S molecule, the weak absorption peak of methylene bridges $-\text{CH}_2-$ and the strong absorption peak of S-O which broadened the peak of Si-O-Si, respectively.

From Figure 3.6 C, it can be seen that the spectra of MCM-TDI-PC4 presents a strong band at 1542 cm^{-1} and its shoulder near 1424 cm^{-1} , which correspond to the phenyl $\nu_{\text{C}_{\text{ar}}-\text{C}_{\text{ar}}}$ and methylene bridges $-\text{CH}_2-$, respectively. The results were closely in agreement with the published data (Huang et al., 2010; Su et al., 2011) and indicated that para-tert-butylcalix[4]arene was successfully bonded on the surface of the MCM-TDI material.

The efficiency of the grafting process was demonstrated by a significant decrease in the isocyanate group band at around 2270 cm^{-1} , with an associated increase of new bands characteristics of the immobilized calix[4]arene derivatives. Meanwhile, the absorption at 2275 cm^{-1} in the spectra of MCM-TDI-C4 and MCM-TDI-C4S disappeared. This indicates that the unattached isocyanate groups reacted with calix[4]arene derivatives, and calix[4]arene derivatives were successfully bonded on the surface of the MCM-TDI. But in the case of MCM-TDI-PC4, the weak absorption peak of the isocyanate group still appears and this may be due to the steric hindrances.

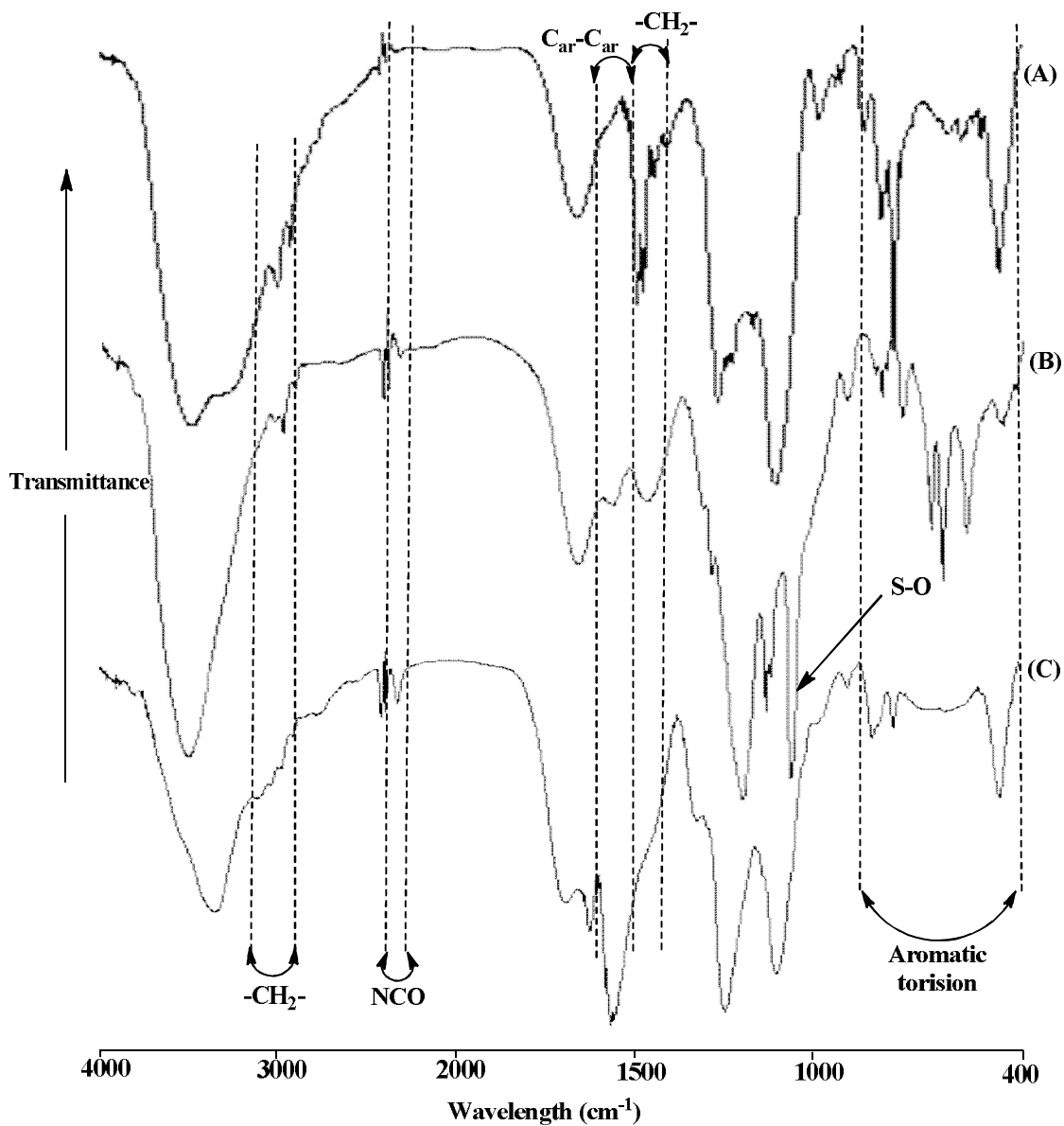


Figure 3.6 FTIR spectra of MCM-TDI-C4 (A), MCM-TDI-C4S (B) and MCM-TDI-PC4 (C)

II. Elemental analysis

Elemental analysis provided further evidence of the successful modification of mesoporous silica. Table 3.1 gives the carbon, hydrogen, nitrogen and sulfur contents of MCM-TDI and mesoporous silica modified with calix[4]arene derivatives. It can be observed that the

amount of carbon in mesoporous silica modified with calix[4]arene derivatives was higher compared to the carbon contents in MCM-TDI.

Table 3.1 Results of elemental analysis for mesoporous silica-TDI, MCM-TDI-C4, MCM-TDI-C4S and MCM-TDI-PC4

Sample	%C	%H	%N	%S
MCM-TDI	18.64	3.04	5.93	-
MCM-TDI-C4	42.64	3.05	1.06	-
MCM-TDI-C4S	33.31	4.16	3.97	4.04
MCM-TDI-PC4	40.53	4.84	4.30	-

III. Thermogravimetric analysis (TGA)

Thermogravimetric analysis of MCM-TDI-calix[4]arene derivatives were determined (Figure 3.7). The weight loss of MCM-TDI-calix[4]arene derivatives occurred at many regions (Table 3.2), and every curve exhibited a stage of weight loss that referred to the loss of a carbamate group. Based on these data, it was proven that the silica was successfully modified with calix[4]arene derivatives.

Table 3.2 Thermogravimetric analysis results of MCM-TDI-C4, MCM-TDI-C4S and MCM-TDI-PC4

Sample	Region °C	Weight-loss %	Assignment
MCM-TDI-C4	45–150	4.9	Moisture
	150–280	8.4	Calix[4]arene
	280–380	21.4	Carbamate group and calix[4]arene
	380–800	32.49	Calix[4]arene
MCM-TDI-C4S	45–150	4.7	Moisture
	150–280	5.9	Carbamate group
	350–800	37.9	Calix[4]arene sulfonate
MCM-TDI-PC4	45–150	2.4	Moisture
	200–350	44.9	Carbamate group and para-tert-butylcalix[4]arene
	400–800	15.7	Para-tert-butylcalix[4]arene

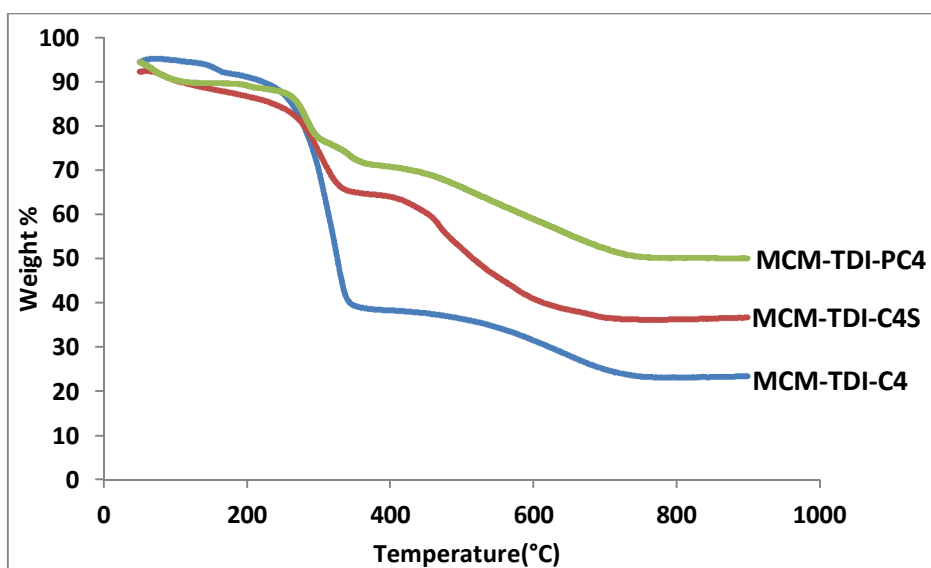


Figure 3.7 TGA analysis of MCM-TDI-C4, MCM-TDI-C4S and MCM-TDI-PC4

As previously discussed (Chapter two, Section 2.1.4), the physical structure of mesoporous silica (high surface area, large pore volume, and others) is one of the major reasons for their effectiveness as a support material. Variations in surface areas, pore volumes and pore sizes have a significant effect on the resulting material. It is therefore necessary to accurately characterize the physical nature of the resulting material.

IV. X-ray powder diffraction (XRD)

Figure 3.8 shows the low angle range X-ray powder diffraction (XRD) patterns of the modified mesoporous silica with calix[4]arene derivatives MCM-TDI-C4, MCM-TDI-C4S and MCM-TDI-PC4. The pure MCM-41 starting material exhibited the peak patterns characteristic of mesoporous silica materials with a hexagonal symmetry (Kresge, et al., 1992): three well-resolved Bragg reflections for 2θ values between 2° , 4° and 5° , one

very intense due to the (100) reflection and two weaker peaks due to (110) and (200) reflections.

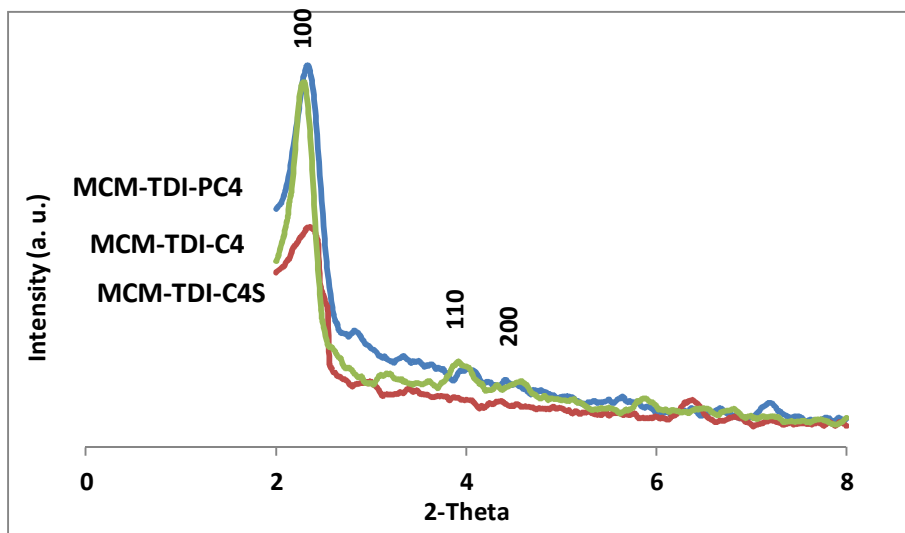


Figure 3.8 X-ray powder diffraction (XRD) analysis of MCM-TDI-C4, MCM-TDI-C4S and MCM-TDI-PC4

Upon functionalization of MCM-41 with calix[4]arene derivatives, the XRD patterns of the samples showed strong (100) peaks and smaller (110) and (200) peak intensities, suggesting that the modification process did not strongly affect the framework integrity of the ordered mesoporous MCM-41. The change in the (100) peak intensities and the small shift to higher 2θ values suggests that calix[4]arene derivatives were present on the internal pore walls of MCM-41 (Sauer, Marlow, & Schuth, 2001). The peaks (110) and (200) showed a decrease in the overall intensities of XRD reflections of MCM-41 after calix[4]arene derivatives functionalization (Figure 3.8). This may be due to the difference of scattering contrast between the amorphous silicate framework and organic moieties, which

are located inside the channels of MCM-41 (Lim & Stein, 1999; Marler, Oberhagemann, Vortmann, & Gies, 1996).

V. Nitrogen adsorption-desorption measurements

In order to further investigate the channel structure of the prepared materials, the characterization of the nitrogen adsorption-desorption was also carried out. The corresponding isotherms are presented in Figure 3.9. They all exhibit the typical Type IV isotherms according to the IUPAC classification (H. Yang, Zhang, Hong, & Zhu, 2004), which correspond to the characteristics of mesoporous materials with highly uniform size distributions.

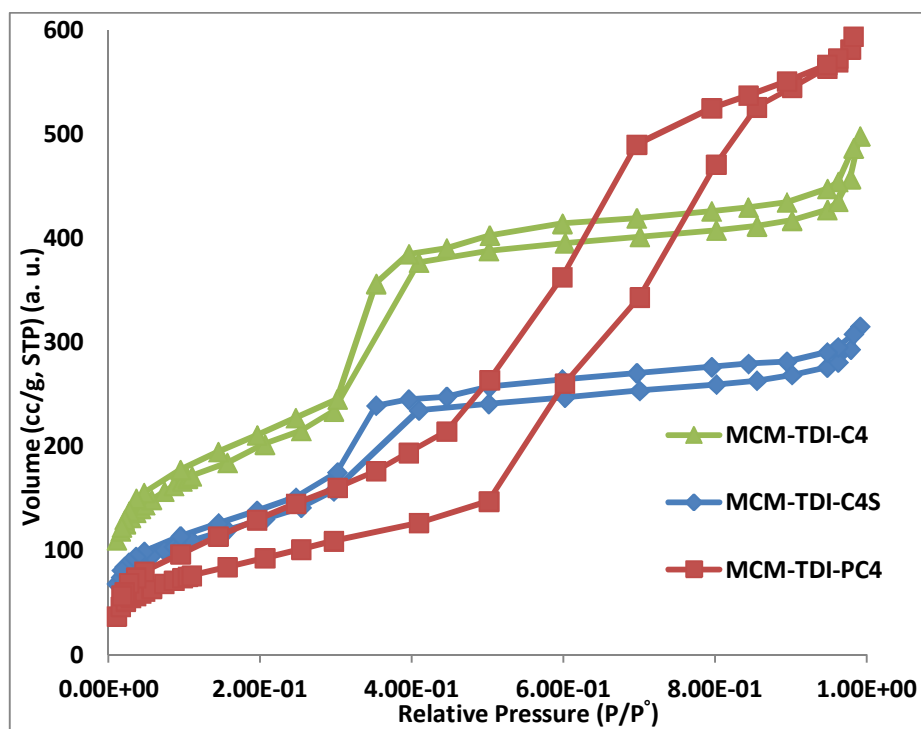


Figure 3.9 Nitrogen adsorption-desorption isotherms of MCM-TDI-C4, MCM-TDI-C4S, and MCM-TDI-PC4

The BET isotherms of the modified samples MCM-TDI-C4 and MCM-TDI-C4S in Figure 3.9 show small hysteresis loops type H1, which is a typical characteristic of mesoporous materials with well-defined cylindrical-like pore channels (Broekhoff, 1979). In case of MCM-TDI-PC4, the BET isotherm shows hysteresis loops type H2, which describes the materials are frequently disordered with not well-defined pore size and shape indicating bottleneck constrictions (Broekhoff, 1979). This may be due to the bulky organic group located inside the pore channel (Caps & Tsang, 2003; Lim & Stein, 1999; Sakthivel, Hijazi, Hanzlik, Chiang, & Kühn, 2005). The structure data of modified mesoporous materials MCM-TDI-C4, MCM-TDI-C4S and MCM-TDI-PC4 (surface area, total pore volume, and pore diameter) are summarized in Table 3.3.

Table 3.3 Structural parameters of MCM-41, MCM-TDI-C4, MCM-TDI-C4S and MCM-TDI-PC4

Sample	S_{BET} (m^2/g)	Pore volume (cm^3/g)	Pore diameter (nm)
MCM-41	993	0.86	2.9
MCM-TDI-C4	733	0.67	3.6
MCM-TDI-C4S	452	0.43	3.8
MCM-TDI-PC4	339	0.32	3.9

The surface area and the total pore volume of all samples have dropped significantly compared with the unfunctionalized sample, MCM-41. The grafted materials also exhibited a broader pore diameter (Table 3.3). The decrease of the pore value and the broad distribution of pore size showed that the calix[4]arene derivatives in the grafted mesoporous samples were mainly located on the internal surfaces of the mesoporous materials (Caps & Tsang, 2003; Lim & Stein, 1999; Sakthivel, et al., 2005). The decrease in the surface area and pore volume were more significant in the case of MCM-TDI-PC4,

and this can be explained as mentioned before due to the presence of bulky organic group, which could lead to partial blockage of the pore channel (Ernst & Selle, 1999).

3.3.3 Characterization of functionalized MCM-41 with CIPTS and TDI as a linker

In this procedure, the MCM-41 was functionalized through a post-synthetic method with 3-chloropropyl triethoxysilane (CIPTS). The chlorine groups were hydrolysed into hydroxyl groups, which react with one of the terminal isocyanate groups of the linking agent (TDI) and forming urethane links. The isocyanate groups at para-positions in TDI would bind with the hydroxyl groups on the surface of OHPTS-MCM preferentially, whereas those at the ortho-positions would be preserved due to steric hindrance within the TDI molecule (R. Arnold, et al., 1957; Simons & Arnold, 1956). The mole amount of the isocyanate groups that reacted with OHPTS-MCM can be regarded as that of TDI that reacted with OHPTS-MCM. The amounts of TDI that reacted with OHPTS-MCM largely depend on the amount of hydroxyls on the surface, therefore in the case of excess of TDI, the amounts of TDI that reacted with OHPTS-MCM were invariable (Che, et al., 2007).

I. Fourier transform infrared spectroscopy (FTIR)

The functionalization of MCM-41 using CIPTS and TDI can be identified using FTIR. Figure 3.10 shows the FTIR spectra of unmodified mesoporous silica and functionalized mesoporous silica with CIPTS and TDI samples, MCM-41 and MCM-PS-TDI, respectively. The spectrum of the unmodified MCM-41 (Figure 3.10 B), as well as the

modified materials (Figure 3.10 A), was dominated by strong bands characteristic of the support matrix, indicating that the support framework remained unchanged.

These bands were present due to the surface hydroxyl groups in the range of 3770–3300 cm^{-1} , and to lattice vibrations in the range 1300–750 cm^{-1} . Bands at about 1215, 1085, 807 and 480 cm^{-1} were assignable to the asymmetric and symmetric stretching ($\nu_{\text{as}}(\text{Si-O-Si})$ and $\nu_{\text{s}}(\text{Si-O-Si})$) of the support framework. The band present at about 970 cm^{-1} was attributable to $\nu(\text{Si-OH})$ vibrations (Alba, et al., 1996; Kureshy, et al., 2005; Shylesh & Singh, 2004).

After anchoring of 3-chloropropyl triethoxysilane (MCM-CIPTS) and subsequent hydrolysis (MCM-OHPTS), the new weak bands arose at 2960 and 2850 cm^{-1} were probably due to the aliphatic ($-\text{CH}_2$) stretching of the propyl chain of the silylating agent (Bhatt et al., 2006), which suggest that the modification of the support material was achieved.

Addition of excess TDI to the MCM-OHPTS resulted in the incorporation of isocyanate functionalities on the surface (MCM-PS-TDI) (Figure 3.10 A). This was evidenced by the appearance of a clearly discernible band at 2282 cm^{-1} corresponding to asymmetric stretching of the appended terminal isocyanate groups, and the appearance of an aromatic C-C stretch at 1560 cm^{-1} in the FTIR spectrum. The signals corresponding to the C=O and C-N stretches of the formed carbamate linkages between the hydroxyl group and the

isocyanate functionality at 1637 cm^{-1} and 1202 cm^{-1} merged with the band of surface hydroxyl groups of mesoporous silica and Si-O-Si band respectively.

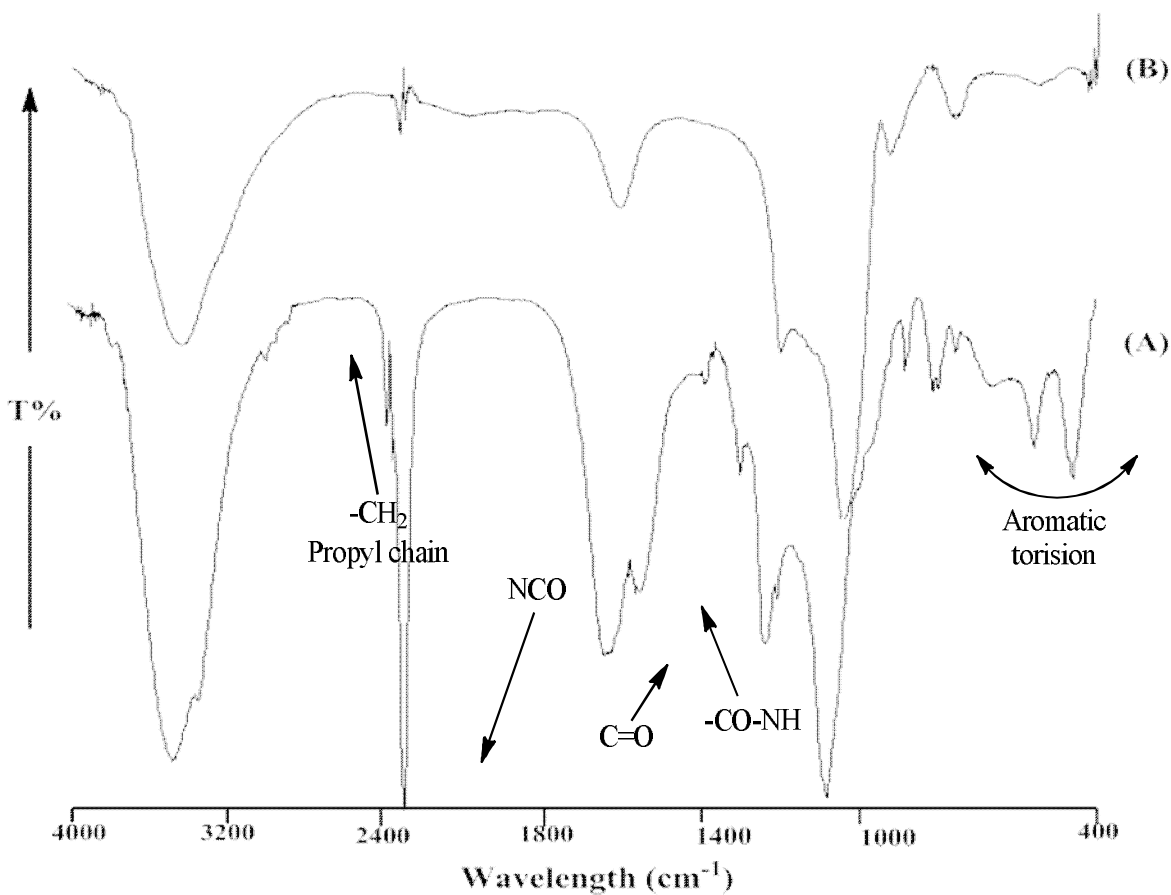


Figure 3.10 Fourier transform infrared spectroscopy (FTIR) spectra of MCM-PS-TDI (A) and MCM-41 (B)

II. Elemental analysis

The carbon and nitrogen content of MCM-PS-TDI increased when compared with the MCM-OHPTS sample, from 3.13% to 20.82% for the total carbon and from 0.14% to 5.03% for the total nitrogen. These data confirmed the attachment of the TDI to the MCM-OHPTS.

III. Thermogravimetric analysis (TGA)

The TGA weight loss curve for MCM-PS-TDI is presented in Figure 3.11. The unmodified MCM-41 (Figure 3.5) as previously established, exhibit a weight loss at about 50 °C corresponding to the loss of physically adsorbed water and with an increase in temperature, the weight loss remained constant, indicating no appreciable condensation of silanol groups on the surface (Iler, 1979; Jaroniec, et al., 1997).

There was a significant change in the weight loss curve with modification of MCM-41 (Figure 3.11). There are three distinct weight-loss regions; the first depicting the loss of any adsorbed water on the surface (between 35 to about 120°C). This was followed by the thermal removal of the organic material in the region of 160-600°C. The removal of organic material took place during the two mass loss steps; the first step was abrupt in the region 160-350°C, which refer to the losses of carbamate group and the organic group in the silylating agent. The second step was broader and considered to complete the decomposition of the remaining organic groups in the region of 400-600°C. The last region of the weight loss curve, above 600°C, may be due to dehydroxylation of the silicate network (Hashemi, et al., 2008).

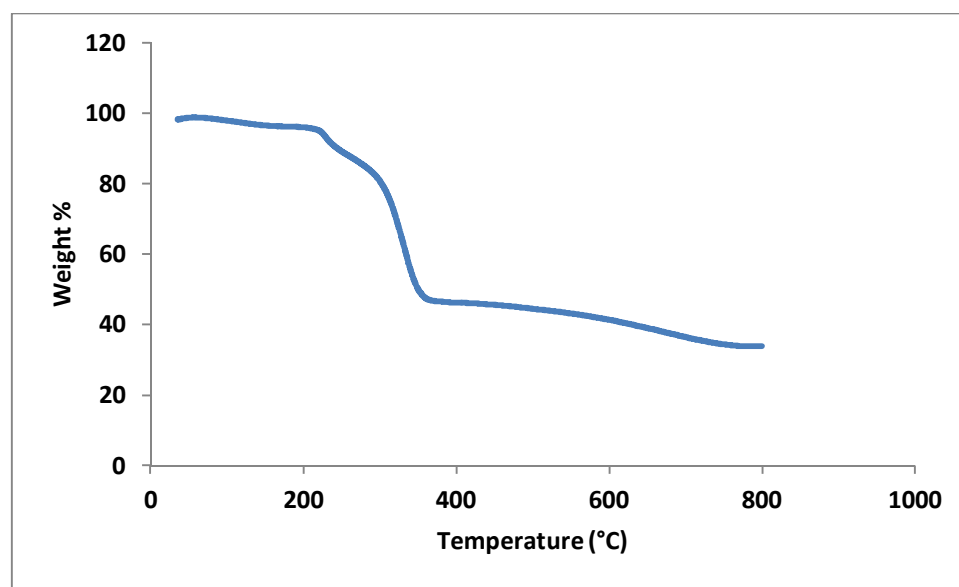


Figure 3.11 Thermogravimetric analysis (TGA) of MCM-PS-TDI

3.3.4 Characterization of functionalized MCM-PS-TDI with calix[4]arene derivatives

I. Fourier transform infrared spectroscopy (FTIR)

Infrared spectroscopy was employed as an important tool to characterize the functional groups of the products. The vibrational spectra obtained from solid samples confirmed the success of the grafting reactions since they displayed bands that are very close to those observed when TDI was used as a linker.

The infrared spectra obtained for MCM-PS-TDI-C4, MCM-PS-TDI-C4S and MCM-PS-TDI-PC4 are shown in Figure 3.12. Typical silica bands associated with the main inorganic backbone can be clearly observed, such as a large, broad band between 3400 and 3200 cm^{-1} attributed to the presence of the O-H stretching frequency of silanol groups bonded to the inorganic structure, and also the intense band related to the Si-O-Si stretching of these

groups at 1080 -1225 cm^{-1} . All spectra showed a large band around 1500- 1650 cm^{-1} due to $\text{C}_{\text{ar}}-\text{C}_{\text{ar}}$ stretching, which confirmed the presence of calix[4]arene derivatives in these materials. The band at 1418 cm^{-1} and 1448 cm^{-1} of MCM-PS-TDI-C4 spectra (Figure 3.12 A), which are referred to $\text{C}_{\text{ar}}-\text{OH}$ and methylene bridges $-\text{CH}_2-$ groups, were broadened with $\text{C}_{\text{ar}}-\text{C}_{\text{ar}}$ stretching at 1541 cm^{-1} . Based on these data, it was proven that the MCM-PS-TDI was successfully modified with calix[4]arene.

The spectrum of MCM-PS-TDI-C4S (Figure 3.12 B) presents new peaks compared to MCM-PS-TDI (Figure 3.10 A). $\text{C}_{\text{ar}}-\text{S}$ peaks and methylene bridges $-\text{CH}_2-$ groups were confirmed by the strong absorptions at 660 and 632 cm^{-1} , and 1443 cm^{-1} , respectively. In addition, the strong absorption peaks for SO_3^- present at 1048 and 1188 cm^{-1} (Xiong, Chen, & Li, 2008). These peaks validated the immobilization of the para-sulfonatocalix[4]arene active groups to the isocyanate functional groups.

In the case of MCM-PS-TDI-PC4, Figure 3.12 C generally shows a strong band at 1542 cm^{-1} and its shoulder near 1418 cm^{-1} , which correspond to the phenyl $\nu\text{C}_{\text{ar}}-\text{C}_{\text{ar}}$ and methylene bridges $-\text{CH}_2-$, respectively, and methyl (CH_3) asymmetric stretching and symmetric vibrations at 2969 and 2862 cm^{-1} , respectively. The weak absorption peak of the isocyanate group appeared in all spectra and this may be due to steric hindrance.

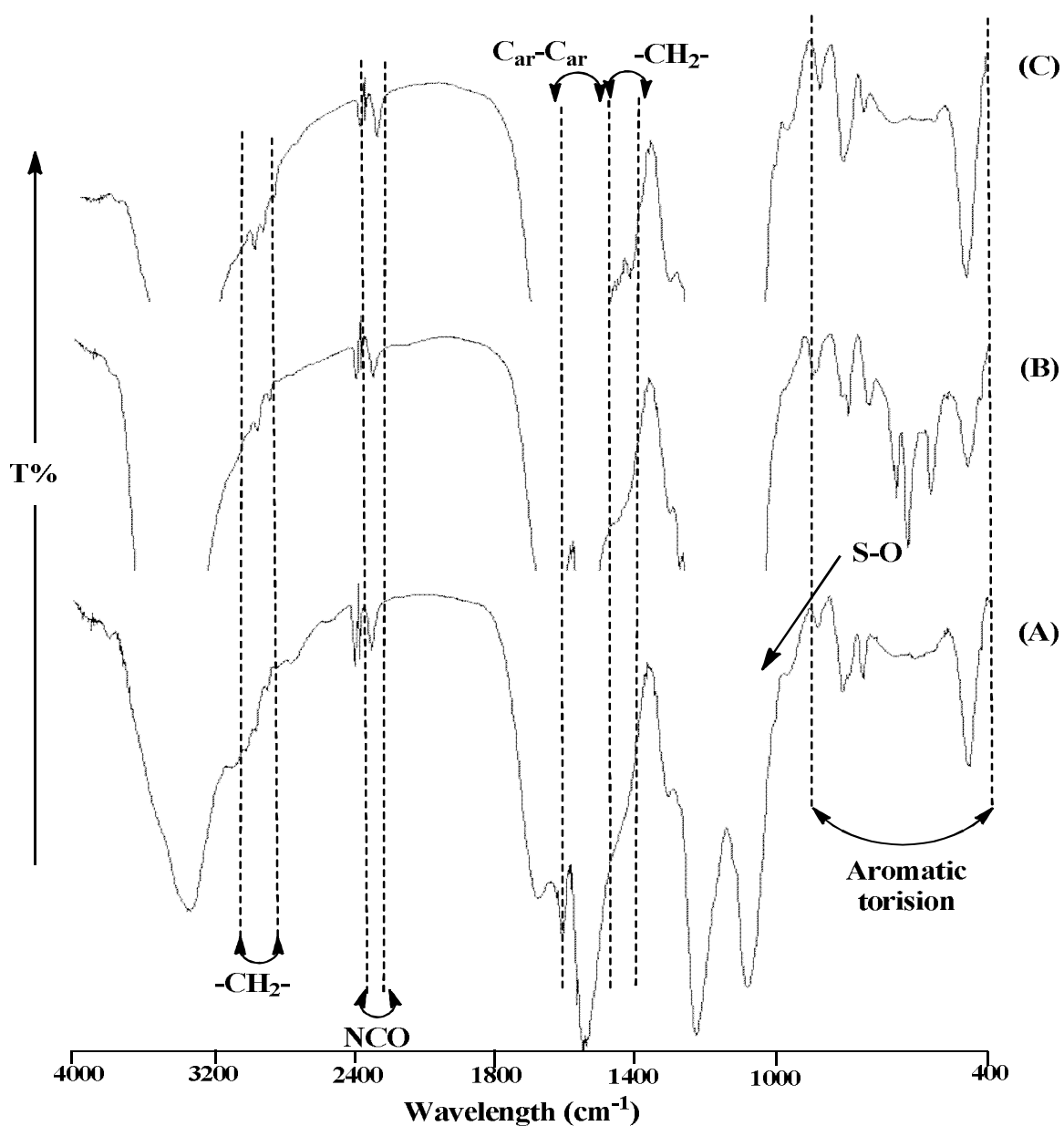


Figure 3.12 FTIR spectra of MCM-PS-TDI-C4 (A), MCM-PS-TDI-C4S (B) and MCM-PS-TDI-PC4 (C)

II. Elemental analysis

Covalent attachment of the calix[4]arene derivatives to MCM-PS-TDI, according to Figure 3.3, was monitored by several techniques. The elemental analysis of the samples (Table

3.4) showed a gradual increase in the carbon content after the modification step. After the reaction of MCM-OHPTS with TDI, the percent of C and N increased from 3.13% and 0.14% to 20.82% and 5.03% respectively, indicating the success of the modification step. After reaction with C4, C4S and PC4, the C content further increased to 30.93%, 25.83% and 33.63% respectively, showing that the calix[4]arene derivatives were attached to the surface.

Table 3.4 Results of elemental analysis for MCM-PS-TDI functionalized with calix[4]arene derivatives

Sample	%C	%H	%N	%S
MCM-PS-TDI-C4	30.93	3.62	5.21	-
MCM-PS-TDI-C4S	25.83	3.23	2.11	3.71
MCM-PS-TDI-PC4	33.63	3.97	4.46	-

III. Thermogravimetric analysis (TGA)

Through the formation of a covalent bond between the calix[4]arene derivatives and the isocyanate group, the calix[4]arene derivatives successfully modified the framework of MCM-PS-TDI materials. Thermal gravimetric analysis was carried out on MCM-PS-TDI-C4, MCM-PS-TDI-C4S and MCM-PS-TDI-PC4 (Figure 3.13).

The functionalized MCM-PS-TDI with calix[4]arene derivatives exhibited a weight loss at about 50°C, which correspond to the loss of physically adsorbed water. With increase in the temperature, there was a significant change in the weight loss curves with functionalized MCM-PS-TDI with calix[4]arene derivatives (MCM-PS-TDI-C4, MCM-PS-TDI-C4S and MCM-PS-TDI-PC4) (Table 3.5). The removal of the organic moiety started at 180-240°C

and continued up to 400 and 600°C. The sharp decrease in weight at 280°C was due to loss of the carbamate group. An additional weight loss occurred at higher temperatures was due to dehydroxylation of the silicate network (Hashemi, et al., 2008).

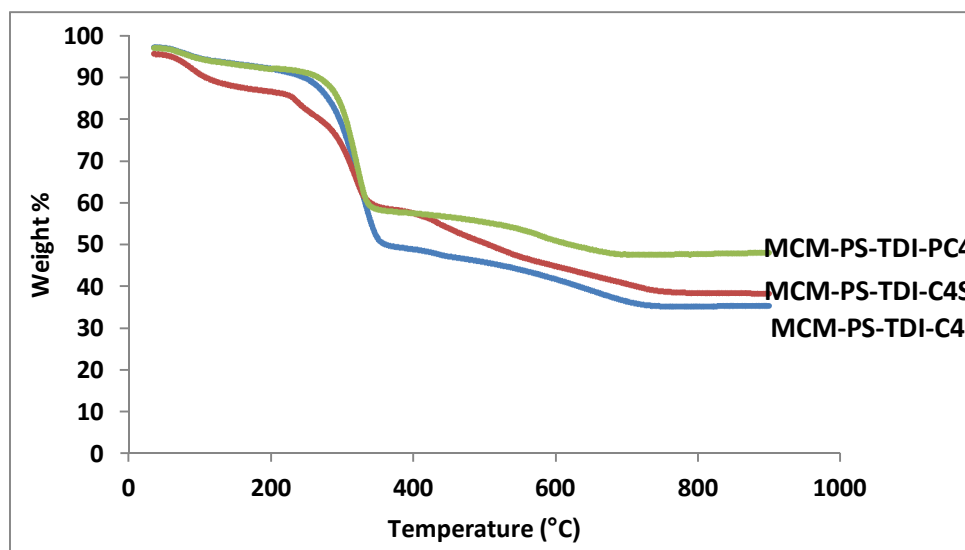


Figure 3.13 TGA analysis of MCM-PS-TDI-C4, MCM-PS-TDI-C4S and MCM-PS-TDI-PC4

Table 3.5 Results of thermogravimetric analysis for MCM-PS-TDI-C4, MCM-PS-TDI-C4S and MCM-PS-TDI-PC4

Sample	Region °C	Weight-loss %	Assignment
MCM-PS-TDI-C4	45–120	3.4	Moisture
	120–200	2.4	Calix[4]arene
	200–350	42.1	Linkers and calix[4]arene
	350–800	14.1	Calix[4]arene
MCM-PS-TDI-C4S	45–150	8.3	Moisture
	280–350	21.8	Linkers
	350–800	19.8	Calix[4]arene sulfonate
MCM-PS-TDI-PC4	45–150	3.3	Moisture
	150–350	34.5	Linkers and para-tert-butylcalix[4]arene
	400–700	10.4	Para-tert-butylcalix[4]arene

IV. X-ray powder diffraction (XRD)

The functionalized ordered mesoporous material, MCM-PS-TDI-C4, MCM-PS-TDI-C4S and MCM-PS-TDI-PC4 were characterized by XRD. The diffraction patterns are shown in Figure 3.14. The XRD patterns of the samples show weak (100) peaks and weaker (110) and (200) peaks. The (100) peak gradually shifts to higher angles, and loss of the peak intensity indicating the presence of the organic moieties on the internal pore walls of MCM-41 (Sauer, et al., 2001). The peaks (110) and (200) showed a decrease in the overall intensities of XRD reflections of MCM-41 after calix[4]arene derivatives functionalization (Figure 3.14). This may be due to the difference of scattering contrast between the amorphous silicate framework and organic moieties, which was located inside the channels of MCM-41 (Lim & Stein, 1999; Marler, et al., 1996).

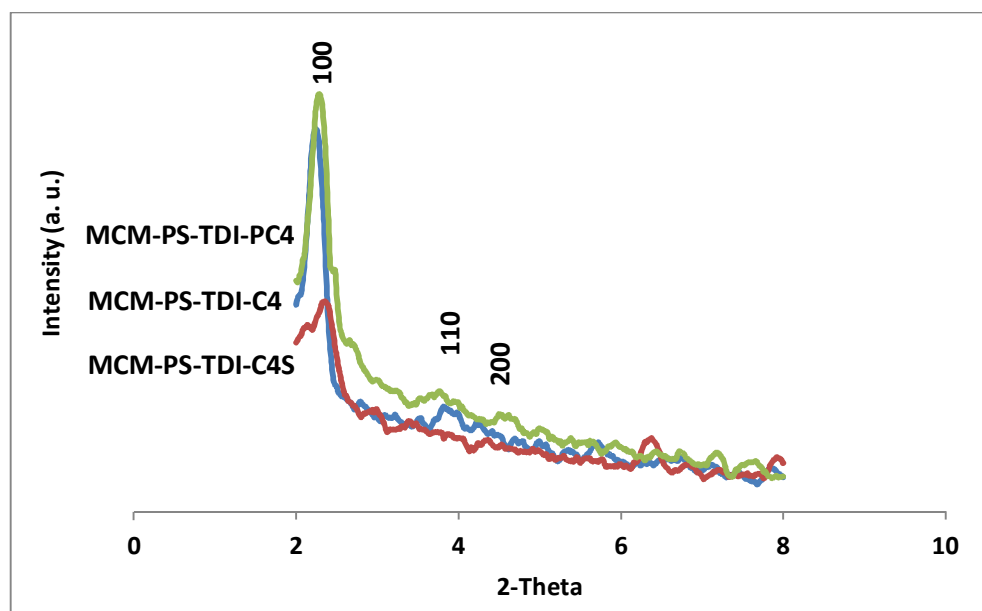


Figure 3.14 XRD analysis of MCM-PS-TDI-C4, MCM-PS-TDI-C4S and MCM-PS-TDI-PC4

V. Nitrogen adsorption-desorption measurements

Nitrogen adsorption-desorption experiments yielded Brunauer-Emmett-Teller (BET) surface area of 993 m²/g for MCM-41 and total pore volume of 0.86. After reaction with the coupling agent and modification with the calix[4]arene derivatives, both the surface area and the total pore volume dropped significantly (Table 3.6).

Figure 3.15 shows the nitrogen adsorption-desorption isotherms for the modified mesoporous silica. All curves presented a Type II isotherm, the characteristic of non-porous or macroporous adsorbent with strong adsorbate-adsorbent interactions. Furthermore, adsorption isotherms were of Type II in the IUPAC classification that represents monolayer/multilayer adsorption. Similar results obtained by Li et al., (H. Li et al., 2008) and they concluded that the presence of a large amount of organic molecule will partially disrupt the assembly process and leading to a decrease in the ordering degree of mesoporous structure.

Type II adsorption isotherm suggests that adsorption of N₂ for the adsorbent materials was moderate or, on the other hand, that the main adsorption process may be ascribed to the van der Waals force. Generally, the isotherm shows that the amount of N₂ adsorbed increased as the relative pressure increased up to a saturation point. A complete adsorption of N₂ as a monolayer onto the surface of adsorbent material is shown by the plateau of the adsorption isotherm. After this point, a large uptake of N₂ was observed close to the saturation pressure and it was assumed that multilayer adsorption took place (i.e. implying the presence of mesopores) (Carmody, Frost, Xi, & Kokot, 2007).

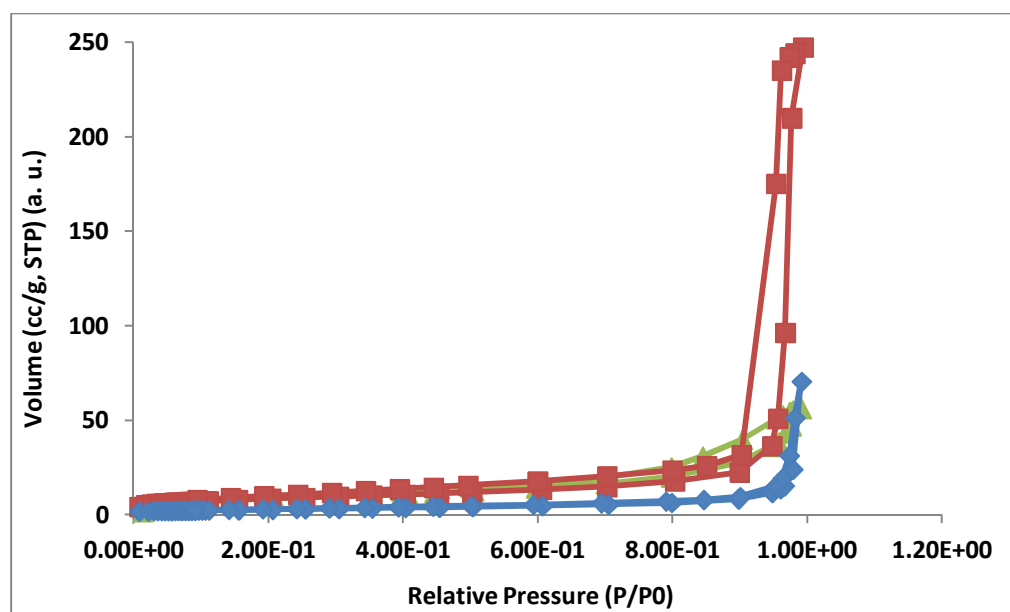


Figure 3.15 Nitrogen adsorption-desorption isotherms of MCM-PS-TDI-C4 (Δ), MCM-PS-TDI-C4S (\square) and MCM-PS-TDI-PC4 (\diamond)

The grafted materials exhibited a broader pore diameter and also displayed a decrease in surface area and pore volume (Table 3.6). The decrease of the pore volume and the surface area were the evidence that the calix[4]arene derivatives in the grafted mesoporous samples were located mainly on the internal surface of the mesoporous materials (Caps & Tsang, 2003; Lim & Stein, 1999; Sakthivel, et al., 2005)

There are commonalities between the three sorbents, namely the low surface area and limited pore volume available for the adsorption processes in the micropores (Table 3.6). This suggests that the main adsorption mechanism for these sorbents occurred on the external surface of the material in the diffusion region (Carmody, et al., 2007).

Table 3.6 Structural parameters of MCM-41, MCM-PS-TDI-C4, MCM-PS-TDI-C4S and MCM-PS-TDI-PC4

Sample	S_{BET} (m^2/g)	Pore volume (cm^3/g)	Pore diameter (nm)
MCM-41	993	0.86	2.9
MCM-PS-TDI-C4	32.1	0.45	11.8
MCM-PS-TDI-C4S	30.6	0.38	9.7
MCM-PS-TDI-PC4	10.4	0.11	22.1

In comparison to mesoporous silica functionalized with only TDI, these materials showed different isotherm shape in addition to the lower surface area and pore volume. This can be explained due to the modification steps, as the modification using CIPTS and TDI as a linkers were performed in three steps. Furthermore, the organic bulky modifier (calix[4]arene derivatives, CIPTS and TDI) may block the pore channel, which resulted in lower surface area and pore volume. Previous studies of functionalization of mesoporous silica have reported similar changes (Blasco, Corma, Martínez, & Martínez-Escolano, 1998; S. Kim, Ida, Guliants, & Lin, 2005).

3.4 Summary

In this chapter, we report the successful anchoring of calix[4]arene derivatives onto the MCM-41 surface using toluene-2,4-diisocyanate (TDI) and 3-chloropropyl triethoxysilane (CIPTS). In the first method, calix[4]arene derivatives were covalently attached to the unmodified MCM-41 support using (TDI) as linker. The isocyanate groups at para-positions in TDI would bind with the hydroxyl groups on the surface of mesoporous silica preferentially, whereas those at the ortho-positions would react with the hydroxyl groups at calix[4]arene derivatives. In the second method, MCM-41 was functionalized through a post-synthetic method with 3-chloropropyl triethoxysilane (CIPTS) and TDI. The chlorine

groups were hydrolysed into hydroxyl groups, which then react with one of the terminal isocyanate groups of the linking agent (TDI), forming urethane links. The other terminal isocyanate functionality reacts with the free hydroxyl group present in the calix[4]arene derivatives. Different characterization techniques such as FTIR, XRD, CHN, BET and TGA analyses showed evidences that the calix[4]arene derivatives were covalently attached to the MCM-41 surface and that its channel structure remained unchanged.

CHAPTER 4

SYNTHESIS AND CHARACTERIZATION OF FUNCTIONALIZED ORDERED MESOPOROUS SILICA MCM-41 WITH β - CYCLODEXTRIN

4.1 Introduction

Synthesized porous materials possessing tailored properties is among the most attractive areas of study in material science (Davis, 1993; Holland, Blanford, & Stein, 1998; Imhof & Pine, 1997; Wijnhoven & Vos, 1998; D. Zhao, Feng, et al., 1998). The pioneering mesoporous silica material having regular pore channels ranging from 20-100 Å was reported in 1992 (Beck, Vartuli, et al., 1992; Kresge, et al., 1992). From then on, the mesoporous inorganic materials synthesized through the use of a structure-directing template has been in the limelight (van Bommel, Friggeri, & Shinkai, 2003).

Currently, a new generation of the mesoporous hybrid silica possessing organic groups on their surface of ordered mesoporous silica was created through grafting or anchoring organic guests on the surface of the mesopore channel (X. Feng, et al., 1997; Fryxell et al., 1999; Y. Lin, Fryxell, Wu, & Engelhard, 2001; J. Liu et al., 1998) or directly to the organic groups by condensation of organo-trialkoxysilanes along with tetra-alkoxysilanes (TEOS or TMOS) (Kruk, Asefa, Jaroniec, & Ozin, 2002; Lebeau, Fowler, Hall, & Mann, 1999; Lim, Blanford, & Stein, 1998; C. Liu, Lambert, & Fu, 2003; Duncan J Macquarrie, 1996; Mercier & Pinnavaia, 2000; Mori & Pinnavaia, 2001). This novel group of hybrid

mesoporous materials holds an attractive interest in the field of environmental remediation and chromatographic separation because of the presence of high surface areas and organic functional groups.

β -cyclodextrins (β -CDs) are described as cyclic oligosaccharides comprising of six D-glucopyranose units linked by α -(1,4)-linkage. They can be represented in a spatial way as a torus having wide and narrow openings that respectively correspond to secondary and primary hydroxyl groups and can encapsulate many compounds because of the hydrophobic character of the internal cavity (Szejtli, 1998). This unique feature has been used in pharmaceutical, food, cosmetic and textile industries, and has long been utilized in the field of catalysis, environmental remediation, chemical sensing and enantiomeric separations (Hashimoto, 2002; Szejtli, 1998; K. Takahashi, 1998). Particular applications call for the immobilization of cyclodextrins or cyclodextrin derivatives in an insoluble support. Various studies have been conducted with the help of organic materials (Cserhádi, 1994; L. Janus et al., 1999; Ma & Li, 1999), metal surfaces (Hill, Fallourd, & Klockow, 1999; Nelles et al., 1996) and inorganic oxide supports.

For the latter supports, mesoporous silica is the most commonly utilized for the production of functionalized materials owing to their great physical strength and chemical inertness (Bibby & Mercier, 2003; Y.-Q. Feng, Xie, & Da, 2000; Guo et al., 2010; Huq, Mercier, & Kooyman, 2001; H. Kim et al., 2010; C. Liu, et al., 2003; C. Liu, Lambert, & Fu, 2004; Park, Lee, & Kim, 2009).

A variety of coupling agents have also been utilized to functionalize mesoporous silica such as organosilanes with particular functional groups; for instance, chloride, carboxylic acid, thiol and amine. Isocyanates are considered to be highly reactive with –OH groups, leading to the formation of urethane bonds (Chun, et al., 2002; Xia & Song, 2006), which depend on the diisocyanate utilized and at least as strong as those obtained with the organosilane binders (Chun, et al., 2002).

In this part, mesoporous silica MCM-41 was functionalized with β -cyclodextrins molecule by post-grafting methods using linking agents consisting of an organosilane (3-chloropropyl triethoxysilane-CIPTS) and a diisocyanate (TDI). Both methods used toluene-2,4-diisocyanate (TDI) as a coupling agent, where one of the isocyanate endings attached to the organosilane -OH ending (method 1), or to the silica surface (method 2), while the other isocyanate ending remains available for the reaction with β -cyclodextrins. Another main purpose of this chapter is to identify and select an effective adsorbent from prepared materials at chapters three and four for removal of organotin compounds (tributyltin TBT, triphenyltin TPT and dibutyltin DBT).

4.2 Experimental

4.2.1 Materials

The chemicals used in this part of the thesis are as follows: Mesoporous silica [Aldrich, surface area of 993 m²/g, average diameter of 2.9 nm] as silica source while β -cyclodextrins [C₄₂H₇₀O₃₅, Acros] was the organic modifier. 3-chloropropyl triethoxysilane

(CIPTS) [C₉H₂₁ClO₃Si, Aldrich] and toluene-2,4-diisocyanate (TDI) [C₉H₆N₂O₂, Aldrich] were the organic linker. Triethylamine [C₆H₁₅N, SAFC] was used as the catalyst. Toluene [Fisher, dried before use by using molecular sieves], ethanol [Fisher] and acetone [Fisher] were used as solvents. Water was purified using Milli-Q purification equipment. The structures of some of these compounds are shown in Figure 4.1. For screening experiments, tributyltin chloride (C₁₂H₂₇ClSn, Aldrich), triphenyltin chloride (C₁₈H₁₅ClSn, Fluka) and dibutyltin dichloride (C₈H₁₈Cl₂Sn, Aldrich) concentrations were adjusted by successive dilutions with Milli-Q water of an 8.42 mM solutions in methanol stored at 4°C in the dark.

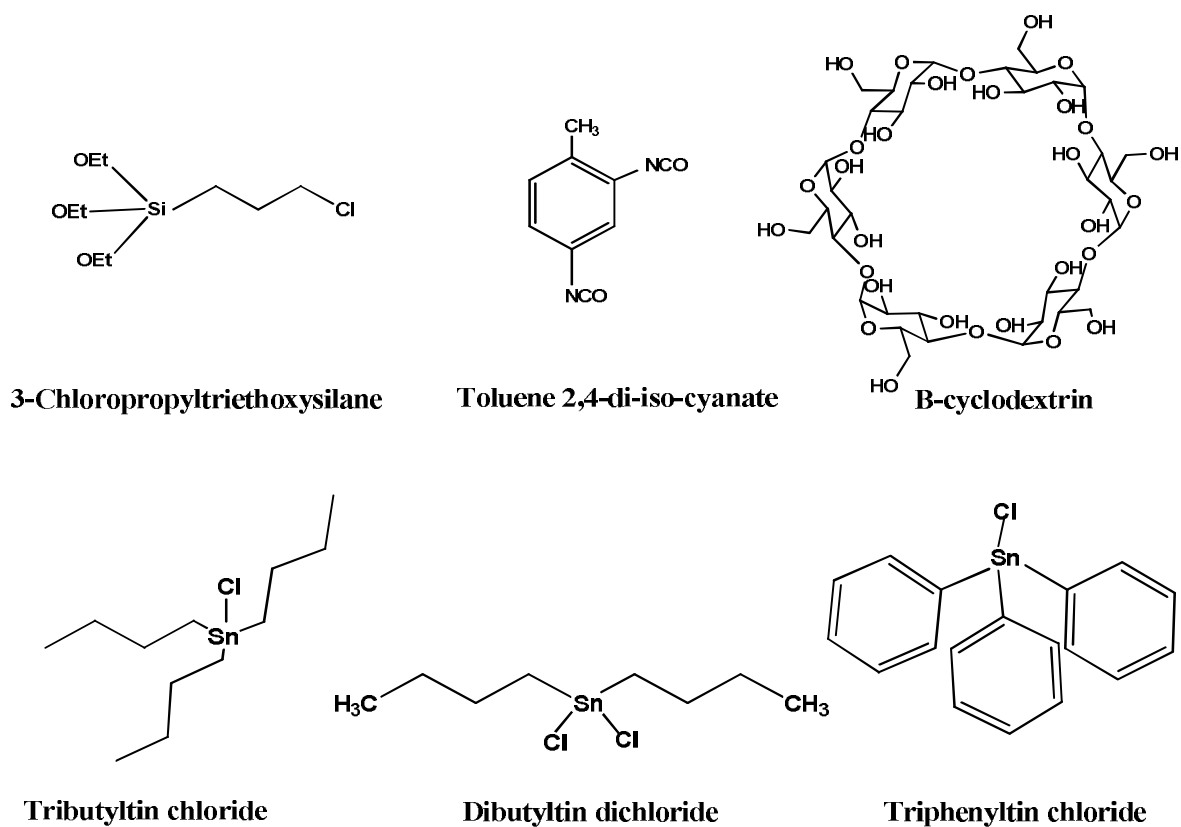


Figure 4.1 Molecular structures of some materials

4.2.2 Instrumentation

In addition to the characterization techniques that were discussed previously in detail in Chapter three Section 3.2.2, inductively coupled plasma mass spectrometry (ICP-MS) was used for the adsorption measurements.

All the adsorption measurements were carried out using an Agilent Technology 7500 series inductively coupled plasma mass spectrometry ICP-MS for the determination of organotin compounds in aqueous solutions. The ICP-MS condition was shown in Table 4.1. A series of Sn standard solutions were used to construct the calibration curve, where a good linear relationship was observed.

Table 4.1 ICP-MS conditions

Parameter	Value
RF power (W)	1550
Sampling depth (mm)	8
Carrier gas flow (L/min)	0.9
Make-up gas flow (L/min)	0.28
O ₂ /Ar mixed gas	0
Chamber temperature	2°C
Nebuliser	Babington
Cones	Ni

4.2.3 Synthesis methods

4.2.3.1 Preparation of 3-hydroxypropyl triethylsilyl functionalized MCM-41

Surface functionalization of MCM-41 with CIPTS was carried out by a procedure described by Feng et al. (X. Feng, et al., 1997). The modification of the surface of MCM-41 was performed according to Figure 4.2 (route a).

The MCM-41 support was dehydrated (150°C, overnight) and a self-assembled monolayer of the initial silane was produced by suspending 1.0 g of MCM-41 in 40 ml of toluene in a 100 ml round-bottom flask. The suspension was stirred vigorously for 5 min before adding 0.30 ml of DI water and the stirring was continued for 2 h. A slight excess of the silane (10 %), 2.18 ml of 3-chloropropyl triethoxysilane corresponding to 9.07 mmol was then added and the solution was refluxed for 6 h. The solids were then filtered and washed copiously with toluene and acetone to remove the unreacted silane and then dried overnight. The obtained modified material was denoted as CIPTS-MCM. The chlorine groups present in the CIPTS-MCM were hydrolysed into hydroxyl groups by heating 1.0 g of the solid material with a solution of methanol: water (1:1) for 2 h at 60°C. The hydrolysed material (OHPTS-MCM) was filtered and dried at 110°C overnight.

4.2.3.2 Immobilizing β -cyclodextrins onto the functionalized MCM-41

β -cyclodextrin was anchored on the MCM-41 surface by using TDI as a linking agent (Figure 4.2, route (a) and (b)). The materials were prepared by refluxing the hydroxyl modified material, OHPTS-MCM (route a), and the unmodified MCM-41 (route b) with excess of TDI (dried by molecular sieve for 24 h) in a dry nitrogen atmosphere at 80°C for 4 h (M. Yang, et al., 2007). After cooling down, the material was filtered, washed and dried overnight.

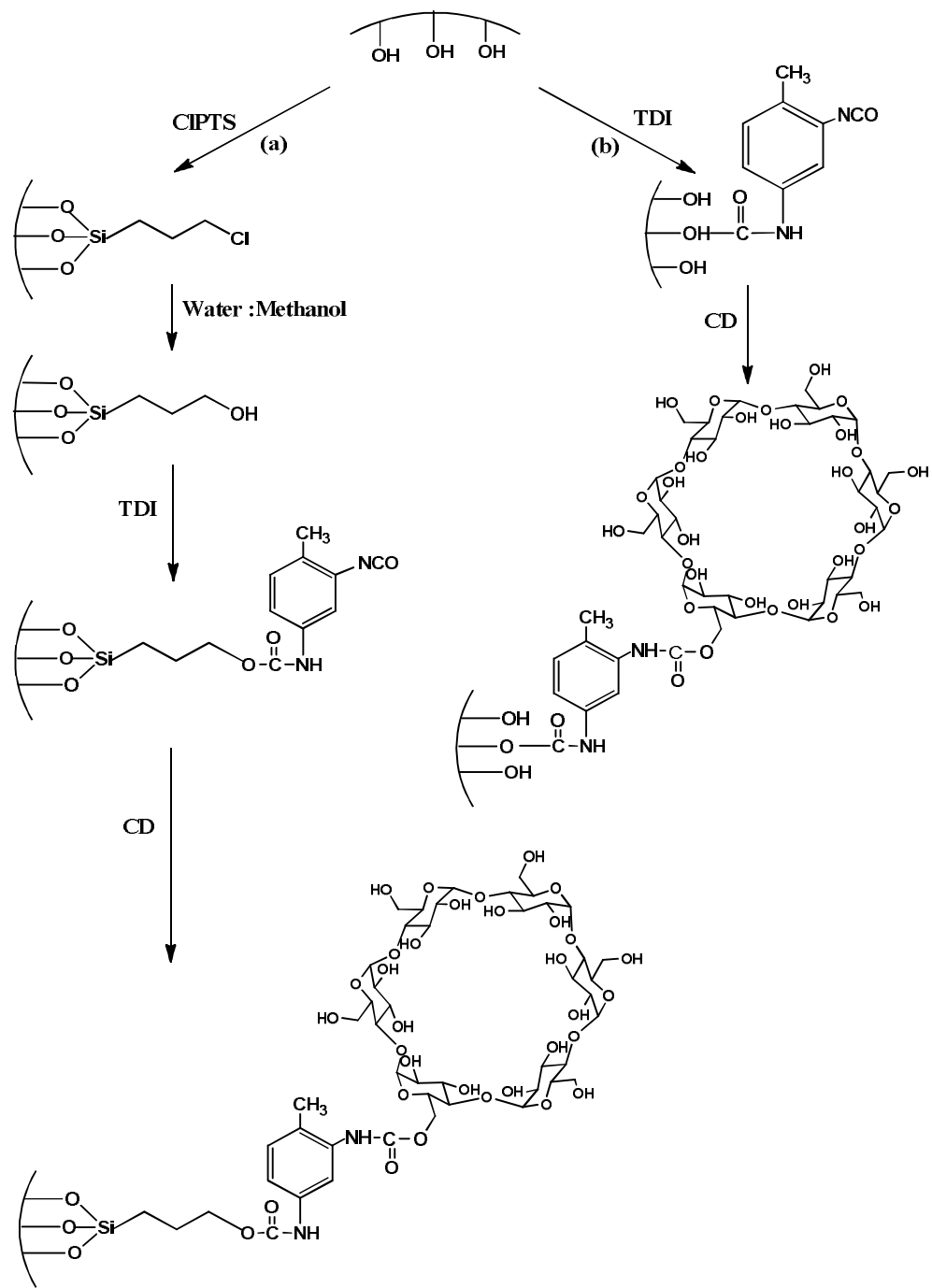


Figure 4.2 Preparation of modified mesoporous silica with β -cyclodextrin

1.8 mmol and 2.0 mmol β -cyclodextrin (calculated from Section 3.2.3.3) were added into the modified mesoporous silica with TDI (route a and b respectively) (1.0 gm) suspension with toluene (dried by molecular sieve for 24 h). Subsequently, few drops of triethylamine were added and the reaction temperature was kept at 80°C for 24 h under continuous stirring. The obtained modified materials were filtered, washed by toluene and acetone and was later dried. The materials obtained from the OHPTS/TDI-method (route a) were denoted as MCM-PS-TDI- β -CD, and those obtained from the TDI-method (route b) were labeled as MCM-TDI- β -CD.

4.2.3.3 Screening experiments

The screening experiments were performed according to the batch method. Eight samples (MCM-TDI-C4, MCM-TDI-PC4, MCM-TDI-C4S, MCM-PS-TDI-C4, MCM-PS-TDI-PC4, MCM-PS-TDI-C4S, MCM-TDI- β -CD and MCM-TDI- β -CD) were screened for their ability in organotin compounds removal (tributyltin TBT, triphenyltin TPT and dibutyltin DBT). The screening experiments were repeated 3 times and the average of the resulting removal efficiency was reported.

In this method, 0.01 g of modified mesoporous silica with calix[4]arene derivatives and β -cyclodextrin were mixed with 10 ml organotin solutions at 2 mg/L into 50-ml Teflon reactors (FEP, Nalgene). The mixtures were sealed and shaken at 180 rpm and 30°C for 3 h. The mixtures were then filtered using 0.45 μ m microporous membrane filters. The concentration of organotin remaining (C_e) in aqueous phase after the sorption was then

determined by ICP-MS. The amount of organotin sorbed by modified mesoporous silica with calix[4]arene derivatives and β -cyclodextrin (q_e) was calculated as:

$$q_e = \frac{(C_o - C_e)V}{w} \quad 4.1$$

where q_e is the amount of organotin adsorbed (mg/g), C_o is the initial aqueous concentration of organotin (mg/L), C_e is the concentration of organotin after shaking for a certain period of time (mg/L), V is the volume of the solution (L) and w is the mass of the modified mesoporous silica (g). Experiments were performed in triplicate and the results were averaged.

4.3 Results and discussion

β -cyclodextrin was anchored on the MCM-41 support using TDI as a linking agent. However, two different methodologies were used. In the first method (Figure 4.2, (a)) of OHPTS/TDI-method, MCM-41 was functionalized through a post-synthetic method with 3-chloropropyl triethoxysilane (CIPTS). The chlorine groups were hydrolysed into hydroxyl groups, which react with one of the terminal isocyanate groups of the linking agent, forming urethane links. The other terminal isocyanate functionality reacts with the free hydroxyl groups present in the β -cyclodextrin. In the second method (Figure 4.2, (b)) of TDI method, β -cyclodextrin was covalently attached to the unmodified MCM-41 support using (TDI) as linker. The isocyanate groups at para-positions in TDI would bind with the

hydroxyl groups on the surface of mesoporous silica preferentially, whereas those at the ortho-positions would react with hydroxyl group at β -cyclodextrin.

4.3.1 Characterization of functionalized MCM-41 with β -cyclodextrin

I. Fourier transform infrared spectroscopy (FTIR)

Infrared spectroscopy was employed to characterize the functional groups of the products. The vibrational spectra obtained from solid samples confirmed the success of the grafting reactions.

The typical MCM-41 silica bands associated with the main inorganic backbone that have been discussed previously in Chapter 3 Sections 3.3.1 and 3.3.3 were present. Additional bands were also observed in both spectra that confirmed the presence of organic pendant groups. After anchoring of 3-chloropropyl triethoxysilane (MCM-CIPTS) and subsequent hydrolysis (MCM-OHPTS), new weak bands arose at 2960 and 2850 cm^{-1} , probably due to the aliphatic ($-\text{CH}_2$) stretching of the propyl chain of the silylating agent, which suggest that the modification of the support material was achieved (Bhatt, et al., 2006; Caps & Tsang, 2003).

Addition of excess TDI to the MCM-OHPTS and MCM-41 resulted in the incorporation of isocyanate functionalities on the surface of the MCM-OHPTS (Figure 4.3 B) and mesoporous silica (Figure 4.3 C). This was evidenced by the appearance of a clearly discernible band at 2282 cm^{-1} corresponding to the asymmetric stretching of the appended

terminal isocyanate groups, and the appearance of an aromatic C-C stretch at 1560 cm^{-1} in the FTIR spectrum. The signals corresponding to the C=O and C-N stretches of the formed carbamate linkages between the hydroxyl group and the isocyanate functionality at 1637 cm^{-1} and 1202 cm^{-1} merged with the band of surface hydroxyl groups of mesoporous silica and Si-O-Si band, respectively. The surface isocyanate functionalities could then be treated with β -cyclodextrin in dry toluene at 80°C for 24 h.

These functionalization reactions were again followed by FTIR spectroscopy to monitor the appearance and disappearance of some peaks (Figure 4.3 D and Figure 4.3 E). In detail, the absence of the -NCO characteristic band at about 2282 cm^{-1} , indicates that both functional groups of toluene-2,4-diisocyanate have reacted (Oliveira, et al., 2007). In addition, the bands at 2927 and 2850 cm^{-1} were more intense and a new band arose at 1425 cm^{-1} , which may be due to the (-CH₂) bending (Bhatt, et al., 2006).

The efficiency of the grafting process was demonstrated by a significant decrease in the isocyanate group band at around 2280 cm^{-1} , with an associated increase of new bands characteristics of the immobilized β -cyclodextrin. Meanwhile, the absorption at 2282 cm^{-1} in the spectra of MCM-PS-TDI- β -CD and MCM-TDI- β -CD disappeared. This indicates that the unattached isocyanate groups reacted with β -cyclodextrin, and β -cyclodextrin was successfully bonded on the surface of the MCM-TDI and MCM-PS-TDI.

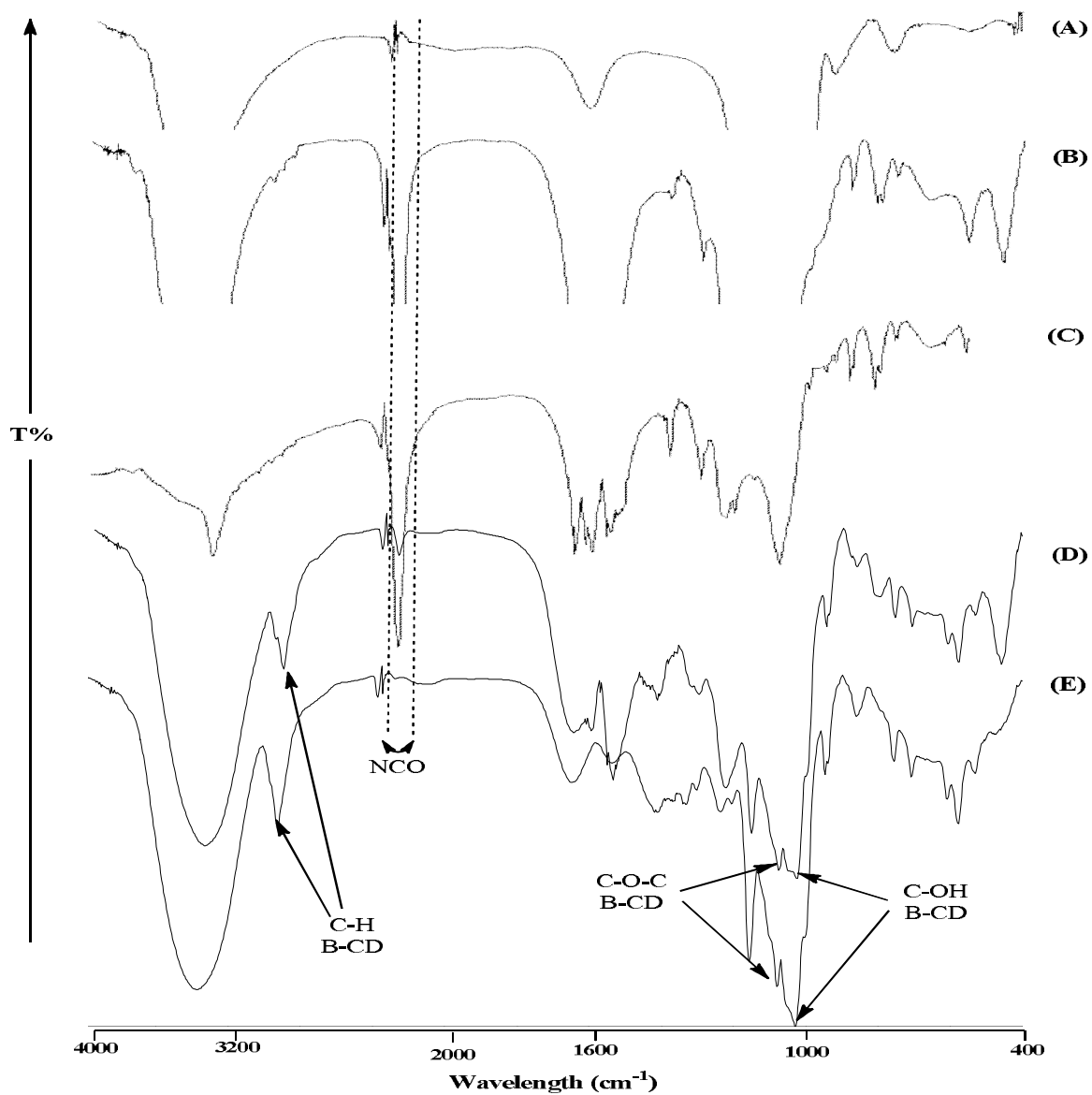


Figure 4.3 FTIR spectra of MCM-41 (A), MCM-PS-TDI (B) MCM-TDI (C), MCM-PS-TDI- β -CD (D) and MCM-TDI- β -CD (E)

II. Thermogravimetric analysis

Thermogravimetric analysis of functionalized mesoporous silica MCM-PS-TDI- β -CD, and MCM-TDI- β -CD were determined (Figure 4.4). Functionalized mesoporous silica curves exhibited a stage of weight loss below 100°C due to the loss of the adsorbed water. After

the initial loss of adsorbed water, the removal of the linkers occurred (Table 4.2). The removal of β -cyclodextrin started at 310°C and continued up to 600°C. An additional weight loss occurred at higher temperatures due to further condensation of the silicate walls, as observed in other mesoporous silicates.

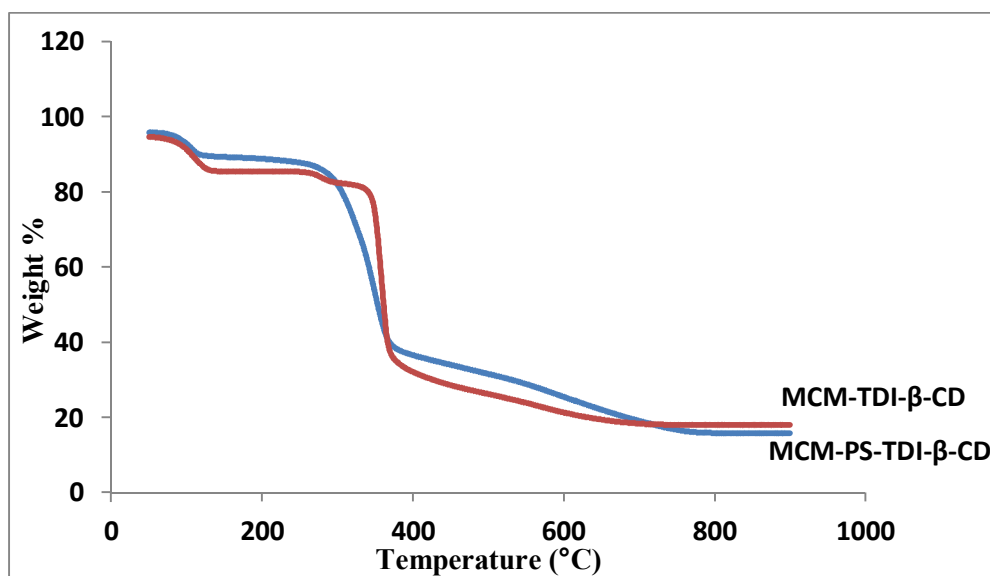


Figure 4.4 TGA analysis of MCM-PS-TDI-β-CD and MCM-TDI-β-CD

Table 4.2 Thermogravimetric analysis results of MCM-PS-TDI-β-CD and MCM-TDI-β-CD

	Region° C	Weight-loss %	Assignment
MCM-PS-TDI- β-CD	50-120	6.7	Moisture
	150-400	53.2	PTS, carbamate group and β-CD
	400-600	20.1	β-CD
MCM-TDI- β-CD	50-120	9.2	Moisture
	240-310	3.5	Carbamate group
	310-600	63.8	β-CD

III. Elemental analysis

Covalent attachment of β -cyclodextrin to MCM-PS-TDI, according to Figure 4.2, was monitored by several techniques. The elemental analysis of the samples (Table 4.3) showed a gradual increase in the carbon content after the modification step. After reaction of MCM-PS with TDI, the percent of C and N rose from 3.13% and 0.14% to 20.82% and 5.03%, respectively, indicating the success of the modification step. After reaction with β -cyclodextrin, the carbon content further increased (Table 4.3), showing that β -cyclodextrin was attached to the silicate surface.

Table 4.3 Results of elemental analysis for MCM-PS, MCM-PS-TDI, MCM-PS-TDI- β -CD, MCM-TDI, MCM-TDI- β -CD

	%C	%H	%N
MCM-PS	3.13	3.24	0.14
MCM-PS-TDI	20.82	4.21	5.03
MCM-PS-TDI- β -CD	39.01	6.60	3.61
MCM-TDI	18.64	3.04	5.93
MCM-TDI- β -CD	36.41	5.21	4.72

IV. XRD diffraction

Figure 4.5 shows the low angle range of XRD patterns for the modified mesoporous silica MCM-41 with β -cyclodextrin materials. The XRD patterns of the samples show strong (100) peaks and smaller (110) and (200) peak intensities, suggesting that the modification process did not strongly affect the framework integrity of the ordered mesoporous MCM-41. The change in the (100) peak intensities and the small shift to higher 2θ values suggests that β -cyclodextrin was present on the internal pore walls of MCM-41 (Sauer, et al., 2001), which leads to an increase of phase cancellation between scattering from the walls and the

pore regions (Hammond, Prouzet, Mahanti, & Pinnavaia, 1999; Köhn & Fröba, 2001), and this was significant in the case of MCM-PS-TDI- β -CD. It can also be noticed that the (100) peak has become broader in the case of MCM-TDI- β -CD, indicating a slight alteration of the order of the mesoporous structure.

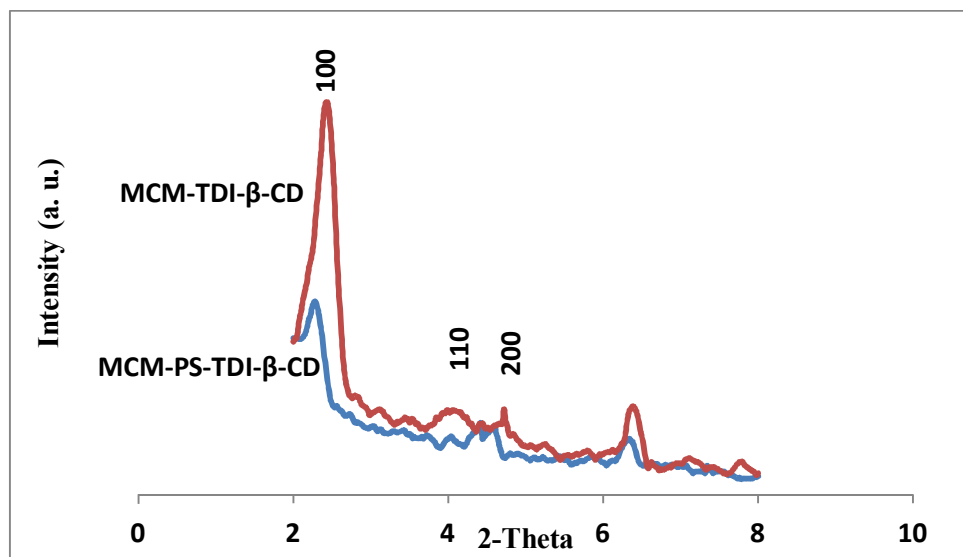


Figure 4.5 XRD analysis of MCM-PS-TDI- β -CD and MCM-TDI- β -CD

V. Nitrogen adsorption-desorption measurements

In order to further investigate the channel structure of these materials, the characterization of the nitrogen adsorption-desorption was also carried out. The corresponding isotherms are presented in Figure 4.6. MCM-TDI- β -CD exhibited the typical type Type IV isotherm according to the IUPAC classification, but MCM-PS-TDI- β -CD exhibited Type III isotherm (describing adsorption on non-porous or macroporous adsorbent with weak adsorbate-adsorbent interactions). In addition, the modified sample MCM-TDI- β -CD showed hysteresis loops type H2, which described that materials were frequently disordered

with not well-defined pore size and shape, indicating bottleneck constrictions (Broekhoff, 1979).

The structure data of these mesoporous materials (BET surface area, total pore volume and pore diameter) are summarized in Table 4.4. The prepared materials showed a decrease in the BET surface area and pore volume, which suggests the presence of bulky materials inside the support porous system (H. Yang, et al., 2004).

Table 4.4 Structural parameters of MCM-41, MCM-PS-TDI- β -CD and MCM-TDI- β -CD

Sample	S_{BET} (m ² /g)	Pore volume (cm ³ /g)	Pore diameter (nm)
MCM-41	993	0.86	2.9
MCM-PS-TDI- β -CD	14	0.023	6.7
MCM-TDI- β -CD	147	0.17	4.48

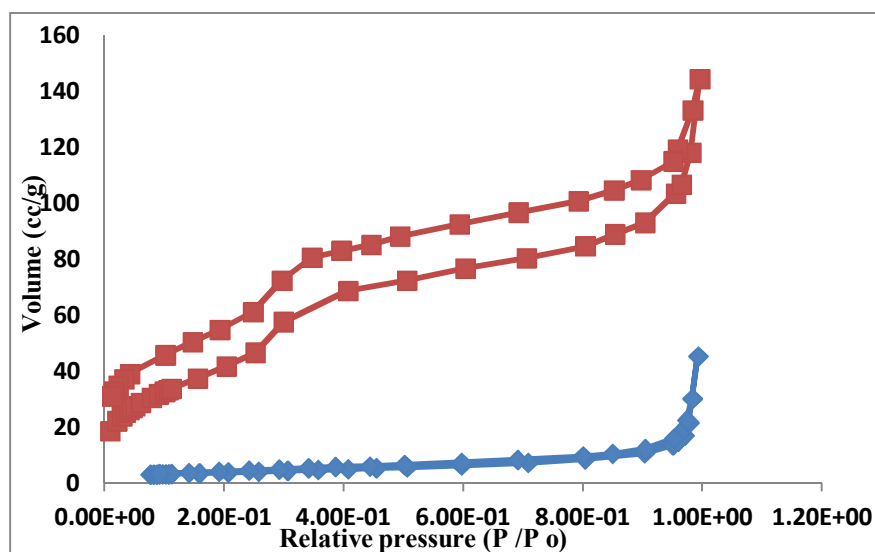


Figure 4.6. Nitrogen adsorption-desorption isotherms of (\diamond) MCM-PS-TDI- β -CD, and (\square)MCM-TDI- β -CD

In comparison to mesoporous silica functionalized with calix[4]arene derivatives, these materials showed different isotherm shape in addition to the lower surface area and pore volume. This can be explained by the organic bulky modifier (β -cyclodextrin) that may block the pore channel, which result in lower surface area and pore volume (Blasco, et al., 1998; S. Kim, et al., 2005). Furthermore, Li et al., (H. Li, et al., 2008) confirmed that the presence of bulky organic molecule will partially disrupt the assembly process and leading to a decrease in the ordering degree of mesoporous structure.

4.3.2 Screening results

To identify and select an efficient adsorbent, a total of eight samples were screened for organotin compounds removal. The removal percentages of the eight modified mesoporous silica MCM-41 were calculated and presented in Figure 4.7. Some of the samples showed an efficient adsorption of organotin compounds, as the organotin compounds removal percentages in three samples (MCM-TDI-C4, MCM-TDI-PC4 and MCM-TDI-C4S) were more than 80%. Furthermore, the removal percentages of MCM-TDI-PC4 were more than 95%.

Although S_{BET} for MCM-TDI-PC4 was lower ($339 \text{ m}^2/\text{g}$) in comparison with other mesoporous silica modified with calix[4]arene derivatives using TDI as linker (MCM-TDI-C4 and MCM-TDI-C4S, 733 and $452 \text{ m}^2/\text{g}$, respectively), however its adsorption capacity was higher. This can be attributed to the nature of the adsorbent, including the surface area, pore size distribution and hydrophobicity, which can be defined as the concentration of carbon atoms in the matrix, density and type of functional groups present on the surface.

On the other hand, the nature of the adsorbate (polarity, hydrophobicity and size of the molecule) also plays an important role in the adsorption process (Salame & Bandosz, 2003).

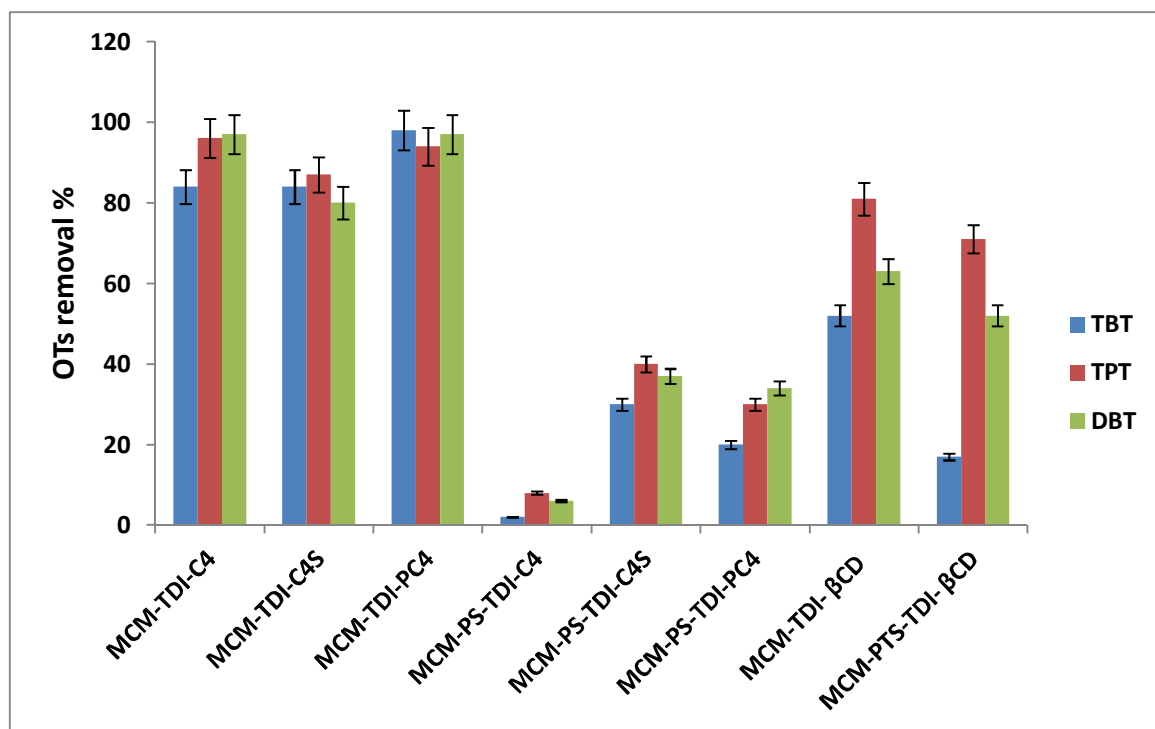


Figure 4.7 Removal percentage of TBT, TPT and DBT by modified mesoporous silica MCM-41 with calix[4]arenes derivatives and β -cyclodextrin adsorbents

The first layer capacity was defined as the calixarene loading, while the second layer inherently represents all external adsorption sites, including those on the residual oxide surface, as well as any non-cavity sites associated with calixarenes (for example, on the outer surface of the tert-butyl groups). The latter also includes interstitial sites between adjacent grafted calixarenes (Thompson, J. Cope, Swift, & Notestein, 2011).

A comparison of materials MCM-TDI-C4, MCM-TDI-PC4 and MCM-TDI-C4S, in which the only difference in calixarene structure is the R group, shows that the uptake increased as the size of the hydrophobic R group changes from H to tert-butyl. This suggests that the upper-rim calixarene functional groups contribute substantially to the degree of uptake, but the pore diameter could also play an important role.

These results suggested that differences in the adsorption between materials were largely influenced by the non-specific van der Waals interactions occurring between the n-butyl chain of butyl group in TBT and DBT, as well as the alkyl R groups on the calixarene upper rim. This is consistent with the result found by Thompson et al.,(2011). Their results displayed that most of the butanol uptake occurred at the calixarene sites and the activity depends on the calixarene chemical structure. The butanol uptake increased with grafted silica with calixarenes containing tert-butyl groups, which provide hydrophobic cavities capable of hydrophobic interactions with n-butyl chains.

Furthermore, the higher TBT capacities of the MCM-TDI-PC4 compared to MCM-TDI-C4 and MCM-TDI-C4S can be explained by the fact that MCM-TDI-PC4 contains a broader pore size distribution (Figure 4.8). The nitrogen sorption isotherms Figure 3.9 were Type IV for all samples, confirming their mesoporous nature. However, slightly different hysteresis loop were noted for MCM-TDI-PC4 compared with MCM-TDI-C4 and MCM-TDI-C4S. The broader hysteresis loop for MCM-TDI-PC4 suggested that this material contained pores with different shapes and size (Idris et al., 2013). Despite having a similar

average pore size to MCM-TDI-C4 and MCM-TDI-C4S, MCM-TDI-PC4 differed in a sense that it has a broader pore size distribution (Figure 4.8).

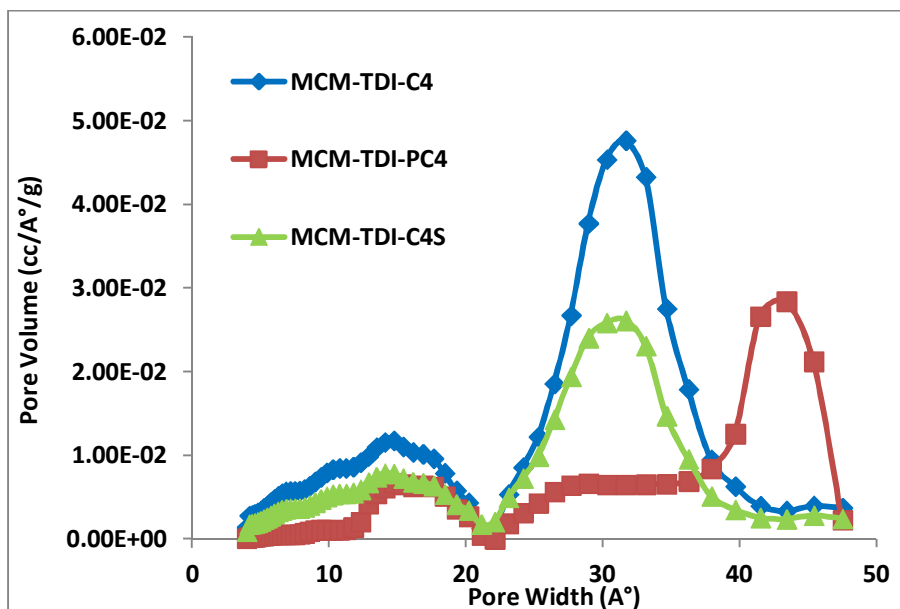


Figure 4.8 BET pore size distribution patterns of the MCM-TDI-C4, MCM-TDI-PC4 and MCM-TDI-C4S.

However, modified mesoporous silica with calix[4]arene using CIPTS and TDI as linking agent (MCM-PS-TDI-C4, MCM-PS-TDI-PC4 and MCM-PS-TDI-C4S) have reported 40% removal percentages, and thus were considered unsuitable as organotin compounds adsorbents. The low sorption efficiency of the former material can be attributed to the low surface area and limited pore volume available for adsorption processes, and this suggests that the main adsorption mechanism for these sorbents occurs only on the external surface (Carmody, et al., 2007).

Moreover, MCM-TDI- β -CD and MCM-PS-TDI- β -CD showed low sorption efficiency for TBT and moderate sorption efficient for DBT. The sorption behavior of organotin compounds was considered to be primarily due to the organic modifier. The reduction in sorption behaviour was due to the presence of β -cyclodextrin, which blockage the porous and resulted in low surface are and pore volume. In addition, β -cyclodextrin may have low affinity towards organotin compounds sorption.

4.4 Summary

In this part, we report the successful anchoring of β -cyclodextrin onto the MCM-41 surface using two methods. In the first method, MCM-41 surface was functionalized with 3-chloropropyl triethoxysilane (CIPTS). The chlorine groups were hydrolysed into hydroxyl groups, which reacted with one of the terminal isocyanate groups of the linking agent, forming urethane links. The other terminal isocyanate functionality reacts with the free hydroxyl group present in the β -cyclodextrin. In the second method, TDI was directly used as a binder. Urethane bonds were formed between the terminal isocyanate group and the silanol groups present on the unmodified MCM-41 surface. Different characterization techniques such as FTIR, XRD, CHN, BET and TGA showed evidences that the β -cyclodextrin was covalently attached to the MCM-41 surface.

Modified mesoporous silica MCM-41 with calix[4]arenes derivatives and β -cyclodextrin adsorbents were screened to remove organotin compounds (TBT, TPT and DBT) from aqueous solution, and the removal percentage of MCM-TDI-C4, MCM-TDI-PC4 and MCM-TDI-C4S were more than 80%.

The adsorption process was mainly contributed by the chemical structure of calixarenes. The prepared material MCM-TDI-PC4 has the lowest BET surface area compared to other mesoporous silica modified with calix[4]arene derivatives using TDI as linker, nevertheless it has the highest adsorption efficiency. This was attributed to the hydrophobic R group present on the upper rim of calix[4]arene. Furthermore, the van der Waals interactions between the adsorbent surface and tert-butyl group might be related to this adsorption.

Mesoporous silica modified with calix[4]arenes derivatives showed higher affinity than mesoporous silica modified with β -cyclodextrin. These results probably due to both supramolecules (calix[4]arenes and β -cyclodextrin) have different cavity size and properties.

Recent findings suggested that the modified mesoporous silica MCM-41 with calix[4]arene derivatives using TDI as linker, which has good adsorption efficiency for organotin compounds, could potentially be used as adsorbents.

CHAPTER 5

ISOTHERMS, KINETICS AND THERMODYNAMICS OF TRIBUTYL TIN (TBT) ADSORPTION ON MODIFIED MESOPOROUS SILICA WITH CALIX[4]ARENE DERIVATIVES

5.1 Introduction

Organotin compounds (OTCs) are the most commonly used organometallic compounds in agricultural, industrial and biomedical applications like PVC stabilizers, industrial catalysts, wood preservatives, fungicides and pesticides (Hoch, 2001). Nevertheless, their notoriety probably stems from the use of tributyltin (TBT) as the active biocide in antifouling paints ingredients. TBT is one of the most toxic compounds that is deliberately released into the environment (Goldberg, 1986) and is referred to as a potent endocrine disruptor exhibiting immunotoxic and genotoxic capabilities to a wide range of organisms from bacterial to human beings (Antizar-Ladislao, 2008).

The adverse TBT effects on aquatic ecosystems, in worse cases, is accompanied by the extinction of local mollusc populations (Bryan & Gibbs, 1991), and has eventually led to its usage restriction. Following several unsuccessful legislative measures (Barroso & Moreira, 2002), TBT was consequently banned in Europe in 2003 (Directive 2002/62/EC) and in all the countries in 2008, with the enforcement of the “International Convention on the Control of Harmful Antifouling systems”. However, even with this ban, OTCs sediments level is

still quite high due to the TBT's affinity to particulate matter and its slow process of degradation under anaerobic conditions (Hoch, 2001).

Various processes have been proposed to remove TBT through conventional treatment technologies such as biodegradation (Chong, 2001; Luan, et al., 2006; N. Tam, et al., 2003; N. F. Y. Tam, Chong, & Wong, 2004) and adsorption process. However, adsorption using sorbents is among the widely employed methods to remove pollutants. Systematic examinations of the TBT adsorption through various adsorbents like natural sediments (Brändli, Breedveld, & Cornelissen, 2009; Burton, et al., 2004; Hoch, et al., 2003), pure minerals (Hoch & Weerasooriya, 2005; Weidenhaupt, et al., 1997), organic matters (C. G. Arnold, Ciani, Müller, Amirbahman, & Schwarzenbach, 1998) and black carbons (Brändli, et al., 2009; Fang, et al., 2010) have been carried out.

The adsorption technique is considered to be among the most effective approaches to remove pollutants from effluents. The process is more advantageous over other methods because of the flexibility of the system, low energy consumption and low operating costs. The recent publications concerning adsorption of toxic compounds revealed an increasing interest in the adsorbent synthesis that is capable of completely eliminating organic pollutants. In this regard, supramolecular chemistry has offered more effective solution to determine molecular structures that can serve as building blocks for the production of sophisticated molecules by anchoring functional group in a manner that they offer an appropriate binding site. This was brought about by the creation of macrocyclic molecules including synthetic crown ethers, cryptands, spherands (Feber, 1978), natural cyclodextrins

(Crini & Morcellet, 2002) and calixarenes (Aksoy, et al., 2012; Ertul, et al., 2010; Kamboh, Akoz, Memon, & Yilmaz, 2013; Qureshi, et al., 2011).

The objective of this chapter is to investigate the adsorption efficiency of a prepared sorbents, MCM-TDI-C4, MCM-TDI-PC4 and MCM-TDI-C4S, and specifically to investigate the adsorption behavior of TBT on prepared sorbent.

Widely accepted adsorption equilibrium isotherm models were used to correlate the experimental data. Two-parameter adsorption isotherm models namely Langmuir, Freundlich, Temkin and Dubinin-Radushkevitch isotherm models and three-parameter adsorption isotherms models namely Redlich-Peterson isotherm and Koble–Corrigan isotherm were used to correlate the adsorption of TBT onto modified MCM-41.

Conventional kinetic models, such as the pseudo-first order, pseudo-second order models and intraparticle diffusion have been used to correlate the experimental data in the current study.

5.2 Experimental

5.2.1 Materials

5.2.1.1 Adsorbents

It was found in Chapter 4, Section 4.3.2 that mesoporous silica MCM-41 modified with calix[4]arene derivatives using TDI as linker (MCM-TDI-C4, MCM-TDI-PC4 and MCM-

TDI-C4S) gave the highest removal percentage for TBT. Therefore, these materials were selected as adsorbents to investigate the adsorption parameters of TBT in this chapter.

5.2.1.2 Adsorbate

Tributyltin TBT was chosen as the representative adsorbate for this part of research. Tributyltin was obtained from Aldrich and used as received. Its molecular formula is illustrated in Figure 5.1.

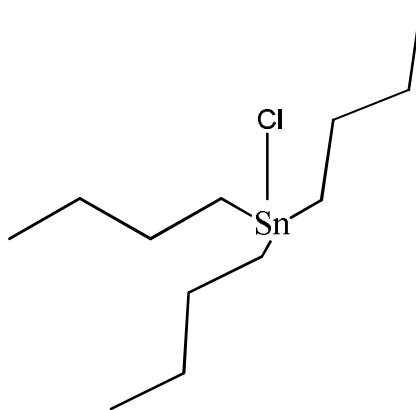


Figure 5.1 Tributyltin molecular formula

Stock solutions were prepared by dissolving tributyltin TBT in methanol and stored at 4°C in the dark, followed by serial dilutions with Milli-Q water of an 8.42 mM. A methanolic stock solution of organotin compound was used due to very low organotin compounds solubility in water.

5.2.2 Adsorption studies

5.2.2.1 Equilibrium contact time

Prior to the equilibrium sorption studies, the equilibrium contact time required for each adsorbent was determined by agitating 10 ml of TBT solution in the prepared materials at predetermined time intervals. The uptake of TBT at any time t (q_t mg/g) was calculated using the following equation:

$$q_t = \frac{(C_o - C_t)V}{w} \quad 5.1$$

where q_t is the amount of TBT adsorbed at time t (mg/g). C_o and C_t (mg/L) are the liquid phase concentrations at initial and any time t , respectively determined by ICP-MS. V is the volume of the solution (L) and W is the mass of adsorbent (g).

The TBT removal efficiency in aqueous solution was calculated by using Equation 5.2:

$$\text{Removal efficiency \%} = \frac{C_o - C_e}{C_o} 100 \quad 5.2$$

where C_o and C_e are the initial and final concentrations of TBT (mg/L) in the solution.

5.2.2.2 Effect of pH

To study the effect of pH on the sorption equilibrium of TBT compound on modified mesoporous silica with calix[4]arene derivatives, the pH of the TBT solutions was initially

adjusted to the range from pH=3 to 8 by the addition of diluted hydrochloric acid (0.01 M, 0.1 M and 1 M) or diluted sodium hydroxide (0.01 M, 0.1 M and 1 M) and the pH was measured with a digital pH meter (Hanna Instruments HI 2213 pH Meter). Other parameters were kept constant.

The concentration of TBT remaining (C_e) in aqueous phase after the sorption was determined by ICP-MS. The amount of TBT sorbed by modified mesoporous silica with calix[4]arene derivatives (q_e) was calculated using Eq.4.1:

5.2.2.3 Effect of initial TBT concentration

A series of TBT solutions with different initial concentration (3-10 mg/L) were added to 0.01 mg of MCM-TDI-C4, MCM-TDI-PC4 and MCM-TDI-C4S. The pH of the TBT solutions was initially adjusted to optimum pH. These reactors were then sealed and agitated in a shaker bath with a speed of 180 rpm for 2 h at different temperatures; 30, 40 and 50°C. The concentration of TBT remaining (C_e) in aqueous phase after the sorption was then determined by ICP-MS.

5.2.2.4 Effect of temperature on the adsorption of TBT

The effect of temperature on the equilibrium adsorption of TBT on the modified mesoporous silica with calix[4]arene derivatives was studied at different temperatures; 30, 40 and 50°C using a temperature controlled water bath (Wise Bath WSB-18). The solution preparation, agitation speed and contact time were similar to those in Section 5.2.2.3. The

concentration of TBT remaining (C_e) in aqueous phase after the sorption was then determined by ICP-MS.

5.2.3 Analytical procedure

All samples were analyzed with an Agilent Technology 7500 series Inductively Coupled Plasma Mass Spectrometry (ICP-MS). The ICP-MS condition is shown in the previous Table 4.1. A series of Sn standard solutions were used to construct the calibration curve, where a good linear relationship was observed.

5.3 Results and discussion

5.3.1 Effect of contact time

Prior to conducting the batch uptake equilibrium experiments, the determination of contact time needed for adsorption equilibrium was required. The TBT uptake by the synthesized mesoporous silica MCM-TDI-C4, MCM-TDI-PC4 and MCM-TDI-C4S is shown in Figure 5.2 as a function of contact time at 30, 40 and 50°C. It is apparent from Figure 5.2 that in the first 10 min, the percentage removal of TBT from aqueous solution increased rapidly and reached up to 81%, 98% and 80% for MCM-TDI-C4, MCM-TDI-PC4 and MCM-TDI-C4S, respectively. After that, the percentage removal of TBT increased slowly until 120 min and then subsequently became constant.

The results indicated that the rate of adsorption of TBT was faster in the initial time of adsorption and has less effect on the rate of adsorption in the latter half of the process. It

was due to the nature of the adsorbent and the available adsorption sites, which affect the rate of adsorption of TBT. This difference in the rate of adsorption may be due to the fact that initially, all adsorbent sites were vacant so the adsorption was high. Later, due to the decrease in the number of adsorption sites on the adsorbents, as well as TBT concentration, the adsorption of TBT became slow. Furthermore, the remaining vacant surface sites were difficult to be occupied due to the repulsive forces, as well as the competition between TBT molecules on the adsorbent surface (Srivastava, Swamy, Mall, Prasad, & Mishra, 2006).

The equilibrium time required for the adsorption of TBT was 2 h for all adsorbents. Prior literature provided varying duration of equilibrium in batch experiments. For instance, Unger et al (Unger, MacIntyre, & Huggett, 1988) revealed that the equilibrium state for TBT was reached after a few minutes to a few hours, while Langston & Pope (Langston & Pope, 1995) revealed that 85.7% of the added TBT amount adsorbed to the solid phase in 2 h.

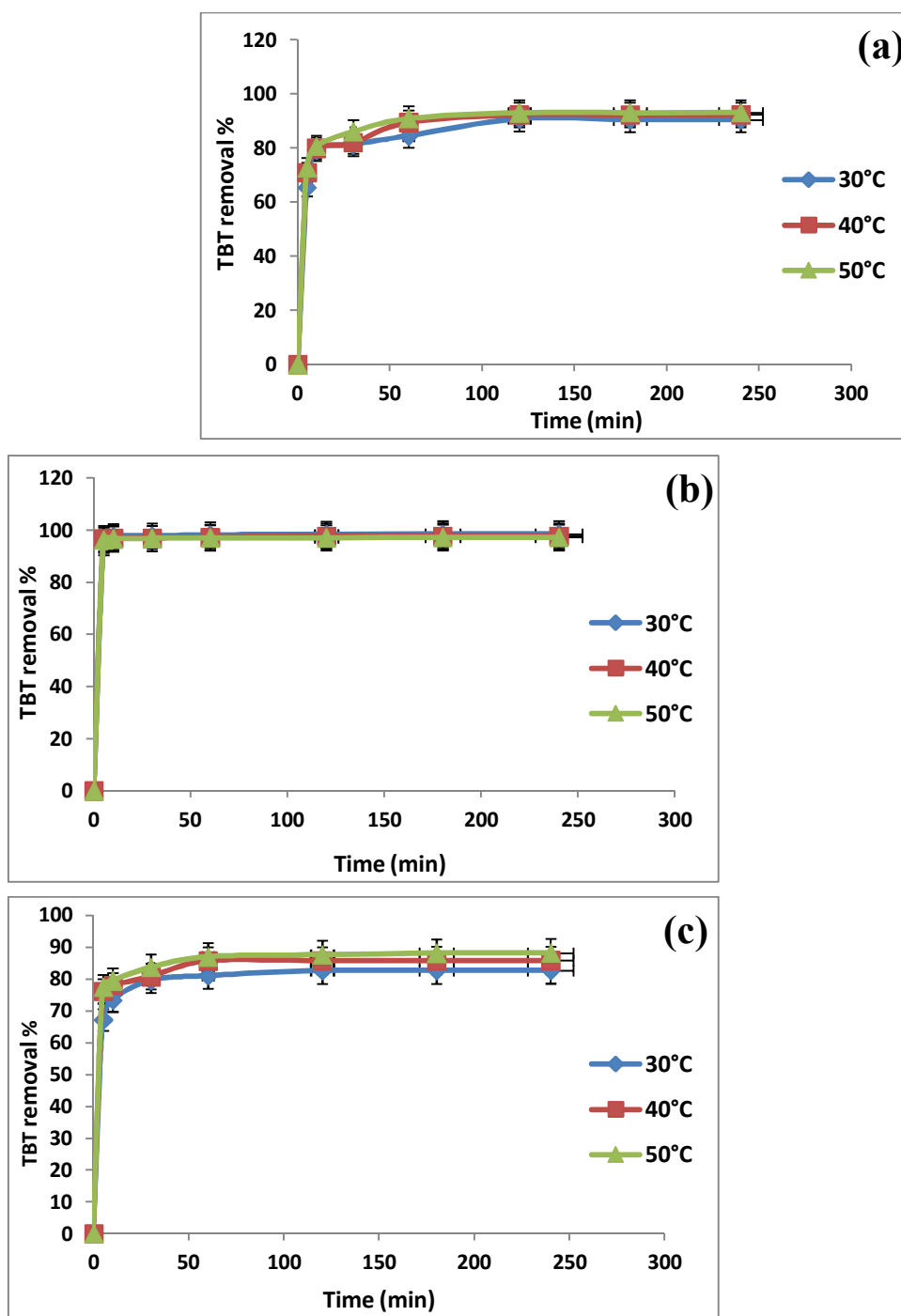


Figure 5.2 Effect of contact time on removal of TBT onto MCM-TDI-C4 (a), MCM-TDI-PC4 (b) and MCM-TDI-C4S (c)

5.3.2 Effect of pH

System pH during adsorption has an important role on the surface characteristics of the adsorbent particles, and consequently the overall adsorption performance. Illustrated in Figure 5.3 is the effect of pH on TBT adsorption onto MCM-TDI-C4, MCM-TDI-PC4 and MCM-TDI-C4S. The adsorption behavior can be explained through the TBT species and the functional group existing in the surface of the adsorbent.

TBT is characterized as a weak acid having a pKa of 6.3 (C. G. Arnold et al., 1997), comprising of cationic form (TBT^+ , $(\text{C}_4\text{H}_9)_3\text{Sn}$) in equilibrium with a neutral form (TBTOH , $(\text{C}_4\text{H}_9)_3\text{SnOH}$) as evident from Equation 5.3;



At $\text{pH} < \text{pKa}$, the adsorption process of TBT^+ is governed by electrostatic attraction. However, it is postulated that the major driving force of adsorption at $\text{pH} > \text{pKa}$ is the hydrophobic character of the TBT compound, which is less effective than the electrostatic interaction (Hoch, Alonso - Azcarate, & Lischick, 2002). With a pH of over 6, the superior species are TBTOH, while the superior species of tributyltin at acidic pH are the TBT^+ . However, in acidic conditions, adsorbent surface becomes a significantly protonated surface that goes against the uptake of TBT^+ form due to electrostatic repulsion.

The TBT maximum adsorption took place at a medium pH for all adsorbents, and this is in analogous to the TBT adsorption by the beech charcoal and soot black carbon (Fang, et al.,

2010). At higher pH ($\text{pH} > \text{pK}_a$), the adsorption decreased due to the TBT species (TBTOH), which are not favorable for those three materials.

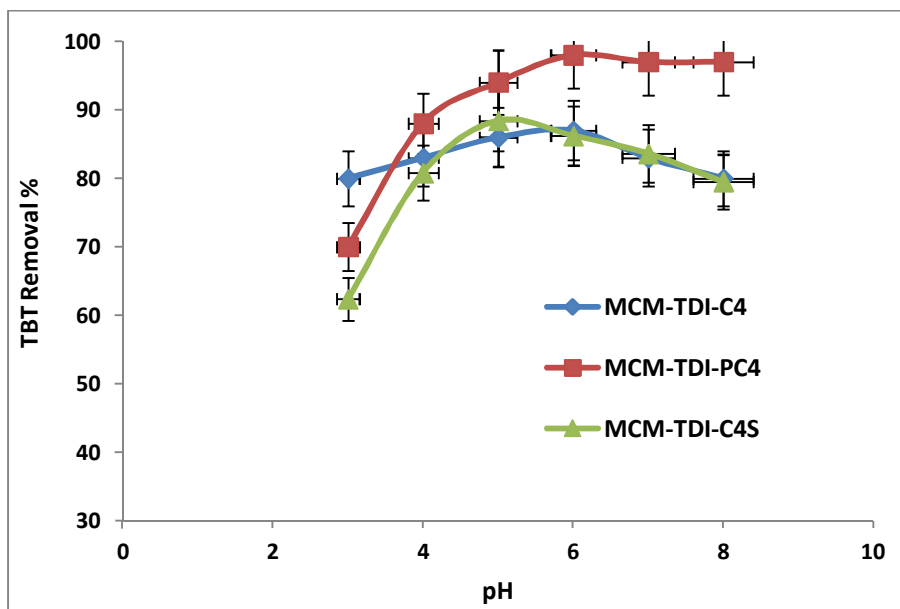


Figure 5.3 Effect of pH on removal of TBT

It was observed that the anchoring of calixarenes onto solid surfaces played an important role in governing both the adsorption process and interaction between adsorbate and sorbent surfaces (Kamboh, et al., 2011b; Memon, et al., 2011; Sayin & Yilmaz, 2011b).

Calix[4]arenes are able to bind some cations, anions and neutral molecules to form inclusion complexes in aqueous solution. Intermolecular forces that are characterized as weak, such as ion-dipole, dipole-dipole, dipole-induced dipole, van der Waals, electrostatic interaction, hydrogen bonding and hydrophobic interaction ($\text{CH}-\pi$ or $\pi-\pi$) have been evidenced to cooperatively contribute to the inclusion complexation of guest molecules with calixarenes (Durmaz, Alpaydin, Sirit, & Yilmaz, 2006). In our case, the complex

stability of calixarenes was attributed to a great extent to van der Waals forces and hydrophobic interaction (CH- π) for all materials. In addition, electrostatic interaction could be considered when MCM-TDI-C4S material was used as adsorbent (the presence of sulfonated anion).

5.3.3 Effect of initial TBT concentration

The adsorption experiments at initial TBT concentrations from 3 to 10 mg/L were also performed with maintaining the adsorbent amount of 0.01g at optimum pH, and the results are represented in Figure 5.4. The results indicate that the percentage removal decreased and the adsorption capacity increased with an increase in the initial TBT concentration for all adsorbents (at 30°C). The decrease in the percentage removal of TBT can be explained with the fact that all adsorbents have a limited number of active sites, which would have become saturated above a certain concentration. The decrease in the percentage removal was significant in the case of MCM-TDI-C4 and MCM-TDI-C4S. This indicates that the MCM-TDI-PC4 materials have higher active sites for adsorption of TBT compared to other materials.

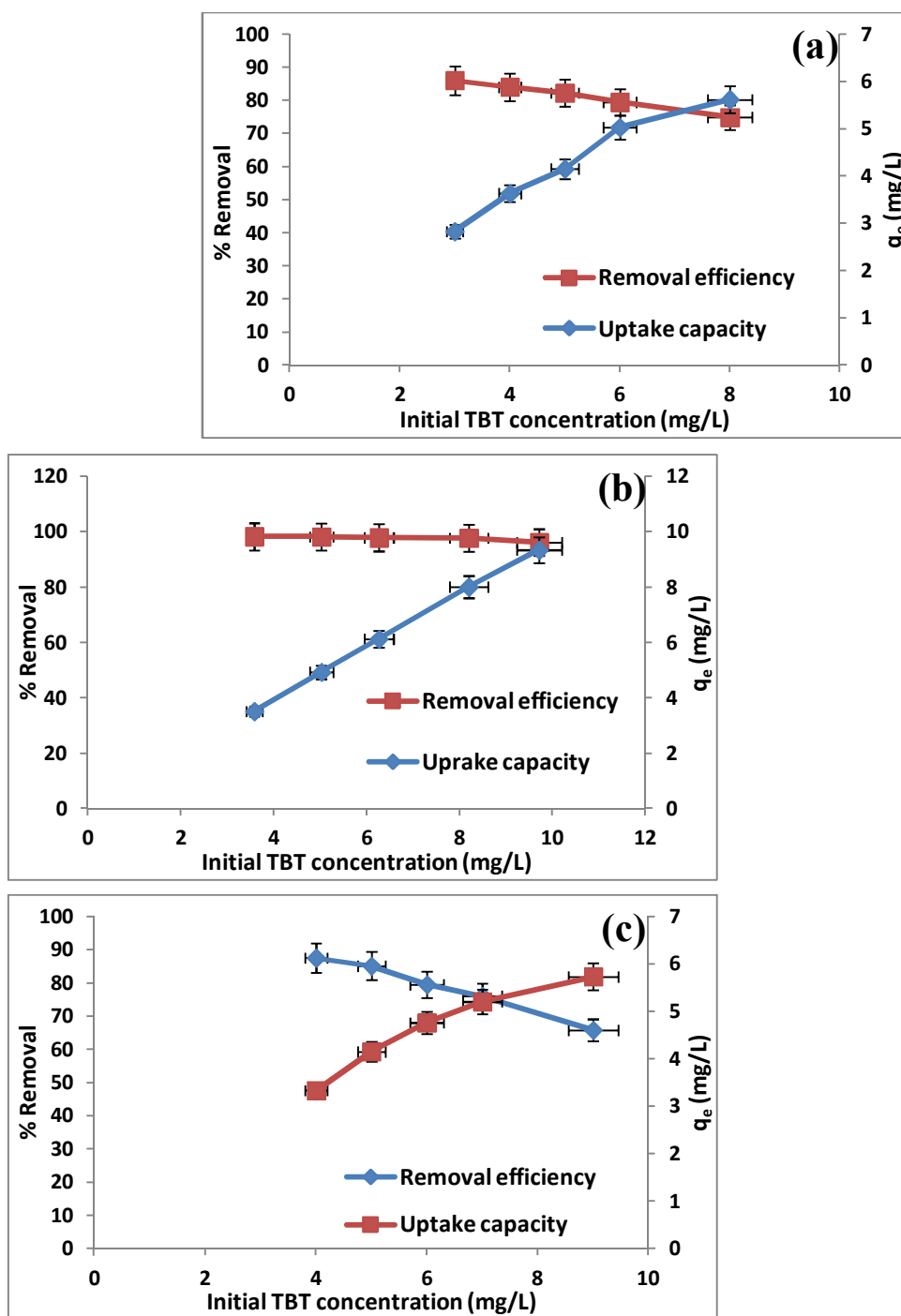


Figure 5.4 Effect of initial TBT concentration on the TBT removal efficiency and uptake capacity by MCM-TDI-C4 (a), MCM-TDI-PC4 (b) and MCM-TDI-C4S (c)

5.3.4 Effect of solution temperature

The temperature influences the adsorption equilibrium and its variations produce a displacement from or toward the phase adsorbed. Also, an increase in temperature generally improves the solubility of the molecules (if in the liquid phase) and their diffusion within the pores of the adsorbent materials (Cotoruelo et al., 2012). The effect of varying temperature on the adsorption of TBT by MCM-TDI-C4, MCM-TDI-PC4 and MCM-TDI-C4S was examined under temperatures of 30, 40 and 50°C, and the experimental results are listed in Figure 5.5.

The bigger adsorptive capacities of TBT were observed in the higher temperature range for MCM-TDI-C4 and MCM-TDI-C4S materials. This was due to the increasing tendency of TBT to adsorb from the solution to the interface with an increase in temperature. The continuous increase in the adsorption capacity indicated that the adsorption process was endothermic. The TBT adsorption uptakes by MCM-TDI-PC4 were found to decrease with increase in the solution temperature from 30 to 50°C. The decrease in adsorption capacity with the increase in temperature is known to be due to the enhancement of the desorption step in the sorption mechanism. It is also due to the weakening of sorptive forces between the active sites on the prepared material and TBT, and also between adjacent TBT molecules on the sorbed phase (Tan, Ahmad, & Hameed, 2008). This result indicated that the adsorption reaction of TBT adsorbed by MCM-TDI-PC4 is an exothermic. A further discussion of temperature in light of the thermodynamic parameters is provided in Section 5.3.7.

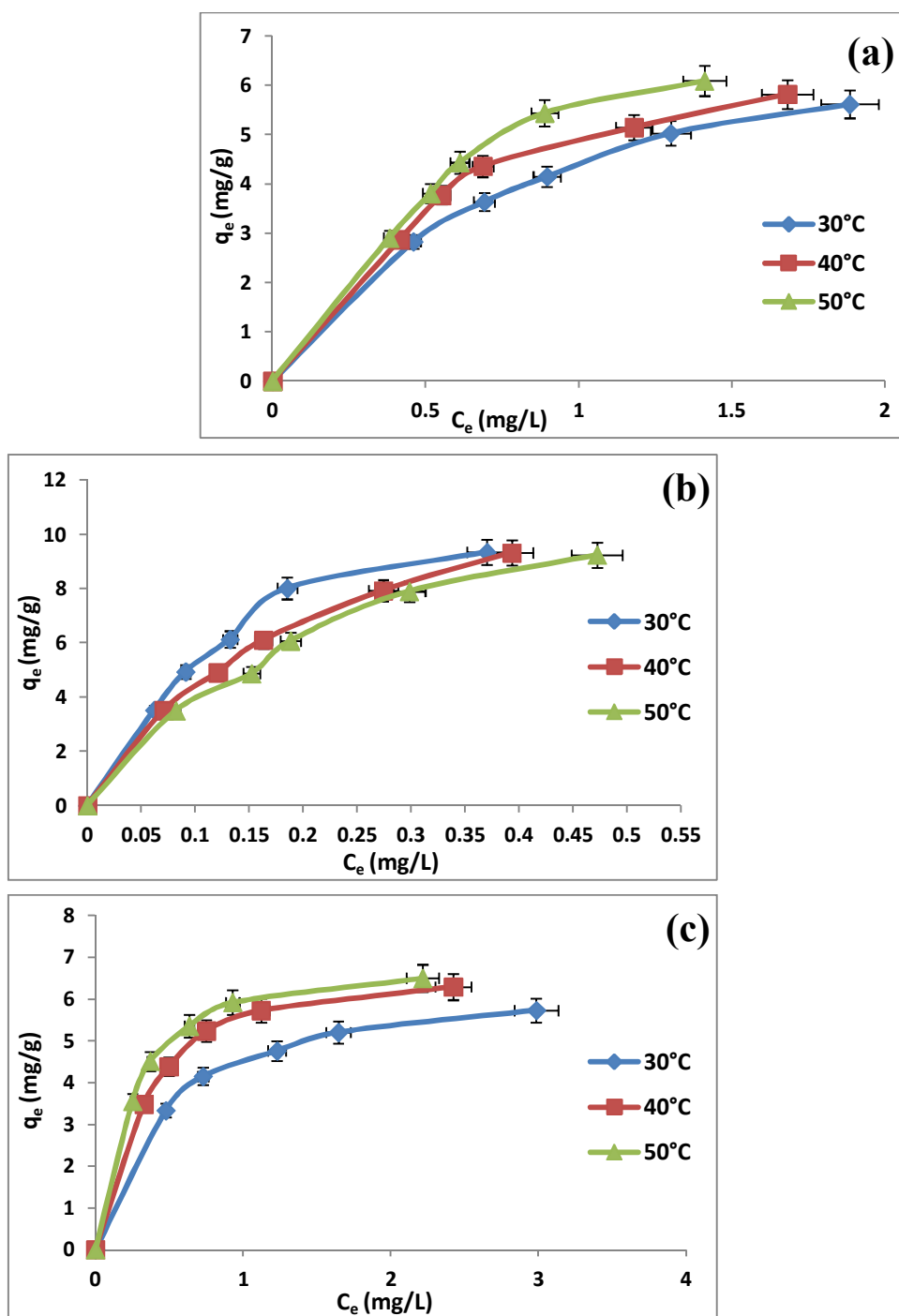


Figure 5.5 Adsorption isotherm for TBT on MCM-TDI-C4 (a), MCM-TDI-PC4 (b) and MCM-TDI-C4S (c) at different temperatures

5.3.5 Adsorption isotherm models

Various isotherm equations have been proposed and utilized, with some of them are characterized by a strong theoretical base, while others are empirical in nature. In the current study, because of the novelty of the adsorbent developed, it is imperative to reach the right equilibrium relationship between solid and liquid phase concentrations of TBT. It also requires the examination of the obtained experimental TBT removal equilibrium data by MCM-TDI-C4, MCM-TDI-PC4 and MCM-TDI-C4S with various isotherm models proposed in literature in order to determine which one is the most suitable among them. In the current study, two-parameter isotherms proposed by Freundlich, Langmuir, Temkin, and Dubinin-Radushkevitch (D-R), and three-parameter isotherms proposed by Redlich-Peterson and Koble-Corrigan were examined with the equilibrium data obtained from the experiments.

I. Freundlich isotherm

To account for the possible multilayer adsorption and non-linear energy distribution for the adsorption sites, the Freundlich isotherm was studied. The Freundlich constants, K_F and n (Eq. 2.12) were calculated from Figure 5.6. The highest K_F values referred to MCM-TDI-PC4, which indicate the highest TBT uptake from aqueous solution by this adsorbent (Table 5.1).

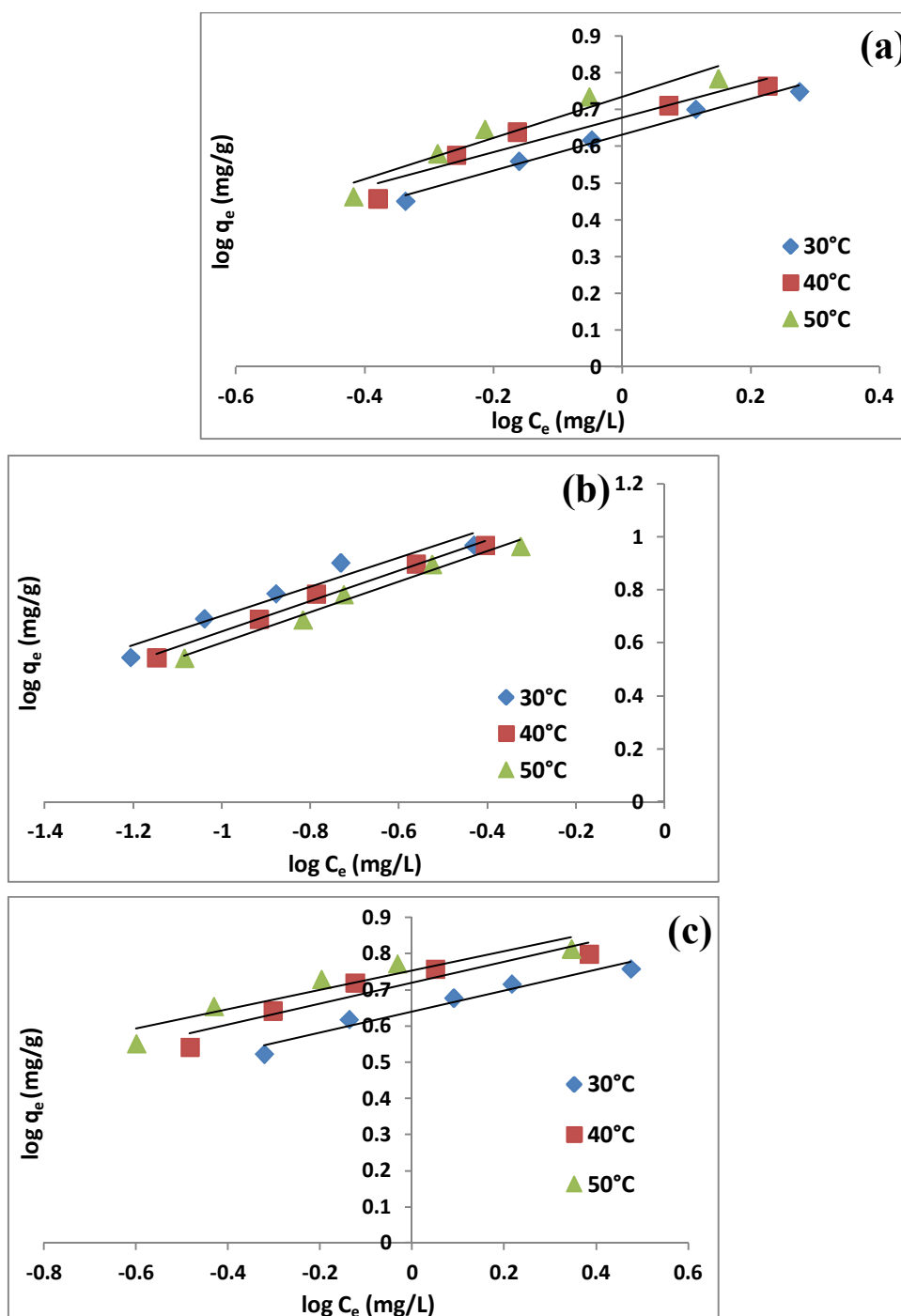


Figure 5.6 Freundlich isotherm of TBT adsorbed onto MCM-TDI -C4 (a), MCM-TDI-PC4 (b) and MCM-TDI-C4S (c)

The values of n , which is an indicator of the adsorption intensity, were more than unity, which represents a favorable adsorption condition for all materials. In addition, higher

values of n in the case of MCM-TDI C4S indicates the formation of relatively strong bond between TBT and the adsorbent (Ramu, Kannan, & Srivathsan, 1992).

Table 5.1 Isotherm constants and correlation coefficient of determination for various adsorption isotherms for the adsorption of TBT onto MCM-TDI-C4 (a), MCM-TDI-PC4 (b) and MCM-TDI-C4S (c)

Adsorbent	Adsorption isotherm	Isotherm parameter	Temperature		
			30	40	50
(a)	Freundlich	$K_F(L/g)$	4.2815	4.7588	5.4225
		n	2.0354	2.1322	1.7879
		R^2	0.9845	0.9309	0.9307
	Langmuir (II)	$q_m(mg/g)$	8.4104	9.1659	12.1212
		$K_L(L/mg)$	1.1009	1.1693	0.8629
		R^2	0.9992	0.9609	0.9719
	Temkin	A_T	2.0189	2.0038	2.4706
		$K_T(L/mg)$	8.8305	11.3189	9.1593
		R^2	0.997	0.9735	0.9704
	Dubinin-Radushkevitch	$q_d(mg/g)$	6.0376	6.4967	7.3075
		$\beta(mol^2/kJ^2)$	3.01×10^{-3}	2.6×10^{-3}	2.6×10^{-3}
		$E(kJ/mol)$	12.8689	13.6495	13.6495
		R^2	0.9823	0.9898	0.9957
	Redlich–Peterson	g	0.9301	0.9689	0.8918
		$B_R(L/mg)$	1.2792	1.3577	1.1522
		$A_R(L/g)$	10.0043	11.5734	11.9312
		R^2	0.9986	0.9554	0.924
	Koble–Corrigan	p	1.0176	2.1208	1.8879
		A_K	9.4697	35.4609	30.8642
		B_K	1.1468	5.9397	4.4907
		R^2	0.9992	0.9959	0.9986
(b)	Freundlich	$K_F(L/g)$	17.8525	16.4626	15.0038
		n	1.8205	1.7422	1.7382
		R^2	0.9365	0.9928	0.9814
	Langmuir (II)	$q_m(mg/g)$	16.4204	14.2653	13.9276
		$K_L(L/mg)$	4.5111	4.5226	3.9888
		R^2	0.9875	0.9975	0.9852

Table 5.1 (Continued)

	Temkin	A_T	3.3637	3.4397	3.427
		$K_T(L/mg)$	48.1922	36.8125	31.3889
		R^2	0.9731	0.9945	0.9832

(c)	Dubinin-Radushkevitch	$q_d(\text{mg/g})$	12.8559	11.8829	11.4662
		$\beta(\text{mol}^2/\text{kJ}^2)$	6.7×10^{-4}	1.01×10^{-3}	1.01×10^{-3}
		$E(\text{kJ/mol})$	27.2991	22.2896	22.2896
		R^2	0.9861	0.9937	0.9788
	Redlich-Peterson	g	0.998	0.9992	0.9883
		$B_R(\text{L/mg})$	4.8264	4.4406	3.8395
		$A_R(\text{L/g})$	76.1627	64.2147	55.2684
		R^2	0.9657	0.9943	0.971
	Koble-Corrigan	p	1.383	0.849	0.742
		A_K	238.0952	40.4858	25.4453
		B_K	21.0238	2.1053	0.9033
		R^2	0.9958	0.9988	0.9897
Freundlich	$K_F(\text{L/g})$	4.3631	5.2396	5.6572	
	n	3.4507	3.4602	3.7439	
	R^2	0.9526	0.8943	0.8919	
Langmuir (II)	$q_m(\text{mg/g})$	6.6577	7.593	7.5757	
	$K_L(\text{L/mg})$	2.1396	2.6552	3.6666	
	R^2	0.9952	0.9881	0.9875	
Temkin	A_T	1.2949	1.3988	1.3319	
	$K_T(\text{L/mg})$	30.9003	45.1689	73.7734	
	R^2	0.9801	0.9367	0.9366	
Dubinin-Radushkevitch	$q_d(\text{mg/g})$	5.7552	6.5463	6.7282	
	$\beta(\text{mol}^2/\text{kJ}^2)$	2.3×10^{-3}	1.6×10^{-3}	1.0×10^{-3}	
	$E(\text{kJ/mol})$	14.5919	17.2655	22.2896	
	R^2	0.9866	0.9993	0.9979	
Redlich-Peterson	g	0.9893	0.999	0.9937	
	$B_R(\text{L/mg})$	2.2506	2.8092	3.9357	
	$A_R(\text{L/g})$	14.7273	20.9121	29.1639	
	R^2	0.9989	0.9968	0.9972	
Koble-Corrigan	p	1.1583	1.4241	1.4278	
	A_K	16.8919	35.5872	54.6448	
	B_K	2.6892	5.3594	8.1366	
	R^2	0.9964	0.9993	0.9984	

The coefficients of determination were revealed to be good for the three prepared materials (Table 5.1). To determine a better fit with other isotherms, the results were analyzed with the other six isotherms proposed in literature.

II. Langmuir isotherm

The Langmuir isotherm and their corresponding linearized forms are shown in Chapter 2, Section 2.2.1.1. It was observed that the Langmuir isotherm can be linearized to at least four different types. Out of the four different types of linearized Langmuir isotherm equations, Langmuir I (Eq. 2.6) and Langmuir II (Eq. 2.7) are the most commonly used by several researchers because of the minimized deviations from the fitted equation resulting in the best error distribution (Ho, 2004).

The maximum monolayer capacity, q_m obtained from Langmuir model II (Figure 5.7) and K_L were shown in Table 5.1. The higher TBT capacities of the MCM-TDI-PC4 compared to MCM-TDI-C4 and MCM-TDI-C4S was explained previously in Chapter 4, Section 4.3.2. Since a high K_L value indicates a high affinity (Y. J. Pan, Hsieh, & Yen, 2011), thus MCM-TDI-PC4 showed the highest affinity for TBT adsorption.

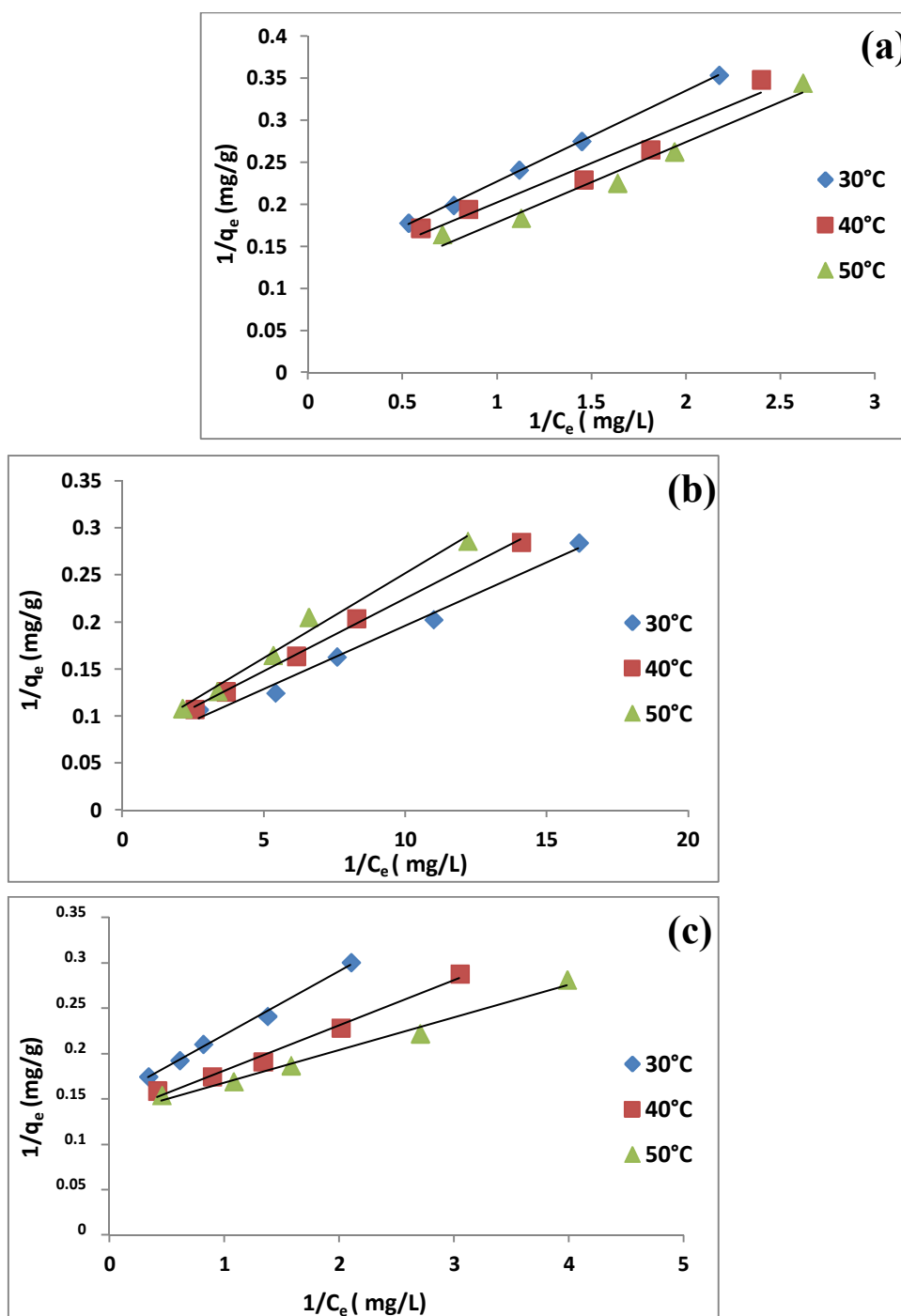


Figure 5.7 Langmuir isotherm Type II of TBT adsorbed onto MCM-TDI-C4 (a), MCM-TDI-PC4 (b) and MCM-TDI-C4S (c)

The significantly high values of the determination coefficients (Langmuir II) for all materials indicate a good agreement between the values obtained from the experiments and isotherm parameters. This reinforces TBT monolayer adsorption onto the surface of MCM-TDI-C4, MCM-TDI-PC4 and MCM-TDI-C4S. Moreover, the Freundlich isotherm has a lower R^2 values in comparison to the best fit Langmuir (II) isotherm, indicating the unsuitable use of the Freundlich isotherm relation for TBT onto MCM-TDI-C4, MCM-TDI-PC4 and MCM-TDI-C4S surfaces.

It was observed that the separation factor R_L (Figure 5.8) are between 0 and 1, which indicated that these three adsorption processes were favorable, and the degree of favorability was in the order of MCM-TDI-PC4>MCM-TDI-C4S>MCM-TDI-C4, which was consistent with the K_L values (indicator of the affinity) order for the three adsorbents. The R_L values decreased with an increase in initial TBT concentration, indicating that the adsorption was more favorable at higher TBT concentration.

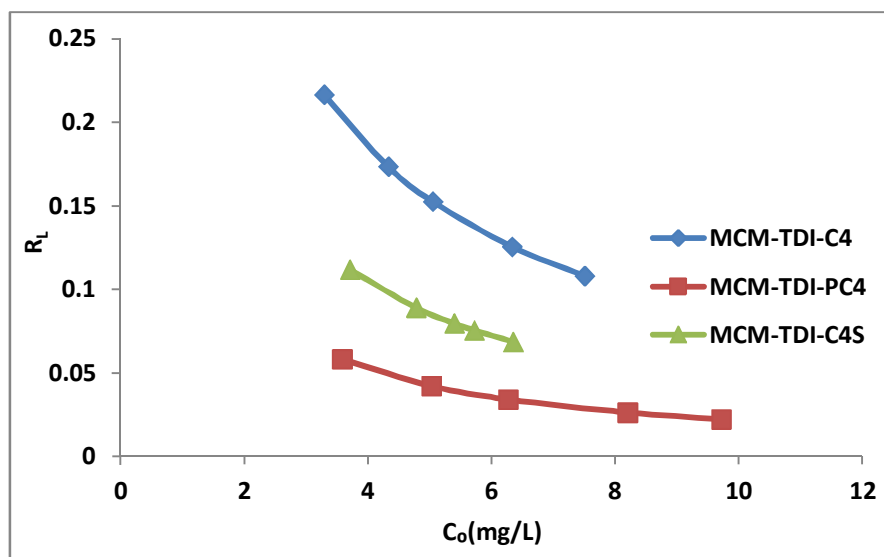
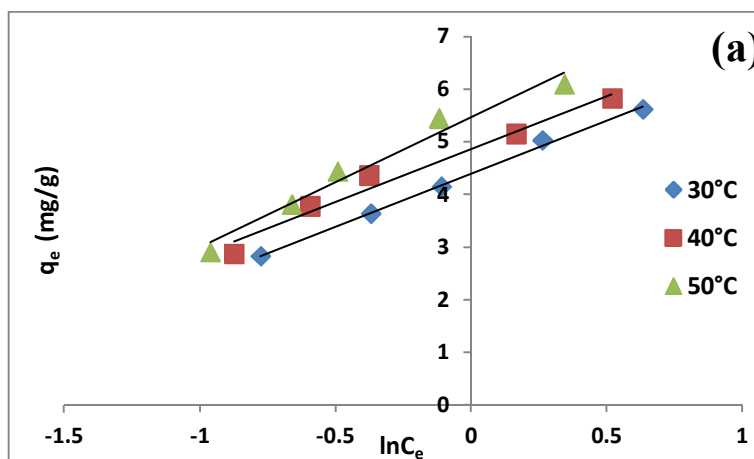


Figure 5.8 Values of R_L for adsorption of TBT onto MCM-TDI-C4, MCM-TDI-PC4 and MCM-TDI-C4S

III. Temkin isotherm

The Temkin isotherm assumes that the fall in the heat of sorption is linear and the distribution of binding energies as uniform. The Temkin isotherm plot for MCM-TDI-C4, MCM-TDI-PC4 and MCM-TDI-C4S adsorbents is presented in Figure 5.9 and the corresponding isotherm parameters are given in Table 5.1.



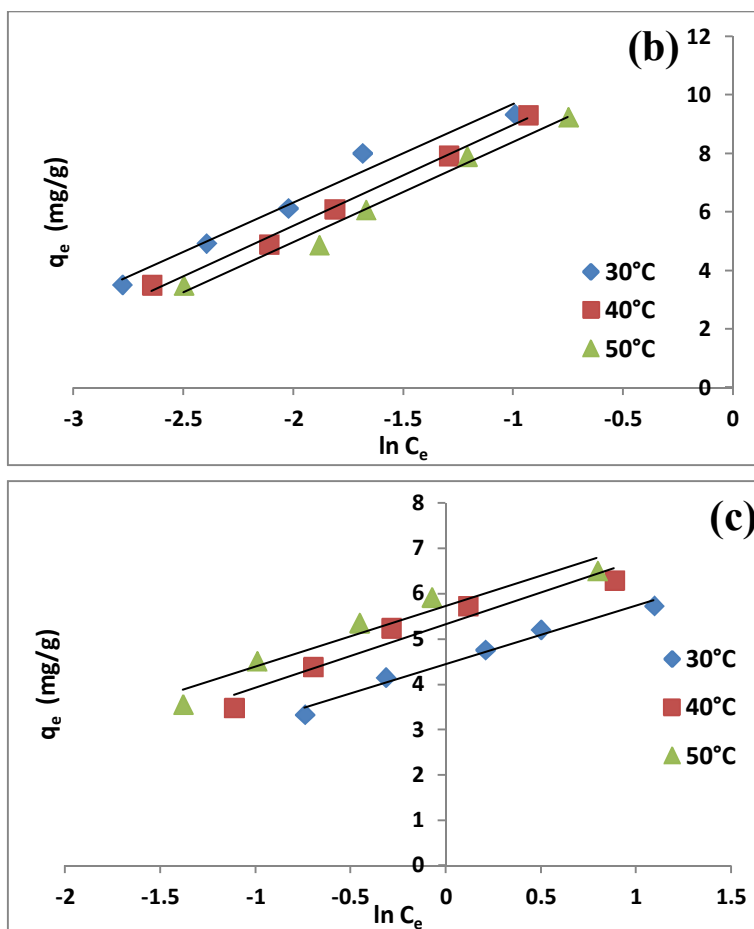


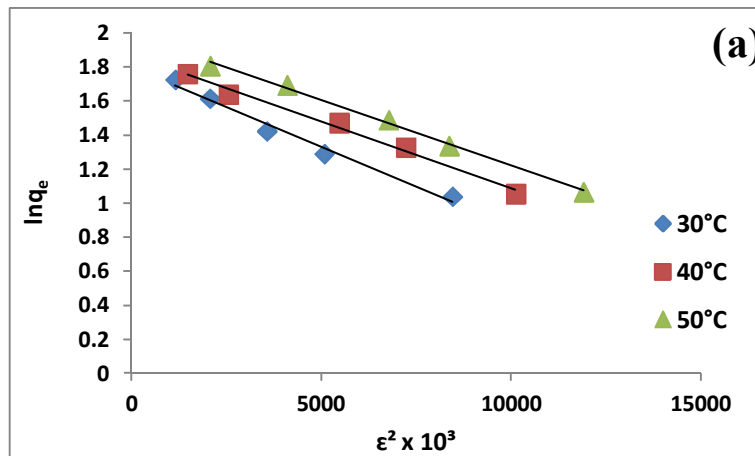
Figure 5.9 Temkin isotherm of TBT adsorbed onto MCM-TDI-C4 (a), MCM-TDI-PC4 (b) and MCM-TDI-C4S (c)

The correlation coefficients obtained from Temkin isotherm model were comparable to those obtained from Langmuir model linear forms II, and they were slightly higher than those obtained from Freundlich isotherm model. This result indicates that the experimental data fitted well to Temkin model and since the Temkin R^2 values were found to be higher than Freundlich, therefore the adsorbent seemed to show more affinity towards linear energy distribution than the non-linear.

IV. Dubinin-Radushkevitch (D–R) isotherm

Dubinin-Radushkevitch equation can be used to estimate the characteristic porosity and the apparent free energy of adsorption. Figure 5.10 shows Dubinin-Radushkevitch isotherm generated using Eq. (2.16) by plotting $\ln q_e$ versus ϵ^2 of the experimental data for the adsorption of TBT by MCM-TDI-C4, MCM-TDI-PC4 and MCM-TDI-C4S. The constants β and q_d were calculated from the slope and the intercept, respectively, and reported in Table 5.1. The mean free energy of adsorption (E) is the free energy change when one mole of ion transferred from infinity in the solution to the surface of the sorbent (T. S. Singh & Pant, 2004).

The calculated mean energy values (Eq. 2.18) of TBT adsorption by MCM-TDI-C4, MCM-TDI-PC4 and MCM-TDI-C4S adsorbents implies that the type of adsorption appears to be physical, chemical and chemical processes, respectively.



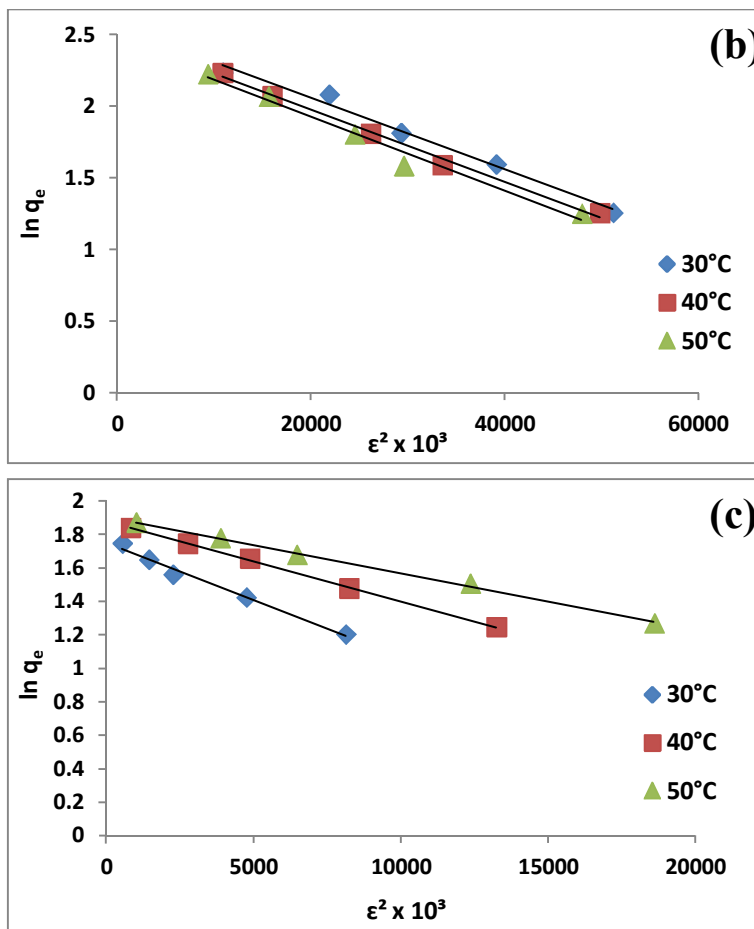


Figure 5.10 Dubinin–Radushkevitch isotherm of TBT adsorbed onto MCM-TDI-C4 (a), MCM-TDI-PC4 (b) and MCM-TDI-C4S (c)

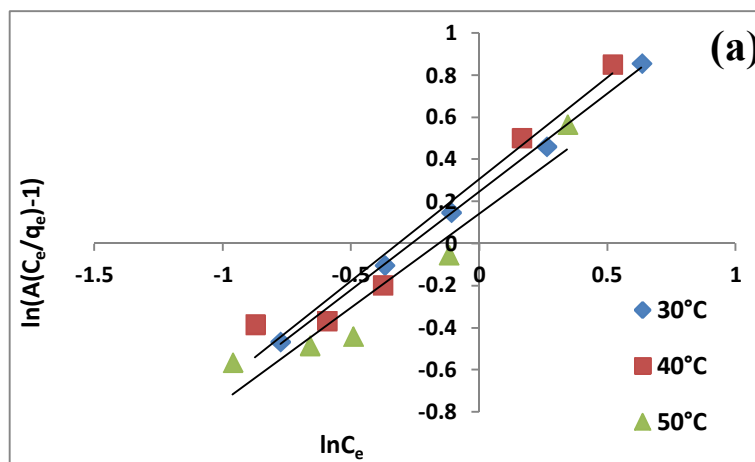
A fairly low porosity factors β -value (< 1) implies that MCM-TDI-C4, MCM-TDI-PC4 and MCM-TDI-C4S adsorbents consist of micropores, thus indicating a surface heterogeneity may arise from the pore structure, as well as adsorbate-adsorbent interaction (Negrea et al., 2011). The adsorption capacities q_d determined through the Dubinin-Radushkevitch isotherm model were lower compared to the q_m values determined using Langmuir isotherm model.

V. Redlich-Peterson isotherm

Since the adsorbents mostly follow Langmuir and Freundlich models, an attempt was made to test its validity with respect to the Redlich-Peterson model, which is essentially a combination of the Langmuir and Freundlich models.

Using the Redlich–Peterson model (Eq.2.20), the parameters A_R , B_R , and g were determined. Since there were three unknowns of Redlich-Peterson model, the unknown constants in this equation need to be obtained by using trial and error method (Solver add-in with Microsoft Excel (Y. Wong, et al., 2004)). The isotherm and its parameters are presented in Figure 5.11 and Table 5.1.

The values of correlation coefficients indicate that Redlich-Peterson isotherm has a good fit to the experimental data. The exponent values of g were close to 1, signifying the applicability of Langmuir model for explaining the obtained equilibrium data, and this indicates that the three adsorption processes were more homogenous than heterogeneous.



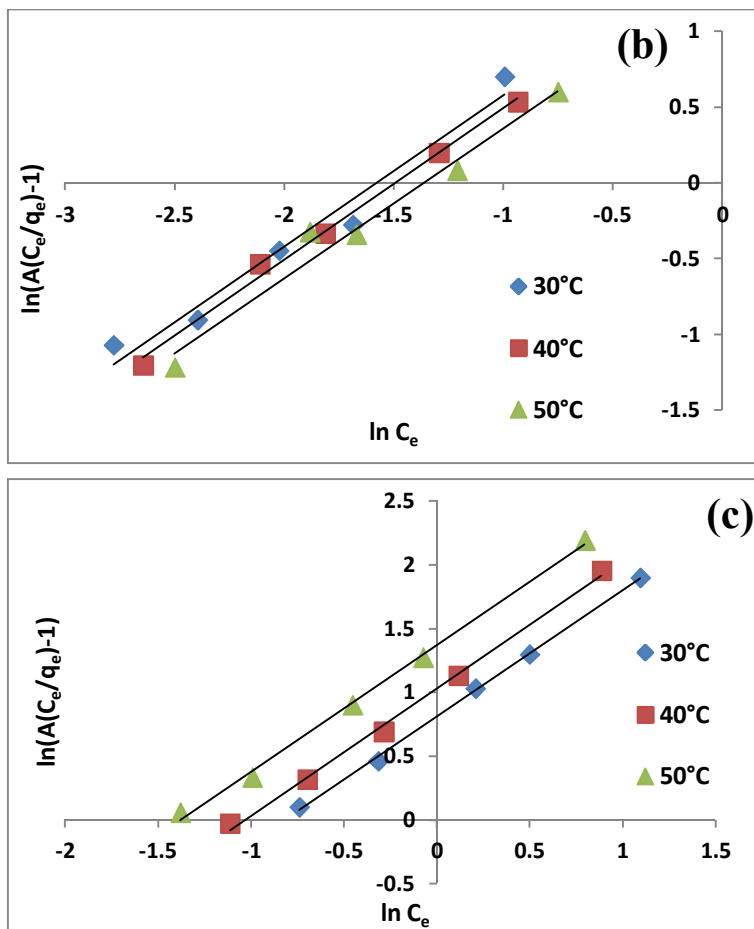
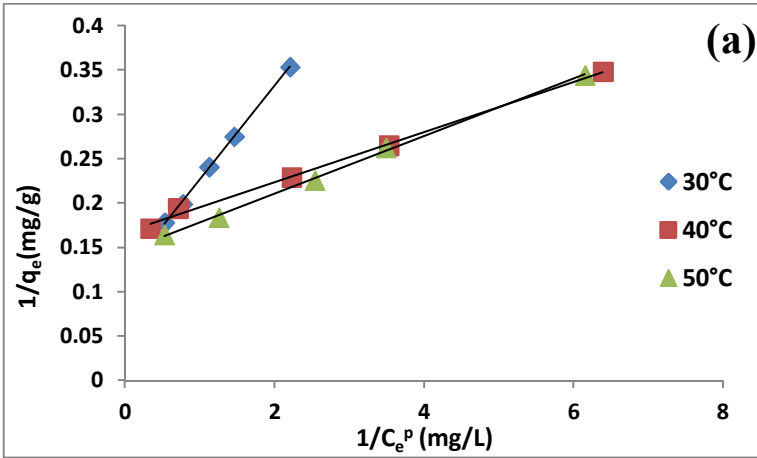


Figure 5.11 Redlich–Peterson isotherm of TBT adsorbed onto MCM-TDI-C4 (a), MCM-TDI-PC4 (b) and MCM-TDI-C4S (c)

VI. Koble–Corrigan isotherm

Koble–Corrigan equation is another isotherm model that depends on the combination of the Langmuir and Freundlich equations. The Koble–Corrigan model’s parameters, A_K , B_K and p , which were obtained by solving Eq. 2.22 using Solver add-in function of the Microsoft excel, are reported in Table 5.1 (Figure 5.12).

The R^2 values at all temperatures and for the three adsorbents were found to be consistently very high by showing the best adherence to this model of all the models studied, which signifies an occurrence of the combination of heterogeneous and homogenous uptake for TBT through the synthesized MCM-TDI-C4, MCM-TDI-PC4 and MCM-TDI-C4S adsorbents. The correlation coefficient values for Langmuir (II) model was more than Freundlich model, which imply that the primary mechanism of the TBT adsorption process was the homogeneous uptake.



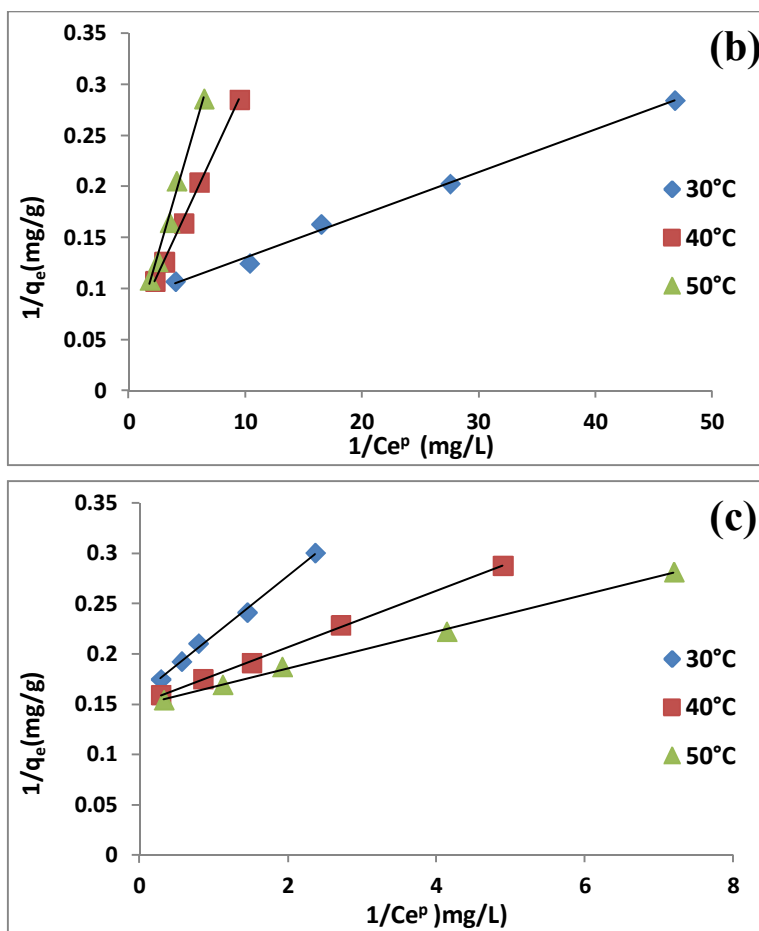


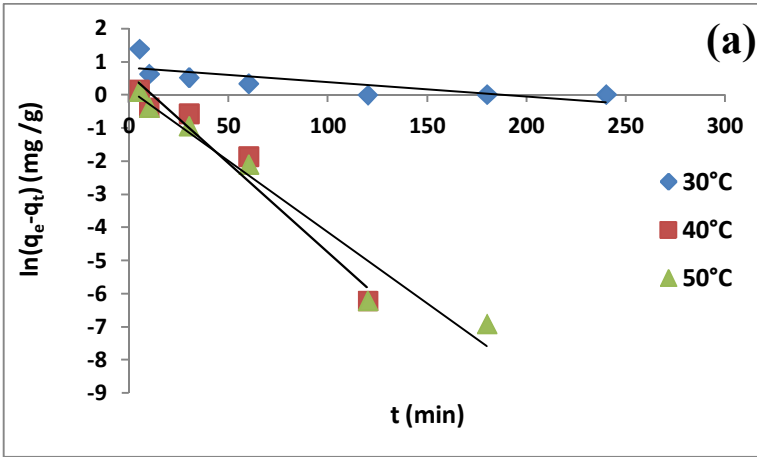
Figure 5.12 Koble–Corrigan isotherm of TBT adsorbed onto MCM-TDI-C4 (a), MCM-TDI-PC4 (b) and MCM-TDI-C4S (c)

5.3.6 Adsorption Kinetic

The adsorption kinetics reveals the rate of adsorbate uptake by the adsorbent during the time (Ho & McKay, 1999a). Pseudo first-order, pseudo second-order and intraparticle diffusion kinetic models were applied for the adsorption of TBT on MCM-TDI-C4, MCM-TDI-PC4 and MCM-TDI-C4S, and the conformity between experimental data and the model-predicted values was expressed by the correlation coefficients (R^2).

I. Pseudo-first order kinetic

At the evaluated experimental temperatures, k_1 and q_e (Eq. 2.25) were calculated using the slope and intercept of plots of $\ln(q_e - q_t)$ versus t (Figure 5.13, Table 5.2). Despite the high correlation coefficients obtained from the pseudo-first order model, the calculated q_e was not consistent with the experimental values, suggesting that the TBT adsorption on MCM-TDI-C4, MCM-TDI-PC4 and MCM-TDI-C4S was not guided by the pseudo-first order kinetics.



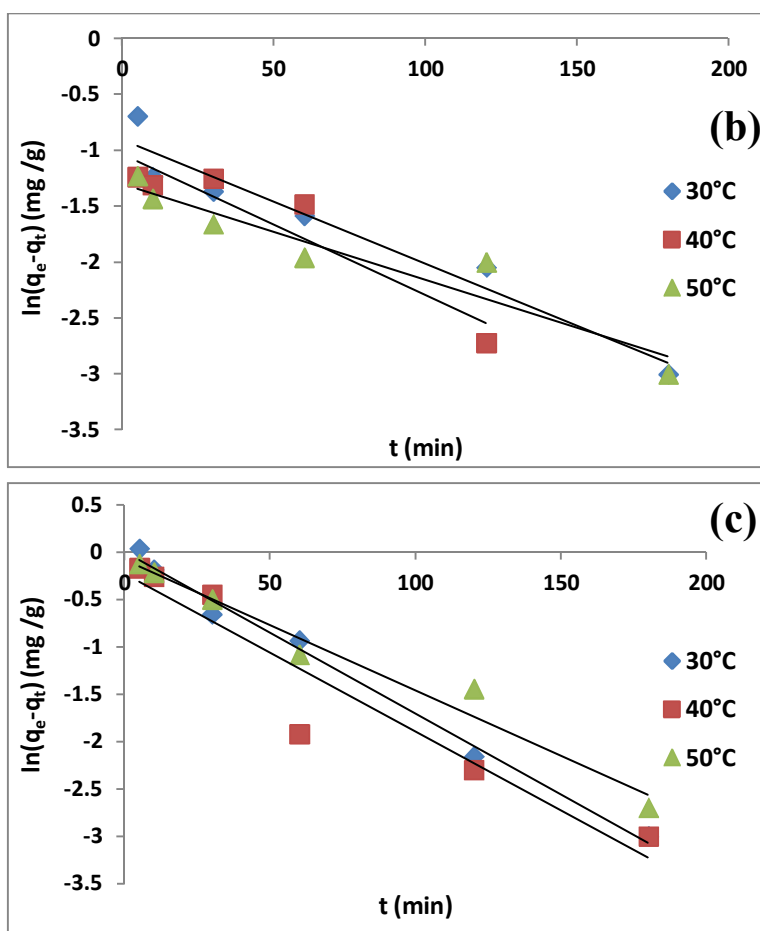


Figure 5.13 Pseudo-first order model plot for the adsorption of TBT onto MCM-TDI-C4 (a), MCM-TDI-PC4 (b) and MCM-TDI-C4S (c)

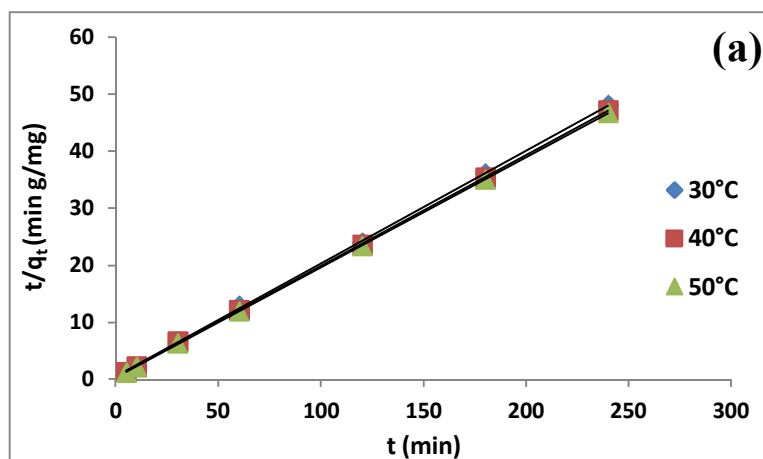
Table 5.2 Calculated kinetic parameters for pseudo-first order and pseudo-second order kinetic models for the adsorption of TBT using MCM-TDI-C4 (a), MCM-TDI-PC4 (b) and MCM-TDI-C4S (c) as adsorbents

	T (°C)	$q_{e,exp}$ (mg/g)	Pseudo-first order			Pseudo-second order			
			K_1 (min^{-1})	$q_{e,cal}$ (mg/g)	R_1^2	K_2 (g/mg min)	$q_{e,cal}$ (mg/g)	h (mg/g min)	R_2^2
(a)	30	5.005	0.0043	2.2619	0.6091	0.0721	5.0531	1.8403	0.9998
	40	5.092	0.0538	1.9102	0.9575	0.0846	5.1493	2.2432	0.9999
	50	5.136	0.0431	1.1864	0.9551	0.1051	5.1813	2.8225	1

	30	6.007	0.011	0.3885	0.9288	0.8932	6.0096	32.2581	1
(b)	40	5.960	0.0126	0.3556	0.88	0.9405	5.963	33.4448	1
	50	5.928	0.0086	0.2723	0.9084	1.6356	5.9276	57.4713	1
	30	5.792	0.0171	1.0029	0.9914	0.1312	5.8275	4.4563	1
(c)	40	6.013	0.0167	0.7993	0.911	0.1625	6.0423	5.9347	1
	50	6.174	0.0138	0.9249	0.9716	0.1353	6.2073	5.2138	1

II. Pseudo-second order kinetic

The model's adsorption parameters q_e and k_2 in Eq. 2.28 were calculated by plotting t/q_t versus t (Figure 5.14, Table 5.2). The linear plot of t/q_t versus t revealed a good fit of consistency to the experimental data with the pseudo-second order kinetic model. The correlation coefficients (R^2) for the second order kinetic model were close to 1, while the values of q_e were consistent with the experimental data. These results showed that the TBT adsorption from aqueous solution on all materials follows the pseudo-second order kinetic model. It can also be seen from the pseudo-second order data that the adsorption rate of TBT, K_2 , was found to be in the order of MCM-TDI-PC4>MCM-TDI-C4S>MCM-TDI-C4. Additionally, the initial adsorption rates, h , were consistent with this order (Table 5.2).



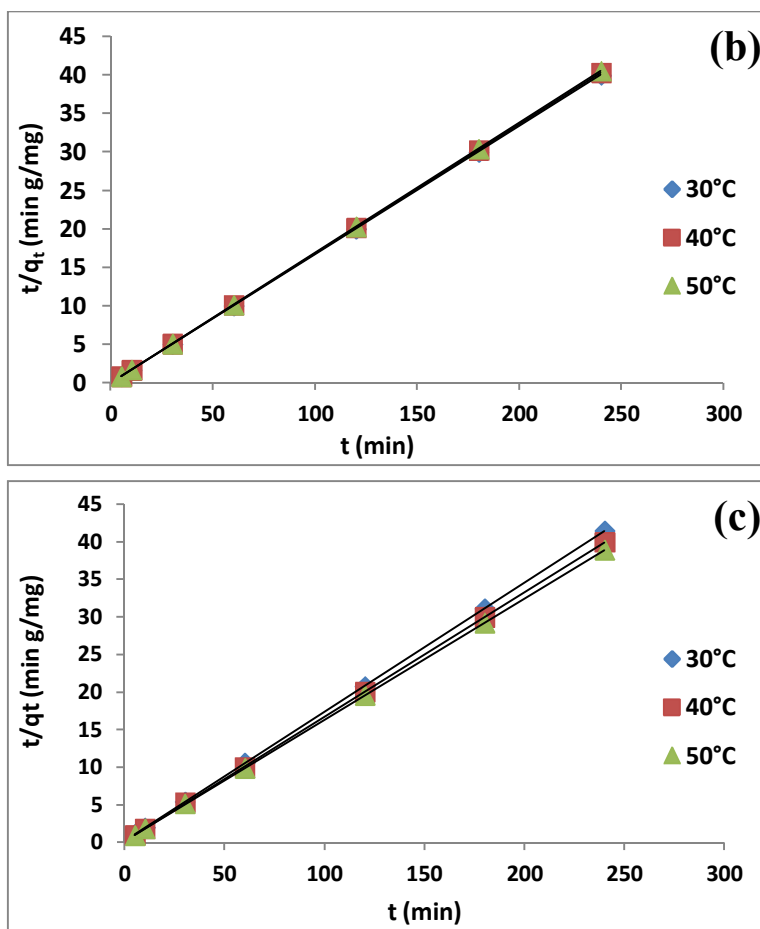


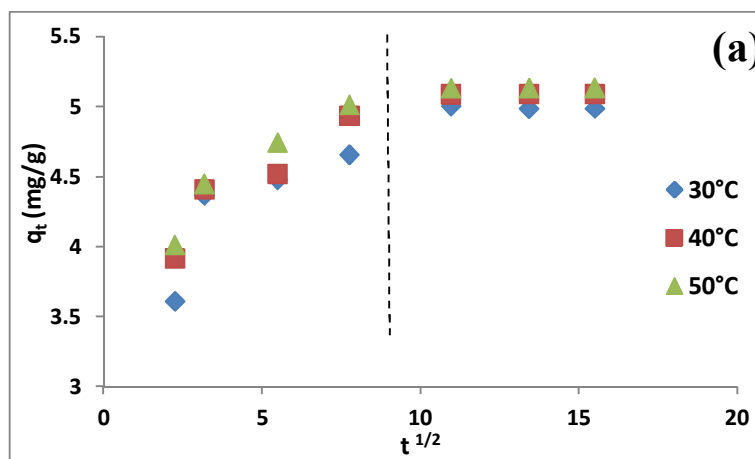
Figure 5.14 Pseudo-second order model plot for the adsorption of TBT onto MCM-TDI-C4 (a), MCM-TDI-PC4 (b) and MCM-TDI-C4S (c)

III. Intraparticle diffusion model

Adsorption of any ions from aqueous phase onto the solid phase consists of many steps which include bulk diffusion, film diffusion and intraparticle diffusion. Because of TBT's probable transportation from aqueous solution to MCM-TDI-C4, MCM-TDI-PC4 and MCM-TDI-C4S by intraparticle diffusion, this type of diffusion is considered as another

kinetic model that should be utilized to examine the rate-determining step for TBT adsorption.

The intraparticle diffusion model's fit with the experimental data is depicted in Figure 5.15 comprising of the plot of q_t versus $t^{1/2}$ and the K_i values (Eq. 2.29), along with the correlation coefficients, are tabulated in Table 5.3. Based on the results, the TBT uptake by the synthesized MCM-TDI-C4, MCM-TDI-PC4 and MCM-TDI-C4S took place in two parts. The first part was an instant adsorption process resulting from the significant attraction between TBT and the adsorbent's external surface. The second part entailed the gradual adsorption which stems from the intraparticle diffusion of TBT molecules through the adsorbent pores. The plots referred to in Figure 5.15 were not linear throughout the whole time range, indicating that intraparticle diffusion was not the only rate limiting mechanism in the process of adsorption. In addition, the plots failed to pass through the origin, which shows that intraparticle diffusion was involved in the uptake process but it did not act as the rate-controlling step.



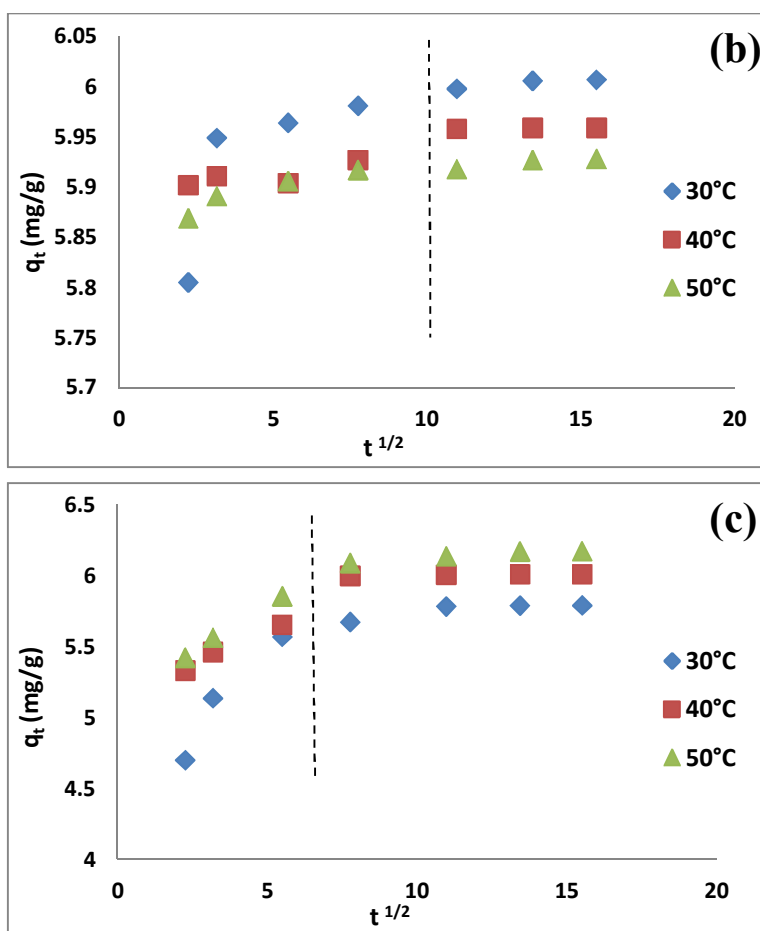


Figure 5.15 Intraparticle diffusion model plot for the adsorption of TBT Onto MCM-TDI-C4 (a), MCM-TDI-PC4 (b) and MCM-TDI-C4S (c)

Table 5.3 Calculated kinetic parameters for intraparticle diffusion model for the adsorption of TBT using MCM-TDI-C4 (a), MCM-TDI-PC4 (b) and MCM-TDI-C4S (c) as adsorbents

	T(°C)	Ki ₁ (mg/g min ^{1/2})	C ₁	R ₁ ²	Ki ₂ (mg/g min ^{1/2})	C ₂	R ₂ ²
(a)	30	0.1537	3.564	0.681	-0.0036	5.0422	0.7471
	40	0.1588	3.7078	0.8776	0.0002	5.0878	0.2937
	50	0.1662	3.7818	0.9168	0.0004	5.1292	0.9976
	30	0.5876	5.7025	0.5876	0.002	5.9768	0.8672

(b)	40	0.0036	5.8944	0.6065	0.0002	5.9557	0.7913
	50	0.008	5.8587	0.898	0.0022	5.8945	0.86
<hr/>							
	30	0.2525	4.2215	0.9414	0.0147	5.5854	0.7363
(c)	40	0.0964	5.1347	0.9822	0.0016	5.9896	0.9499
	50	0.1322	5.1352	0.9981	0.0113	6.0095	0.9363

5.3.7 Adsorption thermodynamic

It is widely acknowledged that parameters of thermodynamic are capable of evaluating the physiochemical adsorptive reaction's orientation and feasibility. Three such parameters used are standard enthalpy (ΔH°), standard free energy (ΔG°) and standard entropy (ΔS°). The values of ΔH° and ΔS° can be calculated from the slope and intercept of $\ln K_c$ versus $1/T$ plot (Eq.2.30, Figure 5.16), respectively. ΔG° can then be calculated using Eq. 2.31.

The calculated values of ΔH° , ΔS° and ΔG° for the adsorption of TBT on MCM-TDI-C4, MCM-TDI-PC4 and MCM-TDI-C4S are shown in Table 5.4. An important difference between the three adsorbents is the magnitude values of thermodynamic parameters. The higher magnitude values of ΔH° , ΔS° and ΔG° for MCM-TDI-C4S compared to MCM-TDI-C4 and MCM-TDI-PC4 may be related to the difference in the mechanisms of adsorption. The TBT adsorption by MCM-TDI-C4S occurred through strong electrostatic interactions, thus the process can lead to significant modifications of the surface groups and of the TBT molecule. In contrast, the TBT adsorption by MCM-TDI-PC4 and MCM-TDI-C4 was more related to the hydrophobic interactions and the process was just the formation of a dense layer of molecules on the surface of the adsorbents material.

The positive ΔH° values for MCM-TDI-C4 and MCM-TDI-C4S and the negative ΔH° value for MCM-TDI-PC4 indicated that the adsorption process was endothermic and exothermic in nature, respectively, which is consistent with the results obtained earlier in the effect of temperature in Section 5.3.4. In addition, the magnitude values of ΔH° indicate that the adsorption of TBT on MCM-TDI-C4 was a physisorption, and the adsorption of TBT on MCM-TDI-PC4 and MCM-TDI-C4S was chemisorption. Additionally, the energy value taken from the D-R model was consistent with these results.

The ΔS° positive values for MCM-TDI-C4 and MCM-TDI-C4S indicate the increased randomness at the interface of solid-solution during the process of sorption. Meanwhile, the negative ΔS° value suggests a decrease in the randomness at the solid/solution interface during the adsorption of TBT onto MCM-TDI-PC4. Furthermore, the solubility of MCM-TDI-C4S adsorbent plays an important role in the magnitude values of ΔS° . As in an aqueous solution, water molecules easily wet hydrophilic MCM-TDI-C4S adsorbent, TBT must received some heat and replace the water molecules and then it could be adsorbed on the MCM-TDI-C4S adsorbent surface. The action is called “solvent replacement”(Gökmen & Serpen, 2002). For TBT molecule with larger molar volume than water molecule, the number of water molecule replaced was larger than that of TBT molecule adsorbed. Hence, the solvent replacement results in the increase of entropy.

The ΔG° values for all adsorbents were negative, which reflect the spontaneous nature of the adsorption processes. The spontaneous adsorption of TBT onto MCM-TDI-PC4 was mainly driven by the enthalpy change, while MCM-TDI-C4 and MCM-TDI-C4S was

mainly driven by the entropy change. Compared to MCM-TDI-C4 and MCM-TDI-PC4, the largest absolute value of ΔG° for MCM-TDI-C4S suggests the most spontaneous nature of the adsorption processes of TBT to MCM-TDI-C4S. It was probably attributed to the electrostatic attraction that occurs at the upper rim of the calix[4]arene (the presence of sulfonated anion) in addition to the hydrophobic interaction with the host cavity (CH- π). The values of ΔG° for MCM-TDI-C4 and MCM-TDI-C4S were found to increase as the temperature increased, indicating high driving force and hence resulting in high adsorption capacity.

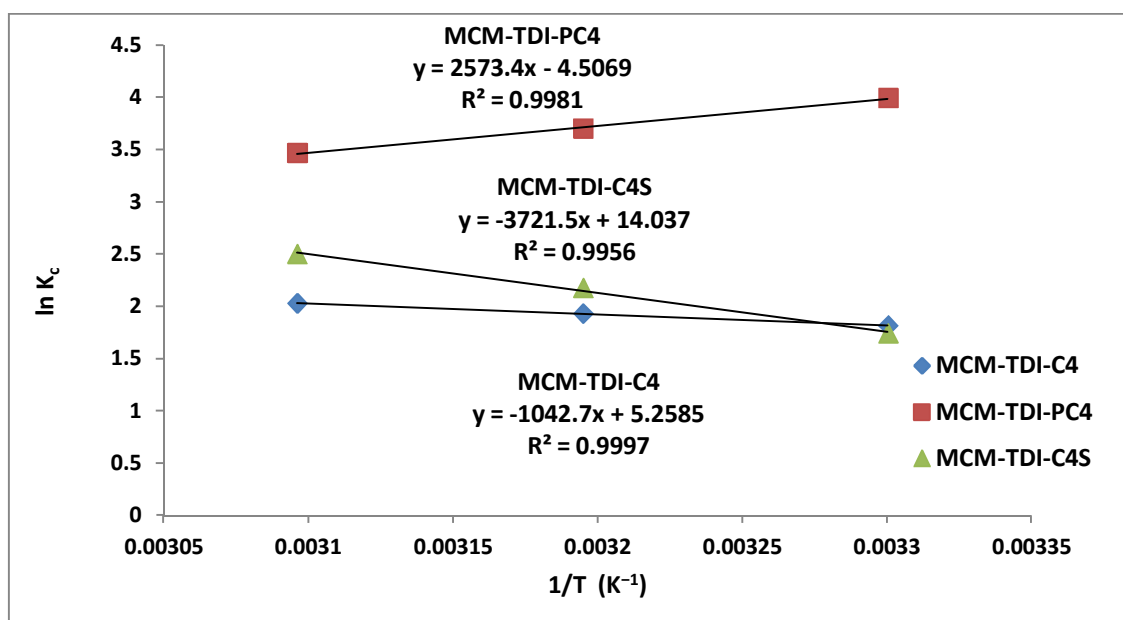


Figure 5.16 Plot of $\ln K_c$ versus $1/T$ for TBT adsorption

Table 5.4 Thermodynamic parameters of TBT adsorption on MCM-TDI-C4, MCM-TDI-PC4 and MCM-TDI-C4S

T (°C)	Thermodynamic parameters
--------	--------------------------

		ΔG° (kJ/mol)	ΔH° (kJ/mol)	ΔS° (J/mol K)
MCM-TDI-C4	30	-4.5779	8.669	43.7192
	40	-5.0151		
	50	-5.4523		
MCM-TDI-PC4	30	-10.0418	-21.3952	-37.4704
	40	-9.6671		
	50	-9.2924		
MCM-TDI-C4S	30	-36.5595	30.8066	120.7609
	40	-37.7671		
	50	-38.9747		

5.4 Summary

In this chapter, the application of modified mesoporous silica for batch adsorption of TBT has been investigated. Several factors that affect the adsorption efficiency were studied. In order to determine the equilibrium time for maximum uptake, a contact time study was performed and it showed that increasing the contact time increased the adsorption capacity of various adsorbents. It was noted that the adsorption increased rapidly in the initial stages and then became slow at the latter stages until the equilibrium was reached. The equilibrium time required for the adsorption of TBT was 2 h for all adsorbents. At equilibrium, with the optimum condition (pH, time and temperature), 93% of TBT was adsorbed by MCM-TDI-C4, 98% adsorbed by MCM-TDI-PC4 and 88% of TBT was adsorbed onto MCM-TDI-C4S.

The pH of a solution is generally recognized as a very effective parameter that governs the adsorption process. The results showed sensitive trends that depended on the type of

adsorbent and pH values. TBT species at low pH lead to the decreased in the adsorption efficiency due to the repulsion forces occurred between the TBT^+ and the protonated active binding sites. However, a significant increase in the adsorption capacity of TBT on the adsorbents was observed when the solution pH was raised. At higher pH ($\text{pH} > \text{pK}_a$), the adsorption decreased may be due to the TBT species (TBT OH), which are not favorable for the modified mesoporous silica with calix[4]arene derivatives.

The equilibrium adsorption of TBT on modified mesoporous silica with calix[4]arene derivatives at various temperatures was studied and the adsorption equilibrium was well described using different adsorption models. The three-parameter isotherm models showed better correlation with the experimental adsorption data than the two-parameter isotherm models, indicating that the surface of the three modified mesoporous silica samples was heterogeneous and calix[4]arene derivatives functional groups created on the mesoporous silica surface make the mesoporous silica surface more heterogeneous. Furthermore, the porosity factors β from Dubinin-Radushkevitch isotherm for TBT were <1 for the three adsorbents. This demonstrates the existence of micropores in addition to mesopores, which confirms the heterogeneity of the surface which arose from the pore structure, as well as adsorbate adsorbent interaction.

Upon comparing the TBT uptake capacities of the different adsorbents as listed in Table 5.5, it is challenging to compare the TBT uptake of the functionalized mesoporous silica in the present study to those done by other researchers because the experiments by different authors were conducted under their own conditions. Nevertheless, it was reasonable to state

that the functionalized mesoporous silica in the present study was equipped with a strong ability for TBT uptake.

Table 5.5 Comparison of adsorption capacities of various materials for TBT

Adsorbent	q_{\max} ($\mu\text{g/g}$)	Reference
MWNT (multiple-wall carbon nanotubes)	2084	(J. b. Zhang, et al., 2009)
MWNT-COOH	1444	(J. b. Zhang, et al., 2009)
Polymeric adsorbent	3350	(Puri, et al., 2004)
Organosorb 200-1	7996	(Vreysen, et al., 2008)
Organosorb 100-1	7986	(Vreysen, et al., 2008)
Norit SAE Super	7998	(Vreysen, et al., 2008)
MCM-TDI-C4	12121	Current study
MCM-TDI-PC4	16420	Current study
MCM-TDI-C4S	7575	Current study

In order to investigate the adsorption processes of TBT on MCM-TDI-C4, MCM-TDI-PC4 and MCM-TDI-C4S, three kinetic models were used, including the pseudo-first order, pseudo-second order and intraparticle diffusion models.

The determination coefficients of the pseudo-second order rate model were larger than 0.9998, and the calculated q_e values also agreed very well with the experimental data. This indicates that the kinetic modeling of TBT adsorbed by the three adsorbents belongs to the pseudo-second order kinetic model. It can also be seen from the pseudo-second order data

that the adsorption rate of TBT, K_2 , was found to be in the order of MCM-TDI-PC4 > MCM-TDI-C4S > MCM-TDI-C4. Additionally, the initial adsorption rates, h , were consistent with this order.

The intraparticle diffusion model was performed to explore the applicability of the model to the TBT-functionalized mesoporous silica system. The intraparticle diffusion model data indicated that the sorption removal of the TBT from aqueous phase on to MCM-TDI-C4, MCM-TDI-PC4 and MCM-TDI-C4S were rather complex process, which involved both boundary layer diffusion and intraparticle diffusion.

The effect of temperature on adsorption was studied and the thermodynamic parameters; free energy, enthalpy, and entropy of adsorption, were calculated. All the adsorption processes were spontaneous at all temperatures (negative free energy), and the enthalpy and entropy values were dependent on the type of adsorbent used.

CHAPTER 6

ISOTHERMS, KINETICS AND THERMODYNAMICS OF TRIPHENYLTIN (TPT) ADSORPTION ON MODIFIED MESOPOROUS SILICA WITH CALIX[4]ARENE DERIVATIVES

6.1 Introduction

Throughout the years, the environment has been the recipient of huge amounts of toxic compounds from natural resources, as well as human activities. Based on the intensity, the impact duration, the system resilience and whether the small quantities of substances are toxic, the results could be monumentally adverse. Organotin compounds are considered as a type of pollutant (e.g., butyltin and phenyltin) utilized in the applications such as antifouling paints, PVC stabilizers, timber treatment and others. In particular, triphenyltin (TPT), an organotin compound (OTC) like tributyltin (TBT), is utilized as an antifouling agent in ship paints since the 1960s. Additionally, OTCs wide utilization as pesticides on high-value food crops is well known (Golub & Doherty, 2004) and also as antifungal agent in the treatments of wood and textiles before they were banned in various countries. Despite the restriction of their use, OTCs may still be present in human dietary sources like fish and seafood (Appel, Bohme, Platzek, Schmidt, & Stinchcombe, 2000).

In the present decade, the removal of TPT from the natural environment is being treated by biological degradation. Along with bacteria and fungi, microalgae are also considered to biosorb and biodegrade TPT (Stasinakis, Thomaidis, Nikolaou, & Kantifes, 2005; Ye et al.,

2013; Yen, Tsai, Su, & Wang, 2001). Systematic examinations of the TPT adsorption through various adsorbents like natural sediments (Brändli, et al., 2009; Burton, et al., 2004; Hoch, et al., 2003), pure minerals (Hoch & Weerasooriya, 2005; Weidenhaupt, et al., 1997), organic matters (C. G. Arnold, et al., 1998), black carbons (Brändli, et al., 2009; Fang, et al., 2010) and recently wheat charcoal (Fang, et al., 2012) have been carried out.

Adsorption isotherm is the most important and fundamental source of information in understanding an adsorption process (Do Duong, 1998; Sykut, et al., 1999). It provides valuable information on how the organotin molecules distribute between the liquid phase and the solid phase when the adsorption process reaches an equilibrium state, which is critical in optimizing the use of adsorbents.

The objectives of this chapter are to investigate the adsorption of TPT from aqueous solution by modified mesoporous silica with calix[4]arene derivatives (MCM-TDI-C4, MCM-TDI-PC4 and MCM-TDI-C4S) at different temperatures and hence to evaluate the thermodynamic parameters of adsorption, i.e. free energy, enthalpy and entropy of adsorption in order to achieve a better understanding of the adsorption process. The effects of various operating parameters such as initial concentration, contact time and pH of the solution were also studied in detail. The kinetic parameters were calculated to determine the adsorption mechanism.

6.2 Experimental

6.2.1 Materials

6.2.1.1 Adsorbents

Since mesoporous silica MCM-41 modified with calix[4]arene derivatives using TDI as linker (MCM-TDI-C4, MCM-TDI-PC4 and MCM-TDI-C4S) gave the highest percentage removal for TPT, therefore these materials were selected as adsorbents to investigate the adsorption parameters of TPT in this chapter.

6.2.1.2 Adsorbate

Triphenyltin chloride TPT was used as an adsorbate in this part of research. Triphenyltin was obtained from Aldrich and used as received. Its molecular formula is illustrated in Figure 6.1.

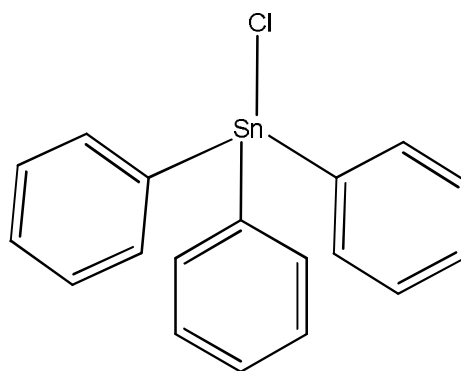


Figure 6.1 Molecular structure of triphenyltin chloride

Stock solutions were prepared by dissolving triphenyltin TPT in methanol and stored at 4°C in the dark, followed by serial dilutions with Milli-Q water of an 8.42 mM. A methanolic stock solution of organotin compound was used due to very low solubility in water.

6.2.2 Equilibrium isotherm and kinetics studies

Batch studies were performed to examine TPT adsorption onto modified mesoporous silica with calix[4]arene derivatives (MCM-TDI-C4, MCM-TDI-C4S and MCM-TDI-PC4) by agitating 10 ml of TPT with 0.01 g of adsorbent materials using a shaker bath (Wise Bath WSB-18) at 180 rpm. After the equilibrium state of adsorption was reached (determined through laboratory tests), samples were taken, filtered through a 0.45 µm membrane filter and TPT concentrations were determined by ICP-MS, and the amount of TPT sorbed by modified mesoporous silica with calix[4]arene derivatives (q_e) were calculated from Eq. 4.1. Experiments were conducted to evaluate the effects of pH, temperature, TPT initial concentration and contact time. The pH of the suspensions of TPT and adsorbent materials was maintained at the desired range by the addition of diluted hydrochloric acid (0.01 M, 0.1 M and 1 M) or diluted sodium hydroxide (0.01 M, 0.1 M and 1 M) during adsorption tests. All adsorption tests were carried out in triplicate.

For the adsorption isotherm study, 0.01 g of adsorbent materials were added to a series of TPT solutions (10 ml) with different initial concentrations ranging from 3-10 mg/L and agitated in a shaker bath (Wise Bath WSB-18) with a speed of 180 rpm for 2 h at different temperatures; 30, 40 and 50°C. The pH of the solutions was initially adjusted to the optimum pH.

To examine the adsorption kinetics, 0.01 g of adsorbent materials were added to 10 ml of TPT solutions and agitated for periods of time ranging from 5 to 240 min before the samples were taken to determine TPT concentrations. The solution pH, agitation speed and temperature were similar as in the adsorption isotherm study.

50 ml Teflon reactors (FEP, Nalgene) were used in all experiments since other studies have shown that this material did not compete for OTCs sorption and did not leach OTCs compounds (Behra, et al., 2003). All reactors used were thoroughly washed with a laboratory detergent (Sparkleen Fisher Scientific Ltd.) and rinsed with tap water. This was followed by rinsing with 10% nitric acid, (prepared from reagent grade nitric acid - BDH chemicals) and deionized water. In order to avoid TPT degradation by photolysis, the samples were covered during the entire experiment. A control was set to which no adsorbent was added in order to determine if TPT was adsorbed by the walls of the reactors. All experiments were triplicated and the average values were used in the analysis.

6.2.3 Analytical procedure

Analytical procedure for adsorption of triphenyltin TPT on modified mesoporous silica with calix[4]arene derivatives (MCM-TDI-C4, MCM-TDI-PC4 and MCM-TDI-C4S) were similar to the procedures mentioned in Chapter 5.

6.3 Results and discussion

6.3.1 Effect of contact time

The TPT removals by the synthesized mesoporous silica MCM-TDI-C4, MCM-TDI-PC4 and MCM-TDI-C4S are shown in Figure 6.2 as a function of contact time at 30, 40 and 50°C. It can be seen from the graph that 88%, 90% and 55% of the initial concentration of TPT was adsorbed onto MCM-TDI-C4, MCM-TDI-PC4 and MCM-TDI-C4S, respectively in the first 10 min. The TPT removal efficiency increased rapidly during the first 10 min and remained nearly constant after 2 h of adsorption, suggesting that the adsorption was fast and reached saturation within 2 h. After this equilibrium period, the amount of adsorbed TPT did not change significantly with time.

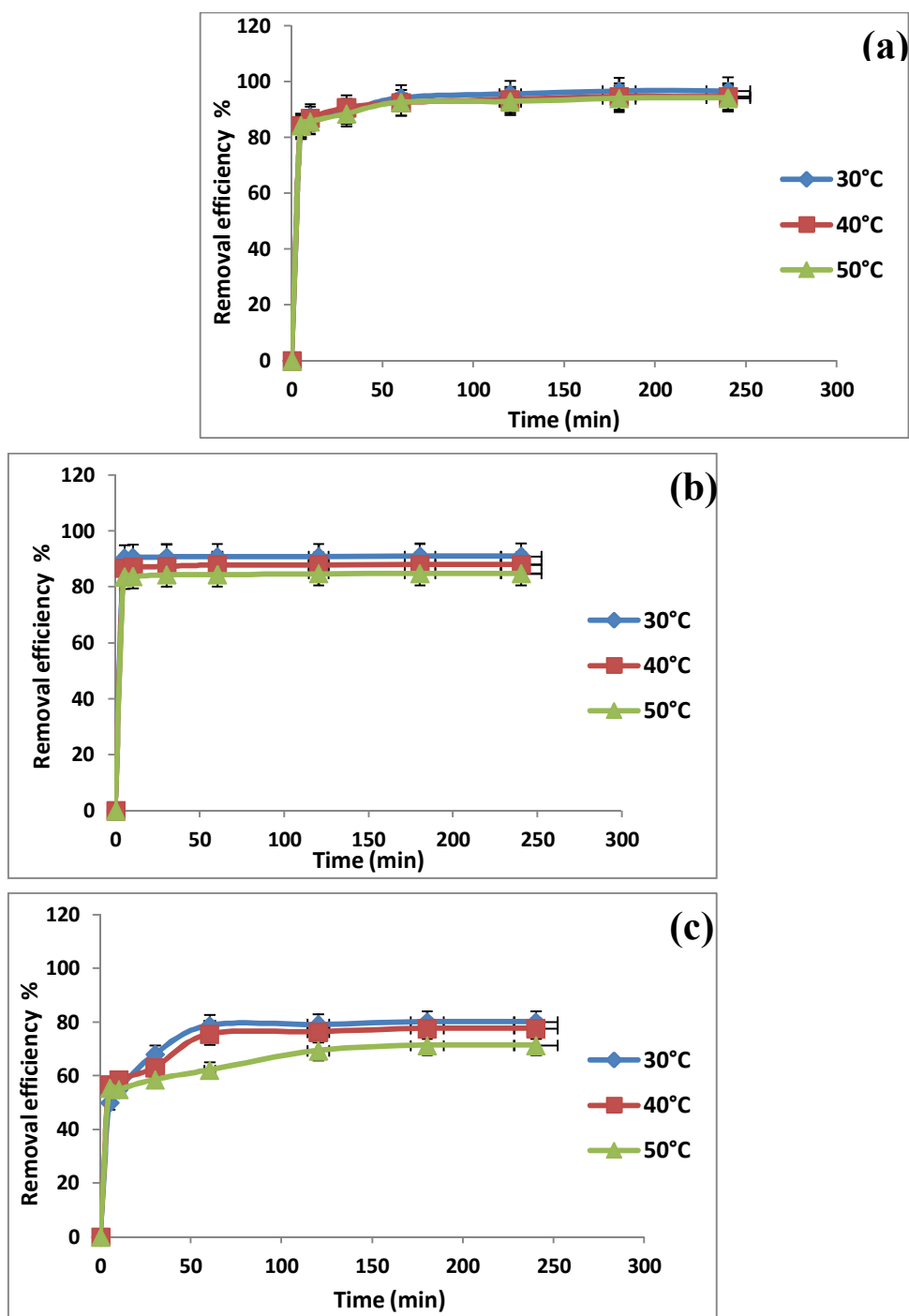


Figure 6.2 Effect of contact time on removal of TPT by MCM-TDI-C4 (a), MCM-TDI-PC4 (b) and MCM-TDI-C4S (c)

6.3.2 Effect of pH

The pH of the solution from which adsorption occurs influences the extent of adsorption. The effect of pH on the adsorption of TPT onto MCM-TDI-C4, MCM-TDI-PC4 and MCM-TDI-C4S was studied in the pH range of 3 to 8 (Figure 6.3).

The dependence of TPT adsorption on the pH can be attributed to two reasons, namely surface charge and species of TPT in aqueous solution. TPT is characterized as a weak acid having a pKa of 5.2 (C. G. Arnold, et al., 1997), composed of a cationic form (TPT⁺, (C₁₈H₁₅)₃Sn⁺) in equilibrium with a neutral form (TPTOH, (C₁₈H₁₅)₃Sn OH) according to Eq. 6.1:



At a low pH (pH < pKa), the superior species are TPT⁺ and the adsorption process is governed by electrostatic attraction. However, it is postulated that with a pH of over 5 (pH > pKa), the superior species are TPTOH and the major driving force of adsorption is the hydrophobic character, which is less effective than the electrostatic interaction (Hoch, et al., 2002). However, in acidic conditions, adsorbent surface becomes a significantly protonated surface that goes against the uptake of TPT⁺ form due to electrostatic repulsion.

As seen from Figure 6.3 the adsorption of TPT onto MCM-TDI-C4 and MCM-TDI-C4S increased with pH up to 4.0 and then declined with further increase in pH. This could be because of the easier adsorption of TPT ions (TPT⁺) into these adsorbents compared to TPT molecules (TPTOH) at high pH. On the other hand, in case of MCM-TDI-PC4 adsorbent,

TPT exhibited high removal percentage value in the pH region higher than their corresponding pKa, which was consistent with the assumption that the complexation of the TPTOH species by MCM-TDI-PC4 was primarily responsible for the sorption of TPT. The maximum removal percentage value was found as 95 % at pH 4.0, 93 % at pH 6.0 and 87 % at pH 4.0 for MCM-TDI-C4, MCM-TDI-PC4 and MCM-TDI-C4S, respectively.

As mentioned before in the previous chapter (Section 5.3.2), the immobilization of calixarenes onto solid surfaces plays an important role in adsorption behavior and the concept of size-shape fit has a key role in forming host compounds inclusion complexes with guest molecules. Hydrophobic interaction of CH- π and the π - π interaction between aromatic ring in calix[4]arene and aromatic ring in TPT and van der Waals forces were considered to determine the complex stability to a large extent. Furthermore, electrostatic interaction could be considered between TPT⁺ and MCM-TDI-C4S adsorbent.

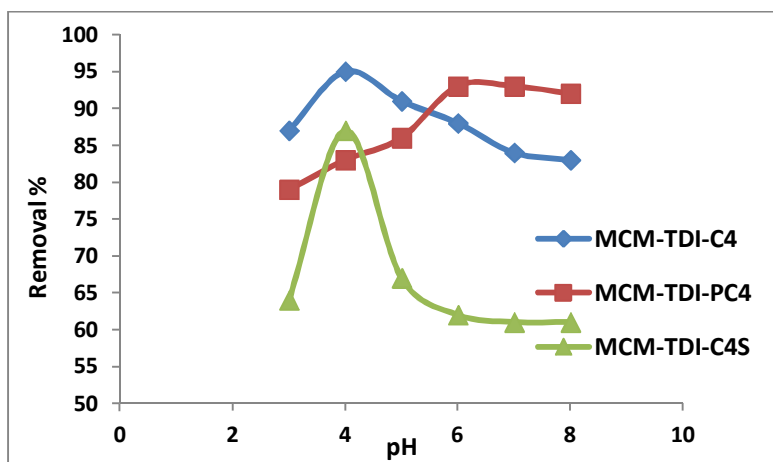


Figure 6.3 Effect of pH on removal of TPT by MCM-TDI-C4, MCM-TDI-PC4 and MCM-TDI-C4S

6.3.3 Effect of initial TPT concentration

The initial TPT concentration plays an important role in the process of adsorption. In order to show the effect of the initial concentration of TPT on the adsorption, sorption experiments were carried out at different initial TPT concentrations which varied from 3 to 12 mg/L (Figure 6.4). The removal efficiency decreased with the increase in the initial concentration of the TPT for all adsorption process. At low initial concentrations, TPT in the solution interacted with the binding sites and thus facilitated high adsorption. At higher concentrations, more TPT have been left un-adsorbed in the solution due to the saturation of binding sites. The TPT adsorption capacity first increased rapidly with increasing of the initial concentration of TPT and then started to decrease sharply in the case of MCM-TDI-C4 and MCM-TDI-C4S, which indicate that these adsorbents have a limited number of binding sites, which would have become saturated above a certain concentration compared to MCM-TDI-PC4 adsorbent.

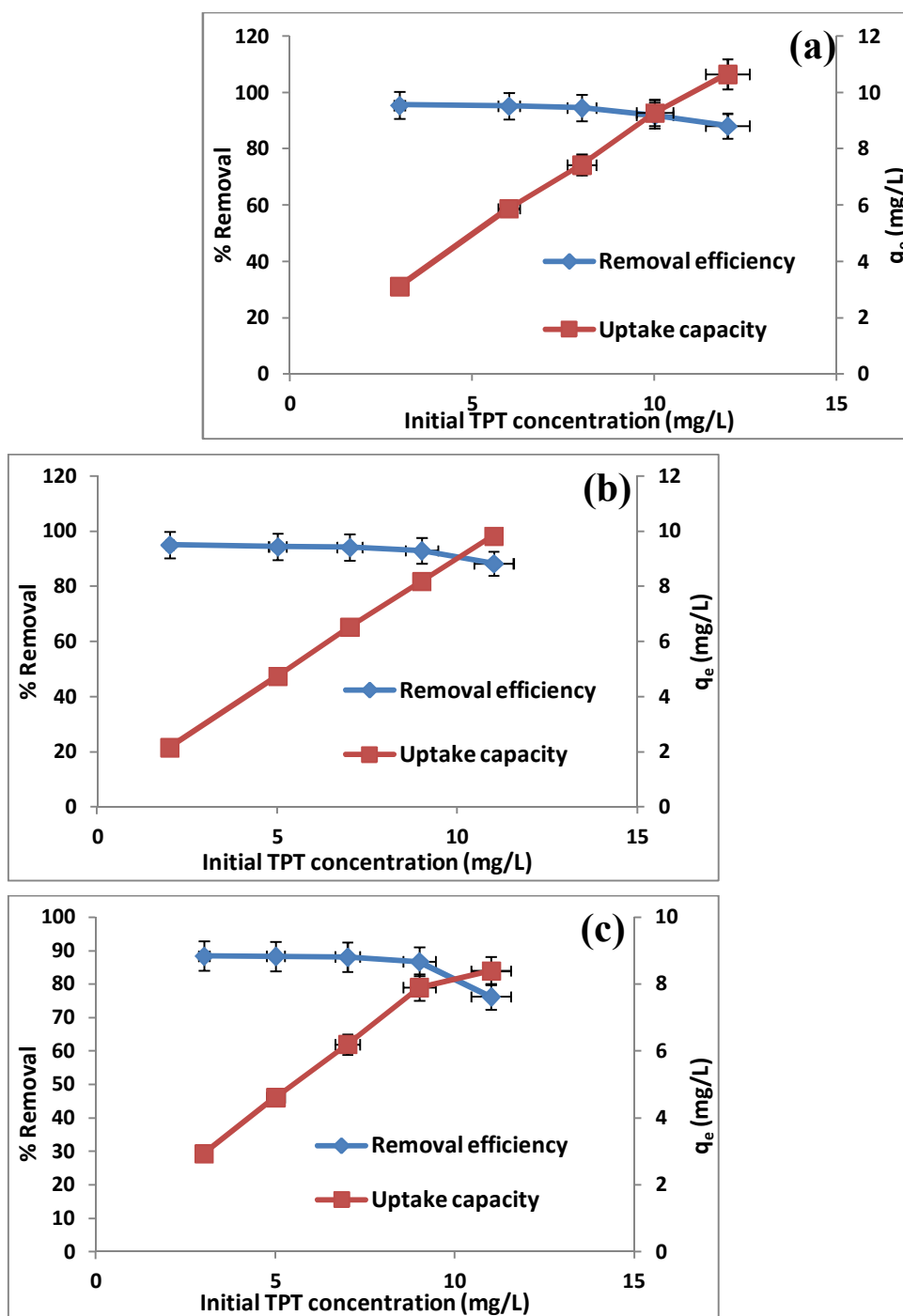


Figure 6.4 Effect of initial TPT concentration on the TPT removal efficiency and uptake capacity by MCM-TDI-C4 (a), MCM-TDI-PC4 (b) and MCM-TDI-C4S (c)

6.3.4 Effect of solution temperature

The temperature of the adsorption medium could be an important factor affecting the adsorption process. Most adsorption process is an exothermic process, whereas some examples of endothermic adsorption have also been reported. The adsorption of TPT by MCM-TDI-C4, MCM-TDI-PC4 and MCM-TDI-C4S appears to be temperature dependent over the temperature range tested (30-50°C) (Figure 6.5). The adsorption capacity of TPT onto all adsorbents decreased significantly with the increasing temperature, and this revealed the exothermic nature of the adsorption processes which was later utilized for the determination of changes in Gibbs free energy (ΔG°), heat of adsorption (ΔH°) and entropy (ΔS°) of the adsorption of TPT from aqueous solutions as provided in Section 6.3.7.

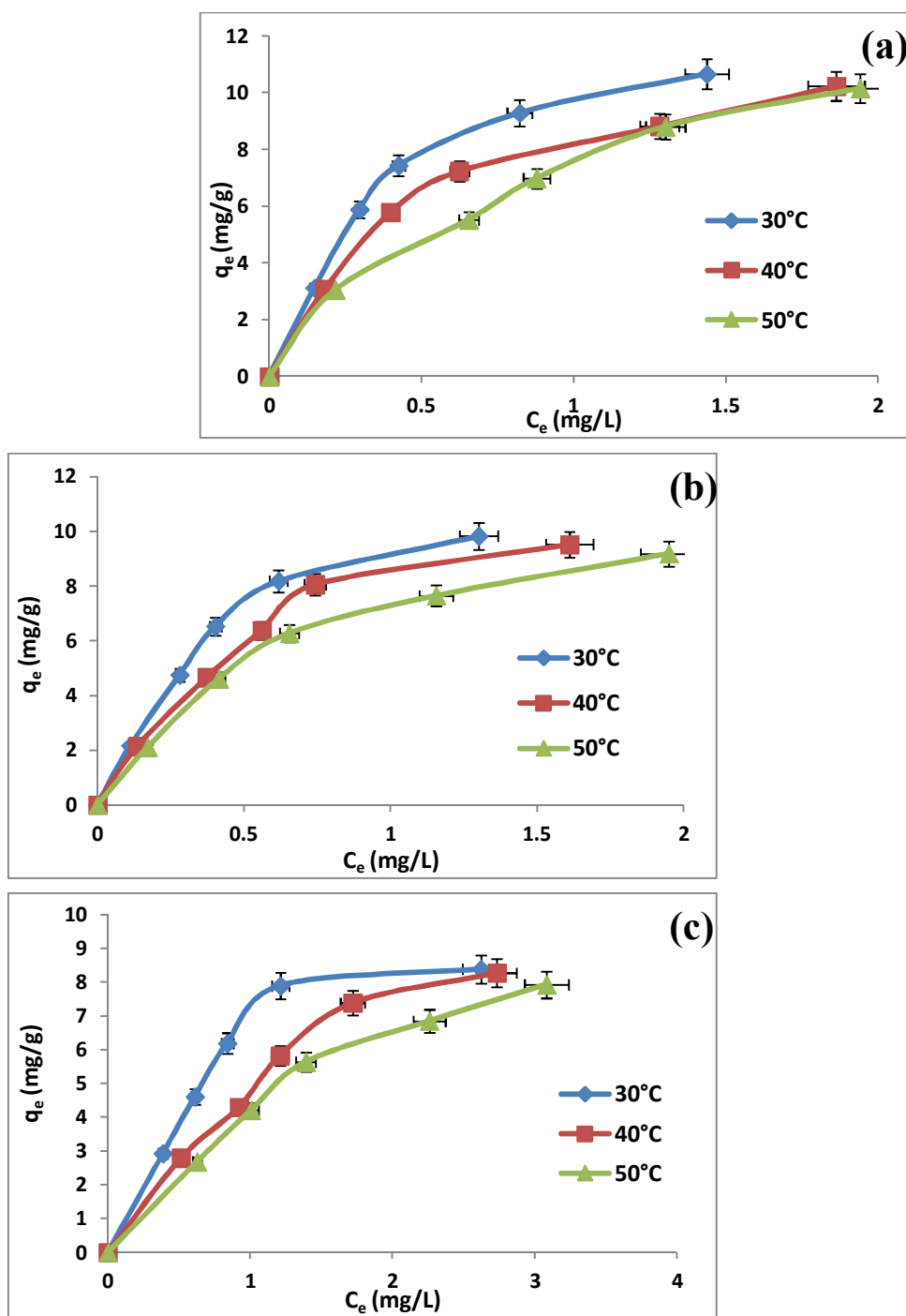


Figure 6.5 Adsorption isotherms for TPT on MCM-TDI-C4 (a), MCM-TDI-PC4 (b) and MCM-TDI-C4S (c) at different temperature

6.3.5 Adsorption isotherm models

The values of isotherm model constants and their respective correlation coefficients are presented in Table 6.1. The experimental data of TPT produced a higher value of correlation coefficients with Langmuir II model (Figure 6.6) than Freundlich model (Figure 6.7), indicating the acceptability of the model of homogeneous sorption phenomena. The values of n , were more than unity, which represents a favorable adsorption condition. The maximum monolayer adsorption capacity q_m from Langmuir were 17.7305, 19.305 and 18.9393 mg/g for MCM-TDI-C4, MCM-TDI-PC4 and MCM-TDI-C4S, respectively.

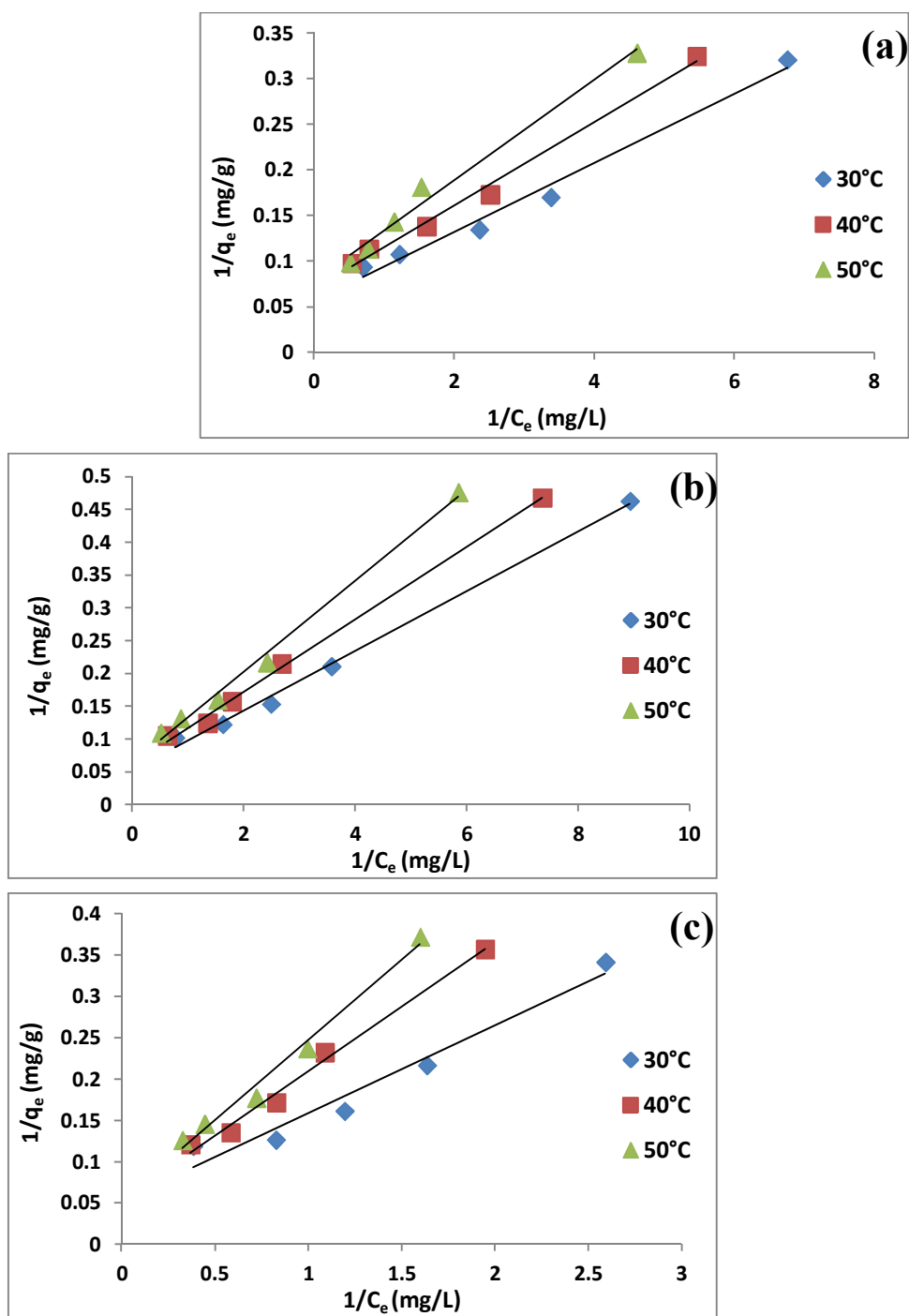


Figure 6.6 Langmuir isotherm Type II of TPT adsorbed onto MCM-TDI-C4 (a), MCM-TDI-PC4 (b) and MCM-TDI-C4S (c)

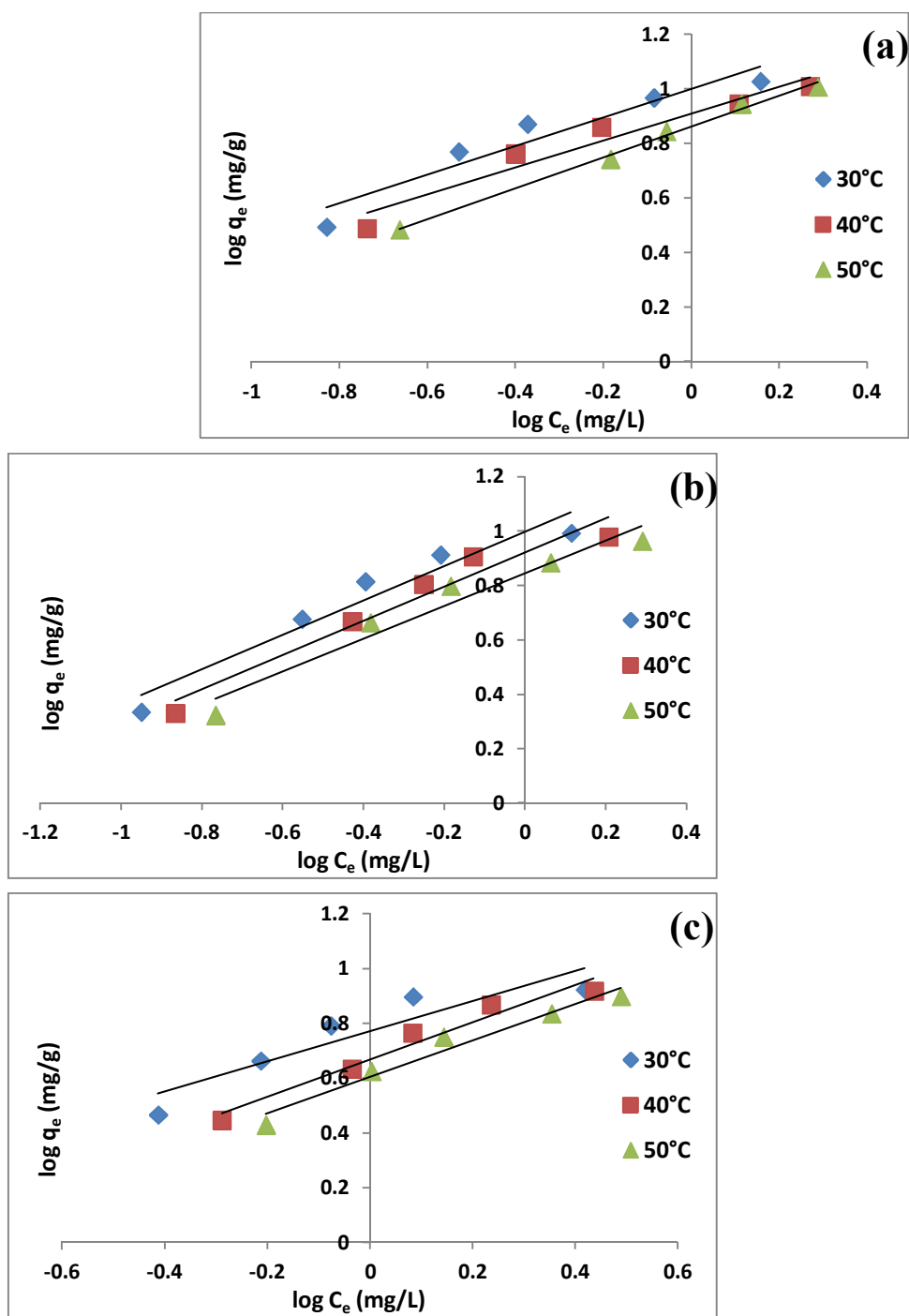


Figure 6.7 Freundlich isotherm of TPT adsorbed onto MCM-TDI-C4 (a), MCM-TDI-PC4 (b) and MCM-TDI-C4S (c)

Table 6.1 Isotherm constants and correlation coefficient of determination for various adsorption isotherms for the adsorption of TPT onto MCM-TDI-C4 (a), MCM-TDI-PC4 (b) and MCM-TDI-C4S (c)

Adsorbents	Adsorption isotherm	Isotherm parameter	Temperature		
			30	40	50
(a)	Freundlich	$K_F(L/g)$	9.9908	8.091	7.2577
		n	1.9091	2.0292	1.7671
		R^2	0.9158	0.9419	0.9935
	Langmuir (II)	$q_m(mg/g)$	17.7305	14.2857	12.7064
		$K_L(L/mg)$	1.4921	1.5351	1.4283
		R^2	0.9835	0.9923	0.9857
	Temkin	A_T	3.3102	2.9828	3.2869
		$K_T(L/mg)$	19.3098	16.4466	10.2755
		R^2	0.9856	0.9925	0.9688
	Dubinin-Radushkevitch	$q_d(mg/g)$	11.3782	10.2308	9.4056
		$\beta(mol^2/kJ^2)$	1.006×10^{-3}	1.67×10^{-3}	2.01×10^{-3}
		$E(kJ/mol)$	22.2939	17.3032	15.772
		R^2	0.9672	0.9925	0.9226
	Redlich–Peterson	g	0.985	0.9915	0.8086
		$B_R(L/mg)$	1.7303	1.6547	1.8081
		$A_R(L/g)$	28.1757	22.7213	20.9664
		R^2	0.9471	0.9836	0.9835
	Koble–Corrigan	p	1.503	1.3165	0.6362
		A_K	75.7576	40	8.5251
		B_K	6.6439	3.636	0.1671
		R^2	0.9997	0.9988	0.9968
(b)	Freundlich	$K_F(L/g)$	9.9586	8.3657	6.9823
		n	1.5837	1.587	1.6664
		R^2	0.935	0.9473	0.9471
	Langmuir (II)	$q_m(mg/g)$	19.305	16.2866	15.8227
		$K_L(L/mg)$	1.1359	1.1103	0.9106
		R^2	0.9953	0.997	0.9944
	Temkin	A_T	3.2484	3.131	2.9162
		$K_T(L/mg)$	17.3739	14.0139	12.1462
		R^2	0.9856	0.9737	0.9977
	Dubinin-Radushkevitch	$q_d(mg/g)$	10.5603	9.6282	9.1011
		$\beta(mol^2/kJ^2)$	1.67×10^{-3}	1.67×10^{-3}	2.01×10^{-3}
		$E(kJ/mol)$	17.265	17.265	15.772
		R^2	0.9924	0.9748	0.9905
	Redlich–Peterson	g	0.9525	0.9304	0.986
		$B_R(L/mg)$	1.2553	1.1985	1.0061
		$A_R(L/g)$	22.7742	18.8305	14.9335

Table 6.1 (Continued)

(c)	Koble–Corrigan	R^2	0.9525	0.9726	0.9623
		p	1.2219	1.0532	1.2922
		A_K	37.7358	20.4498	25.7069
		B_K	2.9584	1.4069	2.4318
		R^2	0.9987	0.9972	0.9997
	Freundlich	$K_F(L/g)$	5.9006	4.6580	4.0169
		n	1.8242	1.4710	1.5033
		R^2	0.841	0.9571	0.9603
	Langmuir (II)	$q_m(mg/g)$	18.9393	18.7266	18.587
		$K_L(L/mg)$	0.4986	0.3421	0.278
		R^2	0.9564	0.9894	0.9862
	Temkin	A_T	2.9731	3.4893	3.2767
		$K_T(L/mg)$	8.2698	4.2274	3.6959
		R^2	0.8952	0.9745	0.9942
	Dubinin-Radushkevitch	$q_d(mg/g)$	9.5401	8.6547	8.2771
		$\beta(mol^2/kJ^2)$	9.1×10^{-4}	1.8×10^{-3}	1.8×10^{-3}
		$E(kJ/mol)$	23.4161	16.5577	16.5577
		R^2	0.9858	0.9576	0.987
	Redlich–Peterson	g	0.7096	0.5352	0.5275
$B_R(L/mg)$		1.4080	1.2412	1.3461	
$A_R(L/g)$		14.7029	10.5369	9.4684	
Koble–Corrigan	R^2	0.8068	0.8657	0.87	
	p	1.7981	1.1232	1.5387	
	A_K	23.31	7.2886	7.6687	
	B_K	2.4569	0.5066	0.8014	
	R^2	0.9942	0.9902	0.9983	

The R_L parameters (Eq. 2.10) maintained between 0 and 1, which showed consistency with the requirement for a favorable adsorption process (Figure 6.8). The order of favorability was consistent with the K_L values order.

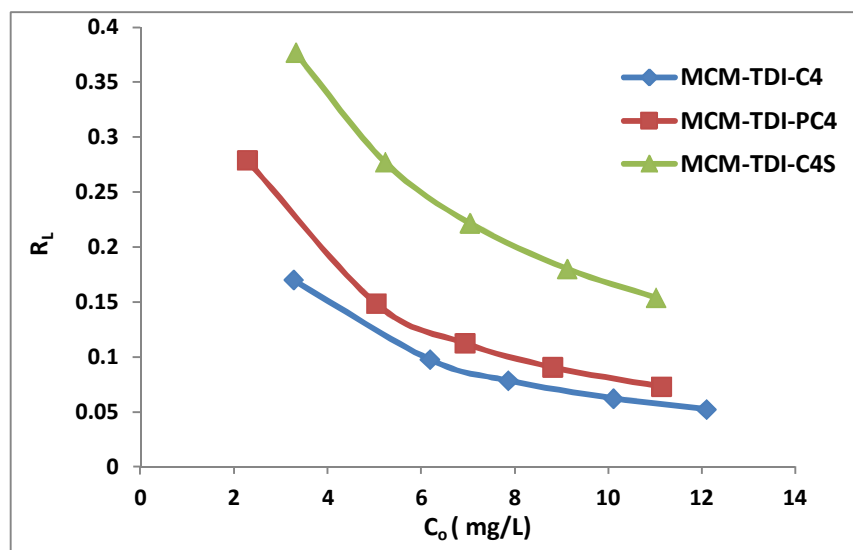


Figure 6.8 Values of R_L for adsorption of TPT onto MCM-TDI-C4, MCM-TDI-PC4 and MCM-TDI-C4S

The results were also fitted by the Temkin model (Figure 6.9), which suggested a reduction in the heat of adsorption along with coverage due to adsorbent–adsorbate interactions. As a result, adsorption of TPT could be characterized by a uniform distribution of binding energies up to a maximum value.

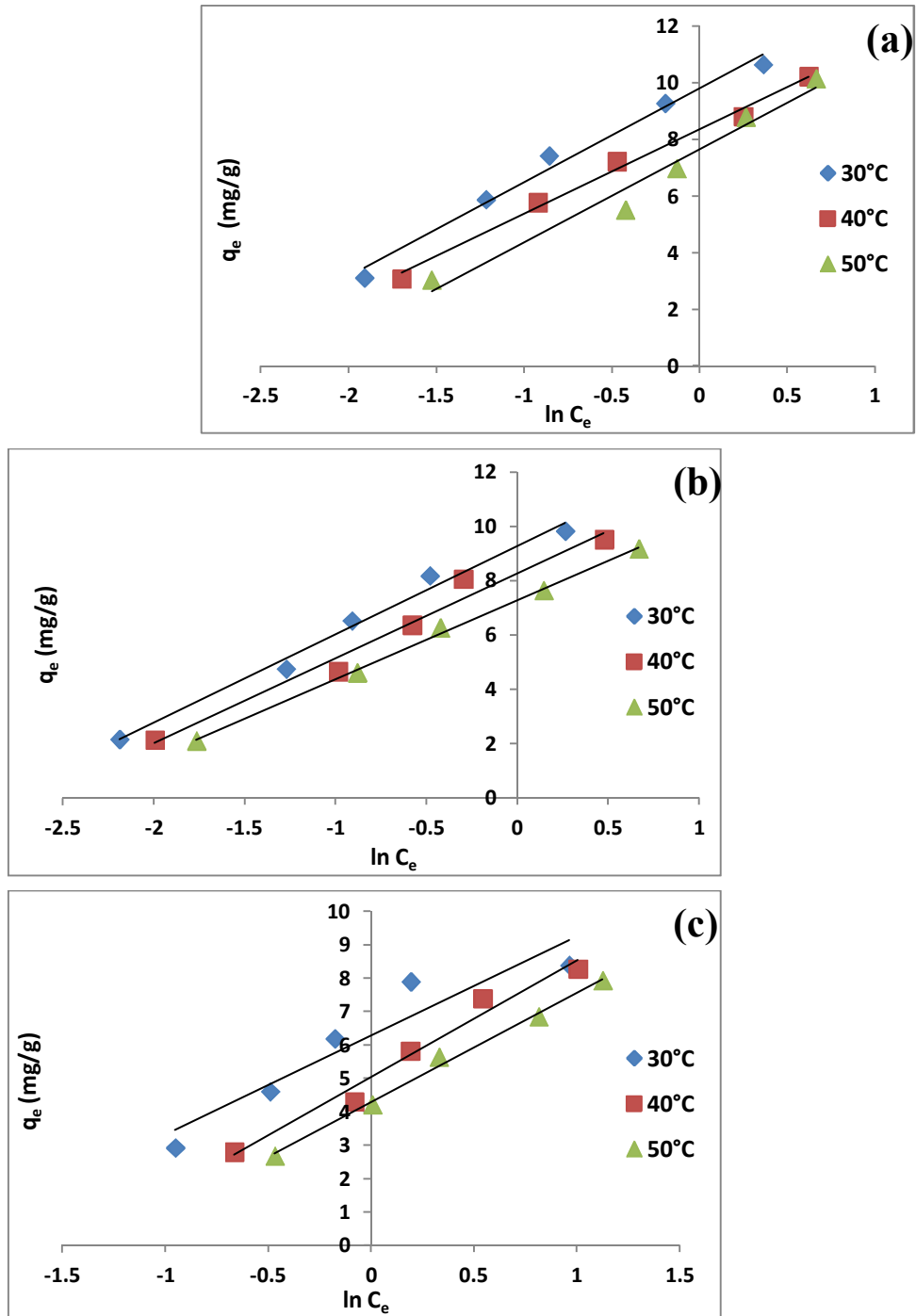


Figure 6.9 Temkin isotherm of TPT adsorbed onto MCM-TDI-C4 (a), MCM-TDI-PC4 (b) and MCM-TDI-C4S (c)

The Dubinin-Radushkevitch isotherm model is a semi-empirical equation where the adsorption is characterized by multilayer involving van der Waals forces (Hutson & Yang, 1997). The model is also utilized in the estimation of the mean free energy adsorption, E . The mean free energies of adsorption of TPT onto MCM-TDI-C4, MCM-TDI-PC4 and MCM-TDI-C4S were almost 16 kJ/mol or more, indicating that the TPT adsorption on all adsorbents took place through chemical adsorption. The values of the porosity factors β (mol^2/kJ^2) were less than unity (Table 6.1, Figure 6.10) imply that all adsorbents consist of micropores, which was consistent with the result in previous chapter and indicated a surface heterogeneity may arise from the pore structure, as well as adsorbate-adsorbent interaction (Negrea, et al., 2011).

The Redlich-Peterson isotherm combines both Langmuir and Freundlich equations elements and the adsorption mechanism is described as a hybrid (homogeneous and heterogeneous) model, which is distinct from an ideal monolayer adsorption. The Redlich-Peterson isotherm constants (Eq. 2.20) were determined through the Solver add-in of Microsoft Excel and are listed in Table 6.1. The coefficients of determination for Redlich-Peterson isotherm model (Figure 6.11) showed a moderate applicability of this model for the adsorption of TPT using MCM-TDI-C4, MCM-TDI-PC4 and MCM-TDI-C4S. The exponent values of g were close to 1, signifying the fit of the Langmuir model for explaining the obtained equilibrium data.

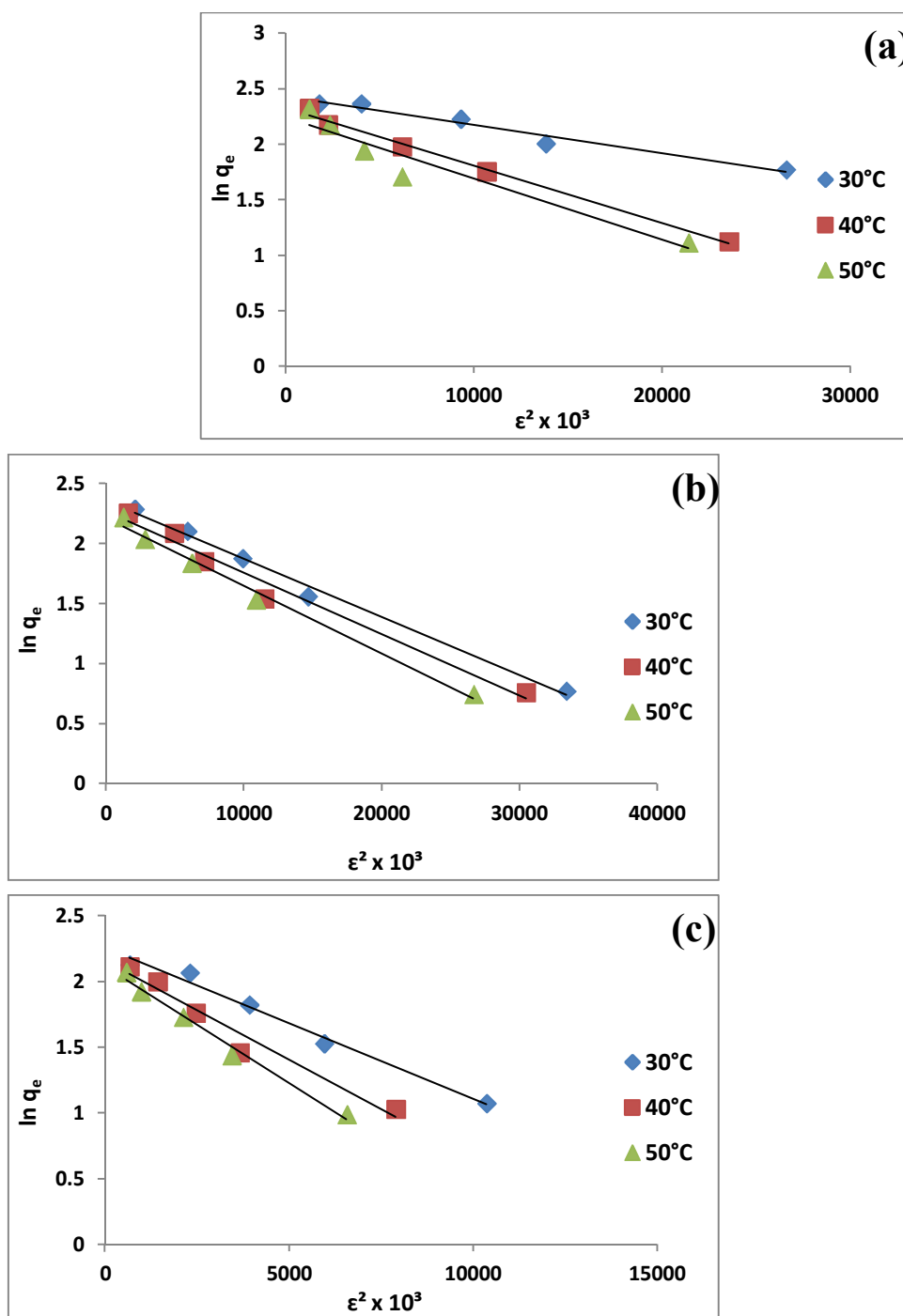


Figure 6.10 Dubinin–Radushkevitch isotherm of TPT adsorbed onto MCM-TDI-C4 (a), MCM-TDI-PC4 (b) and MCM-TDI-C4S (c)

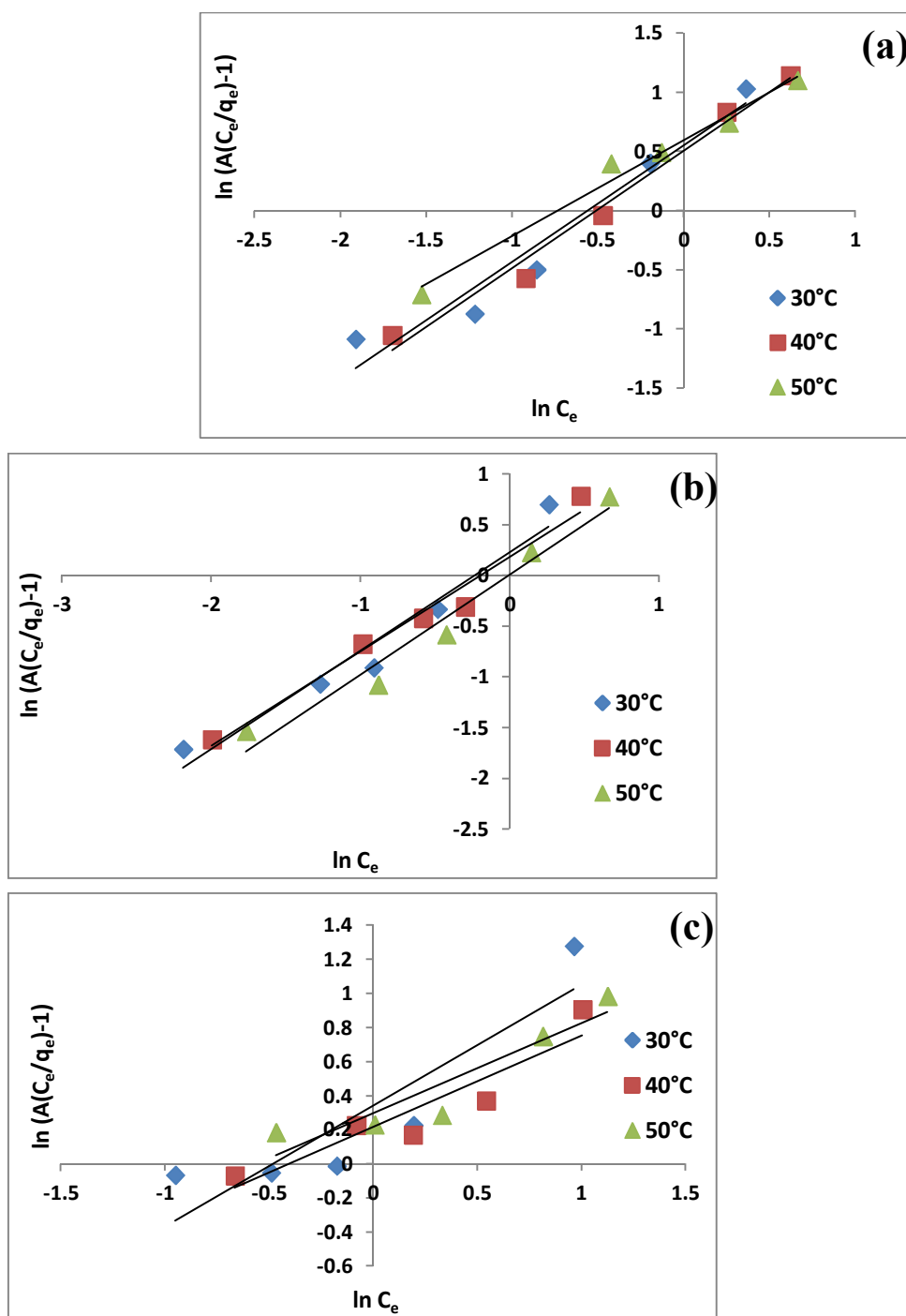


Figure 6.11 Redlich-Peterson isotherm of TPT adsorbed onto MCM-TDI-C4 (a), MCM-TDI-PC4 (b) and MCM-TDI-C4S (c)

Moreover, the Koble–Corrigan model (Figure 6.12) seemed to agree very well with the experimental data of TPT ($R^2 > 0.9902$). This indicates that a combination of heterogeneous and homogeneous uptake occurred for TPT uptake by the prepared MCM-TDI-C4, MCM-TDI-PC4 and MCM-TDI-C4S. By comparing the coefficients of determination of the Langmuir and Freundlich models, we inferred that homogenous uptake was the main mechanism of the TPT adsorption process. The corresponding Koble–Corrigan parameters of A_K , B_K and p for different temperatures along with correlation coefficients are also given in Table 6.1.

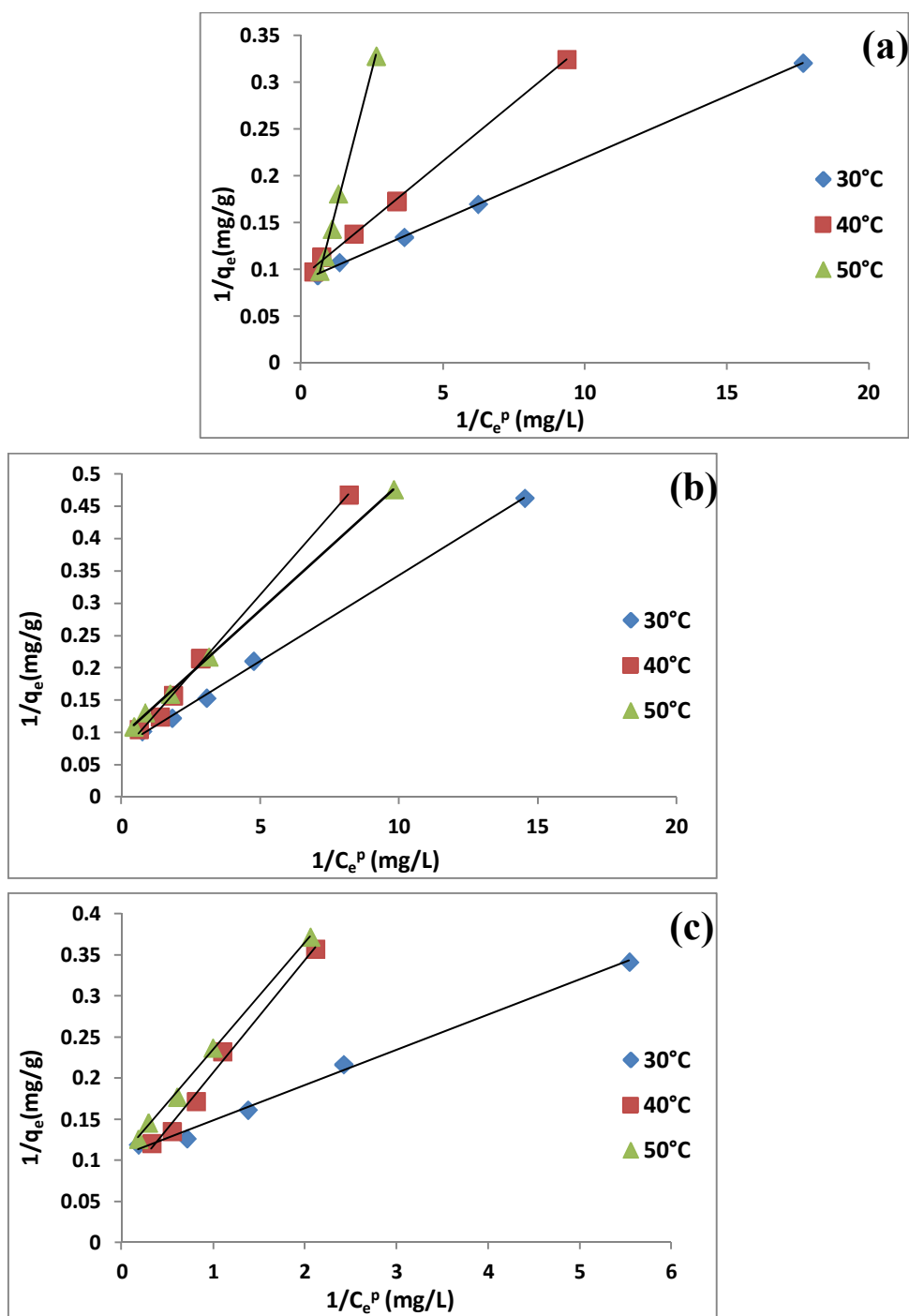


Figure 6.12 Koble-Corrigan isotherm of TPT adsorbed onto MCM -TDI-C4 (a), MCM-TDI-PC4 (b) and MCM-TDI-C4S (c)

6.3.6 Adsorption kinetic

In order to clarify the adsorption kinetics of TPT onto MCM-TDI-C4, MCM-TDI-PC4 and MCM-TDI-C4S adsorbents, three kinetic models, which are pseudo-first order, pseudo-second order and intraparticle diffusion models, were applied to the experimental data.

I. Pseudo-first order kinetic

Figure 6.13 shows a plot of the linearized form of the pseudo-first order model for the sorption of TPT at various temperatures. Although the correlation coefficients for the linear plots of $\ln (q_e - q_t)$ against time from the pseudo-first order model were greater than 0.916, the experimental data deviated considerably from the theoretical data (Table 6.2), confirming that the pseudo-first order model was not appropriate for describing the adsorption kinetics of TPT onto adsorbents.

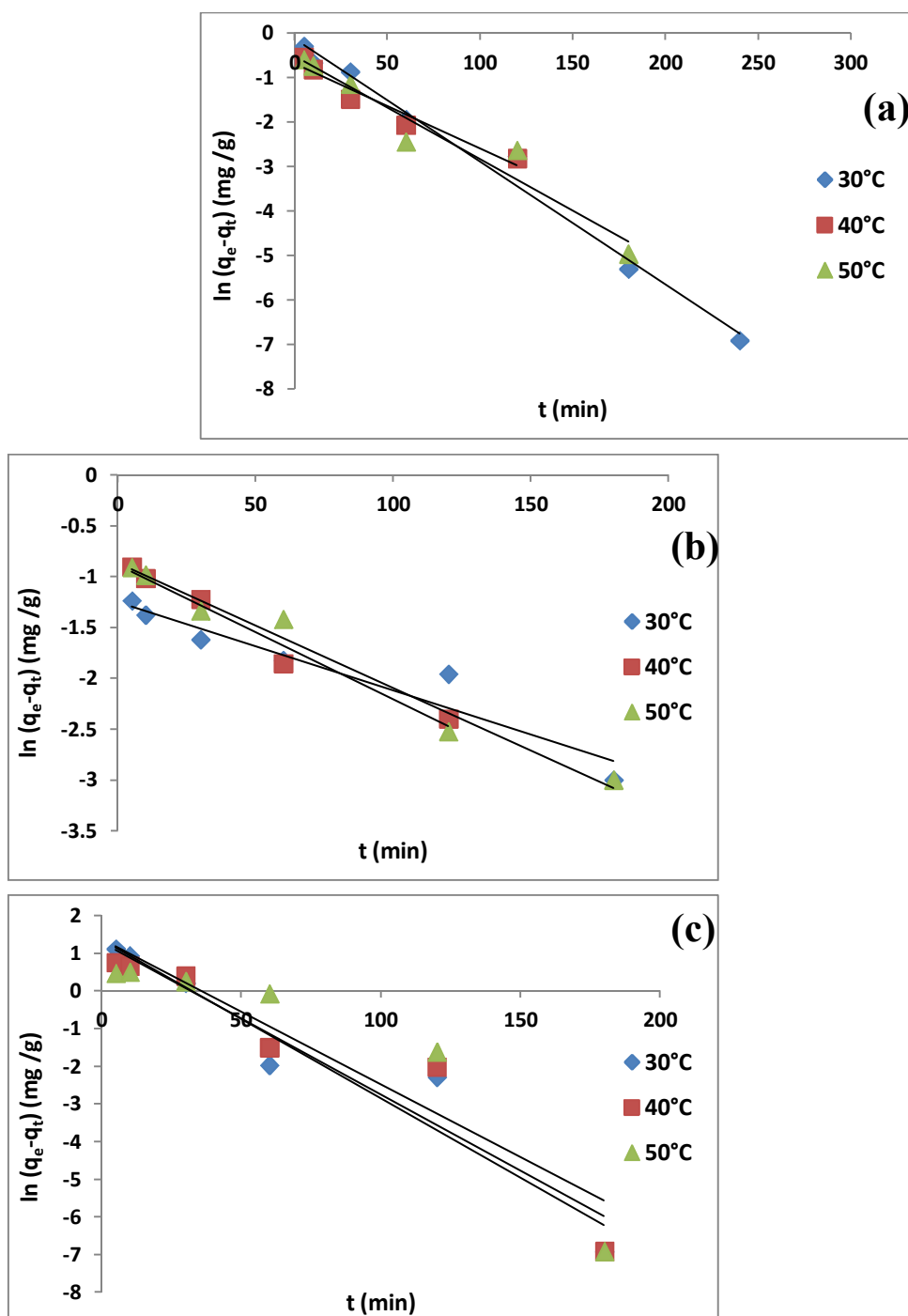


Figure 6.13 Pseudo-first order model plot for the adsorption of TPT onto MCM-TDI-C4 (a), MCM-TDI-PC4 (b) and MCM-TDI-C4S (c)

Table 6.2 Calculated kinetic parameters for pseudo first-order and pseudo-second order kinetic

models for the adsorption of TPT using MCM-TDI-C4 (a), MCM-TDI-PC4 (b) and MCM-TDI-C4S (c) as adsorbents

	T (°C)	q _{e,exp} (mg g ⁻¹)	Pseudo-first order			Pseudo-second order			
			K ₁ (min ⁻¹)	q _{e,cal} (mg g ⁻¹)	R ₁ ²	K ₂ (g mg ⁻¹ min ⁻¹)	q _{e,cal} (mg g ⁻¹)	h (mg l ⁻¹ min ⁻¹)	g ⁻¹
(a)	30	5.491	0.0276	0.874	0.9838	0.1101	5.5248	3.363	0.9999
	40	5.373	0.0191	0.506	0.9436	0.153	5.3966	4.4267	1
	50	5.341	0.0231	0.593	0.9405	0.142	5.3648	4.0749	1
(b)	30	9.257	0.0087	0.286	0.9166	1.422	9.259	9.259	1
	40	8.954	0.0132	0.4129	0.9736	0.8589	8.9605	8.961	1
	50	8.628	0.0123	0.42029	0.9775	0.7367	8.6355	8.6355	1
(c)	30	8.18	0.0421	3.9129	0.9321	0.0294	8.34	2.0433	0.9998
	40	7.925	0.0404	3.6466	0.915	0.0262	8.0645	2.0483	0.9996
	50	7.278	0.0386	3.9964	0.8571	0.0217	7.4239	1.4263	0.999

II. Pseudo-second order kinetic

The pseudo-second order rate constant K_2 , q_e and R^2 are given in Table 6.2 (Figure 6.14). From Table 6.2, it was evident that the calculated q_e values agreed with the experimental q_e values well, and also, the correlation coefficients for the pseudo-second order kinetic plots at all the studied adsorbents and temperatures were higher than 0.999. It can thus be easily concluded that the ongoing reactions proceeds via a pseudo-second order mechanism rather than a pseudo-first order mechanism. Furthermore, the adsorption rate of TPT, K_2 , was found to be in the order of MCM-TDI-PC4>MCM-TDI-C4>MCM-TDI-C4S. Additionally, the initial adsorption rates, h , were consistent with this order.

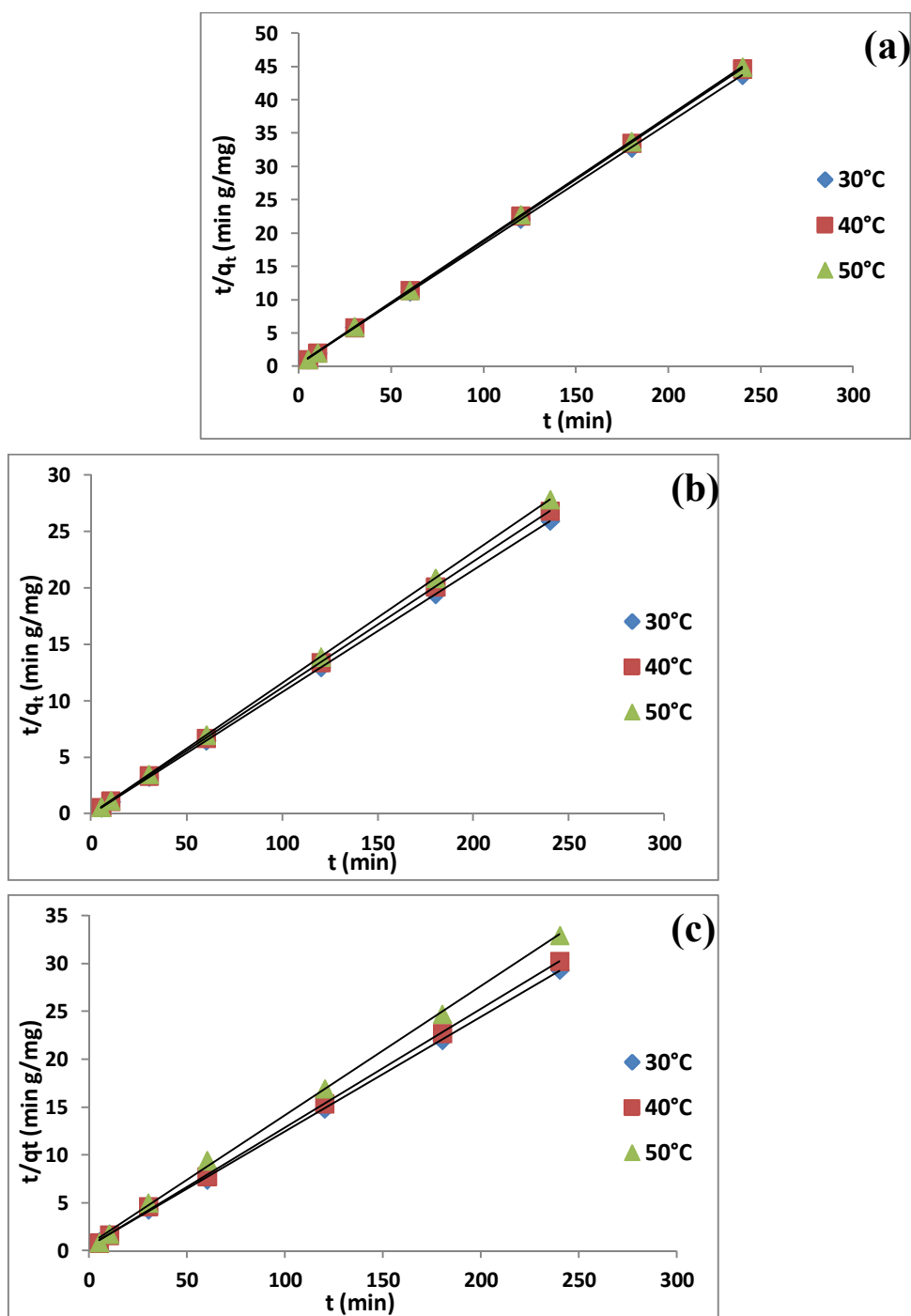


Figure 6.14 Pseudo-second order model plot for the adsorption of TPT onto MCM-TDI-C4 (a), MCM-TDI-PC4 (b) and MCM-TDI-C4S (c)

III. Intraparticle diffusion model

The intraparticle diffusion model's fit with the experimental data is depicted in Figure 6.15, which consists of the plot of q_t versus $t^{1/2}$ and the K_i values (Eq. 2.29), and the correlation coefficients are tabulated in Table 6.3. Based on the results, the TPT uptake by the synthesized adsorbents took place in two phases, namely the surface sorption and intraparticle diffusion. The initial linear portion occurred due to the boundary layer diffusion effect, while the final part was due to the intraparticle diffusion effect. Nevertheless, the correlation coefficients of the intraparticle model were less compared to the pseudo-second order model. The plots failed to pass through the origin, which shows that intraparticle diffusion was involved in the uptake process but it did not act as the rate-controlling step.

Table 6.3 Calculated kinetic parameters for intraparticle diffusion model for the adsorption of TPT using MCM-TDI-C4 (a), MCM-TDI-PC4 (b) and MCM-TDI-C4S (c) as adsorbents

	T (°C)	K_{i1} (mg/g min ^{1/2})	C_1	R_1^2	K_{i2} (mg/g min ^{1/2})	C_2	R_2^2
(a)	30	0.0095	4.7849	0.933	0.0005	5.375	0.8361
	40	0.0078	4.8227	0.9529	8E-06	5.3713	0.7913
	50	0.0078	4.8227	0.9909	0.0006	5.2067	0.8581
(b)	30	0.01	9.1795	0.9571	0.0021	9.2248	0.924
	40	0.019	8.7908	0.9678	0.0019	8.9274	0.8792
	50	0.024	8.45	0.9982	0.0048	8.5607	0.7508
(c)	30	0.5688	3.8232	0.9999	0.0203	7.8776	0.9016
	40	0.1975	5.3489	0.9997	0.0317	7.4582	0.9319
	50	0.1093	5.3547	0.8396	0.1225	5.5349	0.8408

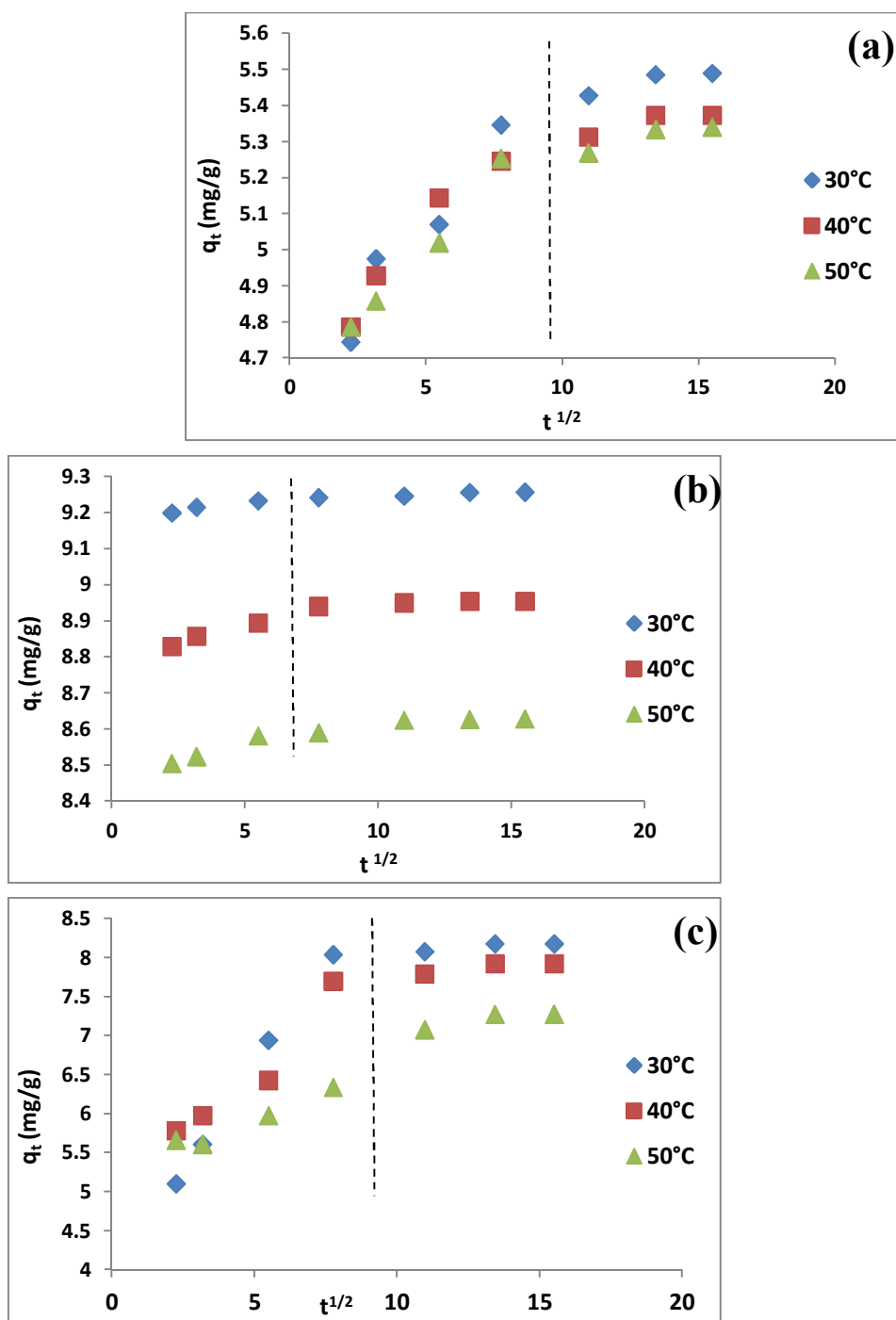


Figure 6.15 Intraparticle diffusion model plot for the adsorption of TPT onto MCM-TDI-C4 (a), MCM-TDI-PC4 (b) and MCM-TDI-C4S (c)

6.3.7 Adsorption thermodynamic

Thermodynamic parameters such as standard free energy (ΔG°), enthalpy (ΔH°), and entropy (ΔS°) of adsorption were calculated in order to explain the thermodynamic nature involved in the adsorption process.

The values of ΔH° and ΔS° were calculated from the slope and intercept of plot between $\ln K_c$ versus $1/T$ (Figure 6.16). The calculated values of ΔH° , ΔS° and ΔG° are listed in Table 6.4.

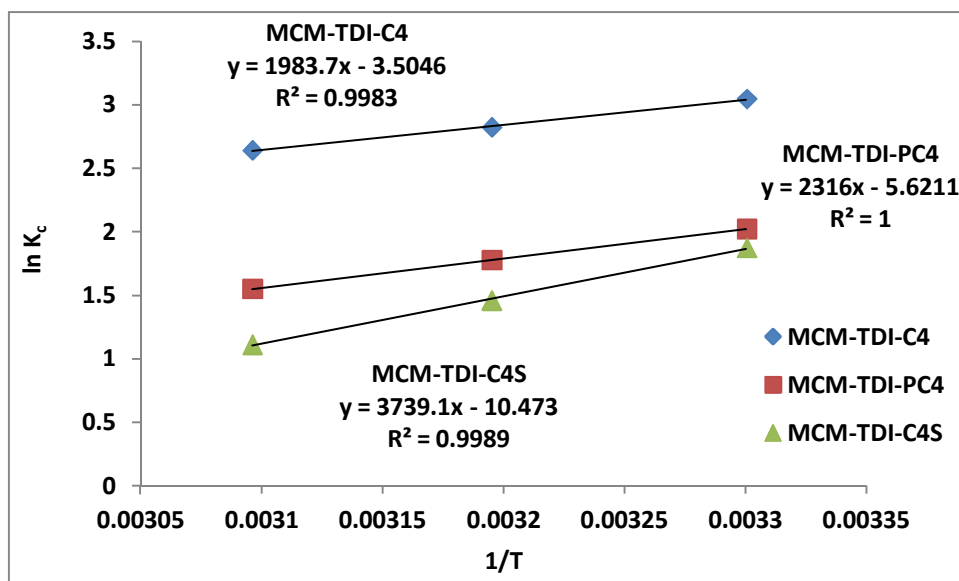


Figure 6.16 Plot of $\ln K_c$ versus $1/T$ for TPT adsorption

All values for the change in ΔG° were negative, implying the thermodynamic feasibility and spontaneous nature of the adsorption of TPT. A decrease in the negative values of ΔG° with the increasing temperatures confirms an increase in the feasibility of adsorption at a low temperature, indicating that high temperatures play a negative role in the adsorption.

Besides, the negative values of the enthalpy (ΔH°) demonstrated that the adsorption process of the TPT onto MCM-TDI-C4, MCM-TDI-PC4 and MCM-TDI-C4S were exothermic, which was consistent with the previous results in the section regarding the temperature effect studies (Section 6.3.4). The decrease in the adsorption capacity with increase in the temperature was known to be due to the enhancement of the desorption step in the sorption mechanism. It was also due to the weakening of sorptive forces between the active sites on the prepared material and the TPT, and also between adjacent TPT molecules on the sorbed phase (Tan, et al., 2008). The magnitude values of ΔH° indicated that the adsorption of TPT on MCM-TDI-C4 and MCM-TDI-PC4 was physisorption and the adsorption of TPT on MCM-TDI-C4S was chemisorption. Otherwise, the energy values taken from the D-R model showed that the adsorption of TPT on all adsorbents was mostly chemisorption. This can be explained as the adsorption processes were a combination of chemisorption and physisorption, and this was confirmed by the better fitting of the three-parameter models than the two-parameter models (Yi et al., 2011).

The negative ΔS° value corresponds to a decrease in randomness at the solid-liquid interface during the adsorption of TPT. The higher magnitude value of ΔS° for MCM-TDI-C4S compared to other adsorbents may be attributed to the difference in the mechanisms of adsorption processes and to the solubility of MCM-TDI-C4S adsorbent, which was resulted by the solvent replacement phenomena as previously mentioned in Chapter 5 Section 5.3.7.

Table 6.4 Thermodynamic parameters of TPT adsorption on MCM-TDI-C4, MCM-TDI-PC4 and MCM-TDI-C4S

T (°C)	Thermodynamic parameters
--------	--------------------------

		ΔG° (kJ/mol)	ΔH° (kJ/mol)	ΔS° (J/mol K)
MCM-TDI-C4	30	-7.6639	-16.4924	-29.137
	40	-7.3725		
	50	-7.0812		
MCM-TDI-PC4	30	-5.0949	-19.2552	-46.734
	40	-4.6275		
	50	-4.1602		
MCM-TDI-C4S	30	-4.7257	-31.1087	-87.0725
	40	-3.8549		
	50	-2.9843		

6.4 Summary

The use of modified mesoporous silica MCM-TDI-C4, MCM-TDI-PC4 and MCM-TDI-C4S in the adsorption of TPT from aqueous solution were investigated in this chapter and the following conclusions can be drawn:

- TPT uptakes by the three adsorbents were rapid and the equilibrium was reached within 2 h.
- The adsorption capacity increased with the increasing of the initial concentration of TPT and the adsorption efficiency decreased with the increasing of the initial concentration of TPT for all adsorbents. These results may be explained by the increased in the number of TPT competing for the available binding sites and also because of the lack of active sites on the adsorbents at higher concentrations.

- The pH of the media affected the adsorption by the sorbents. The optimum pH of the medium was found to be 4.0 for MCM-TDI-C4 and MCM-TDI-C4S. However, TPTOH uptake by MCM-TDI-PC4 was evident.
- Isotherm studies confirmed the combination of heterogeneous and homogenous uptake for TPT through the synthesized adsorbents MCM-TDI-C4, MCM-TDI-PC4 and MCM-TDI-C4S. Furthermore, the porosity factors β from the Dubinin-Radushkevitch isotherm were <1 for the three adsorbents. This demonstrates the existence of micropores in addition to mesopores that confirms the heterogeneity of the surface.
- It was observed that the calculated values of the dimensionless constant separation factor R_L ranged between 0 and 1, which means that the adsorption of TPT onto synthesized adsorbents was favorable over the range of initial TPT concentrations that were applied.
- The adsorption capacities of TPT onto MCM-TDI-C4, MCM-TDI-PC4 and MCM-TDI-C4S were 17.7305, 19.305, and 18.9393 mg/g, respectively, and followed the order of MCM-TDI-PC4 > MCM-TDI-C4S > MCM-TDI-C4.
- The mean free energies of adsorption E calculated from Dubinin-Radushkevitch isotherm indicated that the TPT adsorption on MCM-TDI-C4, MCM-TDI-PC4 and MCM-TDI-C4S took place through chemical adsorption.
- Two adsorption mechanisms, i.e. van der Waals forces and hydrophobic interactions (CH- π and π - π) involved in the adsorption of the TPT. Furthermore, electrostatic interaction could be considered between TPT⁺ and MCM-TDI-C4S adsorbent.

- The adsorption of TPT onto MCM-TDI-C4, MCM-TDI-PC4 and MCM-TDI-C4S could be best fitted by the pseudo-second order kinetic model. The intraparticle diffusion model was used to find both the boundary and intraparticle diffusion rate constants. The sorption data indicated that the mechanism of TPT adsorption by all adsorbents was rather complex and is probably a combination of external mass transfer, intraparticle diffusion and sorption process.
- Adsorptions of TPT onto all adsorbents were spontaneous and the negative values of ΔH° and ΔS° showed the exothermic nature and increase in order of TPT adsorption, respectively.

CHAPTER 7

ISOTHERMS, KINETICS AND THERMODYNAMICS OF DIBUTYLTIN (DBT) ADSORPTION ON MODIFIED MESOPOROUS SILICA WITH CALIX[4]ARENE DERIVATIVES

7.1 Introduction

The search for efficient and economical control strategy for a pollutant is one of the most challenging jobs due to increasingly stringent regulations on environmental pollution. Much effort has been focused on the macrocyclic compound as adsorbent.

Organized studies dedicated to organotin compounds are primarily confined to tributyltin (TBT). TBT is described as a notable environmental pollutant that enters directly to water through industrial employment of organotin biocides and because it is significantly toxic, it also impacts non-target aqueous organisms (C. C. Lee, Wang, Hsieh, & Tien, 2005). As such, several papers have focused on the TBT sorption behaviour by different adsorbents. On the other hand, adsorption of the less alkylated derivative dibutyltin (DBT) is largely overlooked (Dowson, Bubb, & Lester, 1993). In addition, systematic laboratory studies that look into the DBT partitioning between solid and liquid phase are very few and far between. Despite evidence to the fact that the butyltin compounds highest toxicity is presented by the trisubstituted species, it should be noted that DBT also falls under the category of toxic compounds that are highly toxic to rats given a dose of LD₅₀ of 100 mg/kg (Merian, 1991). Moreover, several studies of organisms reported DBT's

accumulated in fish bodies and tissues (Kannan, Corsolini, Focardi, Tanabe, & Tatsukawa, 1996), bird (Kannan, Senthilkumar, Elliott, Feyk, & Giesy, 1998), and even mammals (Kannan, Guruge, Thomas, Tanabe, & Giesy, 1998), and hence making it an environmental concern.

Because of sorbents' low sorption efficiency and regeneration issues, their use is quite limited and hence a more innovative, regenerable and significantly efficient sorbent is required. Accordingly, synthetic materials in the form of calixarenes have generated much interest due to their ability to be platforms for the preparation of macrocyclic hosts that recognized harmful and toxic species (Aksoy, et al., 2012; Ertul, et al., 2010; Kamboh, et al., 2013; Qureshi, et al., 2011). As a result, the chemical immobilization of calixarene framework on the silica surface improves its reusability and results in materials that are significant in the field of separation science (M. A. Kamboh, I. B. Solangi, S. T. H. Sherazi, & S. Memon, 2011c).

The objective of the work in this chapter is to investigate the adsorption behaviour of the modified MCM-41 (MCM-TDI-C4, MCM-TDI-C4S and MCM-TDI-PC4) for dibutyltin DBT. Six isotherm models were compared in order to find out and explain the 'best-fit' model.

7.2 Experimental

7.2.1 Materials

The prepared material MCM-TDI-C4, MCM-TDI-PC4 and MCM-TDI-C4S were used as adsorbents to investigate the adsorption parameters of DBT in this chapter.

Dibutyltin DBT was used as an adsorbate in this part of research. Dibutyltin was obtained from Aldrich and used as received. Its molecular formula is illustrated in Figure 7.1.

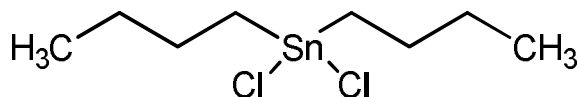


Figure 7.1 Dibutyltin molecular formula

7.2.2 Equilibrium isotherm and kinetics studies

Adsorption studies of dibutyltin DBT on modified mesoporous silica with calix[4]arene derivatives (MCM-TDI-C4, MCM-TDI-C4S and MCM-TDI-PC4) were similar to the procedures mentioned in Chapter 5.

Batch adsorption studies were performed to examine adsorption of DBT onto modified mesoporous silica with calix[4]arene derivatives (MCM-TDI-C4, MCM-TDI-C4S and MCM-TDI-PC4) by agitating 10 ml of solution containing DBT of desired concentration with 0.01 g of adsorbent using a shaker bath (Wise Bath WSB-18) at different

temperatures; 30, 40 and 50°C for 2 h at 180 rpm. The resulting mixture was filtered through a 0.45 µm membrane filter and the DBT concentration was measured using ICP-MS. All the adsorption tests were carried out in triplicates.

The effect of pH on DBT removal was studied using a series of 10 ml solutions containing DBT with 0.01 g adsorbent materials at 30°C. The pH of the solutions was adjusted between pH 3 to pH 8 with an interval of 1 by adding dilute solutions of HCl and NaOH and then shaken for 2 h. To test the effect of contact time, a series of 50 ml Teflon reactors (FEP, Nalgene) with 10 ml DBT solutions and 0.01 g adsorbent materials were shaken for periods of time ranging from 5 to 240 min at different temperatures before the samples were taken from the designated reactors and filtered for DBT measurement using ICP-MS. To examine the effect of temperature on DBT adsorption, adsorbent materials were added to batches of 10 ml DBT solutions at different concentration and shaken for 2 h at a temperature ranging from 30 to 50°C. For the adsorption isotherm study, 0.01 g of adsorbents were added to 10 ml of DBT solutions with different concentrations ranging from 2-8 mg /L and shaken for 2 h at three different levels of temperature ranging from 30 to 50°C at optimum pH.

7.2.3 Analytical procedure

Analytical procedure for adsorption of dibutyltin DBT on modified mesoporous silica with calix[4]arene derivatives (MCM-TDI-C4, MCM-TDI-PC4 and MCM-TDI-C4S) was similar to the procedures mentioned in Chapter 5.

7.3 Results and discussion

7.3.1 Effect of contact time

The relationship between contact time and DBT sorption onto MCM-TDI-C4, MCM-TDI-PC4 and MCM-TDI-C4S at different temperature is presented in Figure 7.2. The rate of DBT adsorption was very rapid, reaching almost 98, 97 and 81%, respectively within 10 min of contact time at 30 °C. Equilibrium was established in 180 min at the end of a rapid adsorption for all adsorbents.

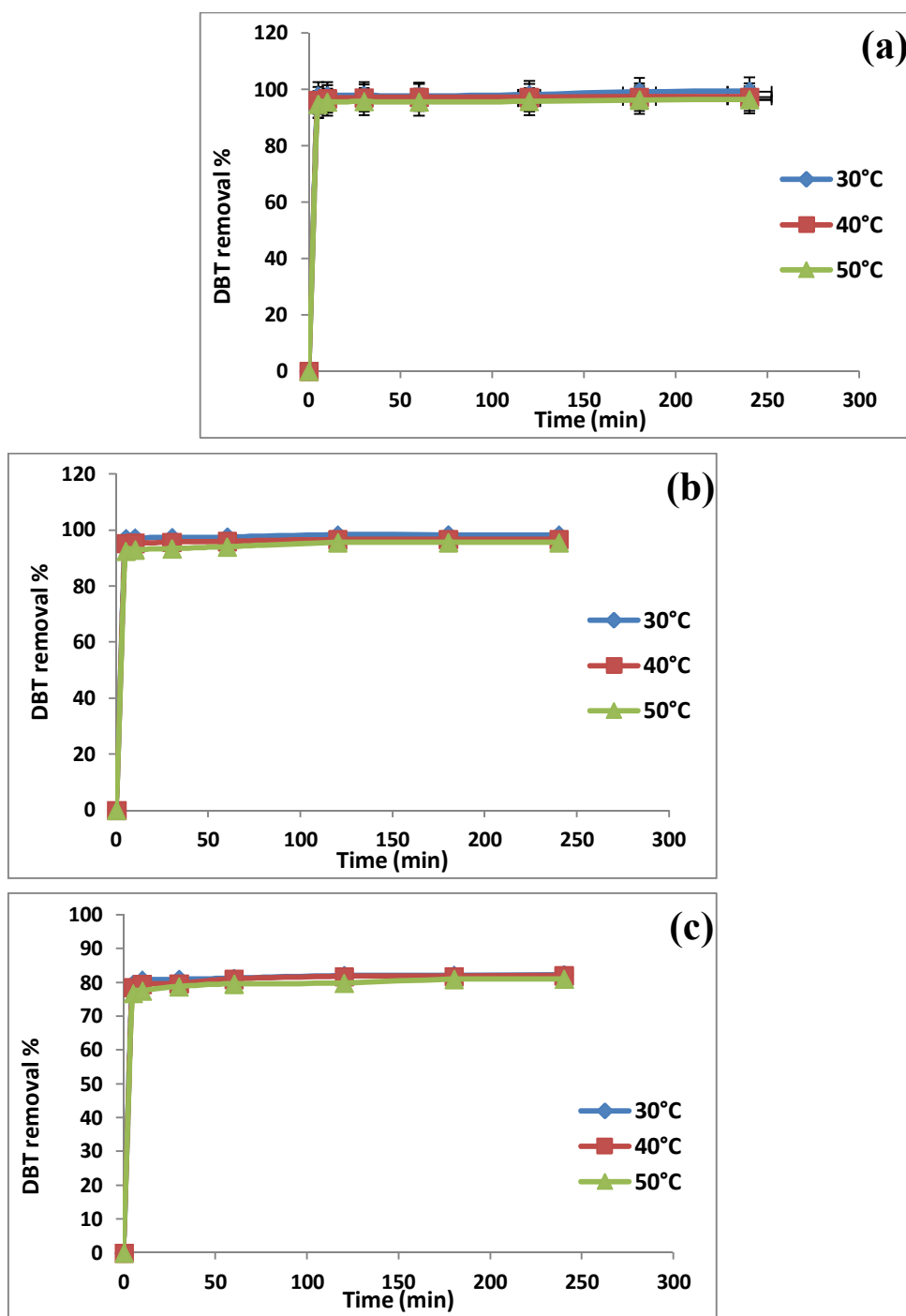


Figure 7.2 Effect of contact time on removal of DBT onto MCM-TDI-C4 (a), MCM-TDI-PC4 (b) and MCM-TDI-C4S (c)

7.3.2 Effect of pH

The pH of solution greatly influences DBT dissociation. Furthermore, pH influences surface properties of the adsorbent through functional group dissociation and also surface charges. At pH 3, the adsorption of DBT onto all adsorbents was found to be very low. It has been suggested that at low pH, H^+ ions were close to the binding sites of the sorbent and this restricts the approach of DBT ions due to repulsion. Adsorption of DBT by MCM-TDI-C4 has been found to increase with the increase in pH and reached maximum at 5.0 (96%), and then decreased with further increase in pH up to 7.0 (Figure 7.3). This conduct can be explained through the DBT species and the functional group existing in the surface of the adsorbent.

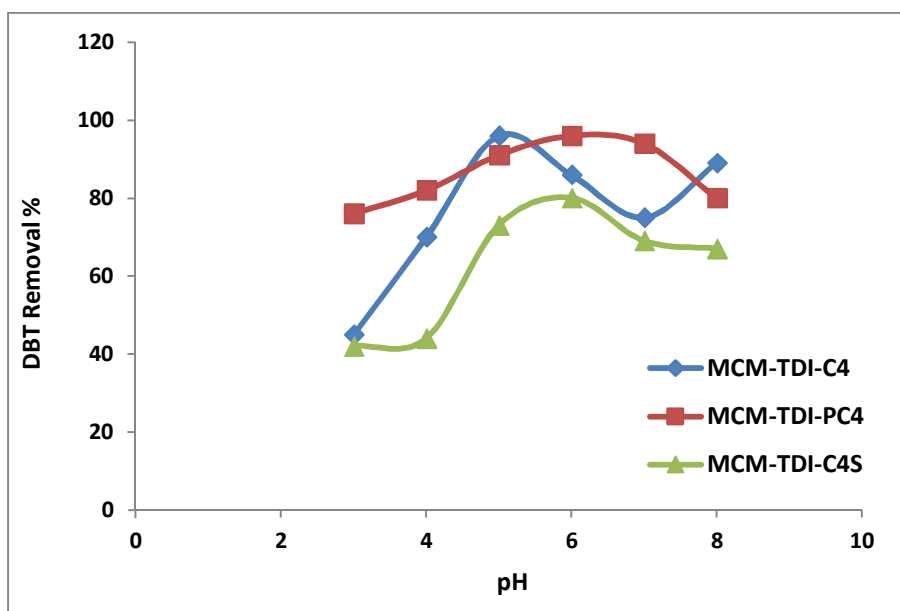
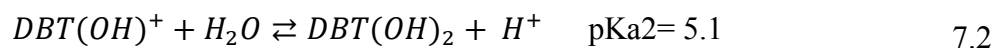
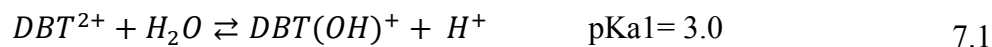


Figure 7.3 Effect of pH on removal of DBT onto MCM-TDI-C4, MCM-TDI-PC4 and MCM-TDI-C4S

The hydrolytic reactions in aqueous solution for dibutyltin (DBT), together with the potentiometrically estimated pKa values recorded by Fang et.al. (Fang, et al., 2012).



At pH <5.1±0.5, the adsorption process of DBT (DBT²⁺ and DBT(OH)⁺) was governed by electrostatic attraction. However, the major driving force of adsorption at higher pH was the hydrophobic character of the DBT (DBT(OH)₂).

The increase of the maximum removal for DBT from pH 3 to 5 can be attributed to the enhancement of the deprotonated surface of the MCM-TDI-C4, and hence increasing the adsorption capacity of MCM-TDI-C4 for the positively charged DBT(OH)⁺ species dominating at pH 5, which is in analogous to the DBT adsorption by the charcoal (Figure 7.4, Fang et al., 2012). Due to the formation of neutral DBT species at pH>5, the dominant DBT(OH)₂ species showed a weaker adsorption to the MCM-TDI-C4 than that at acidic condition (Figure 7.3).

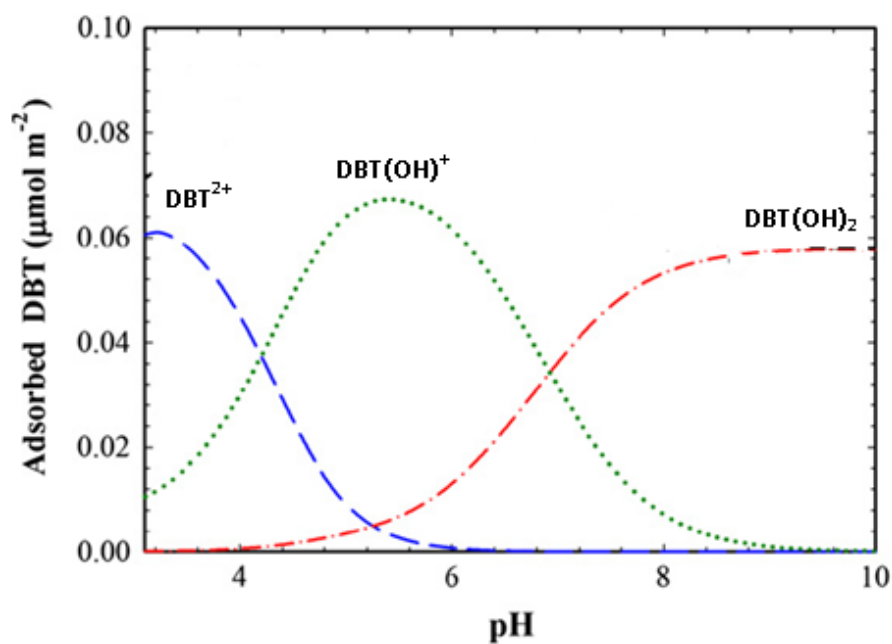


Figure 7.4 Predicted adsorption edges of DBT, calculated by using the pH-dependent Dual Langmuir model

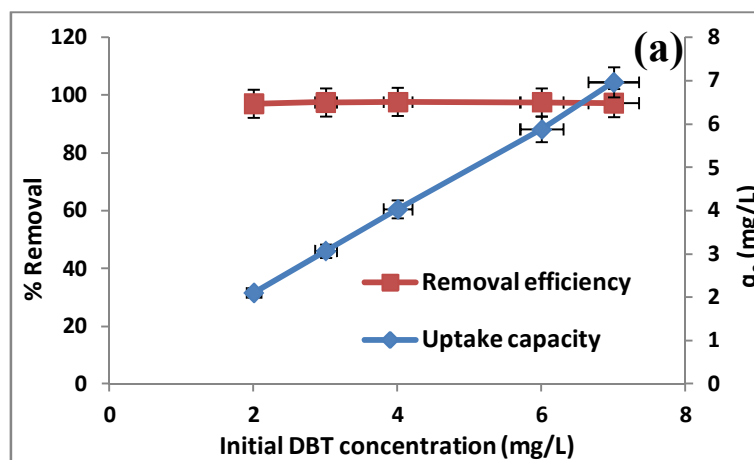
As seen from Figure 7.3 adsorption of DBT onto MCM-TDI-PC4 and MCM-TDI-C4S exhibited a maximum removal at pH 6, and then the removals declined sharply with further increase in pH. This is in good agreement with the result documented for DBT adsorption to clay-rich sediments (Hoch, et al., 2003). In case of MCM-TDI-C4, the removal percentage increased until pH 5 (adsorption of DBT(OH)⁺) and then start to decrease, may be due to the decreasing concentration of DBT(OH)⁺. After that, the removal percentage started to increase and this can be attributed to the DBT species at pH>7 (DBT(OH)₂).

Another key factor that affects the DBT uptake was the presence of calix[4]arenes on the surface of adsorbents. In the current part, the complex stability of calixarenes with DBT was attributed to a great extent to van der Waals forces and hydrophobic interaction (CH- π). Furthermore, calix[4]arenes containing tert-butyl groups provide a more hydrophobic

cavities capable of the hydrophobic interactions with n-butyl chains at DBT (Thompson, et al., 2011). In case of MCM-TDI-C4S adsorbent, the adsorption process was also governed by electrostatic attraction with the sulfonate group present at calix[4]arene sulfonate on the surface of the adsorbent.

7.3.3 Effect of initial DBT concentration

The initial concentration provides an important driving force to overcome all mass transfer resistance of DBT between the aqueous and solid phases. Hence, a higher initial concentration of DBT will increase the adsorption capacity, whereas the DBT removal percentage decreased slightly. Such effect is clearly demonstrated in Figure 7.5. The increase of DBT adsorption capacity at higher initial DBT concentration was due to higher availability of DBT ions in the solution. On the other hand, the decrease in removal percentage was due to the increase in the number of DBT ions competing for the available binding sites in the adsorbents and also due to the lack of binding sites at higher concentration.



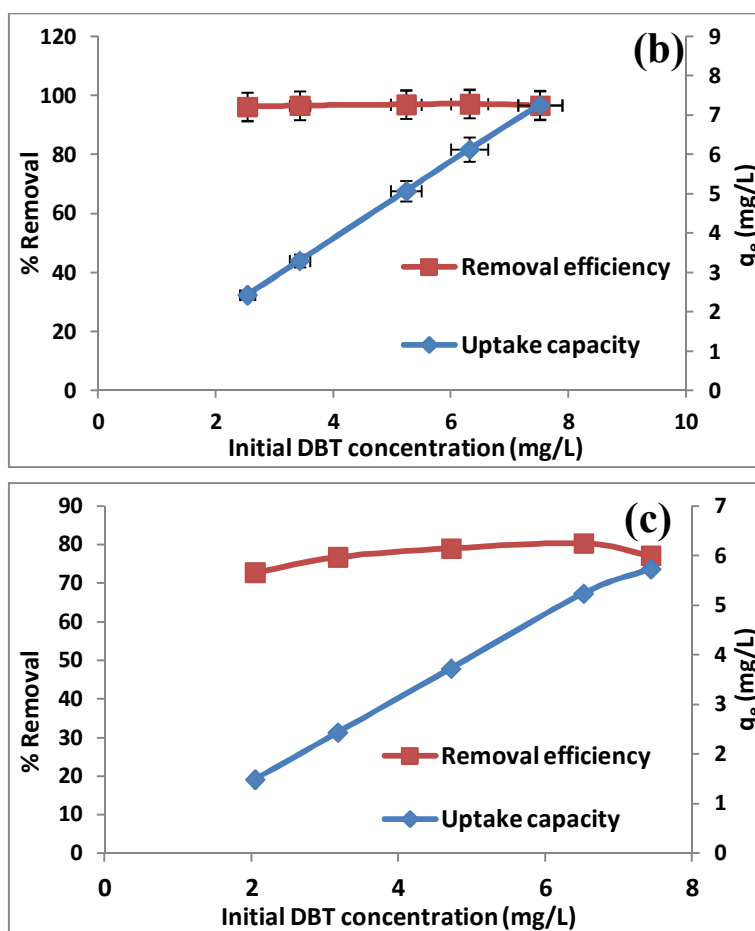
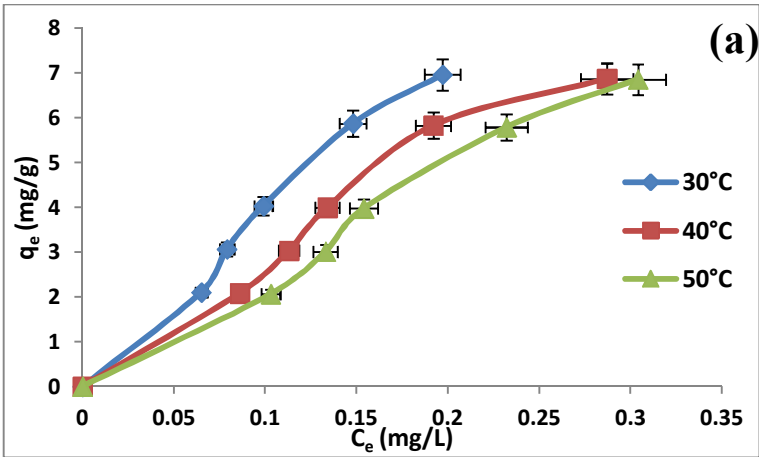


Figure 7.5 Effect of initial DBT concentration on the DBT removal efficiency and uptake capacity by MCM-TDI-C4 (a), MCM-TDI-PC4 (b) and MCM-TDI-C4S (c)

7.3.4 Effect of solution temperature

The effect of temperature on the equilibrium sorption capacity of MCM-TDI-PC4 for DBT was investigated in the temperature range of 30–50°C. As shown in Figure 7.6, the adsorption of DBT was inversely proportional to the increase of temperature, i.e. increasing the temperature lead to a decrease in the equilibrium uptakes, which suggested that the adsorption was characterized as an exothermic process. The decreased in adsorption capacity at higher temperature may be attributed to the deactivation of the adsorbent

surface or the destruction of some active sites on the adsorbent surface due to bond rupture (Aksu & İšođlu, 2005). Moreover, the heteroporous structure of the adsorbent, the considerable interactions among the molecules of adsorbent and adsorbate, and the cooperative adsorption in the context of significant concentrations of equilibrium resulted in the observation of the whole isotherm shapes that were noted to be similar to Type V at various temperatures (Rosen, 2004). Through the employment of a typical Langmuir treatment as the base, Giles et.al., (Giles, Smith, & Huitson, 1974) revealed that the S-shape arose when a considerable interaction occurred between the adsorbed molecules encouraging cooperative adsorption, while the L type isotherms arose when a considerable adsorbate-surface interaction occurs.



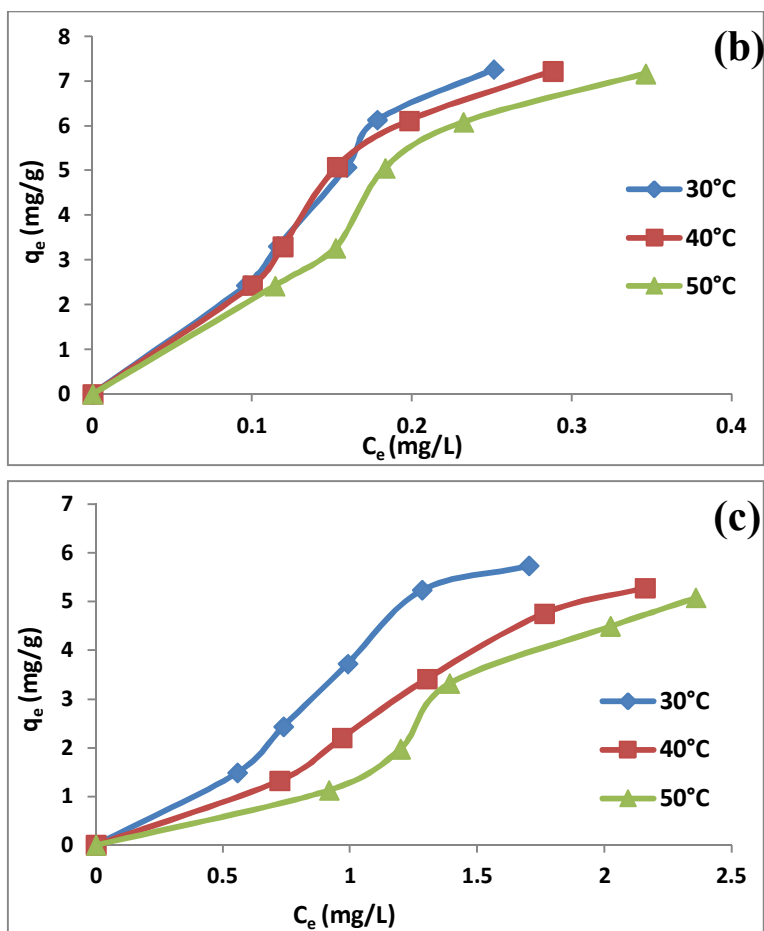


Figure 7.6 Adsorption isotherms for DBT on MCM-TDI-C4 (a), MCM-TDI-PC4 (b) and MCM-TDI-C4S (c) at different temperatures

7.3.5 Adsorption isotherm models

In order to optimize the design of a sorption system to remove DBT from aqueous solutions, it is important to establish the most appropriate correlation for the equilibrium isotherms. The calculated isotherm constants at different temperature and their respective correlation coefficients are given in Table 7.1.

As can be noticed in Figure 7.7, the experimental data were described by Freundlich isotherm, and the values of the parameter $1/n$ were found to be above unity, which

represents a cooperative adsorption. Seliem et.al., also reported that the adsorption of nitrate by synthetic organosilicas (MCM-41) was a cooperative adsorption (Seliem et al., 2013).

Table 7.1 Isotherm constants and correlation coefficients of determination for various adsorption isotherms for the adsorption of DBT onto MCM-TDI-C4 (a), MCM-TDI-PC4 (b) and MCM-TDI-C4S (c)

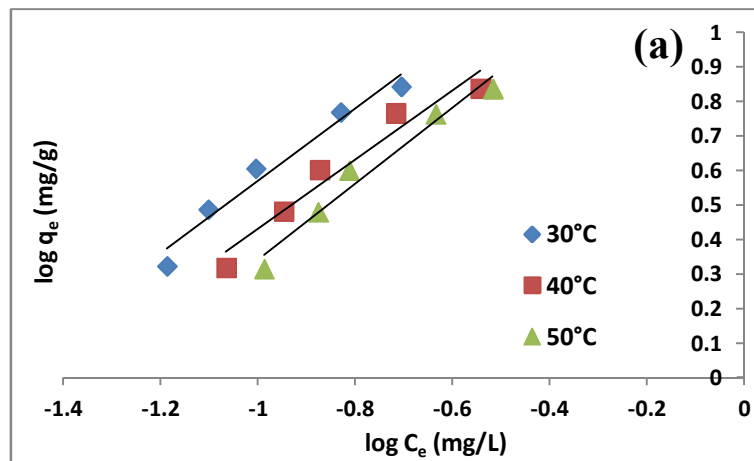
Adsorbent	Adsorption isotherm	Isotherm parameter	Temperature		
			30	40	50
(a)	Freundlich	$K_F(L/g)$	41.3809	27.0022	27.5043
		n	0.9549	0.9981	0.91024
		R^2	0.9634	0.9468	0.9662
	Langmuir (II)	$q_m(mg/g)$	-26.6666	-31.8471	-19.6463
		$K_L(L/mg)$	-1.2097	-0.7494	-0.9714
		R^2	0.9518	0.9612	0.9618
	Temkin	A_T	4.3935	4.1604	4.5205
		$K_T(L/mg)$	25.2107	19.2433	15.2215
		R^2	0.9987	0.9838	0.9962
	Dubinin-Radushkevitch	$q_d(mg/g)$	16.9404	14.4313	14.8902
		$\beta(mol^2/kJ^2)$	1.3×10^{-3}	1.3×10^{-3}	1.7×10^{-3}
		$E(kJ/mol)$	19.3034	19.3034	17.2655

(b)	Redlich–Peterson	R^2	0.985	0.9814	0.9894	
		g	-0.0472	-0.0019	-0.0986	
		$B_R(\text{L/mg})$	1.2×10^8	1.3×10^8	1.12×10^8	
		$A_R(\text{L/g})$	5.0×10^9	3.6×10^9	3.1×10^9	
	Koble–Corrigan	R^2	0.0507	0.0404	0.1869	
		p	2.6568	2.1233	2.2801	
		A_K	5000	500	476.1905	
		B_K	646	55.65	53.9048	
	<hr/>					
	Freundlich	$K_F(\text{L/g})$	41.1149	29.3697	23.9662	
n		0.8527	0.9754	0.9825		
Langmuir (II)	R^2	0.9533	0.9127	0.9114		
	$q_m(\text{mg/g})$	-15.6985	-25.7069	-30.581		
	$K_L(\text{L/mg})$	-1.4543	-0.9239	-0.6606		
Temkin	R^2	0.9653	0.9291	0.9419		
	A_T	5.2407	4.6313	4.5313		
	$K_T(\text{L/mg})$	16.6564	17.7676	15.0830		
Dubinin-Radushkevitch	R^2	0.9828	0.969	0.9535		
	$q_d(\text{mg/g})$	18.8196	16.1642	14.7626		
	$\beta(\text{mol}^2/\text{kJ}^2)$	1.67×10^{-3}	1.67×10^{-3}	1.67×10^{-3}		
	$E(\text{kJ/mol})$	17.2655	17.2655	17.2655		
Redlich–Peterson	R^2	0.9802	0.9561	0.9523		
	g	-1.7779	-0.0252	-0.0178		
	$B_R(\text{L/mg})$	2.92×10^{13}	7.3×10^7	4.63×10^{12}		
	$A_R(\text{L/g})$	3.22×10^9	2.14×10^9	1.11×10^{14}		

Table 7.1 (Continued)

	Koble–Corrigan	R^2	0.3073	0.0063	0.0031
		p	2.4345	3.0272	2.0072
		A_K	1000	3333.33	232.0952
		B_K	103.8	417.666	22.7143
		R^2	0.9973	0.9967	0.9642
<hr/>					
(c)	Freundlich	$K_F(\text{L/g})$	3.422	2.1938	1.501
		n	0.80411	0.781	0.6411
	Langmuir (II)	R^2	0.9555	0.9733	0.9258
		$q_m(\text{mg/g})$	-0.21867	-0.17645	-0.4205
		$K_L(\text{L/mg})$	-1.8945	-1.4848	-0.8222
	Temkin	R^2	0.5059	0.6268	0.6962
		A_T	4.042	3.7599	4.2556
		$K_T(\text{L/mg})$	2.5723	1.9236	1.4256
	Dubinin-Radushkevitch	R^2	0.9805	0.9947	0.9757
		$q_d(\text{mg/g})$	8.4748	7.3544	8.292
$\beta(\text{mol}^2/\text{kJ}^2)$		2.7×10^{-3}	2.7×10^{-3}	4.6×10^{-3}	
$E(\text{kJ/mol})$		13.5193	13.5193	10.472	

Redlich–Peterson	R^2	0.994	0.9972	0.9777
	g	-0.3036	-0.3144	-0.6206
	$B_R(\text{L/mg})$	3.75955	8.2846	10.5045
	$A_R(\text{L/g})$	16.3276	20.3966	17.3260
Koble–Corrigan	R^2	0.4449	0.6354	0.6126
	p	2.3729	2.3253	3.2216
	A_K	7.3746	3.4317	1.8018
	B_K	0.94469	0.46945	0.2827
	R^2	0.9987	0.9998	0.9879



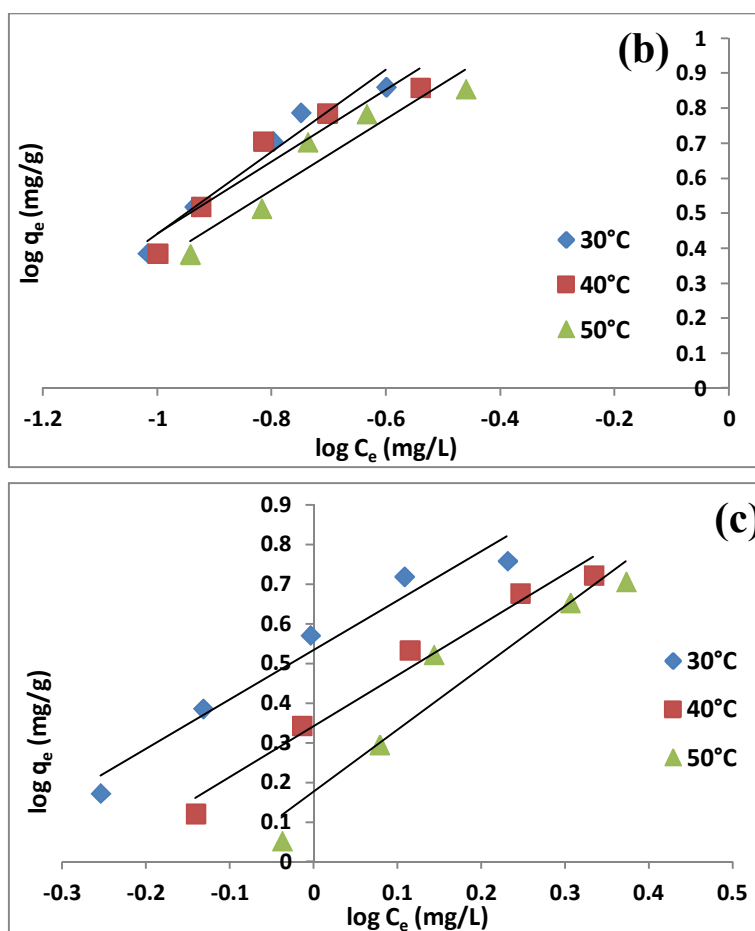


Figure 7.7 Freundlich isotherm of DBT adsorbed onto MCM-TDI-C4 (a), MCM-TDI-PC4 (b) and MCM-TDI-C4S (c)

Since the values of the parameter $1/n$ were above unity, there was a certain degree of deviation with respect to the Langmuir equation. Indeed, although at the first sight, one might think the data could also be described by Langmuir isotherm Figure 7.6 showed an S-shape of the data, which was not taken into the account by the Langmuir equation. Nevertheless, the experimental data of Langmuir adsorption parameters have negative slopes and intercepts, which suggested that the adsorption behavior of the tested systems did not follow the assumption of the Langmuir approach. The negative value of R_L (Figure

7.8) confirmed that the Langmuir type II isotherm was not suitable for the expression of removal rate of DBT (Kayranli, 2011).

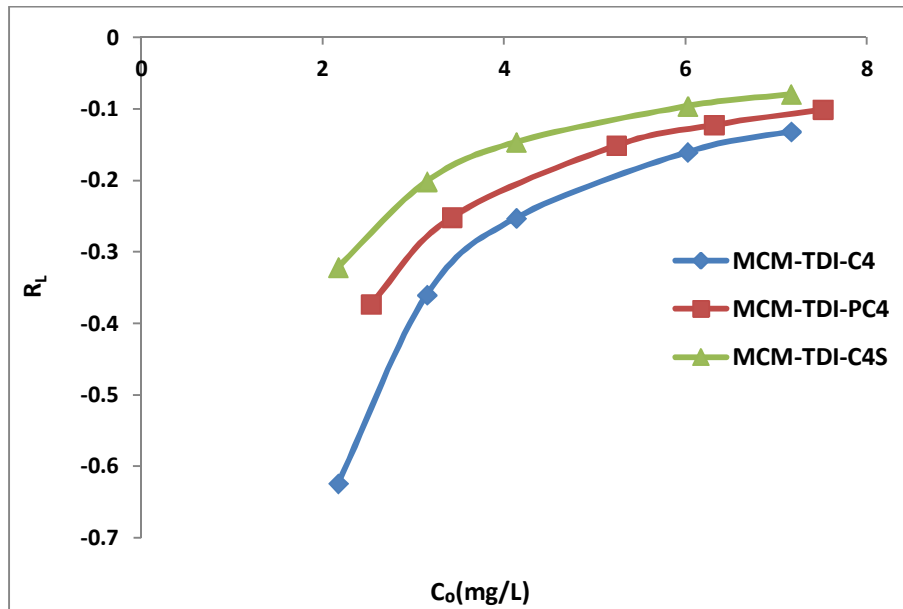


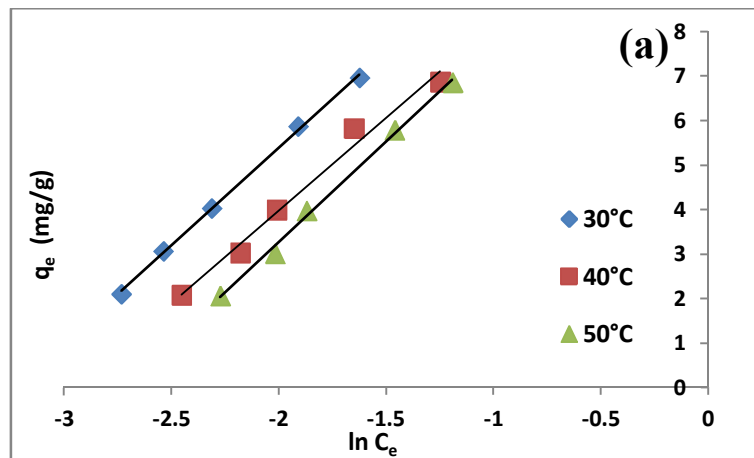
Figure 7.8 Values of R_L for adsorption of DBT onto MCM-TDI-C4, MCM-TDI-PC4 and MCM-TDI-C4S

Redlich–Peterson exponents g were revealed to be less than 0, which showed the inapplicability of this model for the adsorption of DBT using these adsorbents.

The prediction of adsorption isotherms of DBT at 30, 40 and 50°C has also been shown by Temkin isotherm (Figure 7.9, Table 7.1). The equation showed good fit to the experimental results due to the obtained correlation coefficient value. In addition, the Temkin isotherm constant (K_T) was found to be in the order of MCM-TDI-C4 > MCM-TDI-PC4 > CM-TDI-C4S, suggesting the highest interaction between sorbet and sorbent on MCM-TDI-C4.

The values of the porosity factors β from Dubinin-Radushkevitch isotherm model (Figure 7.10) were less than unity (Table 7.1) which implied that all adsorbents consist of micropores and indicated a surface heterogeneity may arise from the pore structure, as well as adsorbate adsorbent interaction (Negrea, et al., 2011). The mean free energies of adsorption E were higher than 16 kJ/mol, indicating that DBT adsorption on MCM-TDI-C4 and MCM-TDI-PC4 adsorbents took place through chemical adsorption and lower than 16 kJ/mol, indicating that the adsorption of DBT on MCM-TDI-C4S was physisorption (Apiratikul & Pavasant, 2008; Vijayaraghavan, et al., 2006).

Based on the correlation coefficient, R^2 , the equilibrium data could be well interpreted by the Koble-Corrigan isotherm model (Figure 7.11), which showed an occurrence of the combination of heterogeneous and homogenous uptake for DBT through the synthesized adsorbents.



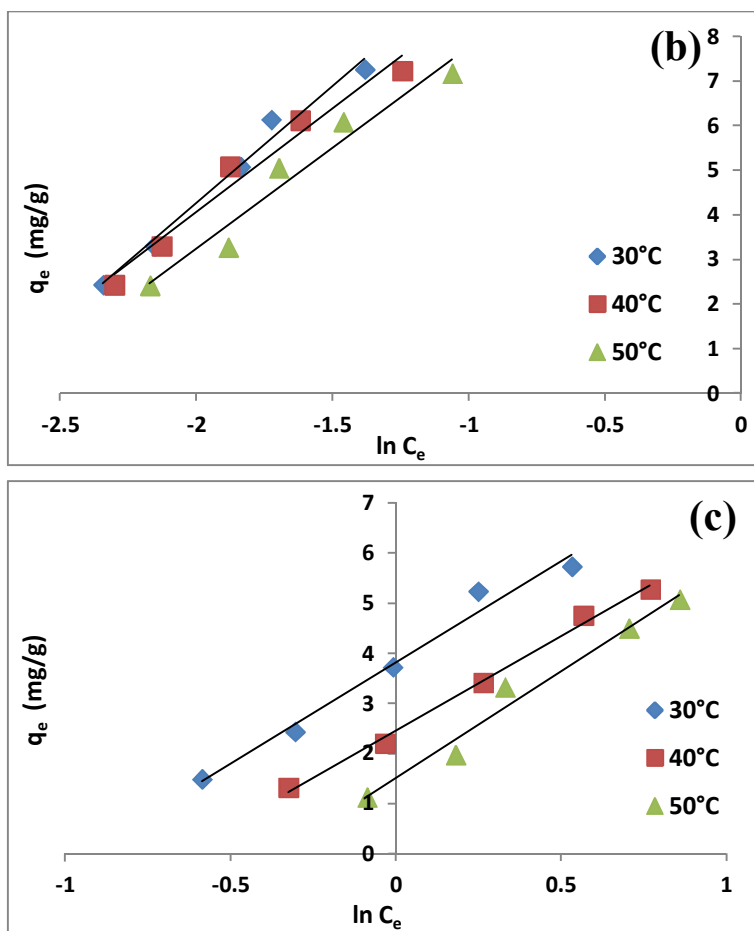


Figure 7.9 Temkin isotherm of DBT adsorbed onto MCM-TDI-C4 (a), MCM-TDI-PC4 (b) and MCM-TDI-C4S (c)

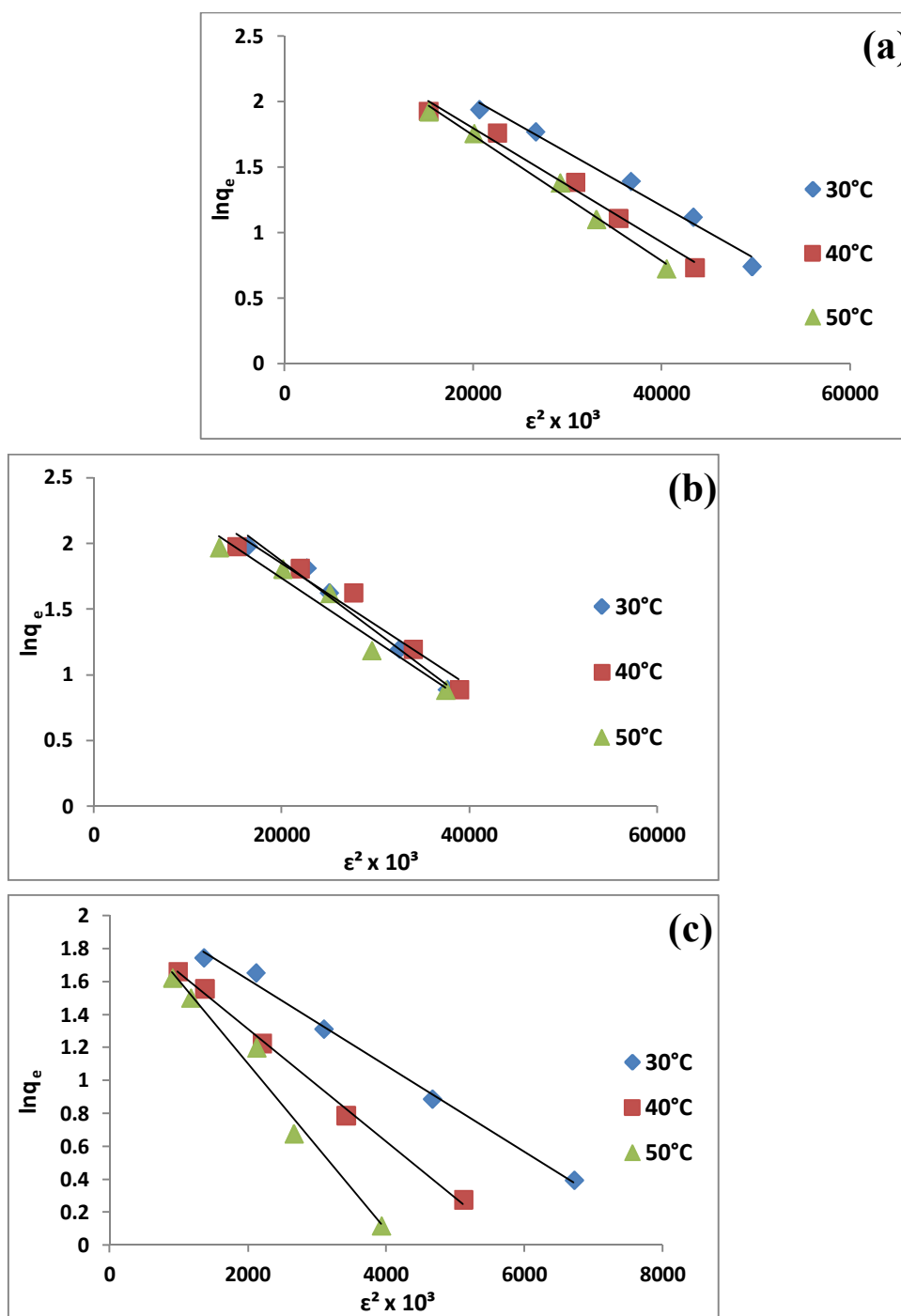


Figure 7.10 Dubinin–Radushkevitch isotherm of DBT adsorbed onto MCM-TDI-C4 (a), MCM-TDI-PC4 (b) and MCM-TDI-C4S (c)

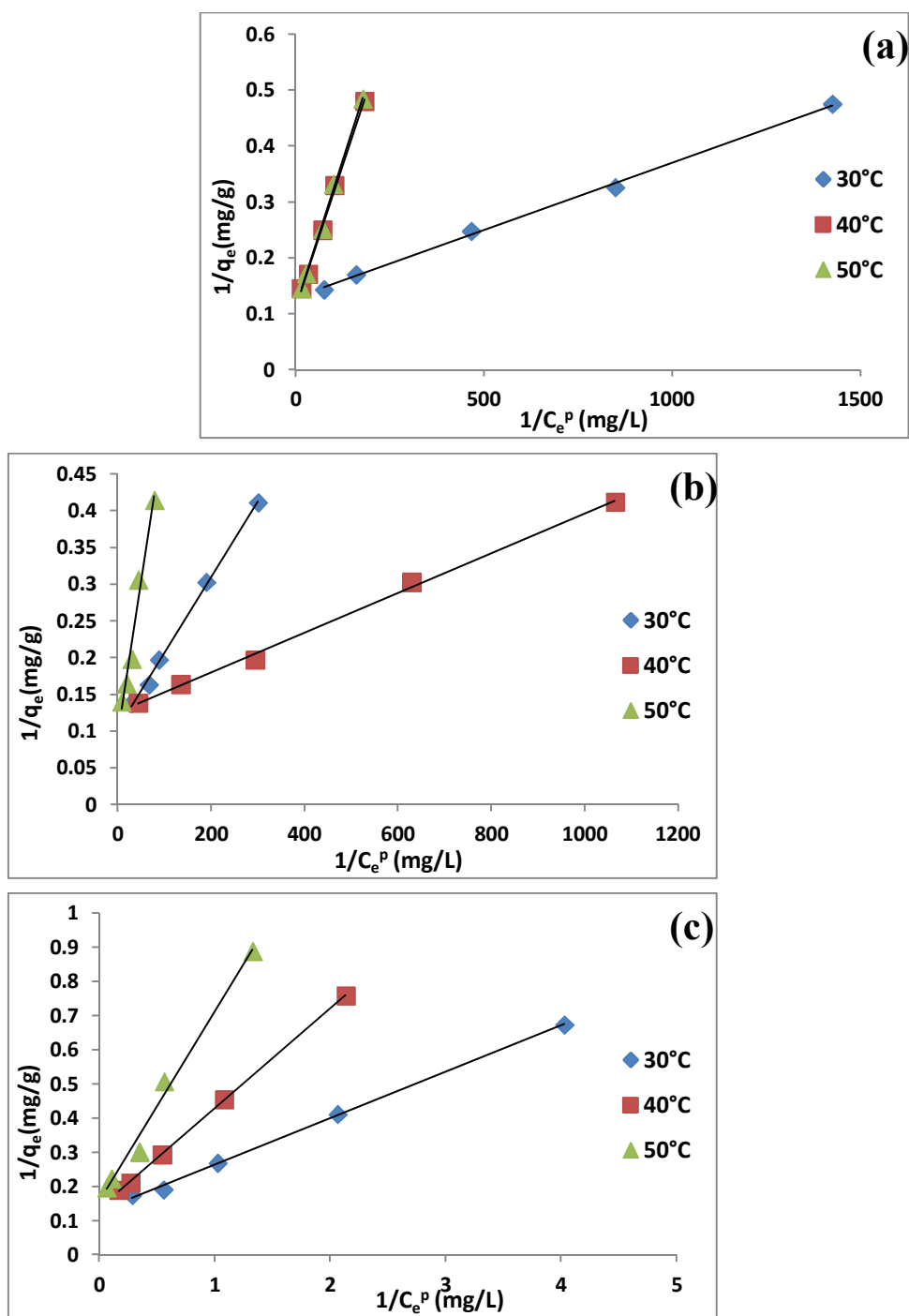


Figure 7.11 Koble–Corrigan isotherm of DBT adsorbed onto MCM-TDI-C4 (a), MCM-TDI-PC4 (b) and MCM-TDI-C4S (c)

7.3.6 Adsorption kinetic

In order to further expose the adsorption mechanism of DBT onto MCM-TDI-C4, MCM-TDI-PC4 and MCM-TDI-C4S and rate-controlling steps, a kinetic investigation was conducted. Pseudo-first order, pseudo-second order and intraparticle diffusion kinetic models have been used for testing the experimental data.

The constants q_e and K_1 from the pseudo-first order kinetic equation were determined experimentally by plotting $\ln(q_e - q_t)$ vs. t (Figure 7.12) and the values are listed in (Table 7.2). The theoretical values ($q_{e,cal}$) were far lower than those experimental data, $q_{e,exp}$, implying that the adsorption process did not fully follow the pseudo-first order adsorption rate expression.

Table 7.2 Calculated kinetic parameters for pseudo-first order and pseudo-second order kinetic models for the adsorption of DBT using MCM-TDI-C4 (a), MCM-TDI-PC4 (b) and MCM-TDI-C4S (c) as adsorbents

	T (°C)	$q_{e,exp}$ (mg g ⁻¹)	Pseudo-first order			Pseudo-second order			
			K_1 (min ⁻¹)	$q_{e,cal}$ (mg g ⁻¹)	R_1^2	K_2 (g mg ⁻¹ min ⁻¹)	$q_{e,cal}$ (mg g ⁻¹)	h (mg g ⁻¹ min ⁻¹)	R_2^2
(a)	30	4.98	0.0102	0.1063	0.7217	0.37966	4.9801	9.4162	1
	40	4.877	0.0188	0.03	0.7745	2.7288	4.878	64.9351	1
	50	4.832	0.0122	0.0709	0.7885	0.71465	4.8333	16.6944	1
(b)	30	8.065	0.0076	0.1061	0.924	0.6006	8.0645	39.0625	1
	40	7.924	0.0311	0.1772	0.923	0.5483	7.9302	34.4827	1
	50	7.833	0.0407	0.4721	0.8793	0.2463	7.8493	15.1745	1
(c)	30	5.868	0.0185	0.1717	0.9668	0.412	5.8754	14.2246	1
	40	5.848	0.0173	0.2334	0.9539	0.2988	5.8582	10.2564	1
	50	5.777	0.02	0.3521	0.8616	0.2069	5.787	6.93	0.999

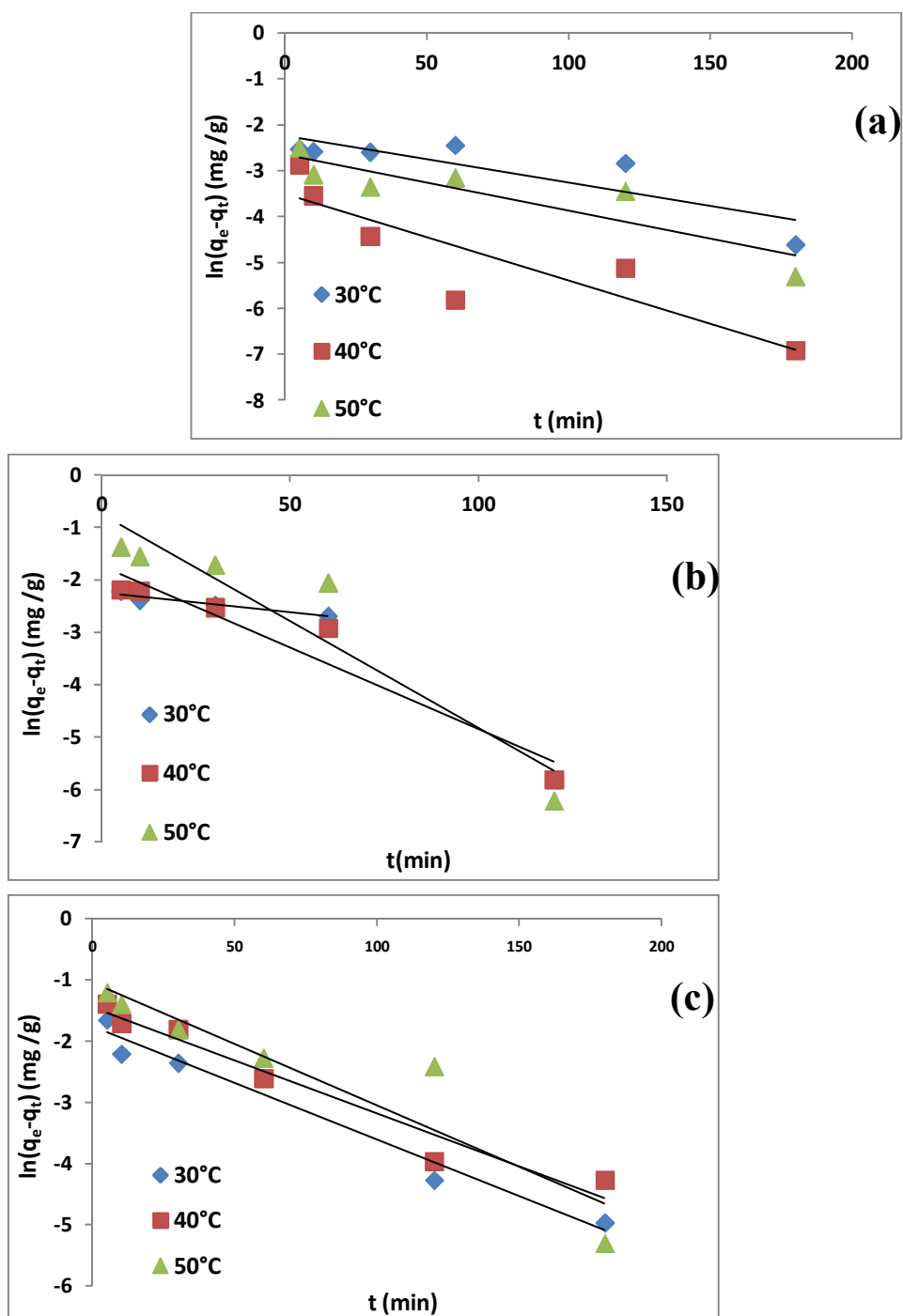


Figure 7.12 Pseudo-first order model plot for the adsorption of DBT onto MCM-TDI-C4 (a), MCM-TDI-PC4 (b) and MCM-TDI-C4S (c)

By plotting t/q_t against t , straight lines were obtained in all cases and by using pseudo-second order kinetic equation, the second order rate constant (K_2) and q_e values were determined from the plots (Figure 7.13). A comparison of the pseudo-first order and pseudo-second order adsorption rate constant on different adsorbents and temperatures is presented in Table 7.2. It is important to note that for a pseudo-first order model, the correlation coefficient was less than the pseudo-second order coefficient. The values of correlation coefficient for the pseudo-second order were very high ($R^2 > 0.9999$), and the theoretical $q_{e,cal}$ values were closer to the experimental $q_{e,exp}$ values. In the view of these results, it can be said that the pseudo-second order kinetic model provided a good correlation for the adsorption of DBT onto adsorbents at different temperatures in contrast to the pseudo-first order model.

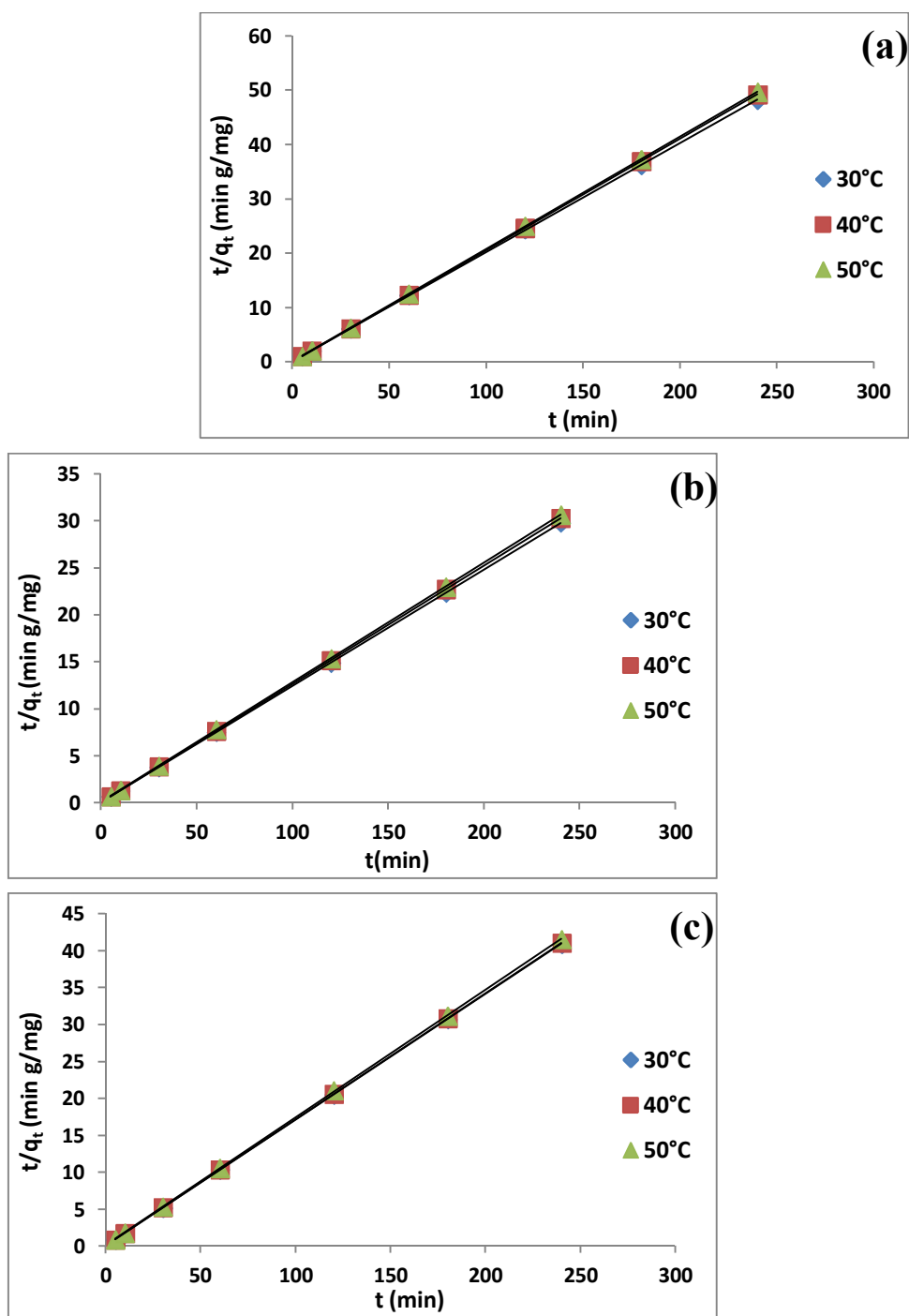


Figure 7.13 Pseudo-second order model plot for the adsorption of DBT onto MCM-TDI-C4 (a), MCM-TDI-PC4 (b) and MCM-TDI-C4S (c)

The intraparticle diffusion coefficient for the sorption of DBT was calculated from the slope of the plot between the amounts of DBT sorbed, q_t vs. $t^{1/2}$ (Figure 7.14, Table 7.3). According to this model, if the plot of q_t versus $t^{1/2}$ gives a straight line, then the adsorption process is controlled by intraparticle diffusion, whereas if the data exhibit multi-linear plots, then two or more steps influence the adsorption process. In the present study, the plots presents multi-linearity (Figure 7.14), indicating two steps took place in the process. At first, the sharper portion may be considered as an external surface adsorption or faster adsorption stage. The second portion described the gradual adsorption stage, where the intraparticle diffusion was rate-controlled. Since the plots failed to pass through the origin, the intraparticle diffusion model did not act as the rate-controlling step.

Table 7.3 Calculated kinetic parameters for intraparticle diffusion model for the adsorption of DBT using MCM-TDI-C4 (a), MCM-TDI-PC4 (b) and MCM-TDI-C4S (c) as adsorbents

	T (°C)	Ki ₁ (mg/g min ^{1/2})	C ₁	R ₁ ²	Ki ₂ (mg/g min ^{1/2})	C ₂	R ₂ ²
(a)	30	0.0013	4.8982	0.7033	0.0121	4.7974	0.9582
	40	0.0126	4.7986	0.8605	0.0005	4.8686	0.3954
	50	0.0126	4.7319	0.7353	0.006	4.7401	0.9377
(b)	30	0.0067	7.9458	0.9296	-0.0018	8.0842	0.9911
	40	0.0111	7.7835	0.9847	0.0007	7.914	0.7913
	50	0.0212	7.541	0.9678	0.0002	7.8288	0.2937
(c)	30	0.0176	5.6684	0.7073	0.0031	5.8201	0.9976
	40	0.0278	5.5509	0.91	0.0041	5.7822	0.9034
	50	0.0353	5.4083	0.9836	0.0203	5.4758	0.83

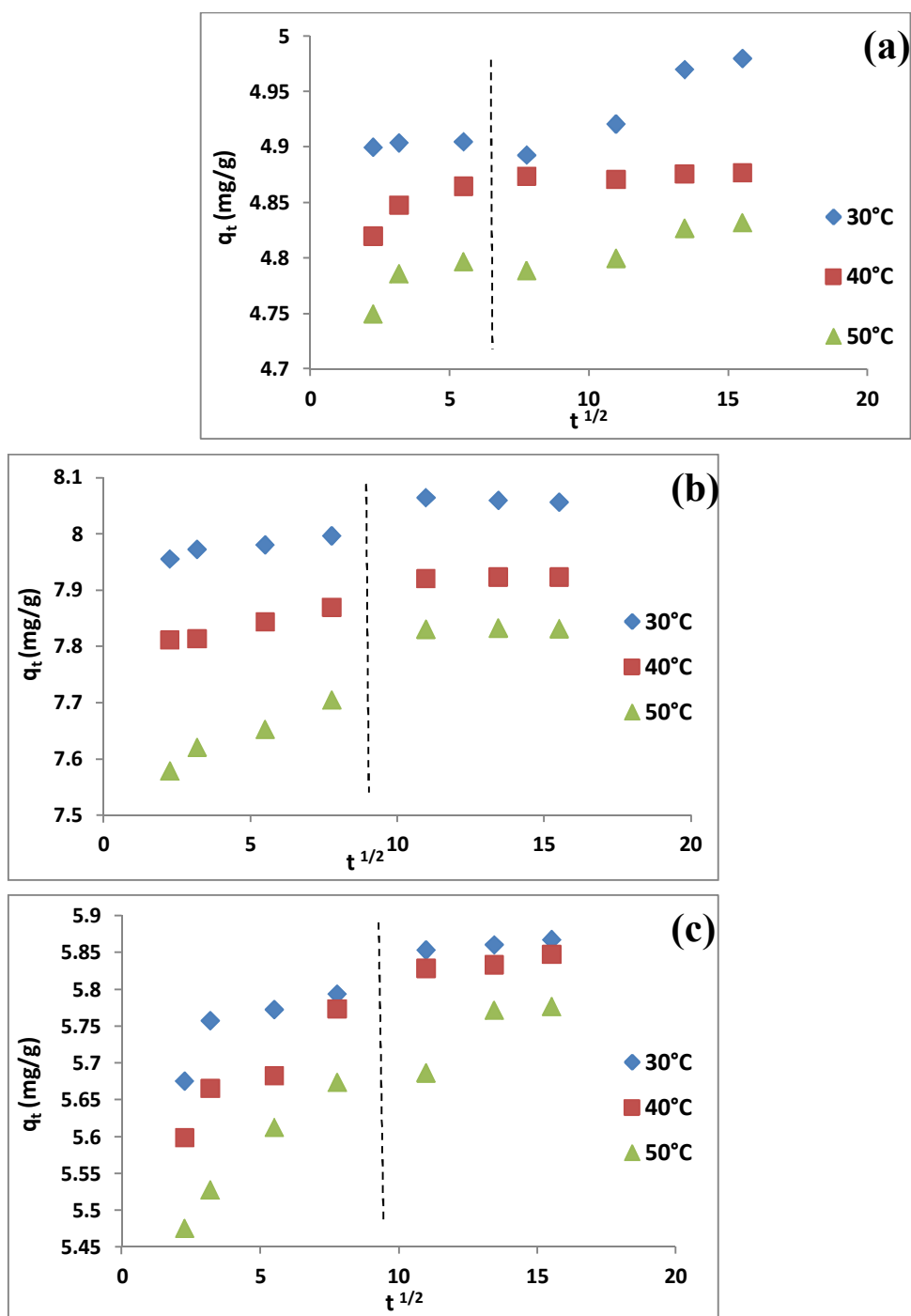


Figure 7.14 Intraparticle diffusion model plot for the adsorption of DBT onto MCM-TDI-C4 (a), MCM-TDI-PC4 (b) and MCM-TDI-C4S (c)

7.3.7 Adsorption thermodynamic

The $\ln K_c$ value versus $1/T$ plot (Figure 7.15) was used to determine the thermodynamic parameters, and the values are given in Table 7.4. The negative value of ΔG° indicated the feasibility of the process and indicated the spontaneous nature of the adsorption. ΔG° value was more negative with decreasing temperature, which suggests that lower temperature makes the adsorption easier. This was also supported by the decrease in the value of uptake capacity of the sorbent with the rise in temperature (Section 7.3.4).

The negative value of ΔH° implied that the adsorption phenomenon was exothermic. The magnitude of ΔH° indicated that the adsorption of DBT on MCM-TDI-C4 and MCM-TDI-PC4 was physisorption, and the adsorption of DBT on MCM-TDI-C4S was chemisorption, which was inconsistent with results from the D-R model energy value. This can be explained as the adsorption processes were a combination of chemisorption and physisorption, and this was confirmed by the better fitting of the three-parameter models than the two-parameter models (Yi, et al., 2011).

The negative value of ΔS° suggested a decrease in the randomness at the solid-liquid interface during the adsorption of DBT on all adsorbents. The higher magnitude value of ΔS° for MCM-TDI-C4S compared to other adsorbents may be attributed to the difference in the mechanisms of adsorption processes and to the solubility of MCM-TDI-C4S adsorbent, which resulted in the solvent replacement phenomena as mentioned previously in Chapter 5 Section 5.3.7.

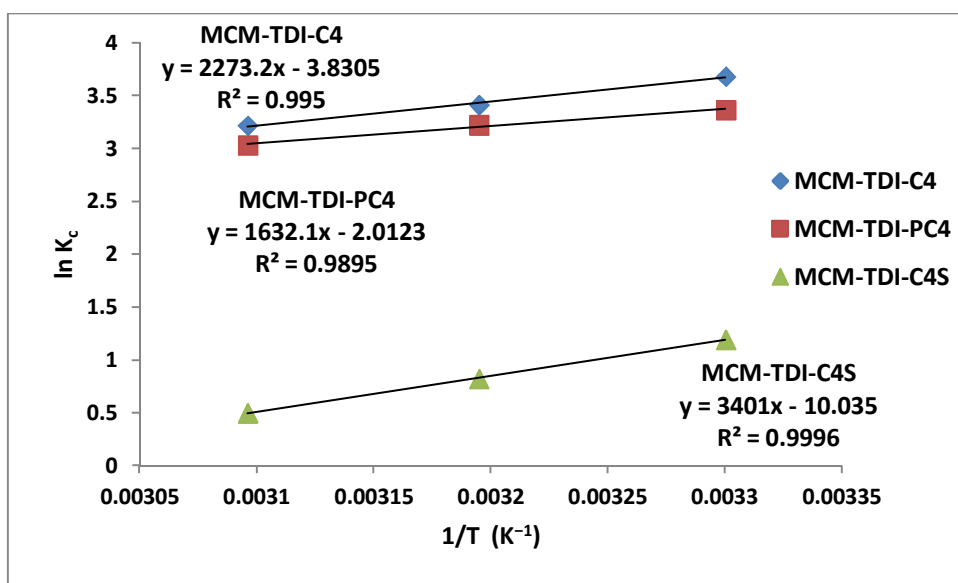


Figure 7.15 Plot of $\ln K_c$ versus $1/T$ for DBT adsorption

Table 7.4 Thermodynamic parameters of DBT adsorption on MCM-TDI-C4, MCM-TDI-PC4 and MCM-TDI-C4S

	T (°C)	Thermodynamic parameters		
		ΔG° (kJ/mol)	ΔH° (kJ/mol)	ΔS° (J/mol K)
MCM-TDI-C4	30	-9.245	-18.89	-31.83
	40	-8.927		
	50	-8.608		
MCM-TDI-PC4	30	-8.5	-13.5692	-16.7302
	40	-8.3327		
	50	-8.1654		
MCM-TDI-C4S	30	-2.9949	-28.2623	-83.3908
	40	-2.1609		
	50	-1.3271		

7.4 Summary

This chapter investigated the adsorption of DBT onto the prepared materials MCM-TDI-C4, MCM-TDI-PC4 and MCM-TDI-C4S from aqueous solution as a function of adsorption time, initial DBT concentration, temperature and pH. In addition, thermodynamic parameters such as free energy, enthalpy and entropy of adsorption were evaluated. The amounts of DBT adsorbed by these adsorbents were strongly influenced by the initial concentration of the adsorbate, contact time, solution pH and temperature. The main findings of this chapter could be summarized as follows:

- All the adsorption isotherms exhibited asymptote (S) shape, which resulted from the heteroporous structure of the adsorbent and the strong interaction exists between the adsorbed molecules, which encourages cooperative adsorption.
- Two-parameter and three-parameter models were used to evaluate the adsorption isotherms. The Koble–Corrigan equation described the experimental data better than the other models, which indicated a combination of heterogeneous and homogenous uptake for DBT.
- The adsorption capacity increased with the increasing of the initial concentration of DBT. The adsorption equilibrium time was found to be approximately 180 min, indicating a rapid adsorption has occurred. The adsorbed DBT decreased with rising temperature, indicating an exothermic process.
- Over the whole pH range investigated, sorption was governed by complexation of the corresponding DBT cation ($\text{DBT}(\text{OH})^+$) by MCM-TDI-C4 and $\text{DBT}(\text{OH})_2$ by

MCM-TDI-PC4 and MCM-TDI-C4S. The determining factors of the DBT binding were postulated as (i) van der Waals forces, (ii) hydrophobic interactions and (iii) electrostatic attraction.

- The batch kinetic studies showed that the kinetic adsorption of DBT onto MCM-TDI-C4, MCM-TDI-PC4 and MCM-TDI-C4S fitted well by the pseudo-second order model, and the steps of film diffusion and intraparticle diffusion were not the rate-limiting step
- All thermodynamic parameters were negative. This indicated that the adsorption of DBT onto prepared materials was an exothermic and spontaneous process, and the mobility of the adsorbate on the surface of the adsorbent becomes more restricted compared with those in the solution.

CHAPTER 8

CONCLUSIONS AND RECOMMENDATIONS

8.1 Conclusions

The research presented in this thesis summarizes works toward the synthesis and characterization of macrocyclic compound functionalized on mesoporous silica as efficient adsorbents for the complexation of organotin compounds. These materials were synthesized using highly ordered mesoporous silicas MCM-41 with calix[4]arene and β -cyclodextrin as organic modifier via post-synthetic modification strategies. A two-step chemical modification was shown to be an effective way to immobilize the macrocyclic compounds that possessed a cone-shaped molecule. The use of 3-chloropropyl triethoxysilane and toluene-2,4-diisocyanate as an organic linker was explored. The physiochemical properties of the prepared materials were characterized. The choice of the aforementioned strategy and organic modifier were essential for increasing the organotin compounds adsorption capacity.

Following these successful approaches, a screening study for organotin compounds removal using the modified samples prepared in this work was performed. In general, modified samples with calix[4]arene as organic modifier and toluene-2,4-diisocyanate as organic linker exhibited the highest organotin compounds uptake than other samples.

The equilibrium sorption studies of tributyltin (TBT), triphenyltin (TPT) and dibutyltin (DBT) on functionalized mesoporous silica with calix[4]arene, p-tert-butylcalix[4]arene and p-sulfonatocalix[4]arene were investigated by studying the effect of solution pH, initial organotin compounds concentration, contact time and temperature. Adsorption isotherms, using the two-parameter isotherm models and three-parameter isotherm models were determined. Finally, kinetics and thermodynamics parameters of TBT, TPT and DBT for these three adsorbents were also investigated.

Experimental parameters such as adsorbate initial concentration, adsorption contact time, solution pH and temperature have considerable effects on the adsorption process. Organotin compounds compound uptake increased as adsorbate initial concentration increases for all adsorbents. The rate of organotin compounds adsorption was very rapid and the equilibrium states were attained at almost 120-180 min. The optimal pH, temperature, maximum adsorption capacity, the most fitted isotherm and kinetic models and thermodynamic parameters are summarized in Table 8.1.

In general, the results obtained in this work confirmed that the mesoporous silica functionalized with calix[4]arene derivatives prepared in this work can be applied for organotin compounds removal and is superior to the other adsorbents that have been used in literature.

Table 8.1 Summarized results for adsorption of TBT,TPT, and DBT onto MCM-TDI-C4, MCM-TDI-PC4 and MCM-TDI-C4S

Adsorbate		MCM-TDI-C4	MCM-TDI-PC4	MCM-TDI-C4S
TBT	Maximum capacity	12.1212	16.4204	7.5757
	Removal %	88	98	93
	Temperature effect	Endothermic	Exothermic	Endothermic
	pH	5	6	5
	Best fitting isotherm	K-C > D-R	K-C > L(II)	K-C > R-P
	Best fitting kinetic	second order	second order	second order
	ΔH°	+ 8.6	-21.4	+30.9
	ΔG° (at 30°C)	-4.5779	-10.0418	-36.5595
ΔS°	43.7192	-37.4704	120.7609	
TPT	Maximum capacity	17.7305	19.305	18.9393
	Removal %	96	95	88
	Temperature effect	Exothermic	Exothermic	Exothermic
	pH	4	6	4
	Best fitting isotherm	K-C > L(II)	K-C > L(II)	K-C >D-R
	Best fitting kinetic	second order	second order	second order
	ΔH°	-16.5	-19.3	-31.1
	ΔG° (at 30°C)	-7.6639	-5.0949	-4.7257
ΔS°	-29.137	-46.734	-87.0725	
DBT	Maximum capacity	16.9404	18.8196	8.4748
	Removal %	97	97	80
	Temperature effect	Exothermic	Exothermic	Exothermic
	pH	5	6	6
	Best fitting isotherm	K-C > T	K-C > T	K-C > D-R
	Best fitting kinetic	second order	second order	second order
	ΔH°	-18.9	-13.6	-28.3
	ΔG° (at 30°C)	-9.245	-8.5	-2.9949
ΔS°	-31.83	-16.7302	-83.3908	

8.2 Recommendations for future work

The followings are the recommendations for future work:

- Synthesis of calix[4]arene derivatives functionalized onto different support material such as nanoparticles and magnetic nanoparticles for other potential applications is worth trying.
- Application of the novel ordered mesoporous silica with calix[4]arene functionalities deserves to be further explored due to its attractive physical and chemical properties. It is expected that this new material will show remarkable improvement in adsorbing phenol, aromatic amines and dyes.
- Application of the β -cyclodextrin-loaded mesoporous silica is significant in some adsorption and separation process. The β -cyclodextrin-loaded on the mesoporous silica may modify the mesoporous silica and hence show much higher adsorption capacity for some organic pollutants which arise from the inclusion complex.
- More work is necessary to understand the adsorption mechanism behind as the competitive adsorption of DBT on the adsorbents appears to be an uncommon behavior.
- Regeneration of the adsorbents and desorption study need to be attempted in order to reuse the adsorbents.

Reference

- Abay, I., Denizli, A., Bişkin, E., & Salih, B. (2005). Removal and pre-concentration of phenolic species onto β -cyclodextrin modified poly(hydroxyethylmethacrylate-ethyleneglycoldimethacrylate) microbeads. *Chemosphere*, 61(9), 1263-1272.
- Adhikari, B. B., Kanemitsu, M., Kawakita, H., Jumina, & Ohto, K. (2011). Synthesis and application of a highly efficient polyvinylcalix[4]arene tetraacetic acid resin for adsorptive removal of lead from aqueous solutions. *Chemical Engineering Journal*, 172(1), 341-353. doi: 10.1016/j.cej.2011.06.015
- Ahmad, A. A., & Hameed, B. H. (2010). Fixed-bed adsorption of reactive azo dye onto granular activated carbon prepared from waste. *Journal of Hazardous Materials*, 175(1-3), 298-303.
- Akira, H. (1996). Preparation and structures of supramolecules between cyclodextrins and polymers. *Coordination Chemistry Reviews*, 148(0), 115-133. doi: 10.1016/0010-8545(95)01157-9
- Akira, H. (1997). Construction of supramolecular structures from cyclodextrins, polymers. *Carbohydrate Polymers*, 34(3), 183-188. doi: 10.1016/s0144-8617(97)00023-4
- Aksoy, T., Erdemir, S., Yildiz, H. B., & Yilmaz, M. (2012). Novel water-soluble calix[4,6]arene appended magnetic nanoparticles for the removal of the carcinogenic aromatic amines. *Water, Air, and Soil Pollution*, 223(7), 4129-4139. doi: 10.1007/s11270-012-1179-4
- Aksu, Z., & İsoğlu, İ. A. (2005). Removal of copper(II) ions from aqueous solution by biosorption onto agricultural waste sugar beet pulp. *Process Biochemistry*, 40(9), 3031-3044. doi: <http://dx.doi.org/10.1016/j.procbio.2005.02.004>
- Alba, M. D., Luan, Z., & Klinowski, J. (1996). Titanosilicate Mesoporous Molecular Sieve MCM-41: Synthesis and Characterization. *The Journal of Physical Chemistry*, 100(6), 2178-2182. doi: 10.1021/jp9515895
- Allen, S. J., McKay, G., & Porter, J. F. (2004). Adsorption isotherm models for basic dye adsorption by peat in single and binary component systems. *Journal of Colloid and Interface Science*, 280, 322-333.

- Alpaydin, S., Saf, A. O., Bozkurt, S., & Sirit, A. (2011). Kinetic study on removal of toxic metal Cr(VI) through a bulk liquid membrane containing p-tert-butylcalix[4]arene derivative. *Desalination*, 275(1-3), 166-171. doi: 10.1016/j.desal.2011.02.048
- Anbia, M., & Lashgari, M. (2009). Synthesis of amino-modified ordered mesoporous silica as a new nano sorbent for the removal of chlorophenols from aqueous media. *Chemical Engineering Journal*, 150(2-3), 555-560.
- Antizar-Ladislao, B. (2008). Environmental levels, toxicity and human exposure to tributyltin (TBT)-contaminated marine environment. A review. *Environment International*, 34(2), 292-308.
- Antochshuk, V., & Jaroniec, M. (2002). 1-Allyl-3-propylthiourea modified mesoporous silica for mercury removal. *Chem. Commun.*(3), 258-259.
- Anwander, R., Palm, C., Stelzer, J., Groeger, O., & Engelhardt, G. (1998). Silazane-silylation of mesoporous silicates: Towards tailor-made support materials. *Studies in Surface Science and Catalysis*, 117, 135-142.
- Apiratikul, R., & Pavasant, P. (2008). Batch and column studies of biosorption of heavy metals by *Caulerpa lentillifera*. *Bioresource Technology*, 99(8), 2766-2777.
- Appel, K. E., Bohme, C., Platzek, T., Schmidt, E., & Stinchcombe, S. (2000). Organotin compounds in consumer relevant products and food. *Organozinnverbindungen in verbrauchernahen produkten und lebensmitteln*, 5(2), 67-77.
- Arena, G., Casnati, A., Contino, A., Mirone, L., Sciotto, D., & Ungaro, R. (1996). Synthesis of new calixcrowns and their anchoring to silica gel for the selective separation of Cs⁺ and K⁺. *Chemical Communications*(19), 2277-2278.
- Armengol, E., Corma, A., Fernández, L., García, H., & Primo, J. (1997). Acid zeolites as catalysts in organic reactions. Acetylation of cyclohexene and 1-methylcyclohexene. *Applied Catalysis A: General*, 158(1), 323-335.
- Arnold, C. G., Ciani, A., Müller, S. R., Amirbahman, A., & Schwarzenbach, R. P. (1998). Association of triorganotin compounds with dissolved humic acids. *Environmental Science & Technology*, 32(19), 2976-2983.

- Arnold, C. G., Weidenhaupt, A., David, M. M., Müller, S. R., Haderlein, S. B., & Schwarzenbach, R. P. (1997). Aqueous speciation and 1-octanol-water partitioning of tributyl- and triphenyltin: effect of pH and ion composition. *Environmental Science & Technology*, 31(9), 2596-2602.
- Arnold, R., Nelson, J., & Verbanc, J. (1957). Recent advances in isocyanate chemistry. *Chemical Reviews*, 57(1), 47-76.
- Arora, A., & Damodaran, S. (2011). Removal of soy protein-bound phospholipids by a combination of sonication, β -cyclodextrin, and phospholipase A 2 treatments. *Food Chemistry*, 127(3), 1007-1013.
- Atwood, J., & Lehn, J.-M. (1996). *Comprehensive supramolecular chemistry*. (New York): Pergamon.
- Ayanda, O. S., Fatoki, O. S., Adekola, F. A., & Ximba, B. J. (2013). Activated Carbon-Fly Ash-Nanometal Oxide Composite Materials: Preparation, Characterization, and Tributyltin Removal Efficiency. *Journal of Chemistry*, 2013, 15. doi: 10.1155/2013/148129
- Badi, N., Guégan, P., Legrand, F.-X., Leclercq, L., Tilloy, S., & Monflier, E. (2010). β -Cyclodextrins modified by alkyl and poly(ethylene oxide) chains: A novel class of mass transfer additives for aqueous organometallic catalysis. *Journal of Molecular Catalysis A: Chemical*, 318(1-2), 8-14. doi: 10.1016/j.molcata.2009.11.015
- Badruddoza, A. Z. M., Hazel, G. S. S., Hidajat, K., & Uddin, M. S. (2010). Synthesis of carboxymethyl- β -cyclodextrin conjugated magnetic nano-adsorbent for removal of methylene blue. *Colloids and Surfaces A: Physicochemical and Engineering Aspects*, 367(1-3), 85-95.
- Badruddoza, A. Z. M., Tay, A. S. H., Tan, P. Y., Hidajat, K., & Uddin, M. S. (2011). Carboxymethyl- β -cyclodextrin conjugated magnetic nanoparticles as nano-adsorbents for removal of copper ions: Synthesis and adsorption studies. *Journal of Hazardous Materials*, 185(2-3), 1177-1186.
- Baekeland, L. H. (1908). *U.S. Patent*, 942,699.
- Bansal, R. C. (2005). *Activated carbon adsorption*: CRC press.

- Barroso, C. M., & Moreira, M. H. (2002). Spatial and temporal changes of TBT pollution along the Portuguese coast: Inefficacy of the EEC directive 89/677. *Marine Pollution Bulletin*, 44(6), 480-486.
- Barton, T. J., Bull, L. M., Klemperer, W. G., Loy, D. A., McEnaney, B., Misono, M., . . . Yaghi, O. M. (1999). Tailored porous materials. *Chemistry of Materials*, 11(10), 2633-2656.
- Beck, J. S., Calabro, D. C., McCullen, S. B., Pelrine, B. P., Schmitt, K. D., & Vartuli, J. C. (1992). Method for functionalizing synthetic mesoporous crystalline material: US Patent 5,145,816.
- Beck, J. S., Vartuli, J. C., Roth, W. J., Leonowicz, M. E., Kresge, C. T., Schmitt, K. D., . . . Schlenker, J. L. (1992). A new family of mesoporous molecular sieves prepared with liquid crystal templates. *Journal of the American Chemical Society*, 114(27), 10834-10843.
- Becker van Slooten, K., Merlini, L., Stegmueller, L. M., Alencastro, L. F. D., & Tarradellas, J. (1994). Contamination des boues de stations d'épuration suisses par les organoétains. *Gas-Wasser-Abwasser*, 74, 104-110.
- Behra, P., Lecarme-Théobald, É., Bueno, M. t., & Ehrhardt, J.-J. (2003). Sorption of tributyltin onto a natural quartz sand. *Journal of Colloid and Interface Science*, 263(1), 4-12. doi: 10.1016/s0021-9797(03)00238-8
- Bender, M., & Komiyama, M. (1978). *Cyclodextrin Chemistry*: Springer.
- Berto, D., Giani, M., Boscolo, R., Covelli, S., Giovanardi, O., Massironi, M., & Grassia, L. (2007). Organotins (TBT and DBT) in water, sediments, and gastropods of the southern Venice lagoon (Italy). *Marine Pollution Bulletin*, 55(10-12), 425-435. doi: 10.1016/j.marpolbul.2007.09.005
- Bhatt, A. P., Pathak, K., Jasra, R. V., Kureshy, R. I., Khan, N.-u. H., & Abdi, S. H. R. (2006). Chiral lanthanum–lithium–binaphthol complex covalently bonded to silica and MCM-41 for enantioselective nitroaldol (Henry) reaction. *Journal of Molecular Catalysis A: Chemical*, 244(1–2), 110-117. doi: <http://dx.doi.org/10.1016/j.molcata.2005.08.045>
- Bibby, A., & Mercier, L. (2003). Adsorption and separation of water-soluble aromatic molecules by cyclodextrin-functionalized mesoporous silica. *Green chemistry*, 5(1), 15-19.

- Blasco, T., Corma, A., Martínez, A., & Martínez-Escolano, P. (1998). Supported heteropolyacid (HPW) catalysts for the continuous alkylation of isobutane with 2-butene: The benefit of using MCM-41 with larger pore diameters. *Journal of Catalysis*, 177(2), 306-313. doi: <http://dx.doi.org/10.1006/jcat.1998.2105>
- Bouchard, N., Pelletier, É., & Fournier, M. (1999). Effects of butyltin compounds on phagocytic activity of hemocytes from three marine bivalves. *Environmental Toxicology and Chemistry*, 18(3), 519-522. doi: 10.1897/1551-5028(1999)018<0519:eobcop>2.3.co;2
- Boven, G., Oosterling, M. L., Challa, G., & Jan Schouten, A. (1990). Grafting kinetics of poly (methyl methacrylate) on microparticulate silica. *Polymer*, 31(12), 2377-2383.
- Boyer, I. J. (1989). Toxicity of dibutyltin, tributyltin and other organotin compounds to humans and to experimental animals. *Toxicology*, 55(3), 253-298.
- Brändli, R. C., Breedveld, G. D., & Cornelissen, G. (2009). Tributyltin sorption to marine sedimentary black carbon and to amended activated carbon. *Environmental Toxicology and Chemistry*, 28(3), 503-508.
- Brewster, M. E., & Loftsson, T. (2007). Cyclodextrins as pharmaceutical solubilizers. *Advanced Drug Delivery Reviews*, 59(7), 645-666. doi: 10.1016/j.addr.2007.05.012
- Broekhoff, J. C. P. (1979) Mesopore Determination from Nitrogen Sorption Isotherms: Fundamentals, Scope, Limitations. *Vol. 3* (pp. 663-684).
- Bryan, G. W., & Gibbs, P. E. (1991). Impact of low concentrations of tributyltin (TBT) on marine organisms: a review. *Metal Toxicology: Concepts and Applications*. Lewis Publishers, MI, 323-361.
- Bryan, G. W., Gibbs, P. E., & Burt, G. R. (1988). A comparison of the effectiveness of tri-n-butyltin chloride and five other organotin compounds in promoting the development of imposex in the dog-whelk, *Nucella lapillus*. *Journal - Marine Biological Association*, 68(4), 733-744.
- Bueno, M., Astruc, A., Astruc, M., & Behra, P. (1998). Dynamic sorptive behavior of tributyltin on quartz sand at low concentration levels: effect of pH, flow rate, and monovalent cations. *Environmental Science & Technology*, 32(24), 3919-3925.

- Burkett, S. L., Sims, S. D., & Mann, S. (1996). Synthesis of hybrid inorganic-organic mesoporous silica by co-condensation of siloxane and organosiloxane precursors. *Chemical Communications*(11), 1367-1368.
- Burton, E. D., Phillips, I. R., & Hawker, D. W. (2004). Sorption and desorption behavior of tributyltin with natural sediments. *Environmental Science & Technology*, 38(24), 6694-6700.
- Cabou, J., Bricout, H., Hapiot, F., & Monflier, E. (2004). Methylated- β -cyclodextrins: useful discriminating tools for substrate-selective reactions in aqueous organometallic catalysis. *Catalysis Communications*, 5(5), 265-270. doi: 10.1016/j.catcom.2004.03.001
- Cai, K., Li, J., Luo, Z., Hu, Y., Hou, Y., & Ding, X. (2011). β -Cyclodextrin conjugated magnetic nanoparticles for diazepam removal from blood. *Chemical Communications*, 47(27), 7719-7721.
- Caps, V., & Tsang, S. C. (2003). Heterogenisation of Os species on MCM-41 structure for epoxidation of trans-stilbene. *Applied Catalysis A: General*, 248(1-2), 19-31. doi: 10.1016/s0926-860x(03)00106-6
- Carmody, O., Frost, R., Xi, Y., & Kokot, S. (2007). Surface characterisation of selected sorbent materials for common hydrocarbon fuels. *Surface Science*, 601(9), 2066-2076. doi: <http://dx.doi.org/10.1016/j.susc.2007.03.004>
- Casnati, A., Barbosa, S., Rouquette, H., Schwing-Weill, M. J., Arnaud-Neu, F., Dozol, J. F., & Ungaro, R. (2001). New efficient calixarene amide ionophores for the selective removal of strontium ion from nuclear waste: Synthesis, complexation, and extraction properties. *Journal of the American Chemical Society*, 123(49), 12182-12190.
- Casu, B., Reggiani, M., & Sanderson, G. R. (1979). Methylated cycloamyloses (cyclodextrins) and their inclusion properties. *Carbohydrate Research*, 76(1), 59-66.
- Che, J., Xiao, Y., Wang, X., Pan, A., Yuan, W., & Wu, X. (2007). Grafting polymerization of polyacetal onto nano-silica surface via bridging isocyanate. *Surface and Coatings Technology*, 201(8), 4578-4584.
- Chen, M., Ding, W., Wang, J., & Diao, G. (2013). Removal of azo dyes from water by combined techniques of adsorption, desorption, and electrolysis based on a supramolecular sorbent. *Industrial and Engineering Chemistry Research*, 52(6), 2403-2411.

- Chen, M., Shang, T., Fang, W., & Diao, G. (2011). Study on adsorption and desorption properties of the starch grafted p-tert-butyl-calix[n]arene for butyl Rhodamine B solution. *Journal of Hazardous Materials*, 185(2-3), 914-921. doi: 10.1016/j.jhazmat.2010.09.107
- Chen, Q. Y., Xiao, J. B., Chen, X. Q., Jiang, X. Y., Yu, H. Z., & Xu, M. (2006). The adsorption of phenol, m-cresol and m-catechol on a β -cyclodextrin derivative-grafted chitosan and the removal of phenols from industrial wastewater. *Adsorption Science and Technology*, 24(7), 547-557.
- Chen, X., Ji, M., M. Wai, C., & R. Fisher, D. (1998). Carboxylate-derived calixarenes with high selectivity for actinium-225. *Chemical Communications*(3), 377-378.
- Cheremisinoff, N. P., & Cheremisinoff, P. N. (1993). *Carbon adsorption for pollution control*: PTR Prentice Hall.
- Chicano, J. J., Ortiz, A., Teruel, J. A., & Aranda, F. J. (2001). Organotin compounds alter the physical organization of phosphatidylcholine membranes. *Biochimica et Biophysica Acta (BBA)-Biomembranes*, 1510(1), 330-341.
- Chiu, K. L., & Ng, D. H. L. (2012). Synthesis and characterization of cotton-made activated carbon fiber and its adsorption of methylene blue in water treatment. *Biomass and Bioenergy*, 46, 102-110.
- Choi, S. H., Chung, J. W., Priestley, R. D., & Kwak, S. Y. (2012). Functionalization of polysulfone hollow fiber membranes with amphiphilic β -cyclodextrin and their applications for the removal of endocrine disrupting plasticizer. *Journal of Membrane Science*, 409-410, 75-81.
- Chong, A. M. Y. (2001). *Toxicity of organotin, and its biosorption and biodegradation by microalgae*. MPhil, City University of Hong Kong, Hong Kong.
- Chouyyok, W., Panpranot, J., Thanachayanant, C., & Prichanont, S. (2009). Effects of pH and pore characters of mesoporous silicas on horseradish peroxidase immobilization. *Journal of Molecular Catalysis B: Enzymatic*, 56(4), 246-252.
- Chow, S. C., Kass, G. E., McCabe, M. J., & Orrenius, S. (1992). Tributyltin increases cytosolic free Ca^{2+} concentration in thymocytes by mobilizing intracellular Ca^{2+} , activating a Ca^{2+} entry pathway, and inhibiting Ca^{2+} efflux. *Archives of biochemistry and biophysics*, 298(1), 143-149.

- Chowdhury, Z. Z., Zain, S. M., Khan, R. A., & Ashraf, M. A. (2011). Preparation, characterization and adsorption performance of the KOH-activated carbons derived from kenaf fiber for lead (II) removal from waste water. *Scientific Research and Essays*, 6(29), 6185-6196.
- Chun, Y. S., Ha, K., Lee, Y.-J., Lee, J. S., Kim, H. S., Park, Y. S., & Yoon, K. B. (2002). Diisocyanates as novel molecular binders for monolayer assembly of zeolite crystals on glass. *Chemical Communications*(17), 1846-1847.
- Colosio, C., Tomasini, M., Cairoli, S., Foa, V., Minoia, C., Marinovich, M., & Galli, C. L. (1991). Occupational triphenyltin acetate poisoning: A case report. *British Journal of Industrial Medicine*, 48(2), 136-139.
- Cooke, G., Tryphonas, H., Pulido, O., Caldwell, D., Bondy, G., & Forsyth, D. (2004). Oral (gavage), in utero and postnatal exposure of Sprague–Dawley rats to low doses of tributyltin chloride. Part 1: toxicology, histopathology and clinical chemistry. *Food and chemical toxicology*, 42(2), 211-220.
- Cooney, J. J., & Wuertz, S. (1989). Toxic effects of tin compounds on microorganisms. *Journal of industrial Microbiology*, 4(5), 375-402.
- Cornforth, J. W., Hart, P. A., Nicholls, G. A., Rees, R. J., & Stock, J. A. (1955). Antituberculous effects of certain surface-active polyoxyethylene ethers. *British journal of pharmacology and chemotherapy*, 10(1), 73-86.
- Cornforth, J. W., Morgan, E. D., Potts, K. T., & Rees, R. J. W. (1973). Preparation of antituberculous polyoxyethylene ethers of homogeneous structure. *Tetrahedron*, 29(11), 1659-1667.
- Cotoruelo, L. M., Marqués, M. D., Díaz, F. J., Rodríguez-Mirasol, J., Rodríguez, J. J., & Cordero, T. (2012). Adsorbent ability of lignin-based activated carbons for the removal of p-nitrophenol from aqueous solutions. *Chemical Engineering Journal*, 184, 176-183.
- Cremer, J. E. (1958). The biochemistry of organotin compounds: the conversion of tetraethyltin into triethyltin in mammals. *Biochemistry*, 68, 685-692.
- Crini, G., & Morcellet, M. (2002). Synthesis and applications of adsorbents containing cyclodextrins. *Journal of Separation Science*, 25(13), 789-813. doi: 10.1002/1615-9314(20020901)25:13<789::aid-jssc789>3.0.co;2-j

- Croft, A. P., & Bartsch, R. A. (1983). Synthesis of chemically modified cyclodextrins. *Tetrahedron*, 39(9), 1417-1474.
- Cserháti, T. (1994). Relationship between the physicochemical parameters of 3, 5-dinitrobenzoic acid esters and their retention behaviour on β -cyclodextrin polymer support. *Analytica Chimica Acta*, 292(1), 17-22.
- Cucinotta, V., Contino, A., Giuffrida, A., Maccarrone, G., & Messina, M. (2010). Application of charged single isomer derivatives of cyclodextrins in capillary electrophoresis for chiral analysis. *Journal of Chromatography A*, 1217(7), 953-967. doi: 10.1016/j.chroma.2009.11.094
- Czarniecki, M. F., & Breslow, R. (1978). Very Fast acylation of β -cyclodextrin by bound p-nitrophenyl ferrocinnamate. *Journal of the American Chemical Society*, 100(24), 7771-7772.
- Dabrowski, A. (2001). Adsorption-from theory to practice. *Advances in Colloid and Interface Science*, 93(1-3), 135-224.
- Danil De Namor, A. F., Aparicio-Aragon, W., Nwogu, N., El Gamouz, A., Piro, O. E., & Castellano, E. E. (2011). Calixarene and resorcarene based receptors: From structural and thermodynamic studies to the synthesis of a new mercury(II) selective material. *Journal of Physical Chemistry B*, 115(21), 6922-6934. doi: 10.1021/jp110195f
- Davis, M. E. (1993). Organizing for better synthesis. *Nature*, 364(6436), 391-393.
- Debouzy, J. C., Crouzier, D., & Gabelle, A. (2007). Physicochemical properties and membrane interactions Of Per(6-Desoxy-6-Halogenated) Cyclodextrins. *Annales Pharmaceutiques Françaises*, 65(5), 331-341. doi: 10.1016/s0003-4509(07)92596-1
- Deng, L., Su, Y., Su, H., Wang, X., & Zhu, X. (2007). Sorption and desorption of lead (II) from wastewater by green algae *Cladophora fascicularis*. *Journal of Hazardous Materials*, 143(1-2), 220-225. doi: <http://dx.doi.org/10.1016/j.jhazmat.2006.09.009>
- Dias, H. M. A. M., Berbicz, F., Pedrochi, F., Baesso, M. L., & Matioli, G. (2010). Butter cholesterol removal using different complexation methods with beta-cyclodextrin, and the contribution of photoacoustic spectroscopy to the evaluation of the complex. *Food Research International*, 43(4), 1104-1110.

- Do Duong, D. (1998). *Adsorption analysis: equilibria and kinetics* (Vol. 2): Imperial College Press.
- Dong, K., Qiu, F., Guo, X., Xu, J., Yang, D., & He, K. (2013). Adsorption Behavior of Azo Dye Eriochrome Black T from Aqueous Solution by β -Cyclodextrins/Polyurethane Foam Material. *Polymer - Plastics Technology and Engineering*, 52(5), 452-460.
- Dowson, P. H., Bubb, J. M., & Lester, J. N. (1993). A study of the partitioning and sorptive behaviour of butyltins in the aquatic environment. *Applied Organometallic Chemistry*, 7(8), 623-633. doi: 10.1002/aoc.590070805
- Ducoroy, L., Bacquet, M., Martel, B., & Morcellet, M. (2008). Removal of heavy metals from aqueous media by cation exchange nonwoven PET coated with β -cyclodextrin-polycarboxylic moieties. *Reactive and Functional Polymers*, 68(2), 594-600.
- Durmaz, M., Alpaydin, S., Sirit, A., & Yilmaz, M. (2006). Chiral Schiff base derivatives of calix[4]arene: synthesis and complexation studies with chiral and achiral amines. *Tetrahedron: Asymmetry*, 17(16), 2322-2327. doi: <http://dx.doi.org/10.1016/j.tetasy.2006.08.008>
- EFSA. (2004). Opinion of the scientific panel on contaminants in the food chain on a request from the commission to assess the health risks to consumers associated with exposure to organotins in foodstuffs. (Question N°EFSA-Q-2003-110). *European Food Safety Authority*, 102, 1–119.
- Epstein, R. L. (1991). Organotin residue determination in poultry and turkey sample survey in the United States. *Journal of Agricultural and Food Chemistry*, 39(5), 917-921.
- Ernst, S., & Selle, M. (1999). Immobilization and catalytic properties of perfluorinated ruthenium phthalocyanine complexes in MCM-41-type molecular sieves. *Microporous and Mesoporous Materials*, 27(2–3), 355-363. doi: [http://dx.doi.org/10.1016/S1387-1811\(98\)00268-6](http://dx.doi.org/10.1016/S1387-1811(98)00268-6)
- Ertul, Ş., Bayrakci, M., & Yilmaz, M. (2010). Removal of chromate and phosphate anion from aqueous solutions using calix[4]arene receptors containing proton switchable units. *Journal of Hazardous Materials*, 181(1-3), 1059-1065. doi: 10.1016/j.jhazmat.2010.05.121
- Fadeev, A. Y., & McCarthy, T. J. (2000). Self-Assembly Is Not the Only Reaction Possible between Alkyltrichlorosilanes and Surfaces: Monomolecular and Oligomeric Covalently Attached

Layers of Dichloro- and Trichloroalkylsilanes on Silicon. *Langmuir*, 16(18), 7268-7274. doi: 10.1021/la000471z

- Fan, L., Zhang, Y., Luo, C., Lu, F., Qiu, H., & Sun, M. (2012). Synthesis and characterization of magnetic β -cyclodextrin-chitosan nanoparticles as nano-adsorbents for removal of methyl blue. *International Journal of Biological Macromolecules*, 50(2), 444-450.
- Fang, L., Borggaard, O. K., Christensen, J. H., Holm, P. E., & Hansen, H. C. B. (2012). Adsorption of mono- and di-butyltin by a wheat charcoal: pH effects and modeling. *Chemosphere*, 89(7), 863-868. doi: <http://dx.doi.org/10.1016/j.chemosphere.2012.05.010>
- Fang, L., Borggaard, O. K., Marcussen, H., Holm, P. E., & Bruun Hansen, H. C. (2010). The pH-dependent adsorption of tributyltin to charcoals and soot. *Environmental Pollution*, 158(12), 3642-3649. doi: 10.1016/j.envpol.2010.08.003
- Feber, K. (1978). Benzidine and related diaminobiphenyls, *Encyclopedia of Chemical Technology*, 3: Wiley, New York.
- Feng, X., Fryxell, G. E., Wang, L. Q., Kim, A. Y., Liu, J., & Kemner, K. M. (1997). Functionalized monolayers on ordered mesoporous supports. *Science*, 276(5314), 923-926.
- Feng, Y.-Q., Xie, M.-J., & Da, S.-L. (2000). Preparation and characterization of an L-tyrosine-derivatized β -cyclodextrin-bonded silica stationary phase for liquid chromatography. *Analytica Chimica Acta*, 403(1), 187-195.
- Fent, K. (1996a). Ecotoxicology of organotin compounds. *CRC Critical Reviews in Toxicology*, 26(1), 3-117.
- Fent, K. (1996b). Organotin compounds in municipal wastewater and sewage sludge: contamination, fate in treatment process and ecotoxicological consequences. *Science of the Total Environment*, 185(1), 151-159.
- Fent, K., & Mueller, M. D. (1991). Occurrence of organotins in municipal wastewater and sewage sludge and behavior in a treatment plant. *Environmental Science & Technology*, 25(3), 489-493.
- Forsyth, D. S., & Jay, B. (1997). Organotin Leachates in Drinking Water from Chlorinated Poly(vinyl chloride) (CPVC) Pipe. *Applied Organometallic Chemistry*, 11(7), 551-558.

- Frankland, E. (1852). On a new series of organic bodies containing metals. *Philosophical Transactions of the Royal Society of London*, 142, 417-444.
- Fried, D. I., Schlossbauer, A., & Bein, T. (2012). Immobilizing glycopyranose on mesoporous silica via "click-chemistry" for borate adsorption. *Microporous and Mesoporous Materials*, 147(1), 5-9.
- Frouin, H., Lebeuf, M., Saint-Louis, R., Hammill, M., Pelletier, É., & Fournier, M. (2008). Toxic effects of tributyltin and its metabolites on harbour seal (*Phoca vitulina*) immune cells in vitro. *Aquatic Toxicology*, 90(3), 243-251.
- Frouin, H., Pelletier, E., Lebeuf, M., Saint-Louis, R., & Fournier, M. (2010). Toxicology of organotins in marine organisms. A review. *Organometallic Compounds: Preparation, Structure and Properties*, Nova Science Publishers Inc., New York, 1-47.
- Fryxell, G. E. (2006). The synthesis of functional mesoporous materials. *Inorganic Chemistry Communications*, 9(11), 1141-1150.
- Fryxell, G. E., Chouyyok, W., & Rutledge, R. D. (2011). Design and synthesis of chelating diamide sorbents for the separation of lanthanides. *Inorganic Chemistry Communications*, 14(6), 971-974.
- Fryxell, G. E., Liu, J., Hauser, T. A., Nie, Z., Ferris, K. F., Mattigod, S., . . . Hallen, R. T. (1999). Design and synthesis of selective mesoporous anion traps. *Chemistry of Materials*, 11(8), 2148-2154.
- Fu, G. H., Lv, G. X., & Ma, J. T. (2013). The effect of surfactant modification of MCM-41 on supporting ionic liquid for CO₂ adsorption. *Journal of Molecular Catalysis*, 27(3), 218-226.
- Fu, J., He, Q., Wang, R., Liu, B., & Hu, B. (2011). Comparative study of phenol compounds adsorption on mesoporous sieves with different degrees of modification. *Colloids and Surfaces A: Physicochemical and Engineering Aspects*, 375(1-3), 136-140.
- Fujita, K., Yamamura, H., Egashira, Y., & Imoto, T. (1992). A complete set of 6A-azido-6A-deoxy-6X-O-sulfonyl- β -cyclodextrins. *Tetrahedron Letters*, 33(24), 3511-3514. doi: 10.1016/s0040-4039(00)92676-5

- Furer, V., Borisoglebskaya, E., Zverev, V., & Kovalenko, V. (2006). DFT and IR spectroscopic analysis of p-tert-butylthiacalix [4] arene. *Spectrochimica Acta Part A: Molecular and Biomolecular Spectroscopy*, 63(1), 207-212.
- Furue, M., Harada, A., & Nozakura, S.-i. (1975). Preparation of cyclodextrin-containing polymers and their catalysis in ester-hydrolysis. *Journal of Polymer Science: Polymer Letters Edition*, 13(6), 357-360.
- Gabbianelli, R., Falcioni, G., & Lupidi, G. (2002). Photoinduced degradation by iron(III): Removal of triphenyltin chloride from water. *Applied Organometallic Chemistry*, 16(1), 27-33.
- Gadd, G. M. (2000). Microbial interactions with tributyltin compounds: Detoxification, accumulation, and environmental fate. *Science of the Total Environment*, 258(1-2), 119-127.
- Gale, P. A., Chen, Z., Drew, M. G. B., Heath, J. A., & Beer, P. D. (1998). Lower-rim ferrocenyl substituted calixarenes: New electrochemical sensors for anions. *Polyhedron*, 17(4), 405-412. doi: 10.1016/s0277-5387(97)00389-6
- Gao, L., Wang, Y., Wang, J., Huang, L., Shi, L., Fan, X., . . . Li, Z. (2006). A novel ZnII-sensitive fluorescent chemosensor assembled within aminopropyl-functionalized mesoporous SBA-15. *Inorganic Chemistry*, 45(17), 6844-6850.
- Gartner, R. S., Berends, A. M., & Witkamp, G.-J. (1999). Extraction of aluminum from a pickling bath solution by liquid-liquid extraction with calixarenes. *Proceedings of the Engineering Foundation Conference*, 315-326.
- Gärtner, R. S., Berends, A. M., & Witkamp, G. J. (2002). Testing calix(4)arenes for the selective removal of aluminum from a pickling bath solution. *Journal of Supramolecular Chemistry*, 2(1-3), 159-162.
- Gennari, A., Viviani, B., Galli, C. L., Marinovich, M., Pieters, R., & Corsini, E. (2000). Organotins induce apoptosis by disturbance of [Ca(2+)](i) and mitochondrial activity, causing oxidative stress and activation of caspases in rat thymocytes. *Toxicology and applied pharmacology*, 169(2), 185-190.
- Gibbs, P. E., Bebianno, M. J., & Coelho, M. R. (1997). Evidence of the differential sensitivity of neogastropods to tributyltin (TBT) pollution, with notes on a species (*Columbella rustica*) lacking the imposex response. *Environmental Technology*, 18(12), 1219-1224.

- Gibbs, P. E., & Bryan, G. W. (1986). Reproductive failure in populations of the dog-whelk, *Nucella lapillus*, caused by imposex induced by tributyltin from antifouling paints. *Journal - Marine Biological Association*, 66(4), 767-777.
- Gibbs, P. E., Bryan, G. W., Pascoe, P. L., & Burt, G. R. (1987). The use of the dog-whelk, *Nucella lapillus*, as an indicator of tributyltin (TBT) contamination. *Journal - Marine Biological Association*, 67(3), 507-523.
- Gibbs, P. E., Pascoe, P. L., & Burt, G. R. (1988). Sex change in the female dog-whelk, *Nucella lapillus*, induced by tributyltin from antifouling paints. *Journal - Marine Biological Association*, 68(4), 715-731.
- Giles, C. H., Smith, D., & Huitson, A. (1974). A general treatment and classification of the solute adsorption isotherm. I. Theoretical. *Journal of Colloid and Interface Science*, 47(3), 755-765.
- Girard, J.-P., Ferrua, C., & Pesando, D. (1997). Effects of tributyltin on Ca²⁺ homeostasis and mechanisms controlling cell cycling in sea urchin eggs. *Aquatic Toxicology*, 38(4), 225-239.
- Gökmen, V., & Serpen, A. (2002). Equilibrium and kinetic studies on the adsorption of dark colored compounds from apple juice using adsorbent resin. *Journal of Food Engineering*, 53(3), 221-227.
- Goldberg, E. D. (1986). TBT: an environmental dilemma. *Environment: Science and Policy for Sustainable Development*, 28(8), 17-44.
- Golub, M. S., & Doherty, J. D. (2004). Triphenyltin as a potential human endocrine disrupto. *Journal of Toxicology and Environmental Health - Part B: Critical Reviews*, 7(4), 281-295. doi: 10.1080/10937400490452705
- Gubbuk, I. H., Gürfidan, L., Erdemir, S., & Yilmaz, M. (2012). Surface modification of sporopollenin with calixarene derivative: Characterization and application for metal removal. *Water, Air, and Soil Pollution*, 223(5), 2623-2632. doi: 10.1007/s11270-011-1054-8
- Guérin, T., Sirot, V., Volatier, J.-L., & Leblanc, J.-C. (2007). Organotin levels in seafood and its implications for health risk in high-seafood consumers. *Science of the Total Environment*, 388(1), 66-77.

- Gumy, C., Chandsawangbhuwana, C., Dzyakanchuk, A. A., Kratschmar, D. V., Baker, M. E., & Odermatt, A. (2008). Dibutyltin disrupts glucocorticoid receptor function and impairs glucocorticoid-induced suppression of cytokine production. *PLOS ONE*, 3(10), e3545.
- Guo, W., Wang, J., Lee, S. J., Dong, F., Park, S. S., & Ha, C. S. (2010). A General pH-Responsive Supramolecular Nanovalve Based on Mesoporous Organosilica Hollow Nanospheres. *Chemistry-A European Journal*, 16(29), 8641-8646.
- Gupta, V. K., Ludwig, R., & Agarwal, S. (2005). Anion recognition through modified calixarenes: a highly selective sensor for monohydrogen phosphate. *Analytica Chimica Acta*, 538(1-2), 213-218. doi: 10.1016/j.aca.2005.02.008
- Gutsche, C. D. (1991). Calixarenes: a versatile class of macrocyclic compounds. *Kluwer, Dordrecht*.
- Gutsche, C. D. (2008). *Calixarenes: An Introduction 2nd edition*: RSC Publishing.
- Gutsche, C. D., Dhawan, B., No, K. H., & Muthukrishnan, R. (1981). Calixarenes. 4. The synthesis, characterization, and properties of the calixarenes from p-tert-butylphenol. *Journal of the American Chemical Society*, 103(13), 3782-3792.
- Gutsche, C. D., Iqbal, M., & Stewart, D. (1986). Calixarenes. 19. Syntheses procedures for p-tert-butylcalix [4] arene. *The Journal of Organic Chemistry*, 51(5), 742-745.
- Gutsche, C. D., & Muthukrishnan, R. (1978). Calixarenes. 1. Analysis of the product mixtures produced by the base-catalyzed condensation of formaldehyde with para-substituted phenols. *The Journal of Organic Chemistry*, 43(25), 4905-4906. doi: 10.1021/jo00419a052
- Gutsche, C. D., Rogers, J. S., Stewart, D., & See, K.-A. (1990). Calixarenes: paradoxes and paradigms in molecular baskets. *Pure and Applied Chemistry*, 62, 485-491.
- Hall, K., Eagleton, L., Acrivos, A., & Vermeulen, T. (1966). Pore-and solid-diffusion kinetics in fixed-bed adsorption under constant-pattern conditions. *Industrial & Engineering Chemistry Fundamentals*, 5(2), 212-223.
- Hamasaki, T., Sato, T., Nagase, H., & Kito, H. (1993). The mutagenicity of organotin compounds as environmental pollutants. *Mutation Research/Genetic Toxicology*, 300(3), 265-271.

- Hammond, W., Prouzet, E., Mahanti, S., & Pinnavaia, T. J. (1999). Structure factor for the periodic walls of mesoporous MCM-41 molecular sieves. *Microporous and Mesoporous Materials*, 27(1), 19-25.
- Han, E. M., Kim, S. H., Ahn, J., & Kwak, H. S. (2005). Cholesterol removal from homogenized milk with crosslinked β -cyclodextrin by adipic acid. *Asian-Australasian Journal of Animal Sciences*, 18(12), 1794-1799.
- Harlick, P. J., & Sayari, A. (2006). Applications of pore-expanded mesoporous silicas. 3. Triamine silane grafting for enhanced CO₂ adsorption. *Industrial & engineering chemistry research*, 45(9), 3248-3255.
- Hashemi, P., Yarahmadi, A., Azizi, K., & Sabouri, B. (2008). Study of the effects of N fertilization and plant density on the essential oil composition and yield of *Cuminum cyminum* L. seeds by HS-SME. *Chromatographia*, 67(3-4), 253-257.
- Hashimoto, H. (2002). Present status of industrial application of cyclodextrins in Japan. *Journal of Inclusion Phenomena and Macrocyclic Chemistry*, 44(1), 57-62.
- Hata, H., Saeki, S., Kimura, T., Sugahara, Y., & Kuroda, K. (1999). Adsorption of taxol into ordered mesoporous silicas with various pore diameters. *Chemistry of Materials*, 11(4), 1110-1119.
- Hedges, A. (1998). Industrial applications of cyclodextrins. *Chemical Reviews*, 98(5), 2035-2044.
- Heidari, A., Younesi, H., & Mehraban, Z. (2009). Removal of Ni(II), Cd(II), and Pb(II) from a ternary aqueous solution by amino functionalized mesoporous and nano mesoporous silica. *Chemical Engineering Journal*, 153(1-3), 70-79. doi: 10.1016/j.cej.2009.06.016
- Hermens, W. A., Deurloo, M. J., Romeyn, S. G., Verhoef, J. C., & Merkus, F. W. (1990). Nasal absorption enhancement of 17 β -estradiol by dimethyl- β -cyclodextrin in rabbits and rats. *Pharmaceutical research*, 7(5), 500-503.
- Hill, W., Fallourd, V., & Klockow, D. (1999). Investigation of the Adsorption of Gaseous Aromatic Compounds at Surfaces Coated with Heptakis (6-thio-6-deoxy)- β -cyclodextrin by Surface-Enhanced Raman Scattering. *The Journal of Physical Chemistry B*, 103(22), 4707-4713.
- Ho, Y. S. (2004). Selection of optimum sorption isotherm. *Carbon*, 42(10), 2115-2116. doi: <http://dx.doi.org/10.1016/j.carbon.2004.03.019>

- Ho, Y. S., & McKay, G. (1999a). Pseudo-second order model for sorption processes. *Process Biochemistry*, 34(5), 451-465.
- Ho, Y. S., & McKay, G. (1999b). The sorption of lead (II) ions on peat. *Water Research*, 33(2), 578-584.
- Ho, Y. S., Porter, J. F., & McKay, G. (2002). Equilibrium isotherm studies for the sorption of divalent metal ions onto peat: Copper, nickel and lead single component systems. *Water, Air, and Soil Pollution*, 141(1-4), 1-33. doi: 10.1023/a:1021304828010
- Hobler, C., Andrade, A. J. M., Grande, S. W., Gericke, C., Talsness, C. E., Appel, K. E., . . . Grote, K. (2010). Sex-dependent aromatase activity in rat offspring after pre- and postnatal exposure to triphenyltin chloride. *Toxicology*, 276(3), 198-205. doi: 10.1016/j.tox.2010.08.003
- Hoch, M. (2001). Organotin compounds in the environment – an overview. *Applied Geochemistry* 16, 719-743.
- Hoch, M., Alonso-Azcarate, J., & Lischick, M. (2003). Assessment of adsorption behavior of dibutyltin (DBT) to clay-rich sediments in comparison to the highly toxic tributyltin (TBT). *Environmental Pollution*, 123(2), 217-227. doi: 10.1016/s0269-7491(02)00402-5
- Hoch, M., Alonso-Azcarate, J., & Lischick, M. (2002). Adsorption behavior of toxic tributyltin to clay-rich sediments under various environmental conditions. *Environmental Toxicology and Chemistry*, 21(7), 1390-1397.
- Hoch, M., & Weerasooriya, R. (2005). Modeling interactions at the tributyltin–kaolinite interface. *Chemosphere*, 59, 743–752.
- Holland, B. T., Blanford, C. F., & Stein, A. (1998). Synthesis of macroporous minerals with highly ordered three-dimensional arrays of spheroidal voids. *Science*, 281(5376), 538-540.
- Horiguchi, T., Shiraishi, H., Shimizu, M., & Morita, M. (1994). Imposex and organotin compounds in *Thais clavigera* and *T. bronni* in Japan. *Journal of the Marine Biological Association of the United Kingdom*, 74(3), 651-669.

- Horiguchi, T., Shiraishi, H., Shimizu, M., & Morita, M. (1997). Effects of triphenyltin chloride and five other organotin compounds on the development of imposex in the rock shell, *Thais clavigera*. *Environmental Pollution*, 95(1), 85-91.
- Horiguchi, T., Shiraishi, H., Shimizu, M., Yamazaki, S., & Morita, M. (1995). Imposer in Japanese gastropods (Neogastropoda and mesogastropoda): Effects of tributyltin and triphenyltin from antifouling paints. *Marine Pollution Bulletin*, 31(4-12), 402-405. doi: 10.1016/0025-326x(95)00133-8
- Huang, H., Zhao, C., Ji, Y., Nie, R., Zhou, P., & Zhang, H. (2010). Preparation, characterization and application of p-tert-butyl-calix [4] arene-SBA-15 mesoporous silica molecular sieves. *Journal of Hazardous Materials*, 178(1), 680-685.
- Huber, U., Stoeckli, F., & Houriet, J.-P. (1978). A generalization of the Dubinin-Radushkevich equation for the filling of heterogeneous micropore systems in strongly activated carbons. *Journal of Colloid and Interface Science*, 67(2), 195-203.
- Huq, R., Mercier, L., & Kooyman, P. J. (2001). Incorporation of Cyclodextrin into Mesostructured Silica. *Chemistry of Materials*, 13(12), 4512-4519. doi: 10.1021/cm010171i
- Hutson, N. D., & Yang, R. T. (1997). Theoretical basis for the Dubinin-Radushkevitch (DR) adsorption isotherm equation. *Adsorption*, 3(3), 189-195.
- Idris, S. A., Alotaibi, K. M., Peshkur, T. A., Anderson, P., Morris, M., & Gibson, L. T. (2013). Adsorption kinetic study: Effect of adsorbent pore size distribution on the rate of Cr (VI) uptake. *Microporous and Mesoporous Materials*, 165(0), 99-105. doi: <http://dx.doi.org/10.1016/j.micromeso.2012.08.001>
- Iler, R. K. (1979). *The Chemistry of Silica: solubility, polymerization, colloid and surface properties, and biochemistry*. New York: Wiley.
- Imhof, A., & Pine, D. (1997). Ordered macroporous materials by emulsion templating. *Nature*, 389(6654), 948-950.
- Inglezakis, V., & Pouloupoulos, S. (2006). *Adsorption, ion exchange and catalysis: design of operations and environmental applications* (Vol. 3): Elsevier Science.

- Izatt, R. M., Christensen, J. J., & Hawkins, R. T. (1984). Recovery of cesium *U.S. Patent 4* (pp. 477,377).
- Jal, P. K., Patel, S., & Mishra, B. K. (2004). Chemical modification of silica surface by immobilization of functional groups for extractive concentration of metal ions. *Talanta*, *62*(5), 1005-1028.
- Jamali, M. R., Assadi, Y., Shemirani, F., Hosseini, M. R. M., Kozani, R. R., Masteri-Farahani, M., & Salavati-Niasari, M. (2006). Synthesis of salicylaldehyde-modified mesoporous silica and its application as a new sorbent for separation, preconcentration and determination of uranium by inductively coupled plasma atomic emission spectrometry. *Analytica Chimica Acta*, *579*(1), 68-73.
- Jamali, M. R., Assadi, Y., Shemirani, F., & Salavati-Niasari, M. (2007). Application of thiophene-2-carbaldehyde-modified mesoporous silica as a new sorbent for separation and preconcentration of palladium prior to inductively coupled plasma atomic emission spectrometric determination. *Talanta*, *71*(4), 1524-1529.
- Jantzen, E., & Prange, A. (1995). Organometallic species of the elements tin, mercury and lead in sediments of the longitudinal profile of the River Elbe. *Fresenius' journal of analytical chemistry*, *353*(1), 28-33.
- Janus, L., Crini, G., El-Rezzi, V., Morcellet, M., Cambiaghi, A., Torri, G., . . . Vecchi, C. (1999). New sorbents containing beta-cyclodextrin. Synthesis, characterization, and sorption properties. *Reactive and Functional Polymers*, *42*(3), 173-180.
- Janus, R., Kuśtrowski, P., Dudek, B., Piwowarska, Z., Kochanowski, A., Michalik, M., & Cool, P. (2011). Removal of methyl–ethyl ketone vapour on polyacrylonitrile-derived carbon/mesoporous silica nanocomposite adsorbents. *Microporous and Mesoporous Materials*, *145*(1-3), 65-73.
- Jaroniec, C. P., Gilpin, R. K., & Jaroniec, M. (1997). Adsorption and Thermogravimetric Studies of Silica-Based Amide Bonded Phases. *The Journal of Physical Chemistry B*, *101*(35), 6861-6866. doi: 10.1021/jp964002a
- Jenkins, S. M., Ehman, K., & Barone Jr, S. (2004). Structure–activity comparison of organotin species: dibutyltin is a developmental neurotoxicant in vitro and in vivo. *Developmental Brain Research*, *151*(1), 1-12.

- Jensen, K. G., O. Andersen, & Ronne, M. (1991). Direct and indirect assessment of the aneuploidy-inducing potency of organotin compounds. *Alternatives to Laboratory Animals*, 19, 214-218.
- Jin, J., Yang, L., Chan, S. M. N., Luan, T., Li, Y., & Tam, N. F. Y. (2011). Effect of nutrients on the biodegradation of tributyltin (TBT) by alginate immobilized microalga, *Chlorella vulgaris*, in natural river water. *Journal of Hazardous Materials*, 185(2-3), 1582-1586.
- Jones-Lepp, T. L., Varner, K. E., & Heggem, D. (2004). Monitoring Dibutyltin and Triphenyltin in Fresh Waters and Fish in the United States Using Micro-Liquid Chromatography-Electrospray/Ion Trap Mass Spectrometry. *Archives of Environmental Contamination and Toxicology*, 46(1), 90-95. doi: 10.1007/s00244-003-2286-4
- Kaftan, Ö., Açikel, M., Eroğlu, A. E., Shahwan, T., Artok, L., & Ni, C. (2005). Synthesis, characterization and application of a novel sorbent, glucamine-modified MCM-41, for the removal/preconcentration of boron from waters. *Analytica Chimica Acta*, 547(1), 31-41.
- Kamboh, M. A., Akoz, E., Memon, S., & Yilmaz, M. (2013). Synthesis of Amino-Substituted p-tert-Butylcalix[4]arene for the Removal of Chicago Sky Blue and Tropaeolin 000 Azo Dyes from Aqueous Environment. *Water, Air, & Soil Pollution*, 224(2), 1-9. doi: 10.1007/s11270-012-1424-x
- Kamboh, M. A., Solangi, B., Sherazi, S. T. H., & Memon, S. (2011a). Sorption of congo red onto p-tert-butylcalix[4]arene based silica resin. *Journal of the Iranian Chemical Society*, 8(1), 272-279.
- Kamboh, M. A., Solangi, I. B., Sherazi, S. T. H., & Memon, S. (2009). Synthesis and application of calix[4]arene based resin for the removal of azo dyes. *Journal of Hazardous Materials*, 172(1), 234-239.
- Kamboh, M. A., Solangi, I. B., Sherazi, S. T. H., & Memon, S. (2011b). A highly efficient calix[4]arene based resin for the removal of azo dyes. *Desalination*, 268(1-3), 83-89. doi: 10.1016/j.desal.2010.10.001
- Kamboh, M. A., Solangi, I. B., Sherazi, S. T. H., & Memon, S. (2011c). Synthesis and application of p-tert-butylcalix[8]arene immobilized material for the removal of azo dyes. *Journal of Hazardous Materials*, 186(1), 651-658. doi: <http://dx.doi.org/10.1016/j.jhazmat.2010.11.058>

- Kannan, K., Corsolini, S., Focardi, S., Tanabe, S., & Tatsukawa, R. (1996). Accumulation pattern of butyltin compounds in dolphin, tuna, and shark collected from Italian coastal waters. *Archives of Environmental Contamination and Toxicology*, 31(1), 19-23.
- Kannan, K., & Falandysz, J. (1997). Butyltin residues in sediment, fish, fish-eating birds, harbour porpoise and human tissues from the Polish coast of the Baltic Sea. *Marine Pollution Bulletin*, 34(3), 203-207. doi: 10.1016/s0025-326x(96)00146-4
- Kannan, K., Guruge, K. S., Thomas, N. J., Tanabe, S., & Giesy, J. P. (1998). Butyltin residues in southern sea otters (*Enhydra lutris nereis*) found dead along California coastal waters. *Environmental Science and Technology*, 32(9), 1169-1175.
- Kannan, K., Senthilkumar, K., Elliott, J. E., Feyk, L. A., & Giesy, J. P. (1998). Occurrence of butyltin compounds in tissues of water birds and seaducks from the United States and Canada. *Archives of Environmental Contamination and Toxicology*, 35(1), 64-69.
- Kannan, K., Senthilkumar, K., & Giesy, J. P. (1999). Occurrence of butyltin compounds in human blood. *Environmental Science and Technology*, 33(10), 1776-1779. doi: 10.1021/es990011w
- Kannan, K., Tanabe, S., & Tatsukawa, R. (1995). Occurrence of butyltin residues in certain foodstuffs. *Bulletin of Environmental Contamination and Toxicology*, 55(4), 510-516.
- Karim, Z., Adnan, R., & Husain, Q. (2012). A β -cyclodextrin-chitosan complex as the immobilization matrix for horseradish peroxidase and its application for the removal of azo dyes from textile effluent. *International Biodeterioration and Biodegradation*, 72, 10-17.
- Kass, G., & Orrenius, S. (1999). Calcium signaling and cytotoxicity. *Environmental Health Perspectives*, 107(Suppl 1), 25-35.
- Kawanishi, T., Asoh, H., Kato, T., Uneyama, C., Toyoda, K., Teshima, R., . . . Hayakawa, T. (1999). Suppression of Calcium Oscillation by Tri-n-Butyltin Chloride in Cultured Rat Hepatocytes. *Toxicology and applied pharmacology*, 155(1), 54-61.
- Kayranli, B. (2011). Adsorption of textile dyes onto iron based waterworks sludge from aqueous solution; isotherm, kinetic and thermodynamic study. *Chemical Engineering Journal*, 173(3), 782-791. doi: <http://dx.doi.org/10.1016/j.cej.2011.08.051>

- Kim, H., Kim, S., Park, C., Lee, H., Park, H. J., & Kim, C. (2010). Glutathione-Induced Intracellular Release of Guests from Mesoporous Silica Nanocontainers with Cyclodextrin Gatekeepers. *Advanced Materials*, 22(38), 4280-4283. doi: 10.1002/adma.201001417
- Kim, M. L., Stripeikis, J. D., & Tudino, M. B. (2009). Hybrid mesoporous materials for on-line preconcentration of Cr(VI) followed by one-step scheme for elution and colorimetric determination at ultratrace levels. *Talanta*, 77(3), 1068-1074.
- Kim, S., Ida, J., Gulians, V. V., & Lin, Y. S. (2005). Tailoring Pore Properties of MCM-48 Silica for Selective Adsorption of CO₂. *The Journal of Physical Chemistry B*, 109(13), 6287-6293. doi: 10.1021/jp045634x
- Kim, S. H., Ahn, J., & Kwak, H. S. (2004). Crosslinking of beta-cyclodextrin on cholesterol removal from milk. *Archives of pharmacal research*, 27(11), 1183-1187.
- Kim, S. H., Kim, H. Y., & Kwak, H. S. (2007). Cholesterol removal from lard with crosslinked β -cyclodextrin. *Asian-Australasian Journal of Animal Sciences*, 20(9), 1468-1472.
- Kim, Y. M., Lee, J. J., Yin, S. Y., Kim, Y., Lee, J. K., Yoon, Y. P., . . . Lee, M. K. (2002). Inhibitory effects of tributyltin on dopamine biosynthesis in rat PC12 cells. *Neuroscience letters*, 332(1), 13-16.
- Kimbrough, R. D. (1976). Toxicity and health effects of selected organotin compounds: A review. *Environmental Health Perspectives*, vol.14, 51-56.
- Kimura, T., Saeki, S., Sugahara, Y., & Kuroda, K. A. (1999). Organic Modification of FSM-Type Mesoporous Silicas Derived from Kanemite by Silylation. *Langmuir*, 15(8), 2794-2798.
- Klinthong, W., Chao, K. J., & Tan, C. S. (2013). CO₂ capture by as-synthesized amine-functionalized MCM-41 prepared through direct synthesis under basic condition. *Industrial and Engineering Chemistry Research*, 52(29), 9834-9842.
- Koble, R. A., & Corrigan, T. E. (1952). Adsorption isotherms for pure hydrocarbons. *Industrial & Engineering Chemistry*, 44(2), 383-387.
- Kodavanti, P. R. S., Cameron, J. A., Yallapragada, P. R., Vig, P. J., & Desaiyah, D. (1991). Inhibition of Ca²⁺ transport associated with cAMP-dependent protein phosphorylation in rat cardiac sarcoplasmic reticulum by triorganotins. *Archives of toxicology*, 65(4), 311-317.

- Köhn, R., & Fröba, M. (2001). Nanoparticles of 3d transition metal oxides in mesoporous MCM-48 silica host structures: Synthesis and characterization. *Catalysis Today*, *68*(1), 227-236.
- Kono, H., Onishi, K., & Nakamura, T. (2013). Characterization and bisphenol A adsorption capacity of β -cyclodextrin-carboxymethylcellulose-based hydrogels. *Carbohydrate Polymers*, *98*(1), 784-792.
- Kresge, C., Leonowicz, M., Roth, W., Vartuli, J., & Beck, J. (1992). Ordered mesoporous molecular sieves synthesized by a liquid-crystal template mechanism. *Nature*, *359*(6397), 710-712.
- Kristmundsdóttir, T., Loftsson, T., & Holbrook, W. (1996). Formulation and clinical evaluation of a hydrocortisone solution for the treatment of oral disease. *International journal of pharmaceutics*, *139*(1), 63-68.
- Kruk, M., Asefa, T., Jaroniec, M., & Ozin, G. A. (2002). Metamorphosis of ordered mesopores to micropores: periodic silica with unprecedented loading of pendant reactive organic groups transforms to periodic microporous silica with tailorable pore size. *Journal of the American Chemical Society*, *124*(22), 6383-6392.
- Kumar, A., Kumar, S., Kumar, S., & Gupta, D. V. (2007). Adsorption of phenol and 4-nitrophenol on granular activated carbon in basal salt medium: Equilibrium and kinetics. *Journal of Hazardous Materials*, *147*(1-2), 155-166. doi: <http://dx.doi.org/10.1016/j.jhazmat.2006.12.062>
- Kureshy, R. I., Ahmad, I., Khan, N.-u. H., Abdi, S. H. R., Singh, S., Pandia, P. H., & Jasra, R. V. (2005). New immobilized chiral Mn(III) salen complexes on pyridine N-oxide-modified MCM-41 as effective catalysts for epoxidation of nonfunctionalized alkenes. *Journal of Catalysis*, *235*(1), 28-34. doi: <http://dx.doi.org/10.1016/j.jcat.2004.11.002>
- Kwak, H. S., Kim, S. H., Kim, J. H., Choi, H. J., & Kang, J. (2004). Immobilized β -cyclodextrin as a simple and recyclable method for cholesterol removal in milk. *Archives of pharmcal research*, *27*(8), 873-877.
- Lagergren, S. (1898). To the theory of so-called adsorption of dissolved substances. *Kungliga Svenska Vetenskapsakademiens, Handlingar* *42*, 1-39.
- Lamond, T., & Marsh, H. (1964). The surface properties of carbon-II the effect of capillary condensation at low relative pressures upon the determination of surface area. *Carbon*, *1*(3), 281-292.

- Langston, W., & Pope, N. (1995). Determinants of TBT adsorption and desorption in estuarine sediments. *Marine Pollution Bulletin*, 31(1), 32-43.
- Lebeau, B., Fowler, C. E., Hall, S. R., & Mann, S. (1999). Transparent thin films and monoliths prepared from dye-functionalized ordered silica mesostructures. *Journal of Materials Chemistry*, 9(10), 2279-2281.
- Lederer, L. (1894). Eine neue Synthese von Phenolalkoholen. *Journal für Praktische Chemie*, 50(1), 223-226.
- Lee, C. C., Wang, T., Hsieh, C. Y., & Tien, C. J. (2005). Organotin contamination in fishes with different living patterns and its implications for human health risk in Taiwan. *Environmental Pollution*, 137(2), 198-208.
- Lee, J. E., Seo, M. H., Chang, Y. H., & Kwak, H. S. (2010). Cholesterol removal from squid liver oil by crosslinked β -cyclodextrin. *JAACS, Journal of the American Oil Chemists' Society*, 87(2), 233-238.
- Lee, S. E., Chung, J. W., Won, H. S., Lee, D. S., & Lee, Y. W. (2012). Removal of methylmercury and tributyltin (TBT) using marine microorganisms. *Bulletin of Environmental Contamination and Toxicology*, 88(2), 239-244.
- Lee, Y. K., Ganesan, P., & Kwak, H. S. (2012). Optimisation of cross-linking β -cyclodextrin and its recycling efficiency for cholesterol removal in milk and cream. *International Journal of Food Science and Technology*, 47(5), 933-939.
- Lehn, J.-M. (1978). Cryptates: inclusion complexes of macropolycyclic receptor molecules. *Pure Appl. Chem*, 50(9-10), 871-892.
- Lehn, J.-M. (1988). Supramolecular chemistry—scope and perspectives molecules, supermolecules, and molecular devices *Angewandte Chemie International Edition in English*, 27(1), 89-112.
- Lehn, J.-M. (1995). *Supramolecular Chemistry: Concepts and Perspectives*: Wiley-VCH.
- Li, H., Yin, H., Zhang, F., Li, H., Huo, Y., & Lu, Y. (2008). Water-Medium Clean Organic Reactions over an Active Mesoporous Ru(II) Organometallic Catalyst. *Environmental Science & Technology*, 43(1), 188-194. doi: 10.1021/es802094b

- Li, X., Zhao, B., Zhu, K., & Hao, X. (2011). Removal of nitrophenols by adsorption using β -cyclodextrin modified zeolites. *Chinese Journal of Chemical Engineering*, 19(6), 938-943.
- Li, X., Zhu, K., & Hao, X. (2009). Surface modification of zeolite with β -cyclodextrin for removal of p-nitrophenol from aqueous solution. *Water Science & Technology*, 60(2), 329-337.
- Li, Y., Hu, X., Song, X., & Sun, T. (2012). Remediation of cadmium-contaminated soil by extraction with para-sulphonato-thiacalix[4]arene, a novel supramolecular receptor. *Environmental Pollution*, 167, 93-100. doi: 10.1016/j.envpol.2012.03.042
- Lim, M. H., Blanford, C. F., & Stein, A. (1998). Synthesis of ordered microporous silicates with organosulfur surface groups and their applications as solid acid catalysts. *Chemistry of Materials*, 10(2), 467-470.
- Lim, M. H., & Stein, A. (1999). Comparative studies of grafting and direct syntheses of inorganic-organic hybrid mesoporous materials. *Chemistry of Materials*, 11(11), 3285-3295.
- Lima, D., Reis-Henriques, M. A., Silva, R., Santos, A. I., Filipe C. Castro, L., & Santos, M. M. (2011). Tributyltin-induced imposex in marine gastropods involves tissue-specific modulation of the retinoid X receptor. *Aquatic Toxicology*, 101(1), 221-227. doi: 10.1016/j.aquatox.2010.09.022
- Lin, Q., Huo, Q., Su, M., & Wang, L. (2013). Preparation of chitosan/ β -cyclodextrin and its absorption on puerarin. *Asian Journal of Chemistry*, 25(3), 1379-1383.
- Lin, Y., Fryxell, G. E., Wu, H., & Engelhard, M. (2001). Selective sorption of cesium using self-assembled monolayers on mesoporous supports. *Environmental Science & Technology*, 35(19), 3962-3966.
- Liu, A., Hidajat, K., Kawi, S., & Zhao, D. (2000). A new class of hybrid mesoporous materials with functionalized organic monolayers for selective adsorption of heavy metal ions. *Chemical Communications*(13), 1145-1146.
- Liu, C., Lambert, J. B., & Fu, L. (2003). A Novel Family of Ordered, Mesoporous Inorganic/Organic Hybrid Polymers Containing Covalently and Multiply Bound Microporous Organic Hosts. *Journal of the American Chemical Society*, 125(21), 6452-6461. doi: 10.1021/ja0213930

- Liu, C., Lambert, J. B., & Fu, L. (2004). Simple Surfactant-Free Route to Mesoporous Organic–Inorganic Hybrid Silicas Containing Covalently Bound Cyclodextrins. *The Journal of Organic Chemistry*, *69*(6), 2213-2216. doi: 10.1021/jo0352979
- Liu, H., Xu, Y., Li, B., Yin, G., & Xu, Z. (2001). A new highly selective calix[4]arene-based fluorescent probe for Ca²⁺. *Chemical Physics Letters*, *345*(5–6), 395-399. doi: [http://dx.doi.org/10.1016/S0009-2614\(01\)00907-1](http://dx.doi.org/10.1016/S0009-2614(01)00907-1)
- Liu, J.-y., & Jiang, G.-b. (2002). Survey on the presence of butyltin compounds in chinese alcoholic beverages, determined by using headspace solid-phase microextraction coupled with gas chromatography-flame photometric detection. *Journal of agricultural and food chemistry*, *50*(23), 6683-6687.
- Liu, J., Feng, X., Fryxell, G. E., Wang, L. Q., Kim, A. Y., & Gong, M. (1998). Hybrid mesoporous materials with functionalized monolayers. *Advanced Materials*, *10*(2), 161-165.
- Lowell, S., Shields, J. E., Thomas, M. A., & Thommes, M. (2006). *Characterization of porous solids and powders: surface area, pore size and density* (Vol. 16): Springer.
- Lu, F. C. (1994). A review of acceptable daily intake of pesticides assessed by WHO. *Regul. Toxicol. Pharmacol.*, *21*, 352–364.
- Luan, T. G., Jin, J., Chan, S. M. N., Wong, Y. S., & Tam, N. F. Y. (2006). Biosorption and biodegradation of tributyltin (TBT) by alginate immobilized *Chlorella vulgaris* beads in several treatment cycles. *Process Biochemistry*, *41*(7), 1560-1565.
- Lyklema, J. (1995). *Fundamentals of interface and colloid science, solid–liquid interfaces* (1st ed. Vol. II). New York: Academic Press
- Ma, M., & Li, D. (1999). New organic nanoporous polymers and their inclusion complexes. *Chemistry of Materials*, *11*(4), 872-874.
- Macquarrie, D. J. (1996). Direct preparation of organically modified MCM-type materials. Preparation and characterisation of aminopropyl–MCM and 2-cyanoethyl–MCM. *Chemical Communications*(16), 1961-1962.

- Macquarrie, D. J., Maggi, R., Mazzacani, A., Sartori, G., & Sartorio, R. (2003). Understanding the influence of the immobilization procedure on the catalytic activity of aminopropylsilicas in C-C forming reactions. *Applied Catalysis A: General*, 246(1), 183-188.
- Maguire, R. J. (1991). Aquatic environmental aspects of non-pesticidal organotin compounds. *Water quality research journal of Canada*, 26(3), 243-360.
- Mahlambi, M. M., Malefetse, T. J., Mamba, B. B., & Krause, R. W. (2010). β -Cyclodextrin-ionic liquid polyurethanes for the removal of organic pollutants and heavy metals from water: Synthesis and characterization. *Journal of Polymer Research*, 17(4), 589-600.
- Makha, M., & Raston, C. L. (2001). Direct synthesis of calixarenes with extended arms: p-phenylcalix[4,5,6,8]arenes and their water-soluble sulfonated derivatives. *Tetrahedron Letters*, 42(35), 6215-6217. doi: 10.1016/s0040-4039(01)01218-7
- Mamba, B. B., Krause, R. W., Malefetse, T. J., Mhlanga, S. D., Sithole, S. P., Salipira, K. L., & Nxumalo, E. N. (2007). Removal of geosmin and 2-methylisoborneol (2-MIB) in water from Zuikerbosch Treatment Plant (Rand Water) using β -cyclodextrin polyurethanes. *Water SA*, 33(2), 223-227.
- Mamun, A. A., Ma'an, F. R., Zahirah, A. K., Yehya, M. A., Mohammed, A. R. S., Alam, M. Z., . . . Azni, I. (2009). Optimisation of arsenic adsorption from water by carbon nanofibres grown on powdered activated carbon impregnated with nickel. *Journal of Applied Sciences*, 9(17), 3180-3183.
- Manasse, O. (1894). Ueber eine Synthese aromatischer Oxyalkohole. *Berichte der deutschen chemischen Gesellschaft*, 27(2), 2409-2413. doi: 10.1002/cber.189402702239
- Manzo, L., Richelmi, P., & Sabbioni, E. (1981). Poisoning by triphenyltin acetate. Report of two cases and determination of tin in blood and urine by neutron activation analysis. *Clinical Toxicology*, 18(11), 1343-1353.
- Marília, R. M., Delphine, P., Gleiciani, Q. S., Philip, L. L., & Célia, M. R. (2011). Amine-modified MCM-41 mesoporous silica for carbon dioxide capture. *Microporous and Mesoporous Materials*, 143(1), 174-179.
- Marinovich, M., Viviani, B., & Galli, C. L. (1990). Reversibility of tributyltin-chloride-induced protein synthesis inhibition after ATP recovery in HEL-30 cells. *Toxicology letters*, 52(3), 311-317.

- Marler, B., Oberhagemann, U., Vortmann, S., & Gies, H. (1996). Influence of the sorbate type on the XRD peak intensities of loaded MCM-41. *Microporous Materials*, 6(5), 375-383.
- Marwani, H. M., Albishri, H. M., Soliman, E. M., & Jalal, T. A. (2012). Selective adsorption and determination of hexavalent chromium in water samples by chemically modified activated carbon with tris(hydroxymethyl)aminomethane. *Journal of Dispersion Science and Technology*, 33(4), 549-555.
- Matsuno-Yagi, A., & Hatefi, Y. (1993). Studies on the mechanism of oxidative phosphorylation. ATP synthesis by submitochondrial particles inhibited at F₀ by venturicidin and organotin compounds. *Journal of Biological Chemistry*, 268(9), 6168-6173.
- Mattigod, S. V., Feng, X., Fryxell, G. E., Liu, J., & Gong, M. (1999). Separation of complexed mercury from aqueous wastes using self-assembled mercaptan on mesoporous silica. *Separation Science and Technology*, 34(12), 2329-2345.
- McCabe, W. L., Smith, J. C., & Harriott, P. (1956). *Unit operations of chemical engineering* (Vol. 3). New York: McGraw-Hill
- McCusker, L. B., Liebau, F., & Engelhardt, G. (2001). Nomenclature of structural and compositional characteristics of ordered microporous and mesoporous materials with inorganic hosts: (IUPAC recommendations 2001). *Pure and Applied Chemistry*, 73(2), 381-394.
- McKay, G. (1983). The adsorption of dyestuffs from aqueous solution using activated carbon: Analytical solution for batch adsorption based on external mass transfer and. *The Chemical Engineering Journal*, 27(3), 187-196.
- Meador, J. P. (1997). Comparative toxicokinetics of tributyltin in five marine species and its utility in predicting bioaccumulation and acute toxicity. *Aquatic Toxicology*, 37(4), 307-326. doi: [http://dx.doi.org/10.1016/S0166-445X\(96\)00827-2](http://dx.doi.org/10.1016/S0166-445X(96)00827-2)
- Memon, S., Memon, N., & Latif, Y. (2011). An efficient calix[4]arene based silica sorbent for the removal of endosulfan from water. *Journal of Hazardous Materials*, 186(2-3), 1696-1703. doi: 10.1016/j.jhazmat.2010.12.048
- Mercier, L., & Pinnavaia, T. J. (1998). Heavy metal ion adsorbents formed by the grafting of a thiol functionality to mesoporous silica molecular sieves: factors affecting Hg (II) uptake. *Environmental Science & Technology*, 32(18), 2749-2754.

- Mercier, L., & Pinnavaia, T. J. (2000). Direct synthesis of hybrid organic-inorganic nanoporous silica by a neutral amine assembly route: Structure-function control by stoichiometric incorporation of organosiloxane molecules. *Chemistry of Materials*, 12(1), 188-196.
- Merian, E. (1991). *Metals and their compounds in the environment: occurrence, analysis and biological relevance*: VCH Verlagsgesellschaft mbH.
- Miloudi, H., Boos, A., Bouazza, D., Ali-Dahmane, T., Tayeb, A., Goetz-Grandmont, G., & Bengueddach, A. (2007). Acylisoxazolone-impregnated Si-MCM-41 mesoporous materials as promising liquid-solid extractants of metals. *Materials Research Bulletin*, 42(4), 769-775.
- Mirisola, M., Pellerito, A., Fiore, T., Stocco, G., Pellerito, L., Cestelli, A., & Di Liegro, I. (1997). Organometallic Complexes with Biological Molecules: VII. Diorgano- and Triorgano-tin (IV)[meso-tetra (4-carboxyphenyl) porphinate] Derivatives: Solid-state, Solution-phase Structural Aspects and In Vivo Effects. *Applied Organometallic Chemistry*, 11, 499-511.
- Mirzajani, R., Pourreza, N., & Najjar, S. S. A. (2013). β -Cyclodextrin-based polyurethane (β -CDPU) polymers as solid media for adsorption and determination of Pb(II) ions in dust and water samples. *Research on Chemical Intermediates*, 1-13.
- Morabito, R., Chiavarini, S., & Cremisini, C. (1995). Speciation of organotin compounds in environmental samples by GC-MS. In E. A. M. Ph. Quevauviller & B. Griepink (Eds.), *Techniques and Instrumentation in Analytical Chemistry* (Vol. Volume 17, pp. 435-464): Elsevier.
- Moreno-Castilla, C. (2004). Adsorption of organic molecules from aqueous solutions on carbon materials. *Carbon*, 42(1), 83-94. doi: <http://dx.doi.org/10.1016/j.carbon.2003.09.022>
- Morey, M., Davidson, A., & Stucky, G. (1998). Silica-based, cubic mesostructures: synthesis, characterization and relevance for catalysis. *Journal of Porous Materials*, 5(3-4), 195-204.
- Mori, Y., & Pinnavaia, T. J. (2001). Optimizing organic functionality in mesostructured silica: direct assembly of mercaptopropyl groups in wormhole framework structures. *Chemistry of Materials*, 13(6), 2173-2178.
- Mui, L. K. (2009). *Production of activated carbons from waste tyres and bamboo scaffolding for the removal of pollutants from effluents*. PHD, HONG KONG UNIV. OF SCI. AND TECH., HONG KONG.

- Muñoz-Botella, S., Del Castillo, B., & Martín, M. (1995). Cyclodextrin properties and applications of inclusion complex formation. *Ars Pharmaceutica*, *36*(2), 187-198.
- Narita, M., Higuchi, Y., Hamada, F., & Kumagai, H. (1998). Metal sensor of water soluble dansyl-modified thiacalix[4]arenes. *Tetrahedron Letters*, *39*(47), 8687-8690. doi: [http://dx.doi.org/10.1016/S0040-4039\(98\)01899-1](http://dx.doi.org/10.1016/S0040-4039(98)01899-1)
- Negrea, A., Ciopec, M., Lupa, L., Davidescu, C. M., Popa, A., Ilia, G., & Negrea, P. (2011). Removal of AsV by FeIII-Loaded XAD7 Impregnated Resin Containing Di(2-ethylhexyl) Phosphoric Acid (DEHPA): Equilibrium, Kinetic, and Thermodynamic Modeling Studies. *Journal of Chemical & Engineering Data*, *56*(10), 3830-3838. doi: 10.1021/jc200476u
- Nelles, G., Weisser, M., Back, R., Wohlfart, P., Wenz, G., & Mittler-Neher, S. (1996). Controlled orientation of cyclodextrin derivatives immobilized on gold surfaces. *Journal of the American Chemical Society*, *118*(21), 5039-5046.
- Newalkar, B. L., Choudary, N. V., Kumar, P., Komarneni, S., & Bhat, T. S. (2002). Exploring the potential of mesoporous silica, SBA-15, as an adsorbent for light hydrocarbon separation. *Chemistry of Materials*, *14*(1), 304-309.
- Niederl, J. B., & Vogel, H. J. (1940). Aldehyde—Resorcinol Condensations¹. *Journal of the American Chemical Society*, *62*(9), 2512-2514.
- Nirmala, K., Oshima, Y., Lee, R., Imada, N., Honjo, T., & Kobayashi, K. (1999). Transgenerational toxicity of tributyltin and its combined effects with polychlorinated biphenyls on reproductive processes in Japanese medaka (*Oryzias latipes*). *Environmental Toxicology and Chemistry*, *18*(4), 717-721.
- Nishiki, M., Tojima, T., Nishi, N., & Sakairi, N. (2000). β -Cyclodextrin-linked chitosan beads: Preparation and application to removal of bisphenol A from water. *Carbohydrate Letters*, *4*(1), 61-67.
- O'Malley, R. (1983). Physical chemistry, (Atkins, PW). *Journal of Chemical Education*, *60*(2), A63.
- Oberdörster, E., & McClellan-Green, P. (2002). Mechanisms of imposex induction in the mud snail, *Ilyanassa obsoleta*: TBT as a neurotoxin and aromatase inhibitor. *Marine Environmental Research*, *54*(3), 715-718.

- Ogawa, T., & Matsui, M. (1977). A new approach to regioselective acylation of polyhydroxy compounds. *Carbohydrate Research*, 56(1), 1-6.
- Ohhira, S., Watanabe, M., & Matsui, H. (2003). Metabolism of tributyltin and triphenyltin by rat, hamster and human hepatic microsomes. *Archives of toxicology*, 77(3), 138-144.
- Ohshima, T., Miyata, T., & Uragami, T. (2005). Selective removal of dilute benzene from water by various cross-linked poly(dimethylsiloxane) membranes containing tert-butylcalix[4]arene. *Macromolecular Chemistry and Physics*, 206(24), 2521-2529.
- Oishi, K., & Moriuchi, A. (2010). Removal of dissolved estrogen in sewage effluents by β -cyclodextrin polymer. *Science of the Total Environment*, 409(1), 112-115.
- Okutomo, S., Kuroda, K., & Ogawa, M. (1999). Preparation and characterization of silylated-magadiites. *Applied Clay Science*, 15(1-2), 253-264.
- Oliveira, P., Machado, A., Ramos, A., Fonseca, I., Braz Fernandes, F., Botelho do Rego, A., & Vital, J. (2007). A new and easy method for anchoring manganese salen on MCM-41. *Catalysis letters*, 114(3), 192-197.
- Orrenius, S., McCabe, M. J., & Nicotera, P. (1992). Ca^{2+} dependent mechanisms of cytotoxicity and programmed cell death. *Toxicology letters*, 64, 357-364.
- Osa, T., & Suzuki, I. (1996). Cyclodextrins. *Comprehensive Supramolecular Chemistry*; Szejtli, J., Osa, T., Eds: Pergamon: Oxford.
- Özer, A., Akkaya, G., & Turabik, M. (2005). Biosorption of Acid Red 274 (AR 274) on *Enteromorpha prolifera* in a batch system. *Journal of Hazardous Materials*, 126(1), 119-127.
- Ozin, G. A. (2000). Panoscopic materials: Synthesis over 'all' length scales. *Chemical Communications*(6), 419-432.
- Pan, J., Zou, X., Wang, X., Guan, W., Li, C., Yan, Y., & Wu, X. (2011). Adsorptive removal of 2,4-didichlorophenol and 2,6-didichlorophenol from aqueous solution by β -cyclodextrin/attapulgitite composites: Equilibrium, kinetics and thermodynamics. *Chemical Engineering Journal*, 166(1), 40-48.

- Pan, Y. J., Hsieh, C. T., & Yen, C. K. (2011). Dyeing Adsorption Isotherm and Equilibrium Modeling Characteristics of Enzymatic and Caustic Pre-Treated Lyocell Fibers. *Advanced Materials Research*, 332, 568-571.
- Park, C., Lee, K., & Kim, C. (2009). Photoresponsive Cyclodextrin-Covered Nanocontainers and Their Sol-Gel Transition Induced by Molecular Recognition. *Angewandte Chemie International Edition*, 48(7), 1275-1278. doi: 10.1002/anie.200803880
- Pater, J. P., Jacobs, P. A., & Martens, J. A. (1999). Oligomerization of hex-1-ene over acidic aluminosilicate zeolites, MCM-41, and silica-alumina co-gel catalysts: A comparative study. *Journal of Catalysis*, 184(1), 262-267.
- Pérez-Quintanilla, D., Sánchez, A., del Hierro, I., Fajardo, M., & Sierra, I. (2007). Preparation, characterization, and Zn²⁺ adsorption behavior of chemically modified MCM-41 with 5-mercapto-1-methyltetrazole. *Journal of Colloid and Interface Science*, 313(2), 551-562.
- Petter, R. C., Salek, J. S., Sikorski, C. T., Kumaravel, G., & Lin, F. T. (1990). Cooperative binding by aggregated mono-6-(alkylamino)-. beta.-cyclodextrins. *Journal of the American Chemical Society*, 112(10), 3860-3868.
- Pinnavaia, T. (1999). Selective adsorption of Hg²⁺ by thiol-functionalized nanoporous silica. *Chemical Communications*(1), 69-70.
- Prasad, N., Strauss, D., & Reichart, G. (1999). Cyclodextrins inclusion for food, cosmetics and pharmaceuticals. *European Patent*, 1(084), 625.
- Prasad, R., & Schafran, G. C. (2006). Characterization of tributyltin in shipyard waters and removal through laboratory and full-scale treatment. *Water Research*, 40(3), 453-462.
- Price, P. M., Clark, J. H., & Macquarrie, D. J. (2000). Modified silicas for clean technology. *Journal of the Chemical Society, Dalton Transactions*(2), 101-110.
- Pu, Q. M., Ren, F. L., Tan, A. X., & Jiang, F. M. (2012). Synthesis of novel functional mesoporous materials and its adsorption capacity to lead ions. *Yejin Fenxi/Metallurgical Analysis*, 32(10), 45-49.

- Puri, B. K., Muñoz-Olivas, R., & Cámara, C. (2004). A new polymeric adsorbent for screening and pre-concentration of organotin compounds in sediments and seawater samples. *Spectrochimica Acta Part B: Atomic Spectroscopy*, 59(2), 209-214.
- Quevauviller, P., Donard, O., & Bruchet, A. (1991). Leaching of organotin compounds from poly (vinyl chloride)(PVC) material. *Applied Organometallic Chemistry*, 5(2), 125-129.
- Qureshi, I., Qazi, M. A., Bhatti, A. A., Memon, S., Sirajuddin, & Yilmaz, M. (2011). An efficient calix[4]arene appended resin for the removal of arsenic. *Desalination*, 278(1-3), 98-104. doi: 10.1016/j.desal.2011.05.007
- Ramu, A., Kannan, N., & Srivathsan, S. A. (1992). Adsorption of Carboxylic Acids on Fly Ash and Activated Carbon. *Indian journal of environmental health*, 34(3), 192-199.
- Rantakokko, P., Kuningas, T., Saastamoinen, K., & Vartiainen, T. (2006). Dietary intake of organotin compounds in Finland: A market-basket study. *Food Additives and Contaminants*, 23(8), 749-756. doi: 10.1080/02652030600779908
- Rantakokko, P., Turunen, A., Verkasalo, P. K., Kiviranta, H., Männistö, S., & Vartiainen, T. (2008). Blood levels of organotin compounds and their relation to fish consumption in Finland. *Science of the Total Environment*, 399(1-3), 90-95. doi: 10.1016/j.scitotenv.2008.03.017
- Rao, P., Enger, O., Graf, E., Hosseini, Mir W., De Cian, A., & Fischer, J. (2000). Mercaptocalixarenes as Mercury(II) Extractors: Synthesis, Structural Analysis and Extraction Properties of Lipophilic Dimercaptocalix[4]arenes. *European Journal of Inorganic Chemistry*, 2000(7), 1503-1508.
- Raoov, M., Mohamad, S., & Abas, M. R. (2013). Removal of 2,4-dichlorophenol using cyclodextrin-ionic liquid polymer as a macroporous material: Characterization, adsorption isotherm, kinetic study, thermodynamics. *Journal of Hazardous Materials*, 263, 501-516.
- Reader, S., & Pelletier, E. (1992). Identification and determination of butyltin compounds by gas chromatography-ion trap spectrometry. *Analytica Chimica Acta*, 262(2), 307-314.
- Redlich, O., & Peterson, D. L. (1959). A useful adsorption isotherm. *Journal of Physical Chemistry*, 63(6), 1024-1024.

- Regayeg, M., Vocanson, F., Duport, A., Blondeau, B., Perrin, M., Fort, A., & Lamartine, R. (2002). New calixarenes for nonlinear optics: synthesis and conformation of functionalized p-nitrocalix[4]arenes. *Materials Science and Engineering: C*, 21(1–2), 131-135. doi: 10.1016/s0928-4931(02)00071-1
- Revathi, G., Ramalingam, S., Subramaniam, P., & Ganapathi, A. (2011). Removal of direct yellow-12 dye from water by adsorption on activated carbon prepared from ficus racemosa l. *E- Journal of Chemistry*, 8(4), 1536-1545.
- Reynhardt, J. P., Yang, Y., Sayari, A., & Alper, H. (2004). Periodic mesoporous silica-supported recyclable rhodium-complexed dendrimer catalysts. *Chemistry of Materials*, 16(21), 4095-4102.
- Robinson, T., McMullan, G., Marchant, R., & Nigam, P. (2001). Remediation of dyes in textile effluent: a critical review on current treatment technologies with a proposed alternative. *Bioresource Technology*, 77(3), 247-255.
- Rodríguez-Bonilla, P., López-Nicolás, J., Méndez-Cazorla, L., & García-Carmona, F. (2011). Development of a reversed phase high performance liquid chromatography method based on the use of cyclodextrins as mobile phase additives to determine pterostilbene in blueberries. *Journal of Chromatography B*, 879(15–16), 1091-1097. doi: 10.1016/j.jchromb.2011.03.025
- Rosen, M. J. (2004). *Surfactants and Interfacial Phenomena* (3rd ed. Vol. 1): Wiley-VCH.
- Rouquerol, J., Rouquerol, F., & Sing, K. S. (1998). *Absorption by powders and porous solids*: Academic press.
- Rugh, B. W., & Miles, D. (1996). Monitoring the effects of five “nonherbicidal” pesticide chemicals on terrestrial plants using chlorophyll fluorescence. *Environmental Toxicology and Chemistry*, 15(4), 495-500.
- Sadiki, A. I., & Williams, D. T. (1999). A study on organotin levels in Canadian drinking water distributed through PVC pipes. *Chemosphere*, 38(7), 1541-1548. doi: 10.1016/s0045-6535(98)00374-9
- Sadiki, A. I., Williams, D. T., Carrier, R., & Thomas, B. (1996). Pilot study on the contamination of drinking water by organotin compounds from PVC materials. *Chemosphere*, 32(12), 2389-2398.

- Sakthivel, A., Hijazi, A. K., Hanzlik, M., Chiang, A. S. T., & Kühn, F. E. (2005). Heterogenization of [Cu(NCCH₃)₆][B(C₆F₅)₄]₂ and its application in catalytic olefin aziridination. *Applied Catalysis A: General*, 294(2), 161-167. doi: 10.1016/j.apcata.2005.07.018
- Salame, I. I., & Bandosz, T. J. (2003). Role of surface chemistry in adsorption of phenol on activated carbons. *Journal of Colloid and Interface Science*, 264(2), 307-312. doi: [http://dx.doi.org/10.1016/S0021-9797\(03\)00420-X](http://dx.doi.org/10.1016/S0021-9797(03)00420-X)
- Santos, D. O., de Lourdes Nascimento Santos, M., Costa, J. A. S., de Jesus, R. A., Navickiene, S., Sussuchi, E. M., & de Mesquita, M. E. (2013). Investigating the potential of functionalized MCM-41 on adsorption of Remazol Red dye. *Environmental Science and Pollution Research*, 20(7), 5028-5035.
- Santos, M. M., Armada Reis-Henriques, M., Natividade Vieira, M., & Solé, M. (2006). Triphenyltin and tributyltin, single and in combination, promote imposex in the gastropod *Bolinus brandaris*. *Ecotoxicology and Environmental Safety*, 64(2), 155-162. doi: 10.1016/j.ecoenv.2005.02.003
- Sasahara, T., Kido, A., Ishihara, H., Sunayama, T., & Egashira, M. (2005). Highly sensitive detection of volatile organic compounds by an adsorption/combustion-type sensor based on mesoporous silica. *Sensors and Actuators, B: Chemical*, 108(1-2 SPEC. ISS.), 478-483.
- Sasaki, Y., Yamada, H., Sugiyama, C., & Kinae, N. (1993). Increasing effect of tri-n-butyltins and triphenyltins on the frequency of chemically induced chromosome aberrations in cultured Chinese hamster cells. *Mutation Research/Genetic Toxicology*, 300(1), 5-14.
- Sauer, J., Marlow, F., & Schuth, F. (2001). Simulation of powder diffraction patterns of modified ordered mesoporous materials. *Physical Chemistry Chemical Physics*, 3(24), 5579-5584.
- Sayari, A. (1996). Catalysis by Crystalline Mesoporous Molecular Sieves. *Chemistry of Materials*, 8(8), 1840-1852. doi: 10.1021/cm950585+
- Sayari, A., & Hamoudi, S. (2001). Periodic Mesoporous Silica-Based Organic-Inorganic Nanocomposite Materials. *Chemistry of Materials*, 13(10), 3151-3168. doi: 10.1021/cm011039I
- Sayari, A., Hamoudi, S., & Yang, Y. (2005). Applications of pore-expanded mesoporous silica. 1. Removal of heavy metal cations and organic pollutants from wastewater. *Chemistry of Materials*, 17(1), 212-216.

- Sayin, S., Ozcan, F., Memon, S., & Yilmaz, M. (2010). Synthesis and oxoanions (dichromate/arsenate) sorption study of N-methylglucamine derivative of calix[4]arene immobilized onto poly[(phenyl glycidyl ether)-co-formaldehyde]. *Journal of Inclusion Phenomena and Macrocyclic Chemistry*, 67(3), 385-391.
- Sayin, S., Ozcan, F., & Yilmaz, M. (2010). Synthesis and evaluation of chromate and arsenate anions extraction ability of a N-methylglucamine derivative of calix[4]arene immobilized onto magnetic nanoparticles. *Journal of Hazardous Materials*, 178(1-3), 312-319.
- Sayin, S., Ozcan, F., & Yilmaz, M. (2011). Preparation and application of calix[4]arene derivatives bearing pyridinium units-grafted magnetite nanoparticles for removal of dichromate and arsenate anions. *Journal of Macromolecular Science, Part A: Pure and Applied Chemistry*, 48(5), 365-372. doi: 10.1080/10601325.2011.562466
- Sayin, S., & Yilmaz, M. (2011a). Preparation and uranyl ion extraction studies of calix[4]arene-based magnetite nanoparticles. *Desalination*, 276(1-3), 328-335. doi: 10.1016/j.desal.2011.03.073
- Sayin, S., & Yilmaz, M. (2011b). Synthesis of a new calixarene derivative and its immobilization onto magnetic nanoparticle surfaces for excellent extractants toward Cr(VI), As(V), and U(VI). *Journal of Chemical and Engineering Data*, 56(5), 2020-2029. doi: 10.1021/je1010328
- Sayin, S., Yilmaz, M., & Tavasli, M. (2011). Syntheses of two diamine substituted 1,3-distal calix[4]arene-based magnetite nanoparticles for extraction of dichromate, arsenate and uranyl ions. *Tetrahedron*, 67(20), 3743-3753. doi: 10.1016/j.tet.2011.03.012
- Schafran, G. C., Prasad, R., Thorn, F. H., Ewing, R. M., & Soles, J. (2003). Removal of tributyltin in shipyard waters: Characterization and treatment to meet low parts per trillion levels. *Journal of Ship Production*, 19(3), 179-186.
- Schurig, V. (2010). Use of derivatized cyclodextrins as chiral selectors for the separation of enantiomers by gas chromatography. *Annales Pharmaceutiques Françaises*, 68(2), 82-98. doi: 10.1016/j.pharma.2009.11.004
- Seinen, W., Vos, J. G., van Krieken, R., Penninks, A., Brands, R., & Hooykaas, H. (1977). Toxicity of organotin compounds. III. Suppression of thymus-dependent immunity in rats by di-n-butyltindichloride and di-n-octyltindichloride. *Toxicology and applied pharmacology*, 42(1), 213-224.

- Seliem, M. K., Komarneni, S., Byrne, T., Cannon, F. S., Shahien, M. G., Khalil, A. A., & Abd El-Gaid, I. M. (2013). Removal of nitrate by synthetic organosilicas and organoclay: Kinetic and isotherm studies. *Separation and Purification Technology*, 110(0), 181-187. doi: <http://dx.doi.org/10.1016/j.seppur.2013.03.023>
- Seltzer, R. (1987). NMR probes freeze tolerance in arctic insect. *Chemical & Engineering News*, 65(20), 28.
- Serna-Guerrero, R., & Sayari, A. (2007). Applications of pore-expanded mesoporous silica. 7. Adsorption of volatile organic compounds. *Environmental Science & Technology*, 41(13), 4761-4766.
- Shao, D., Sheng, G., Chen, C., Wang, X., & Nagatsu, M. (2010). Removal of polychlorinated biphenyls from aqueous solutions using β -cyclodextrin grafted multiwalled carbon nanotubes. *Chemosphere*, 79(7), 679-685.
- Sharma, K. K., & Asefa, T. (2007). Efficient bifunctional nanocatalysts by simple postgrafting of spatially isolated catalytic groups on mesoporous materials. *Angewandte Chemie - International Edition*, 46(16), 2879-2882.
- Shim, W. J., Kahng, S. H., Hong, S. H., Kim, N. S., Kim, S. K., & Shim, J. H. (2000). Imposex in the rock shell, *Thais clavigera*, as evidence of organotin contamination in the marine environment of Korea. *Marine Environmental Research*, 49(5), 435-451. doi: 10.1016/S0141-1136(99)00084-7
- Shiraishi, Y., Nishimura, G., Hirai, T., & Komazawa, I. (2002). Separation of transition metals using inorganic adsorbents modified with chelating ligands. *Industrial & engineering chemistry research*, 41(20), 5065-5070.
- Shylesh, S., & Singh, A. P. (2004). Synthesis, characterization, and catalytic activity of vanadium-incorporated, -grafted, and -immobilized mesoporous MCM-41 in the oxidation of aromatics. *Journal of Catalysis*, 228(2), 333-346.
- Si, H., Wang, T., & Xu, Z. (2013). Biosorption of methylene blue from aqueous solutions on β -cyclodextrin grafting wood flour copolymer: Kinetic and equilibrium studies. *Wood Science and Technology*, 47(6), 1177-1196.
- Simons, D. M., & Arnold, R. G. (1956). Relative reactivity of the isocyanate groups in toluene-2, 4-diisocyanate. *Journal of the American Chemical Society*, 78(8), 1658-1659.

- Sing, K. S. W., Everett, D. H., Haul, R. A. W., Moscou, L., Pierotti, R. A., Rouquerol, J., & Siemieniowska, T. (1985). Reporting Physisorption Data for Gas/solid Systems with Special Reference to the Determination of Surface Area and Porosity. *Pure Appl. Chem.*, 57(4), 603-619.
- Singh, A., & Bragg, P. (1979). The action of tributyltin chloride on energy-dependent transhydrogenation of NADP⁺ by NADH in membranes of *Escherichia coli*. *Canadian Journal of Biochemistry*, 57(12), 1384-1391.
- Singh, T. S., & Pant, K. (2004). Equilibrium, kinetics and thermodynamic studies for adsorption of As (III) on activated alumina. *Separation and Purification Technology*, 36(2), 139-147.
- Smith, J. M. (1981). *Chemical Engineering Kinetics* (third ed.). New York: McGraw-Hill.
- Snoeij, N., Penninks, A., & Seinen, W. (1988). Dibutyltin and tributyltin compounds induce thymus atrophy in rats due to a selective action on thymic lymphoblasts. *International journal of immunopharmacology*, 10(7), 891-899.
- Sohn, S., & Kim, D. (2005). Modification of Langmuir isotherm in solution systems—definition and utilization of concentration dependent factor. *Chemosphere*, 58(1), 115-123.
- Solangi, I. B., Bhatti, A. A., Kamboh, M. A., Memon, S., & Bhangar, M. I. (2011). Comparative fluoride sorption study of new calix[4]arene-based resins. *Desalination*, 272(1-3), 98-106.
- Solangi, I. B., Memon, S., & Bhangar, M. I. (2009). Synthesis and application of a highly efficient tetraester calix[4]arene based resin for the removal of Pb²⁺ from aqueous environment. *Analytica Chimica Acta*, 638(2), 146-153.
- Solé, M., Morcillo, Y., & Porte, C. (1998). Imposex in the commercial snail *Bolinus brandaris* in the northwestern Mediterranean. *Environmental Pollution*, 99(2), 241-246. doi: 10.1016/s0269-7491(97)00186-3
- Song, W., Hu, J., Zhao, Y., Shao, D., & Li, J. (2013). Efficient removal of cobalt from aqueous solution using β -cyclodextrin modified graphene oxide. *RSC Advances*, 3(24), 9514-9521.
- Srivastava, V. C., Swamy, M. M., Mall, I. D., Prasad, B., & Mishra, I. M. (2006). Adsorptive removal of phenol by bagasse fly ash and activated carbon: equilibrium, kinetics and

thermodynamics. *Colloids and Surfaces A: Physicochemical and Engineering Aspects*, 272(1), 89-104.

St-Jean, S. D., Pelletier, É., & Courtenay, S. C. (2002). Very low levels of waterborne butyltins modulate hemocyte function in the blue mussel *Mytilus edulis*. *Marine Ecology Progress Series*, 236, 155-161.

Stasinakis, A. S., Thomaidis, N. S., Nikolaou, A., & Kantifes, A. (2005). Aerobic biodegradation of organotin compounds in activated sludge batch reactors. *Environmental Pollution*, 134(3), 431-438. doi: <http://dx.doi.org/10.1016/j.envpol.2004.09.013>

Stathi, P., Dimos, K., Karakassides, M. A., & Deligiannakis, Y. (2010). Mechanism of heavy metal uptake by a hybrid MCM-41 material: Surface complexation and EPR spectroscopic study. *Journal of Colloid and Interface Science*, 343(1), 374-380.

Stein, A., Melde, B. J., & Schroden, R. C. (2000). Hybrid inorganic-organic mesoporous silicates-nanoscopic reactors coming of age. *Advanced Materials*, 12(19), 1403-1419.

Stewart, D. R., & Gutsche, C. D. (1999). Isolation, characterization, and conformational characteristics of p- tert-butylcalix[9 - 20]arenes. *Journal of the American Chemical Society*, 121(17), 4136-4146.

Stichnothe, H., Thöming, J., & Calmano, W. (2001). Detoxification of tributyltin contaminated sediments by an electrochemical process. *Science of the Total Environment*, 266(1-3), 265-271.

Stoner, H. B. (1966). Toxicity of triphenyltin. *British Journal of Industrial Medicine*, 23(3), 222-229.

Strand, J., & Jacobsen, J. A. (2005). Accumulation and trophic transfer of organotins in a marine food web from the Danish coastal waters. *Science of the Total Environment*, 350(1-3), 72-85. doi: 10.1016/j.scitotenv.2005.02.039

Stridh, H., Orrenius, S., & Hampton, M. B. (1999). Caspase involvement in the induction of apoptosis by the environmental toxicants tributyltin and triphenyltin. *Toxicology and applied pharmacology*, 156(2), 141-146.

Stucky, G. D., Monnier, A., Schüth, F., Huo, Q., Margolese, D., Kumar, D., . . . Chmelka, B. F. (1994). Molecular and Atomic Arrays in Nano- and Mesoporous Materials Synthesis. *Molecular*

Crystals and Liquid Crystals Science and Technology. Section A. Molecular Crystals and Liquid Crystals, 240, 187-200.

- Su, B.-L., Ma, X.-C., Xu, F., Chen, L.-H., Fu, Z.-Y., Moniotte, N., . . . Vocanson, F. (2011). SBA-15 mesoporous silica coated with macrocyclic calix[4]arene derivatives: Solid extraction phases for heavy transition metal ions. *Journal of Colloid and Interface Science*, 360(1), 86-92. doi: 10.1016/j.jcis.2011.03.084
- Sun, L., Zhang, J., Zuo, Z., Chen, Y., Wang, X., Huang, X., & Wang, C. (2011). Influence of triphenyltin exposure on the hypothalamus-pituitary-gonad axis in male *Sebastiscus marmoratus*. *Aquatic Toxicology*, 104(3-4), 263-269. doi: 10.1016/j.aquatox.2011.04.018
- Sykut, K., Saba, J., & Dabrowski, A. (1999). Adsorption and Its Applications in Industry and Environmental Protection: Elsevier, Amsterdam.
- Sze, M. F. F., Lee, V. K. C., & McKay, G. (2008). Simplified fixed bed column model for adsorption of organic pollutants using tapered activated carbon columns. *Desalination*, 218(1-3), 323-333.
- Szejtli, J. (1998). Introduction and General Overview of Cyclodextrin Chemistry. *Chemical Reviews*, 98(5), 1743-1754.
- Tabakci, M., Erdemir, S., & Yilmaz, M. (2007). Preparation, characterization of cellulose-grafted with calix[4]arene polymers for the adsorption of heavy metals and dichromate anions. *Journal of Hazardous Materials*, 148(1-2), 428-435.
- Tabakci, M., Ersoz, M., & Yilmaz, M. (2006). A calix[4]arene-containing polysiloxane resin for removal of heavy metals and dichromate anion. *Journal of Macromolecular Science - Pure and Applied Chemistry*, 43 A(1), 57-69.
- Tabushi, I., Kuroda, Y., Yokota, K., & Yuan, L. C. (1981). Regiospecific A,C- and A,D-disulfonate capping of .beta.-cyclodextrin. *Journal of the American Chemical Society*, 103(3), 711-712.
- Takahashi, K. (1998). Organic Reactions Mediated by Cyclodextrins. *Chemical Reviews*, 98(5), 2013-2034.

- Takahashi, S., Mukai, H., Tanabe, S., Sakayama, K., Miyazaki, T., & Masuno, H. (1999). Butyltin residues in livers of humans and wild terrestrial mammals and in plastic products. *Environmental Pollution*, 106(2), 213-218. doi: 10.1016/s0269-7491(99)00068-8
- Takemura, H. (2002). Azacalixarenes: synthesis, complexation, and structures. *Journal of Inclusion Phenomena and Macrocyclic Chemistry*, 42(3-4), 169-186.
- Tam, N., Chong, A., & Wong, Y. (2003). Removal of tributyltin (TBT) from wastewater by microalgae. *Water Pollution Vii-Modelling, Measuring and Prediction, International Series on Progress in Water Resources*, 9, 261-271.
- Tam, N. F. Y., Chong, A. M. Y., & Wong, Y. S. (2002). Removal of tributyltin (TBT) by live and dead microalgal cells. *Marine Pollution Bulletin*, 45(1-12), 362-371.
- Tam, N. F. Y., Chong, A. M. Y., & Wong, Y. S. (2004). *Removal of tributyltin (TBT) by free and immobilized Chlorella sorokiniana*. Paper presented at the the 4th World Water Congress and Exhibition, Marrakech, Morocco
- Tamez Uddin, M., Rukanuzzaman, M., Maksudur Rahman Khan, M., & Akhtarul Islam, M. (2009). Adsorption of methylene blue from aqueous solution by jackfruit (*Artocarpus heterophyllus*) leaf powder: A fixed-bed column study. *Journal of Environmental Management*, 90(11), 3443-3450.
- Tan, I., Ahmad, A. L., & Hameed, B. (2008). Adsorption of basic dye on high-surface-area activated carbon prepared from coconut husk: Equilibrium, kinetic and thermodynamic studies. *Journal of Hazardous Materials*, 154(1-3), 337-346.
- Tanev, P. T., & Pinnavaia, T. J. (1995). A neutral templating route to mesoporous molecular sieves. *Science*, 267(5199), 865-867.
- Tanev, P. T., & Pinnavaia, T. J. (1996). Biomimetic templating of porous lamellar silicas by vesicular surfactant assemblies. *Science*, 271(5253), 1267-1269.
- Tatsuya, S. (1999). Stabilisation of fragrance in bathing preparations. *Japanese Patent*, 11.
- Temkin, M., & Pyzhev, V. (1940). Recent modifications to Langmuir isotherms. *Acta Physiochim. USSR*, 12, 217-222.

- Thompson, A. B., J. Cope, S., Swift, T. D., & Notestein, J. M. (2011). Adsorption of n-butanol from dilute aqueous solution with grafted calixarenes. *Langmuir*, 27(19), 11990-11998.
- Tien, C. (1994). *Adsorption calculations and modeling*: Butterworth-Heinemann Boston.
- Tilloy, S., Bertoux, F., Mortreux, A., & Monflier, E. (1999). Chemically modified β -cyclodextrins in biphasic catalysis: a fruitful contribution of the host-guest chemistry to the transition-metal catalyzed reactions. *Catalysis Today*, 48(1-4), 245-253. doi: 10.1016/S0920-5861(98)00379-4
- Treviño-Cordero, H., Juárez-Aguilar, L. G., Mendoza-Castillo, D. I., Hernández-Montoya, V., Bonilla-Petriciolet, A., & Montes-Morán, M. A. (2013). Synthesis and adsorption properties of activated carbons from biomass of *Prunus domestica* and *Jacaranda mimosifolia* for the removal of heavy metals and dyes from water. *Industrial Crops and Products*, 42(1), 315-323.
- Trinh, T., Bartolo, R. G., Dodd, M. T., Lucas, J. M., Buckner, R. Y., & Kajs, T. M. (1999). Methods and compositions for reducing body odor: US Patent 5,897,855.
- Tseng, R. K., & Cooney, J. J. (1995). Action of tributyltin on enzymes of four bacteria. *Environmental Toxicology and Chemistry*, 14(7), 1113-1121.
- Uekama, K., Adachi, H., Irie, T., Yano, T., Saita, M., & Noda, K. (1992). Improved transdermal delivery of prostaglandin E1 through hairless mouse skin: combined use of carboxymethyl-ethyl- β -cyclodextrin and penetration enhancers. *Journal of pharmacy and pharmacology*, 44(2), 119-121.
- Uekama, K., Hirayama, F., & Irie, T. (1998). Cyclodextrin Drug Carrier Systems. *Chemical Reviews*, 98(5), 2045-2076.
- Ueno, S., Kashimoto, T., Susa, N., Ishii, M., Chiba, T., Mutoh, K.-i., . . . Sugiyama, M. (2003). Comparison of hepatotoxicity and metabolism of butyltin compounds in the liver of mice, rats and guinea pigs. *Archives of toxicology*, 77(3), 173-181.
- Unger, M. A., MacIntyre, W. G., & Huggett, R. J. (1988). Sorption behavior of tributyltin on estuarine and freshwater sediments. *Environmental Toxicology and Chemistry*, 7(11), 907-915.

- Uragami, T., Ohshima, T., & Miyata, T. (2005). *Permeation and removal of volatile organic compounds from water through cross-linked poly(dimethylsiloxane) membranes containing calixarene*. Paper presented at the 54th SPSJ Annual Meeting Yokohama; Japan.
- van Bommel, K. J., Friggeri, A., & Shinkai, S. (2003). Organic templates for the generation of inorganic materials. *Angewandte Chemie International Edition*, 42(9), 980-999.
- van Leeuwen, F. W. B., Beijleveld, H., Velders, A. H., Huskens, J., Verboom, W., & Reinhoudt, D. N. (2005). Thiocalix[4]arene derivatives as radium ionophores: a study on the requirements for Ra²⁺ extraction. *Organic & Biomolecular Chemistry*, 3(10), 1993-2001.
- Vansant, E. F., Van Der Voort, P., & Vrancken, K. C. (1995). *Characterization and chemical modification of the silica surface* (Vol. 93): Elsevier Science.
- Verschuuren, H., Kroes, R., Vink, H., & Van Esch, G. (1966). Short-term toxicity studies with triphenyltin compounds in rats and guinea-pigs. *Food and cosmetics toxicology*, 4, 35-45.
- Vighi, M., & Calamari, D. (1985). QSARs for organotin compounds on *Daphnia magna*. *Chemosphere*, 14(11-12), 1925-1932.
- Vijayaraghavan, K., Padmesh, T. V. N., Palanivelu, K., & Velan, M. (2006). Biosorption of nickel(II) ions onto *Sargassum wightii*: Application of two-parameter and three-parameter isotherm models. *Journal of Hazardous Materials*, 133(1-3), 304-308.
- Vreysen, S., Maes, A., & Wullaert, H. (2008). Removal of organotin compounds, Cu and Zn from shipyard wastewaters by adsorption – flocculation: A technical and economical analysis. *Marine Pollution Bulletin*, 56(1), 106-115. doi: 10.1016/j.marpolbul.2007.09.044
- Wan, M. M., Yang, J. Y., Qiu, Y., Zhou, Y., Guan, C. X., Hou, Q., . . . Zhu, J. H. (2012). Sustained release of heparin on enlarged-pore and functionalized MCM-41. *ACS Applied Materials and Interfaces*, 4(8), 4113-4122.
- Wang, G., Xu, W., Wang, X., & Huang, L. (2012). Glycine- β -cyclodextrin-enhanced electrokinetic removal of atrazine from contaminated soils. *Environmental Engineering Science*, 29(6), 406-411.

- Wang, G., Zhou, Y., Wang, X., Chai, X., Huang, L., & Deng, N. (2010). Simultaneous removal of phenanthrene and lead from artificially contaminated soils with glycine- β -cyclodextrin. *Journal of Hazardous Materials*, *184*(1-3), 690-695.
- Weber Jr, W. J., & DiGiano, F. A. (1996). *Process dynamics in environmental systems*. New York: John Wiley & Sons.
- Weber, W., & Morris, J. (1963). Kinetics of adsorption on carbon from solution. *Journal of Sanitary Engineering Division American Society of Civil Engineers*, *89*(17), 31-60.
- Weidenhaupt, A., Arnold, C., Müller, S. R., Haderlein, S. B., & Schwarzenbach, R. P. (1997). Sorption of organotin biocides to mineral surfaces. *Environmental Science & Technology*, *31*(9), 2603-2609.
- Weis, J. S., & Perlmutter, J. (1987). Effects of tributyltin on activity and burrowing behavior of the fiddler crab, *Uca pugilator*. *Estuaries*, *10*(4), 342-346.
- Whalen, M. M., Loganathan, B. G., & Kannan, K. (1999). Immunotoxicity of Environmentally Relevant Concentrations of Butyltins on Human Natural Killer Cells in Vitro. *Environmental research*, *81*(2), 108-116.
- Wijnhoven, J. E., & Vos, W. L. (1998). Preparation of photonic crystals made of air spheres in titania. *Science*, *281*(5378), 802-804.
- Wong, P., Chau, Y., Kramar, O., & Bengert, G. (1982). Structure-toxicity relationship of tin compounds on algae. *Canadian Journal of Fisheries and Aquatic Sciences*, *39*(3), 483-488.
- Wong, Y., Szeto, Y., Cheung, W., & McKay, G. (2004). Adsorption of acid dyes on chitosan—equilibrium isotherm analyses. *Process Biochemistry*, *39*(6), 695-704.
- Wu, H., Liu, L., Pan, F., Hu, C., & Jiang, Z. (2006). Pervaporative removal of benzene from aqueous solution through supramolecule calixarene filled PDMS composite membranes. *Separation and Purification Technology*, *51*(3), 352-358.
- Xia, H., & Song, M. (2006). Preparation and characterisation of polyurethane grafted single-walled carbon nanotubes and derived polyurethane nanocomposites. *Journal of Materials Chemistry*, *16*(19), 1843-1851.

- Xiong, D., Chen, M., & Li, H. (2008). Synthesis of para-sulfonatocalix[4]arene-modified silver nanoparticles as colorimetric histidine probes. *Chemical Communications*(7), 880-882.
- Xu, G., Zhu, W., Gou, P., Zhu, K., & Shen, Z. (2010). Synthesis of calix[4] arene containing pbt-pdms copolyester and its property for separating benzene from its dilute aqueous solution by pervaporation. *Acta Polymerica Sinica*(11), 1327-1332. doi: 10.3724/sp.j.1105.2010.09440
- Xu, X., Lu, P., Zhou, Y., Zhao, Z., & Guo, M. (2009). Laccase immobilized on methylene blue modified mesoporous silica MCM-41/PVA. *Materials Science and Engineering C*, 29(7), 2160-2164.
- Yamasaki, H., Makihata, Y., & Fukunaga, K. (2008). Preparation of crosslinked β -cyclodextrin polymer beads and their application as a sorbent for removal of phenol from wastewater. *Journal of Chemical Technology and Biotechnology*, 83(7), 991-997.
- Yang, H., Coombs, N., & Ozin, G. A. (1997). Morphogenesis of shapes and surface patterns in mesoporous silica. *Nature*, 386(6626), 692-695.
- Yang, H., Zhang, G., Hong, X., & Zhu, Y. (2004). Dicyano-functionalized MCM-41 anchored-palladium complexes as recoverable catalysts for Heck reaction. *Journal of Molecular Catalysis A: Chemical*, 210(1-2), 143-148. doi: 10.1016/j.molcata.2003.09.009
- Yang, H., Zheng, K., Zhang, Z., Shi, W., Jing, S., Wang, L., . . . Zhang, P. (2012). Adsorption and protection of plasmid DNA on mesoporous silica nanoparticles modified with various amounts of organosilane. *Journal of Colloid and Interface Science*, 369(1), 317-322.
- Yang, M., Gao, Y., He, J., & Li, M. (2007). Preparation of polyamide 6/silica nanocomposites from silica surface initiated ring-opening anionic polymerization. *Express Polym Lett*, 1, 433-442.
- Yang, R. T. (2003). *Adsorbents: fundamentals and applications*: Wiley-Interscience.
- Yasmin, T., & Müller, K. (2010). Synthesis and surface modification of mesoporous mcm-41 silica materials. *Journal of Chromatography A*, 1217(20), 3362-3374.
- Ye, J., Yin, H., Peng, H., Bai, J., Xie, D., & Wang, L. (2013). Biosorption and biodegradation of triphenyltin by *Brevibacillus brevis*. *Bioresource Technology*, 129(0), 236-241. doi: <http://dx.doi.org/10.1016/j.biortech.2012.11.076>

- Yen, J.-H., Tsai, C.-C., Su, C.-C., & Wang, Y.-S. (2001). Environmental Dissipation of Fungicide Triphenyltin Acetate and Its Potential as a Groundwater Contaminant. *Ecotoxicology and Environmental Safety*, 49(2), 164-170. doi: <http://dx.doi.org/10.1006/eesa.2001.2053>
- Yi, X. S., Shi, W. X., Yu, S. L., Wang, Y., Sun, N., Jin, L. M., & Wang, S. (2011). Isotherm and kinetic behavior of adsorption of anion polyacrylamide (APAM) from aqueous solution using two kinds of PVDF UF membranes. *Journal of Hazardous Materials*, 189(1-2), 495-501. doi: <http://dx.doi.org/10.1016/j.jhazmat.2011.02.063>
- Yilmaz, A., Yilmaz, E., Yilmaz, M., & Bartsch, R. A. (2006). Removal of azo dyes from aqueous solutions using calix[4]arene and β -cyclodextrin. *Dyes and Pigments*, 74(1), 54-59.
- Yilmaz, E., Memon, S., & Yilmaz, M. (2010). Removal of direct azo dyes and aromatic amines from aqueous solutions using two β -cyclodextrin-based polymers. *Journal of Hazardous Materials*, 174(1-3), 592-597.
- Yousefi, S. R., Ahmadi, S. J., Shemirani, F., Jamali, M. R., & Salavati-Niasari, M. (2009). Simultaneous extraction and preconcentration of uranium and thorium in aqueous samples by new modified mesoporous silica prior to inductively coupled plasma optical emission spectrometry determination. *Talanta*, 80(1), 212-217.
- Yuan, J., Zhang, X., Yu, L., Sun, Z., Zhu, P., Wang, X., & Shi, H. (2011). Stage-specific malformations and phenotypic changes induced in embryos of amphibian (*Xenopus tropicalis*) by triphenyltin. *Ecotoxicology and Environmental Safety*, 74(7), 1960-1966. doi: 10.1016/j.ecoenv.2011.07.020
- Yuliarto, B., Honma, I., Katsumura, Y., & Zhou, H. (2006). Preparation of room temperature NO₂ gas sensors based on W- and V-modified mesoporous MCM-41 thin films employing surface photovoltage technique. *Sensors and Actuators, B: Chemical*, 114(1), 109-119.
- Yuskova, E. A., Ignacio-De Leon, P. A. A., Khabibullin, A., Stoikov, I. I., & Zharov, I. (2013). Silica nanoparticles surface-modified with thiacalixarenes selectively adsorb oligonucleotides and proteins. *Journal of Nanoparticle Research*, 15(10), 1-9.
- Yvon, Y., Hécho, I., & Donard, O. X. (2011). Tributyltin Solubilization and Degradation from Spiked Kaolin Using Different Reagents. *Water, Air, & Soil Pollution*, 219(1-4), 69-79. doi: 10.1007/s11270-010-0684-6

- Zaucke, F., Zöltzer, H., & Krug, H. F. (1998). Dose-dependent induction of apoptosis or necrosis in human cells by organotin compounds. *Fresenius' journal of analytical chemistry*, 361(4), 386-392.
- Zeleňák, V., Badaničová, M., Halamová, D., Čejka, J., Zukal, A., Murafa, N., & Goerigk, G. (2008). Amine-modified ordered mesoporous silica: Effect of pore size on carbon dioxide capture. *Chemical Engineering Journal*, 144(2), 336-342.
- Zhang, J., Shen, Z., Shan, W., Mei, Z., & Wang, W. (2011). Adsorption behavior of phosphate on lanthanum(III)-coordinated diamino-functionalized 3D hybrid mesoporous silicates material. *Journal of Hazardous Materials*, 186(1), 76-83.
- Zhang, J. b., Zhouq, F., Liu, W., & Jiang, G. (2009). The adsorption behavior of multiple-wall carbon nanotubes on tributyltin and their combined cytotoxicity. *Acta Scientiae Circum stantiae*, 29 (5), 1056- 1062.
- Zhang, Z., Hu, J., Zhen, H., Wu, X., & Huang, C. (2008). Reproductive inhibition and transgenerational toxicity of triphenyltin on medaka (*Oryzias latipes*) at environmentally relevant levels. *Environmental Science and Technology*, 42(21), 8133-8139. doi: 10.1021/es801573x
- Zhao, D., Feng, J., Huo, Q., Melosh, N., Fredrickson, G. H., Chmelka, B. F., & Stucky, G. D. (1998). Triblock copolymer syntheses of mesoporous silica with periodic 50 to 300 angstrom pores. *Science*, 279(5350), 548-552.
- Zhao, D., Huo, Q., Feng, J., Chmelka, B. F., & Stucky, G. D. (1998). Nonionic triblock and star diblock copolymer and oligomeric surfactant syntheses of highly ordered, hydrothermally stable, mesoporous silica structures. *Journal of the American Chemical Society*, 120(24), 6024-6036.
- Zhao, X., & Lu, G. (1998). Modification of MCM-41 by surface silylation with trimethylchlorosilane and adsorption study. *The Journal of Physical Chemistry B*, 102(9), 1556-1561.
- Zhao, X. S., Lu, G. Q., & Millar, G. J. (1996). Advances in mesoporous molecular sieve MCM-41. *Industrial and Engineering Chemistry Research*, 35(7), 2075-2090.
- Zhao, X. S., Lu, G. Q., Whittaker, A. K., Millar, G. J., & Zhu, H. Y. (1997). Comprehensive study of surface chemistry of MCM-41 using ²⁹Si CP/MAS NMR, FTIR, pyridine-TPD, and TGA. *Journal of Physical Chemistry B*, 101(33), 6525-6531.

- Zheng, C., Huang, X., Kong, L., Li, X., & Zou, H. (2004). Cross-linked β -cyclodextrin polymer used for bilirubin removal. *Chinese Journal of Chromatography (Se Pu)*, 22(2), 128-130.
- Zhong, N., Ohvo-Rekilä, H., Ramstedt, B., Slotte, J. P., & Bittman, R. (2001). Selective removal of palmitic acid from Langmuir monolayers by complexation with new quaternary ammonium β -cyclodextrin derivatives. *Langmuir*, 17(17), 5319-5323.
- Zhu, G., Zhong, H., Yang, Q., & Li, C. (2008). Chiral mesoporous organosilica spheres: Synthesis and chiral separation capacity. *Microporous and Mesoporous Materials*, 116(1-3), 36-43.
- Zhuang, X., Wan, Y., Feng, C., Shen, Y., & Zhao, D. (2009). Highly Efficient Adsorption of Bulky Dye Molecules in Wastewater on Ordered Mesoporous Carbons. *Chemistry of Materials*, 21(4), 706-716. doi: 10.1021/cm8028577
- Zinke, A., & Ziegler, E. (1944). Zur Kenntnis des Härtungsprozesses von Phenol-Formaldehyd-Harzen, X. Mitteilung. *Berichte der deutschen chemischen Gesellschaft (A and B Series)*, 77(3-4), 264-272. doi: 10.1002/cber.19440770322

List of Publications

1. **Alahmadi Sana M.**, Sharifah Mohamad, Mohd Jamil Bin Maah, (2014). Prediction of optimum sorption isotherm for adsorption of dibutyltin onto mesoporous silica functionalized with calix[4]arene derivatives: comparison of two and three parameter isotherm models. Submitted to *Separation Science and Technology*. (ISI/SCOPUS Cited Publication)
2. **Alahmadi Sana M.**, Sharifah Mohamad, Mohd Jamil Bin Maah, (2014). Isotherm modelling, kinetics and thermodynamic studies for the adsorption of triphenyltin on a mesoporous silica functionalized with calix[4]arene derivatives. Submitted to *Arabian Journal of Chemistry*. (ISI/SCOPUS Cited Publication)
3. **Alahmadi Sana M.**, Sharifah Mohamad, Mohd Jamil Bin Maah, (2014). Comparative study of tributyltin adsorption onto mesoporous silica functionalized with calix[4]arene, p-tert-butylcalix[4]arene and p-sulfonatocalix[4]arene. *Molecules*, 19, 4524-4547. <http://www.mdpi.com/1420-3049/19/4/4524/pdf>. (ISI/SCOPUS Cited Publication)
4. **Alahmadi Sana M.**, Sharifah Mohamad, Mohd Jamil Bin Maah, (2013). Preparation of Organic-Inorganic Hybrid Materials based on MCM-41 and its applications. *Advances in Materials Science and Engineering* - <http://dx.doi.org/10.1155/2013/634863> (ISI/SCOPUS Cited Publication)
5. **Alahmadi, Sana M.**, Sharifah Mohamad, and Mohd Jamil Maah, (2014). Organic Inorganic Hybrid Materials Based on Mesoporous Silica MCM-41 with β -

Cyclodextrin and its Applications. In press, *Asian Journal of Chemistry*. 26(14).
(ISI/SCOPUS Cited Publication)

6. **Sana M. Alahmadi**, Sharifah Mohamad and Mohd Jamil Maah, (2012). Synthesis and Characterization of Mesoporous Silica Functionalized with Calix[4]arene Derivatives. *International Journal of Molecular Sciences*, 13(10), 13726-13736.
(ISI/SCOPUS Cited Publication)
7. **Sana Alahmadi**, (2012). Modification of Mesoporous Silica MCM-41 and its Applications- A review. *Oriental Journal of Chemistry*, 28(1), 1-11. (ISI/SCOPUS Cited Publication)
8. **S.M. Alahmadi**, (2011). Organotin Speciation Analysis Based on Liquid or Gas Chromatography. *Asian Journal of Chemistry*, 23(9), 3787-3791. (ISI/SCOPUS Cited Publication)

Related Publication

9. **Alahmadi Sana Mohammad**, Sharifah Mohamad and Mohd Jamil Maah, (2010). Preparation and Characterization of Silica Modified with Calix[4]arene Derivatives. *Journal of Chemistry and Chemical Engineering*, 4(9), 44-49.

International Conferences Attended

1. **Alahmadi, Sana M.**, Sharifah Mohamad, and Mohd Jamil Maah, International Conference on Nanotechnology (ICONT), 30 May-1 June 2012, Kuantan, Malaysia (Oral presentation).
2. **Alahmadi, Sana M.**, Sharifah Mohamad, and Mohd Jamil Maah, Asian International Conference on Materials, Minerals and Polymer (MAMIP), 23-24 March 2012, Penang, Malaysia (Oral presentation).
3. **Alahmadi, Sana M.**, Sharifah Mohamad, and Mohd Jamil Maah, ASEAN Conference on Scientific and Social Science Research (ACSSSR), 22-23 June 2011, Penang, Malaysia (Oral presentation).
4. **Alahmadi, Sana M.**, Sharifah Mohamad, and Mohd Jamil Maah, 5th International Congress of Chemistry and Environment (ICCE), 27-29 May 2011, Port Dickson, Malaysia (Oral presentation).
5. **Alahmadi, Sana M.**, Sharifah Mohamad, and Mohd Jamil Maah, 3rd International Conference for Young Chemists (ICYC), 23-25 June 2010, Penang, Malaysia (Oral presentation).
6. **Alahmadi, Sana M.**, Sharifah Mohamad, and Mohd Jamil Maah, Regional Annual Fundamental Science Symposium (RAFAS), 8-9 June 2010, Kuala Lumpur, Malaysia (Oral presentation).